พิร์โรลิดินิลเพปไทด์นิวคลีอิกแอซิดโพรบติดฉลากเรืองแสงที่ตอบสนองต่อการเกิดไฮบริด

นายณัฐวุฒิ โยธาพันธ์

วิทยานิพนธ์นี้เป็นส่วนหนึ่งของการศึกษาตามหลักสูตรปริญญาวิทยาศาสตรดุษฎีบัณฑิต
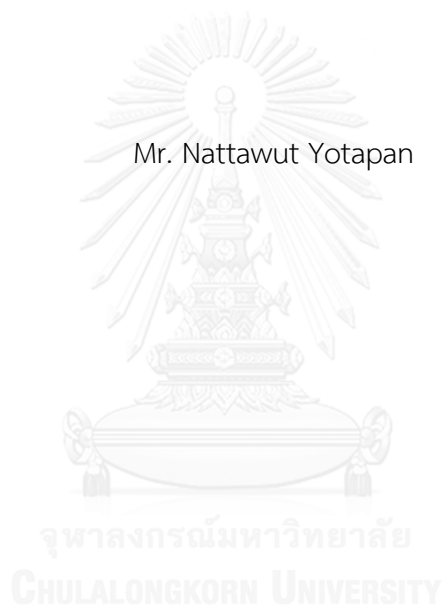สาขาวิชาเคมี ภาควิชาเคมี
คณะวิทยาศาสตร์ จุฬาลงกรณ์มหาวิทยาลัย
ปีการศึกษา 2557
ลิขสิทธิ์ของจุฬาลงกรณ์มหาวิทยาลัย

HYBRIDIZATION RESPONSIVE FLUORESCENCE-
LABELED PYRROLIDINYL PEPTIDE NUCLEIC ACID PROBES

Mr. Nattawut Yotapan

A Dissertation Submitted in Partial Fulfillment of the Requirements

for the Degree of Doctor of Philosophy Program in Chemistry

Department of Chemistry

Faculty of Science

Chulalongkorn University

Academic Year 2014

Thesis Title	HYBRIDIZATION RESPONSIVE FLUORESCENCE-LABELED PYRROLIDINYL PEPTIDE NUCLEIC ACID PROBES
By	Mr. Nattawut Yotapan
Field of Study	Chemistry
Thesis Advisor	Professor Tirayut Vilaivan, D.Phil.

Accepted by the Faculty of Science, Chulalongkorn University in Partial Fulfillment of the Requirements for the Doctoral Degree

⎯⎯⎯⎯⎯⎯⎯⎯⎯⎯⎯⎯⎯⎯⎯⎯⎯Dean of the Faculty of Science

(Professor Supot Hannongbua, Dr.rer.nat.)

THESIS COMMITTEE

⎯⎯⎯⎯⎯⎯⎯⎯⎯⎯⎯⎯⎯⎯⎯Chairman

(Associate Professor Vudhichai Parasuk, Ph.D.)

⎯⎯⎯⎯⎯⎯⎯⎯⎯⎯⎯⎯⎯⎯⎯Thesis Advisor

(Professor Tirayut Vilaivan, D.Phil.)

⎯⎯⎯⎯⎯⎯⎯⎯⎯⎯⎯⎯⎯⎯⎯Examiner

(Assistant Professor Aroonsiri Shitangkoon, Ph.D.)

⎯⎯⎯⎯⎯⎯⎯⎯⎯⎯⎯⎯⎯⎯⎯Examiner

(Assistant Professor Worawan Bhanthumnavin, Ph.D.)

⎯⎯⎯⎯⎯⎯⎯⎯⎯⎯⎯⎯⎯⎯⎯External Examiner

(Associate Professor Chutima Kuhakarn, Ph.D.)

ณัฐวุฒิ โยธาพันธ์ : พิร์โรลิดินิลเพปไทด์นิวคลีอิกแอซิดโพรบติดฉลากเรืองแสงที่ตอบสนองต่อการเกิดไฮบริด (HYBRIDIZATION RESPONSIVE FLUORESCENCE-LABELED PYRROLIDINYL PEPTIDE NUCLEIC ACID PROBES) อ.ที่ปรึกษาวิทยานิพนธ์หลัก: ธีรยุทธ วิไลวัลย์, 203 หน้า.

ในงานวิจัยนี้เราได้พัฒนาเพปไทด์นิวคลีอิกแอซิดโพรบเรืองแสงที่สามารถเปลี่ยนแปลงความเข้มและความยาวคลื่นของการเรืองแสงเมื่อเกิดไฮบริดกับดีเอ็นเอเป้าหมายที่ถูกต้อง ซึ่งโพรบดังกล่าวจะสามารถนำมาใช้ประโยชน์ในการตรวจวัดลำดับเบสของดีเอ็นเอ เพปไทด์นิวคลีอิกแอซิดที่ใช้ในงานวิจัยนี้คือ พิร์โรลิดินิลเพปไทด์นิวคลีอิกแอซิดที่ประกอบด้วย ดี-โพรลีน/2-อะมิโนไซโคลเพนเทนคาร์บอกซิลิก แอซิด เป็นโครงสร้างหลัก (acpcPNA) พีเอ็นเอชนิดนี้แสดงความเสถียร และมีความสามารถจับยึดกับดีเอ็นเอได้อย่างแข็งแรงและจำเพาะเจาะจงกว่าดีเอ็นเอและพีเอ็นเอที่มีจำหน่ายในท้องตลาด ในงานส่วนแรก ได้ทำการสังเคราะห์พีเอ็นเอที่ติดฉลากคู่ที่ตำแหน่งภายในสายของ acpcPNA โดยอาศัย 3-อะมิโนพิร์โรลิดีน-4-คาร์บอกซิลิก แอซิด (APC) ที่ปกป้องด้วยคู่ของหมู่ปกป้องที่ออร์โทโกนัลกัน (Tfa และ o-Nosyl) พีเอ็นเอที่ติดฉลากคู่แบบภายในสายควรจะสามารถเปลี่ยนแปลงการเรืองแสงเนื่องจากอันตรกิริยาที่แตกต่างกัน (quenching หรือ FRET) ระหว่างฉลากทั้งสองชนิดที่อยู่บนพีเอ็นเอสายเดี่ยวและพีเอ็นเอที่จับยึดกับดีเอ็นเอ เป็นที่น่าเสียดายว่าการเรืองแสงเปลี่ยนไปไม่มากนัก และไม่เป็นไปตามที่ออกแบบไว้เนื่องจากเกิดการ quench ระหว่างคู่ FRET ในพีเอ็นเอโพรบที่เป็นสายเดี่ยว งานส่วนที่สองคือการพัฒนา acpcPNA ที่ติดฉลากเรืองแสงและ quencher (anthraquinone) ที่มีสมบัติในการซ้อนทับกับคู่เบส ตรงปลายสาย พีเอ็นเอสายเดี่ยวที่ติดฉลากคู่ตรงปลายสายจะมีการเรืองแสงที่ต่ำ เมื่อมีดีเอ็นเอที่มีลำดับเบสคู่สม การเรืองแสงของ acpcPNA ที่ติดฉลากที่ปลายสายจะเพิ่มขึ้นอย่างมาก (ได้ถึง 18 เท่า) โดยโพรบนี้สามารถแยกความแตกต่างของดีเอ็นเอคู่สมจากดีเอ็นเอที่มีลำดับเบสผิดไปหนึ่งตำแหน่งทั้งตรงกลางและปลายสายได้อย่างจำเพาะเจาะจง นอกจากนี้ยังอาจเพิ่มความจำเพาะขึ้นไปได้อีกโดยใช้ปฏิกิริยาการแทนที่ของสายดีเอ็นเอ (strand displacement reaction) หรือการเพิ่มอุณหภูมิ งานส่วนสามเป็นการติด Nile red ซึ่งเป็นฉลากเรืองแสงชนิด solvatrochromic dye ซึ่งสามารถเปลี่ยนแปลงการเรืองแสงได้ตามสิ่งแวดล้อมที่ตำแหน่งภายในสายของ acpcPNA การเรืองแสงของ apcpPNA ที่ทำการติด Nile red จะเพิ่มขึ้นและเลื่อนไปทางสีน้ำเงินเมื่อมีการจับยึดกับดีเอ็นเอคู่สม และกับดีเอ็นเอที่มีการเพิ่มเบสลงไปซึ่งจับกับพีเอ็นเอแล้วเกิดเป็นโครงสร้างที่มีช่องโป่ง (bulge) จากข้อมูลทางสเปกโตรสโคปี Nile red ทำให้เสนอได้ว่า Nile red เกิดอันตรกิริยากับร่อง (groove) ในไฮบริดของพีเอ็นเอกับดีเอ็นเอที่เป็นคู่สม หรือเกิดอันตรกิริยากับช่องว่างที่ไม่ชอบน้ำของ bulged duplex

ภาควิชา   เคมี   ลายมือชื่อนิสิต --

สาขาวิชา   เคมี   ลายมือชื่อ อ.ที่ปรึกษาหลัก ----------------------------

ปีการศึกษา   2557

5173893623 : MAJOR CHEMISTRY

KEYWORDS: PEPTIDE NUCLEIC ACID / DUAL-FLUORESCENCT LABELED / FLUORESCENCE / FRET PROBES

NATTAWUT YOTAPAN: HYBRIDIZATION RESPONSIVE FLUORESCENCE-LABELED PYRROLIDINYL PEPTIDE NUCLEIC ACID PROBES. ADVISOR: PROF. TIRAYUT VILAIVAN, D.Phil., 203 pp.

In this study, we developed fluorescence peptide nucleic acid (PNA) probes that can change the fluorescence intensity and emission wavelength upon hybridization with correct DNA targets. Such probes should be useful for DNA sequence analyses. The PNA employed in this work is the pyrrolidinyl PNA with an alternating D-proline/2-aminocyclopentane carboxylic acid backbone (acpcPNA) which shows superior stability, as well as binding affinity and specificity than DNA and commercial PNA. In the first part, internally dual-labeled acpcPNA were synthesized using a pair of orthogonally-protected (Tfa and o-Nosyl) 3-aminopyrrolidine-4-carboxylic acid (APC) that was incorporated into the acpcPNA backbone. It was proposed that the fluorescence of internally dual-labeled acpcPNA should change due to different interactions (quenching or FRET) between the two dyes in the single stranded and DNA-hybridized probes. Unfortunately, the fluorescence change was not very high, and was not in accordance with the design due to the quenching between the FRET pairs in single stranded probes. In the second part, dual end-labeled acpcPNA probes bearing a fluorophore and a quencher with end-stacking ability (anthraquinone) were developed. These single-stranded end-labeled probes exhibited very low fluorescence in single stranded state. In the presence of complementary DNA, the fluorescence of the doubly-end labeled acpcPNA was greatly enhanced (up to 18 folds). The probes exhibit good specificity in discriminating between complementary and both internally and terminally mismatched DNA, which could be improved further by a strand displacement reaction or by increasing the temperature. In the third part, the solvatrochromic dye Nile red which can change its fluorescence according to its environment was incorporated into the internal positions of acpcPNA backbone. The fluorescence of the Nile red-modified acpcPNA was enhanced when hybridized with complementary DNA and DNA with inserted base that can form a bulge. Based on spectroscopic data, the Nile red was proposed to interact with the groove in complementary PNA-DNA hybrid, or the hydrophobic pocket formed by the bulged duplex.

Department:	Chemistry	Student's Signature	-------------------------------------
Field of Study:	Chemistry	Advisor's Signature	-------------------------------------
Academic Year:	2014		

ACKNOWLEDGEMENTS

CONTENTS

LIST OF TABLES

LIST OF FIGURES

Figure   Page

Figure   Page

Figure   Page

Figure   Page

Figure   Page

Figure   Page

Figure   Page

LIST OF ABBREVIATIONS

AQ		Anthraquinone
apc		4-amino-cyclopentane carboxylic acid
δ	:	chemical shift
μL	:	microliter
μmol	:	micromole
$[\alpha]_D$	:	specific rotation
A	:	adenine
A^{Bz}	:	N^6-benzoyladenine
Ac	:	acetyl
Ac_2O	:	acetic anhydride
Boc	:	*tert*-butoxycarbonyl
BHQ	:	black hole quencher
Bz	:	benzoyl
c	:	concentration
C	:	cytosine
calcd	:	calculated
C^{Bz}	:	N^4-benzoylcytosine
CCA	:	α-cyano-4-hydroxy cinnamic acid
Cou	:	coumarin
$CDCl_3$	:	deuterated chloroform
DMSO-d6	:	deuterated dimethyl sulfoxide

d	:	doublet
DABCYL	:	4-(4-dimethylaminophenylazo)benzoic acid
DBU	:	1,8-*diazabicyclo*[5.4.0]undec-7-ene
DCM	:	dichloromethane
DIEA	:	diisopropylethylamine
DMF	:	*N,N'*-dimethylformamide
DNA	:	deoxyribonucleic acid
Dpm	:	diphenylmethyl
ds	:	double strand
Dns	:	dansyl
DNB	:	3,5-dinitrobenzoic acid
f	:	enhancement factor
Flu	:	fluorescein
Fmoc	:	9-fluorenylmethoxycarbonyl
FmocOSu	:	9-fluorenylmethyl succinimidyl carbonate
FRET	:	fluorescence resonance energy transfer
g	:	gram
G	:	guanine
G^{Ibu}	:	N^2-isobutyrylguanine
h	:	hour
HATU	:	*O*-(7-azabenzotriazol-1-yl)-*N,N,N',N'*-tetramethyluronium hexafluorophosphate
HOAt	:	1-hydroxy-7-azabenzotriazol
HPLC	:	high performance liquid chromatography

Hz	:	hertz
Ibu	:	isobutyryl
J	:	coupling constant
Lys	:	lysine
m	:	multiplet
M	:	molar
MALDI-TOF	:	matrix-assisted laser desorption/ionization-time of flight
MeCN	:	acetonitrile
MeOH	:	methanol
mg	:	milligram
MHz	:	megahertz
min	:	minute
mL	:	milliliter
mM	:	millimolar
mmol	:	millimol
MS	:	mass spectrometry
m/z	:	mass to charge ratio
nm	:	nanometer
NMR	:	nuclear magnetic resonance
NBD		7-nitrobenzofurazan
Nr		Nile red
°C	:	degree celsius
Pfp	:	pentafluorophenyl
PheR		Phenoxazine red

PNA	:	peptide nucleic acid or polyamide nucleic acid
R_f	:	retention factor
RNA	:	ribonucleic acid
s	:	singlet
ss	:	single strand
t	:	triplet
T	:	thymine
TFA	:	trifluoroacetic acid
THF	:	tetrahydrofuran
TLC	:	thin layer chromatography
T_m	:	melting temperature
TMR	:	*tetramethylrhodamine*
t_R	:	retention time
UV	:	ultraviolet

CHAPTER I

INTRODUCTION

1.1 Peptide Nucleic acid

Peptide nucleic acid (PNA) is a structural mimic of DNA obtained by replacing the deoxyribosephosphate with a polyamide backbone. In 1991, the first PNA with N-(2-aminoethyl)-glysine (aeg) backbone was introduced by Nielsen et al. [1, 2]. This PNA system is now known as aegPNA. The four nucleobases: adenine, cytosine, guanine and thymine were attached to the N-aminoethylglycyl backbone via methylenecarbonyl linkages. (**Figure1.1**). Instead of 5' and 3'-termini, PNA has an amino (N-) and carboxyl (C-) groups. Despite such a dramatic structural difference, aegPNA hybridizes to complementary DNA according to the Watson-Crick's base pairing rules. PNA has no negative charge in the backbone, the unfavorable Coulombic repulsion observed in DNA or RNA duplexes is therefore absence in PNA-DNA hybrids (**Figure 1.1**). Accordingly, PNA can bind with complementary DNA to form PNA-DNA hybrid that is more stable than DNA-DNA hybrid. In addition, PNA hybridizes to DNA with high selectivity, which means that complementary PNA-DNA hybrids are much more stable than the mismatched PNA-DNA hybrids [2].
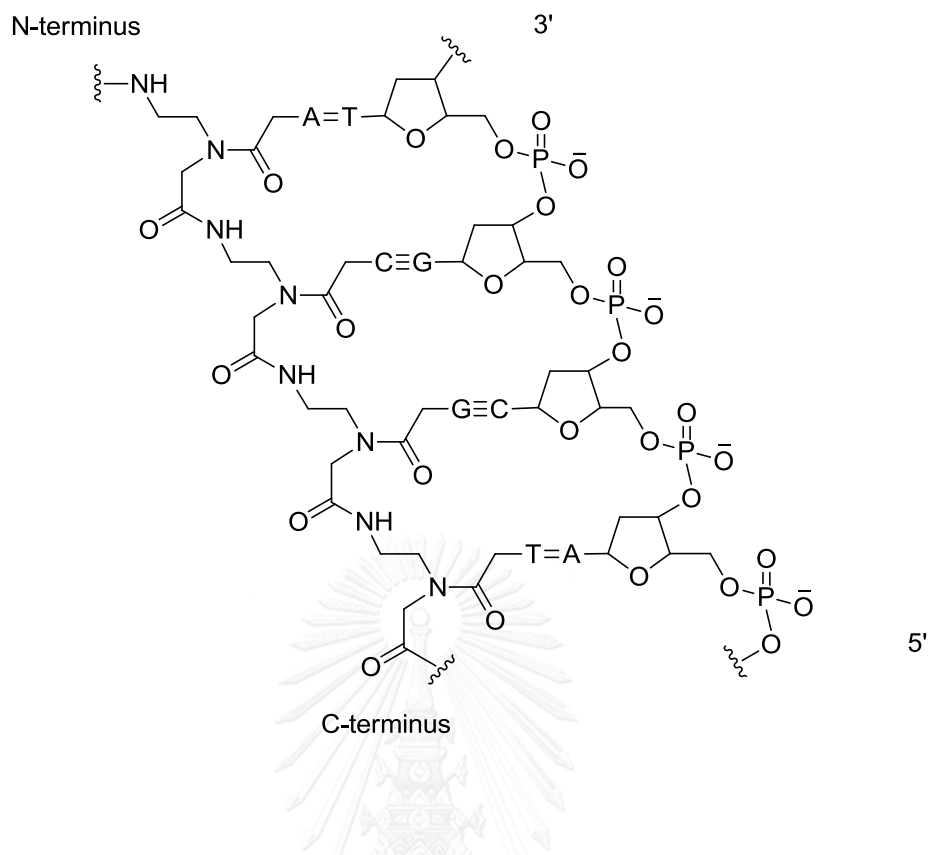
Figure 1.1 A schematic structure of aegPNA hybridized with DNA

In addition to the charge, PNA exhibits many different properties from DNA. PNA is completely resistant to proteases and nucleases [3]. The stability of PNA-DNA hybrid is much less dependent to salt concentration than DNA-DNA hybrids, which is the direct consequence of its uncharged nature [3]. From these advantages, PNA can be applied in several areas involving nucleic acids, which can be classified in three groups [4]. In the first and most popular group, PNA can be used as diagnostic probes for DNA and RNA sensing which can be used for clinical diagnosis and other areas [5, 6]. PNA can also be used as for biological applications such as by controlling genetic expressions by antisense or antigene principle [7-9] and also as tools for manipulation of nucleic acids [10]. In the last and only recently emerging group, PNA is useful in building self-assembled nanoscale structures [11] or devices [12] that can be used for various applications such as drug delivery and many others.

In 2005 Vilaivan et al. developed a new class of PNA called pyrrolidinyl PNA. These PNAs contain a pyrrolidine ring in the backbone which restricts the conformational flexibility of the PNA molecules. The best known member of the pyrrolidinyl PNA family is acpcPNA with a (2R,4R)-prolyl-(1S,2S)-2-aminocyclopentanecarboxylic acid (ACPC) backbone. The nucleobases were attached to the 4-position of the pyrrolidine ring deriving from D-proline. With its conformationally constrained backbone, acpcPNA form a PNA-DNA hybrid with higher affinity and specificity than aegPNA [13, 14]. It also binds to DNA exclusively in antiparallel fashion which is different from aegPNA. A systematic study of the stereochemical effects of the pyrrolidine monomer and ACPC spacer indicates that out of the possible 16 combinations, only the (2R,4R)-proline/(1S,2S)-ACPC and (2R,4S)-proline/(1S,2S)-ACPC diastereomers can form stable hybrids with DNA [15]. In addition, the effects of ring size of the spacer part on DNA hybridization were investigated. The acbcPNA with a four-membered ring spacer (ACBC) showed an improved DNA and RNA binding affinity without compromising the specificity, while the achcPNA with a six-membered ring spacer (ACHC) failed to bind to DNA [16]. This could be explained by comparing the torsional angle (θ) between the NH/CO in the spacer and molecular model of pyrrolidinyl PNA-DNA hybrids [17].

In addition, many other alternatives PNA had been developed during the past 20 years. The most promising one is the γ-PNA independently introduced by Ly et al. [18, 19] and Appella et al. [20]. Pre-organization of the PNA structure, which was controlled by the presence of a substituent at the γ-position of the original aegPNA backbone with a proper stereochemistry, remarkably increases the binding affinity to DNA. These new PNA have potential for much wider range of applications than the original aegPNA.
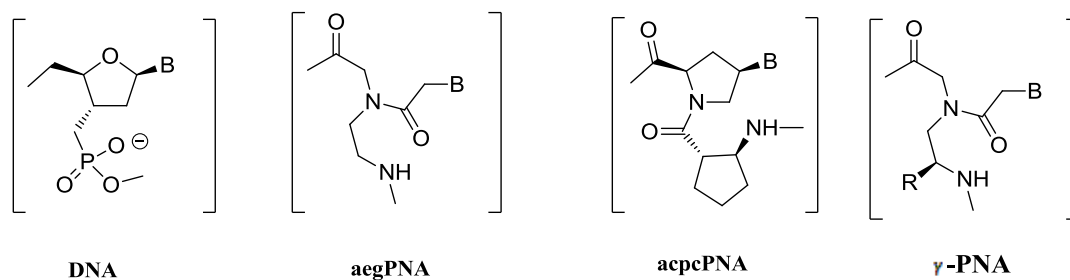
Figure 1.2 Structure of DNA and PNA

1.2 Fluorescence probes

Fluorescence spectroscopy is one of the most important techniques for DNA detection and sequence analysis. Since DNA itself is non-fluorescence, a fluorescence probe is required. The probe may be simply a DNA-binding dye that can interact non-specifically with DNA (or RNA) such as ethidium and the members of SYBR dyes family. However, for DNA sequence analysis purpose, a fluorescence probe that can bind sequence-specifically with good discrimination ability toward single base mismatch is highly desirable. To enable the sequence-specific binding, the probe must contain a recognizing element, which is almost invariably an oligonucleotide or analogues. A number of such fluorescence oligonucleotides probes have been developed over the past two decades. Better known examples include molecular beacons, binary probes and base-discriminating fluorescence probes.

1.2.1 Molecular beacon probes

One of the landmark developments in the area of fluorescence hybridization probes was the introduction of molecular beacons (MBs) by Tyagi and Kramer in 1996 [21]. The molecular beacon is a doubly end-labeled single stranded oligonucleotide that can fold in to a stem-loop structure (**Figure 1.3**). The loop part of the MBs acts as a DNA binding element by carrying a base sequence that is complementary to the target DNA. The stem part is formed by annealing the two complementary "arms" that are five or six bases long on either side of the probe sequence. The two dyes are

attached to the end of both arms. In the absence of the DNA target, the MB stays in a closed form. The formation of the stem keeps these two dyes in close proximity to each other. Hybridization with the DNA target results in destruction of the stem, which changes the distance between the two dyes. The change in distance, and thus interaction between the dyes cause a fluorescence change.

1.2.1.1 Fluorophore-Quencher molecular beacons

In the classical MB [21], a fluorophore (F) and a quencher (Q) were attached to the opposite ends of the molecule. In the closed state, the stem formation results in quenching of the fluorophore therefore resulting in low fluorescence emission. Hybridization with the target DNA in the loop region opens the stem and separates the fluorophore and quencher. This produces a strong fluorescence increase [22-25].
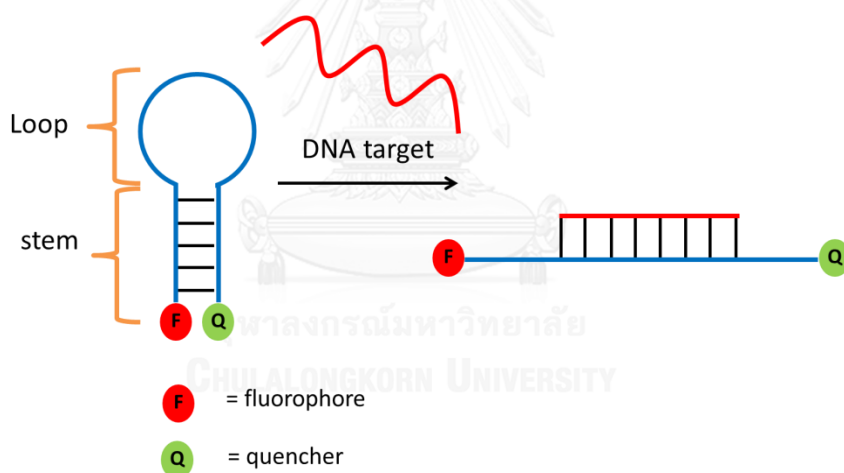
Figure 1.3 A schematic representation of the working principle of the fluorophore-quencher MBs

1.2.1.2 FRET beacons

As an alternative to the fluorophore-quencher MBs described above, there are another type of MB that operates by a Förster resonance energy transfer (FRET) principle FRET MB probes possess two fluorescence dyes – a fluorescence donor (D) and acceptor (A) (a FRET pair) – attached to its opposite ends (**Figure 1.4**). Efficient

FRET requires three conditions to be met [26]. Firstly the dyes must have a good spectra overlap (the emission of the donor should overlap with the absorption of the acceptor). Secondly the dyes should be in a suitable distance – the donor and acceptor molecules must be in close proximity (typically 10–100 Å). Finally, the donor and acceptor transition dipole orientations must be approximately parallel. In the closed state, excitation at the donor fluorophore does not result in fluorescence of the donor because of the energy transfer to the acceptor. Accordingly, the donor fluorophore is quenched, and the fluorescence of the acceptor will be observed. In the presence of the target DNA, hybridization to the MB results in an increase in fluorescence of the donor because now the two fluorophores are separated beyond the FRET distance. The advantage of FRET MBs over the classical MBs is that the change of two fluorescence intensities can be monitored, instead of only one, which should provide more accuracy and reliability.

D = fluorophore donor
A = fluorophore acceptor
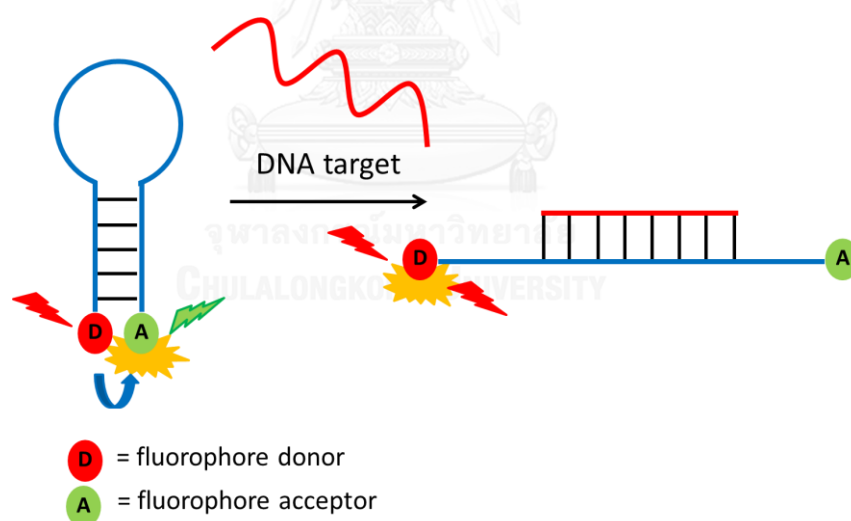
Figure 1.4 A schematic representation of the working principle of the FRET MBs

More recently, Wagenknecht et al. had introduced pyrene and Nile red as an energy transfer pair into the stem of a DNA molecular beacon. The dyes were incorporated into the DNA strand via an ethynyl liker at the position 5 of 2'-deoxyuridine [27-29]. In free MB, excitation at the pyrene wavelength resulted in energy

transfer to the Nile red, thus a red fluorescence was observed. After adding the target DNA in sub-stoichiometric quantities, a white or blue fluorescence were observed as a result of blending between the fluorescence of pyrene (blue) and FRET from pyrene to Nile red (red). Pure blue pyrene fluorescence was observed only after complete hybridization (**Figure 1.5**).
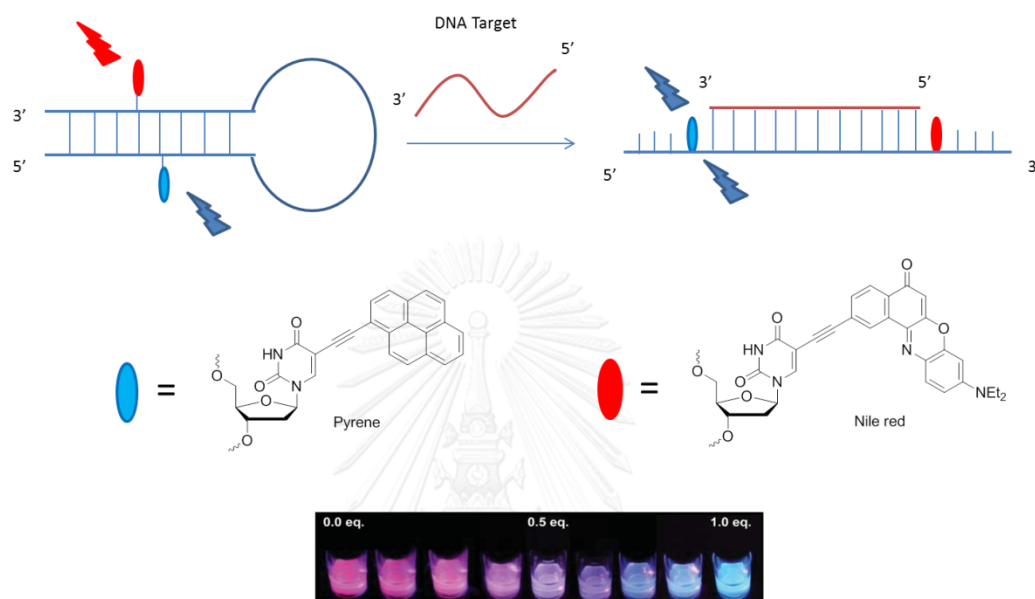
Figure 1.5 A schematic representation of the working principle of the pyrene-Nile red FRET MBs [28]

More recently, the same group reported a new FRET MB probe. Thiazole orange (TO, donor) and thiazole red (TR, acceptor) were incorporated into the stem of the MB. In the closed form, only fluorescence emission of the TR was observed because of the energy transfer from TO. In the open form, TO fluorescence was increased while TR fluorescence was decreased because the two flourophore were separated [30]. This design allows much more efficient contact between the two dyes and therefore the FRET and also color contrast are much better than the classical FRET MB with the fluorescein/tetramethylrhodamine FRET pairs at the end of the stems.
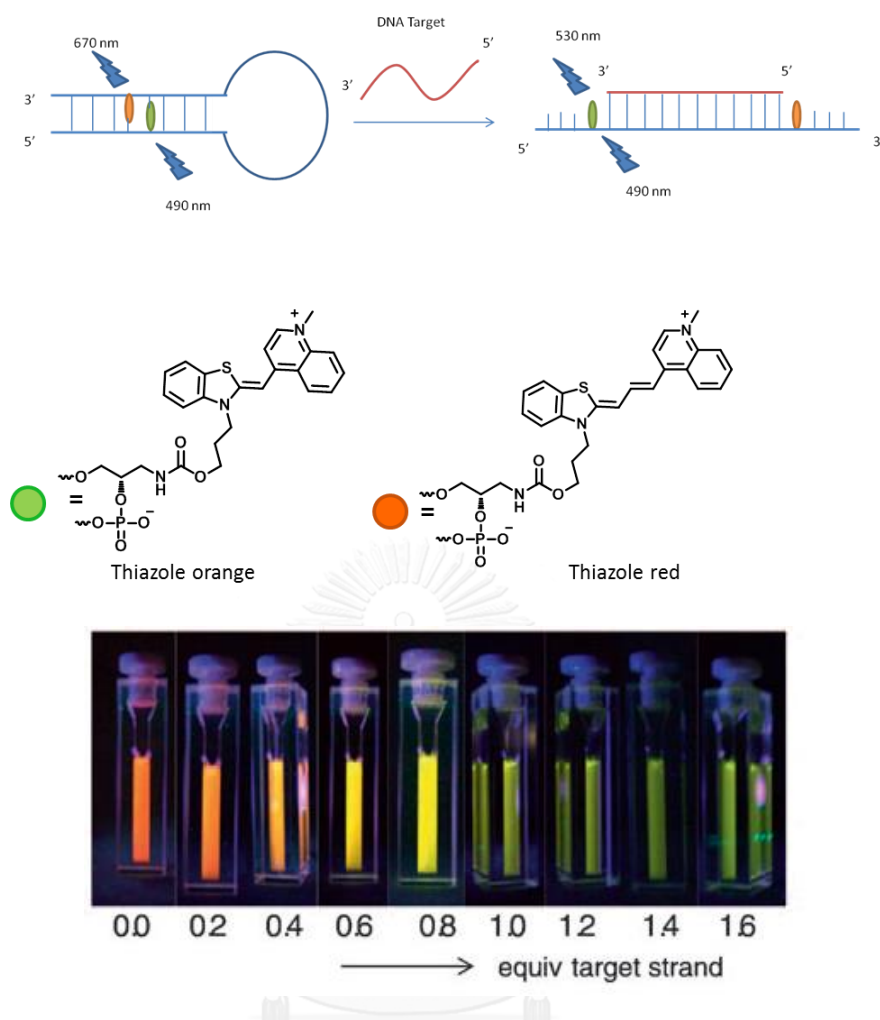
Figure 1.6 A schematic representation of the working principle of the TO-TR FRET MBs [30]

1.2.1.3 Quencher-free molecular beacon probes

Recently, it has been shown that certain modified oligonucleotide probes carrying just one fluorophore can function as MB even without the quencher moiety. These can be regarded as "quencher-free molecular beacons" [31]. Like normal MBs, the quencher-free MBs must be able recognize the complementary DNA in a sequence specific manner. To allow fluorescence change, there must be some mechanisms to differentiate the fluorophore in the free and hybridized states, e.g. by interactions with nucleobases or DNA (interacalation or groove binding). These often change the properties and hence the fluorescence behavior of the fluorophores. For example, Kim

and co-workers designed a MB containing a fluorescence nucleoside analogue and demonstrated its utility as a quencher-free probe for DNA detection [31, 32]. The fluorescent base analogue UFL, having a fluorene anchored to the nucleobase of deoxyuridine through an ethynyl linker, was incorporated it into the central position of the hairpin loop (**Figure 1.7**). This quencher-free MB showed an increased fluorescence upon hybridization to complementary DNA with high specificity is due to disruption of quenching interactions in the single-stranded probe DNA between the fluorophore and the nucleobases.
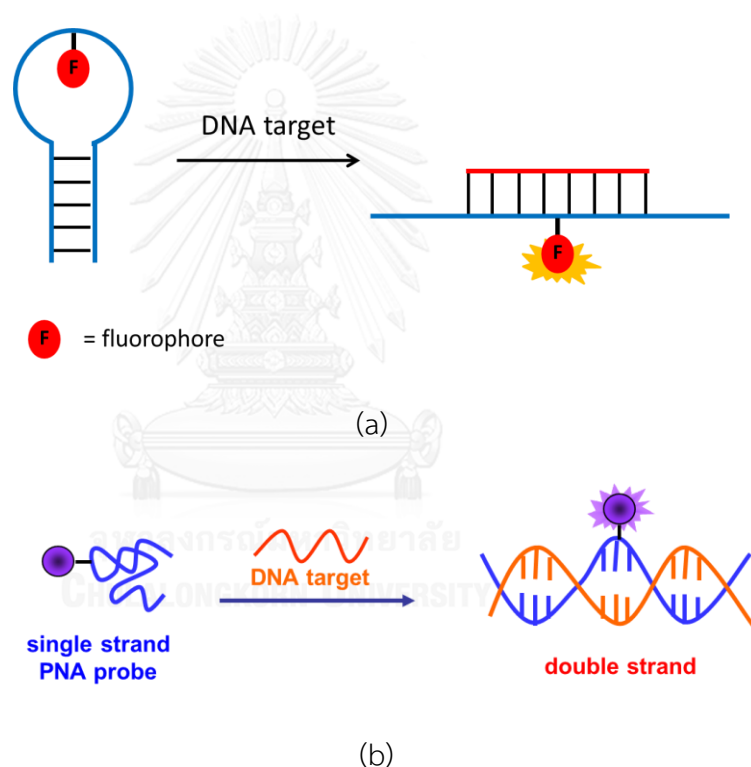
Figure 1.7 Schematic representations of the working principle of the (a) quencher-free MB and (b) linear probe

A related work by Saito also demonstrated a similar concept [32, 33]. Instead of fluorene, the DNA was modified by a pyrene attached to the nucleobase. The fluorescence change does not require the presence of the stem-loop structure. Thus this represents an example of linear probe which offers a number of advantages over

structured probes including the simple design and fast hybridization kinetics. However, the discrimination power may not be ideal because mismatched targets can still form relatively stable hybrids with the probe.

1.2.1.4 Excimer-Monomer Switching MBs

In addition to quenching, FRET and quencher-free, another type of interactions between fluorophores that had been employed for DNA sequence detection is the formation of excimers or exciplexes. Fluorophore dimer can form via π-stacking or dipole-dipole interactions, which results in a smaller gap between highest occupied molecular orbital (HOMO) and lowest unoccupied molecular orbital (LUMO) and thus emission at longer wavelength. Consequently, there are several reports about hybridization probes and molecular beacons based on this principle [34-38]. For example, a linear DNA probe with two pyrenes attached can form excimer as the free probe or in the presence of mismatched DNA target. But hybridization with the target DNA resulted in pyrene monomer emission or total quenching due to interaction of pyrene with the DNA duplex [39].
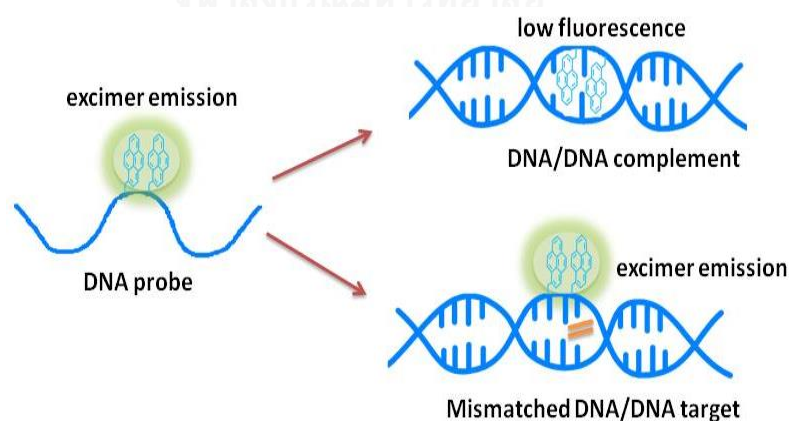
Figure 1.8 A schematic represenctation of the working principle of the excimer-monomer swiching MBs [39]
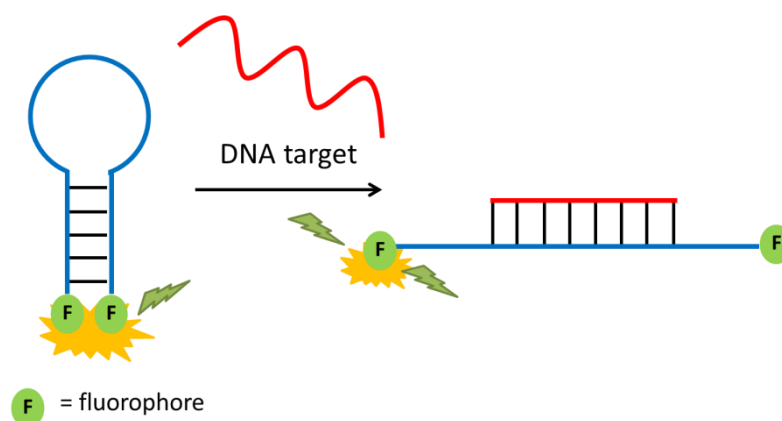
Figure 1.9 A schematic representation of the working principle of the excimer-monomer switching MBs [36]

In another work, a DNA beacon with two pyrene labels at each terminus was reported by Inouye [36]. In the stem-loop conformation, excimer formation from the two pyrenes resulted in the excimer emission. After addition of the target DNA, the two pyrenes were separated. As the result, the monomer emission was increased while the excimer emission was diminished. In a relate work, Saito group [37] designed a novel excimer probe by attaching two pyrene units in the stem of a MB. In the absence of target, the pyrene was quenched by base G nearby. In the open state, the pyrene excimer was observed.
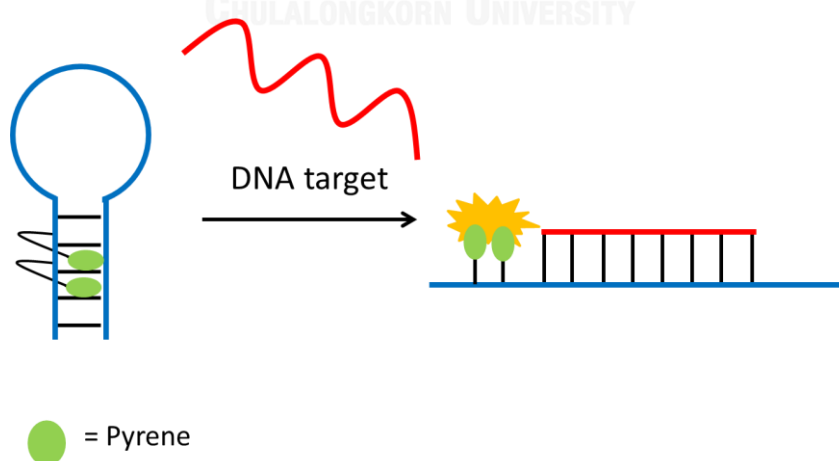
Figure 1.10 A schematic representation of the working principle of the excimer-monomer switching MBs [37]

1.2.1.5 Multilabel MBs

To increase the efficiency of MB probes further, multilabel MBs have been developed. These multilabeld MB carry more than two dyes such as a FRET pair (donor and acceptor dyes) and a quencher (Q) (**Figure 1.11a**) [40, 41]. The MBs are non-fluorescent in the absence target DNA due to the quenched fluorescence donor in their close conformation. Upon hybridization to their target DNA, the energy transfer from donor to acceptor fluorophores results in distinctive emission colors

(a)

(b)
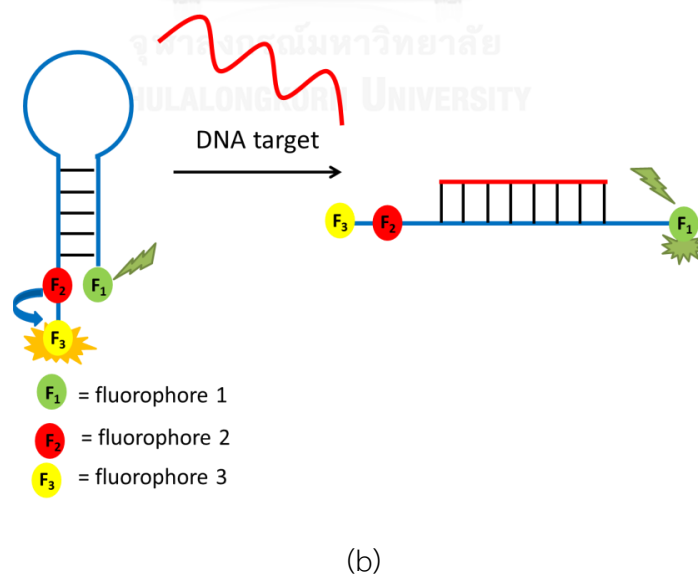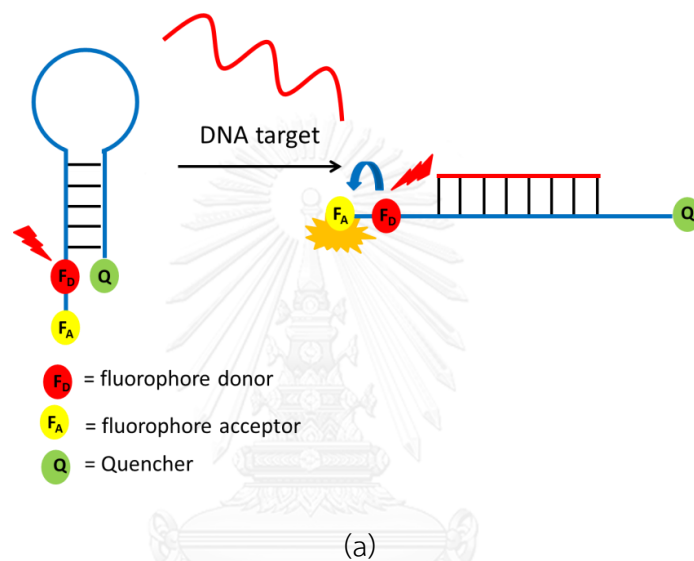
Figure 1.11 Schematic representations of the working principle of the multilabel MBs with (a) a FRET pair and a quencher and (b) two FRET pairs, three dyes [40, 42]

In 2001, Tong et.al. developed a three–dye MB [42]. In this approach, a fluorophore donor (F1) and a FRET pair (F2 and F3) are linked to different ends of MBs (**Figure 1.11b**). In the absence of the DNA target, energy transfer from the fluorescence donor to the intermediate (F2), and then subsequently to the fluorescence acceptor (F3), which results in mainly the F3 emission. In the presence of target DNA, the fluorescence donor and the FRET pair were separated. This results in the most intense emission from the fluorescence donor. The main advantage of the three MBs is that the MB is detectable in both its closed and open conformations, which allows processes such as cellular delivery to be monitored.

In 2008, Tan et al. designed a new MB containing two pyrene units at the 5' and 3'-terminus and a DABCYL quencher. In the stem-loop conformation, no fluorescence signal was observed because of quenching of the pyrene by the DABCYL. After hybridization with the target DNA, the stem was opened and the two pyrene units were separated from the quencher, resulting in an increased excimer fluorescence [41].

1.3 PNA-based MB and hybridization probes

PNA is very promising as a probe for DNA diagnosis because of its better hybridization affinity and selectivity than DNA. In addition, PNA is much more chemically and biologically stable than DNA. The development of PNA and other XNA-based fluorescence DNA and RNA probes had therefore attracted considerable interests over the past several years [43]. PNA probes labeled with an environment sensitive dye such as pyrene or thiazole orange [44-46], a fluorophore-quencher pair or two or more different fluorophores have been developed as MB [46, 47]. Most importantly, the stem-loop structure is not required for PNA-based beacons because PNA usually fold into a compact structure in the aqueous environment [46, 47]. This folding forces the dyes to interact with the nucleobases (single dye labeling) or to interact with each other (multiple dye labeling). Hybridization with the DNA target unfold the PNA, and separate the dyes, resulting in fluorescence change.

1.3.1 Singly-labeled PNA probes

In an early example, Svanvik et al. developed a so-called light-up PNA probes for detection of nucleic acids by attaching thiazole orange (TO) at the *N*-termini of aegPNA (**Figure 1.12**) [44]. The advantage of using PNA over DNA is that there is generally low background fluorescence because the TO dye does not interact appreciably with single stranded PNA.[48]In single-stranded state, TO-labeled PNA probes showed low fluorescence intensities due to free rotation of the bond connecting the two rings of the TO dyes. When hybridized with their complementary DNA targets, the fluorescence emissions were markedly increased as a result of interaction between thiazole orange and the hanging part of the DNA strand, which in turns restricted the free rotation [45]. A similar concept was adopted by Seitz, who incorporated TO as a base surrogate into PNA [39, 45, 49]. The so-called Forced Intercalation (FIT) probe exhibits a large fluorescence increase in the presence of DNA. Intercalation of the TO dye within the PNA-DNA helix results in efficient restriction of rotation, which enforces a coplanar arrangement even in the excited state. In presence of single base mismatch DNA, the fluorescent signal of TO dye was significantly lower because of the TO dye could undergo torsional motions that led to rapid depletion of the excited state as illustrated in **Figure 1.12.**

a)

(b)
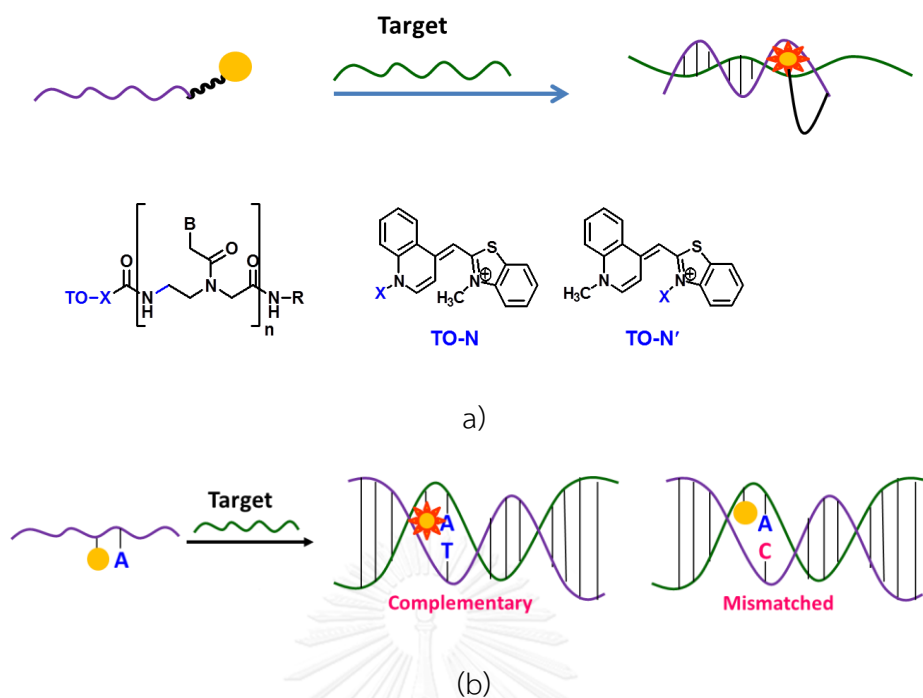
Figure 1.12 Schematic representations of the working principle of (a) light-up probes and (b) FIT-probes

In 2005, Appella et al. reported a prototype of quencher-free PNA probes for DNA sequence detection with single mismatch specificity. The fluorene fluorophore was attached to the side-chain of a lysine inserted at the γ-position of the aegPNA backbone *via* an amide bond (**Figure 1.13**) [46]. The fluorene-labeled PNA probes showed an increase in fluorescence emission upon binding to complementary DNA targets, which was explained by the detachment of the fluorene chromopore from the nucleobases, which act as the quencher in the single stranded probe.
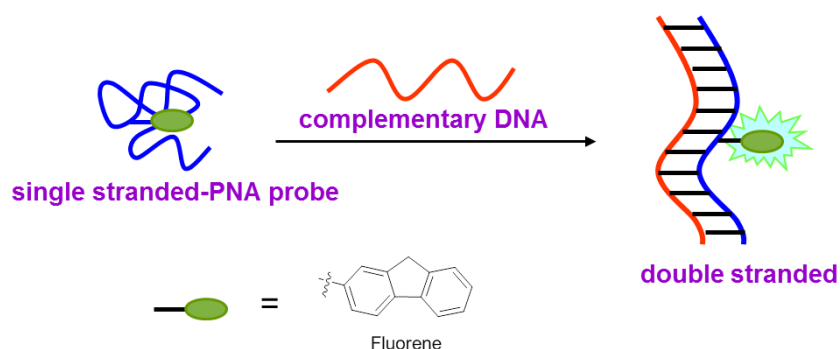
Figure 1.13 Schematic representations of the working principle of fluorene-labeled quencher-free aegPNA probes

1.3.2 Doubly-labeled PNA probes

In the early 2000, Seitz and Frank-Kamenetski independently reported a stemless PNA beacon consisting of a fluorophore and a quencher attached to each end of the PNA strand [47, 50, 51]. Due to the hydrophobicity of PNA, the fluorophore is in close contact with the quencher in the single stranded state in the aqueous environment without requiring the conventional stem-loop structure as in DNA. Kuhn and co-workers reported the use of PNA opener in combination with stemless PNA molecular beacons for direct detection of DNA targets sequence in double-stranded DNA [50]. Moreover, the use of stemless PNA beacons improved the specificity of the detection against single mismatched targets (**Figure 1.14**).
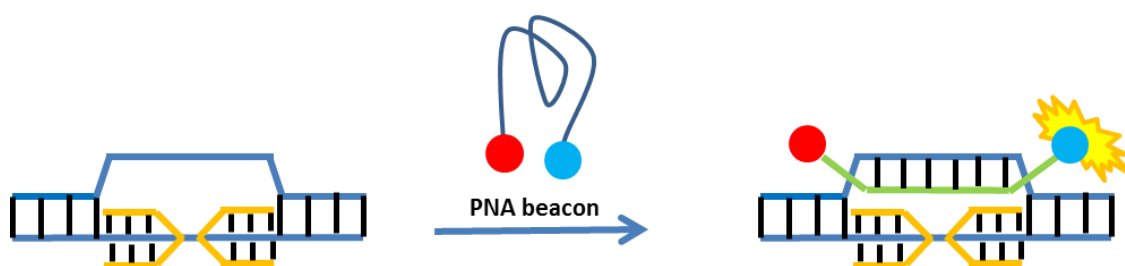
Figure 1.14 Schematic representations of a hybridization of PNA beacons bearing a fluorophore-quencher pair to double-stranded DNA target in the presence of PNA openers.

More recently, Seitz [52] developed dual fluorophore version of FIT PNA probe. Thiazole orange (TO) was employed as the fluorescene donor and NIR667 was used as the florophore acceptor as well as the quencher. The single stranded form, the fluorescene of both fluorophores were not observed because quenching by the NIR667. In the duplex form, the NIR667 become fluorescence because the TO transferred the energy to the NIR667. The advantage over the singly labeled FIT probe is an extended applicability to various sequence context. Other related dual labeled FIT PNA probes with very high fluorescence change were very recently reported by the same group [53]. Their applications in cell imaging had also been demonstrated [54, 55].
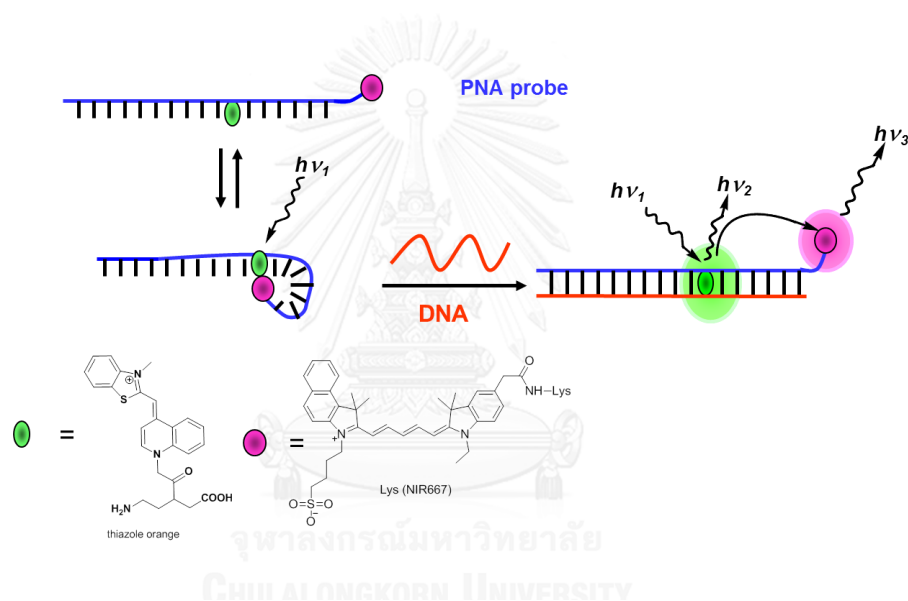
Figure 1.15 Schematic representations of thaizole orange and NIR667 modified forced intercalation (FIT) PNA probes

1.4 Fluorescence probes deriving from pyrrolidinyl PNA

The high binding affinity to complementary DNA and the powerful discrimination for single mismatched DNA, together with the high directional specificity make the new acpcPNA system a potential candidate for the development of a highly effective probe for DNA sequence determination. Vilaivan group has demonstrated applications of acpcPNA as a probe for DNA sequence detection with various techniques. The high mismatch discrimination ability of the acpcPNA combination with

ion-exchange technique led to successful applications in mass spectrometric detection of single nucleotide polymorphisms (SNP) [56]. AcpcPNA is uncharged, so it cannot be absorbed by a solid ion-exchange support (Q-sepharose) in single stranded state. Complementary DNA formed a negatively charged acpcPNA-DNA duplex, which can be subsequently trapped on the Q-sepharose and can be analyzed for the presence of PNA directly by MALDI-TOF mass spectrometry. A similar analysis, with positively charged magnetic nanoparticles was also developed, which facilitate the sample preparation [57, 58].

Ananthanawat et al. used a surface plasmon resonance (SPR) technique to demonstrate the performance of acpcPNA in comparison with DNA, and aegPNA in terms of base-pairing specificity and ability to discriminate single base mutation, direction of binding (parallel or antiparallel). The results confirmed that acpcPNA possesses better specificity than both DNA and aegPNA [59].

Some fluorescence labeled acpcPNA probes that can change the fluorescence signal in response to the presence of correct DNA target were reported in the past few years. The first example was the apcpPNA bearing a pyrene-modified nulceobase developed by Boonlua et al [60]. The modified base (U^{py}) was incorporated into the acpcPNA in place of thymine. In the single stranded form, the fluorescence emission was low. Addition of complementary DNA increased the fluorescence 1.0-14.0 folds, depending on the sequence).

Development of PNA probe with modified base requires tedious synthesis of the monomer. Optimization of the performance of the probe by changing the dye is also difficult because new the monomer and the new PNA must be re-synthesized. The post-synthetic modification approach whereby the label is attached at a pre-defined position in the PNA molecule is highly preferable. Reenabthue et al. [61]. developed a new (3*R*,4*S*)-3-aminopyrrolidine-4-carboxylic acid (APC) spacer – an aza analogue of the ACPC spacer (**Figure 1.17**) that can be inserted anywhere in the acpcPNA molecule without affecting the overall conformation, stability and specificity of the modified PNA-DNA hybrids. The APC-modified acpcPNA contains a secondary amine which can be further labeled with fluorophores bearing a carboxyl group *via* an

amide bond. Pyrene-modified acpcPNA showed a low fluorescence in the single form as a result of quenching by nucleobases (especially T). The fluorescence was increased markedly after hybridization with the complementary DNA, but only when the pyrene label was placed at the internal position of the PNA, regardless of the nature of the neighboring bases [62]. Molecular dynamics simulations suggested that the pyrene is located in the groove in the complementary duplexes and intercalated within the base stacks in the single mismatched duplexes [62].

a) apc-modified PNA   b) fluorophore labeled acpcPNA
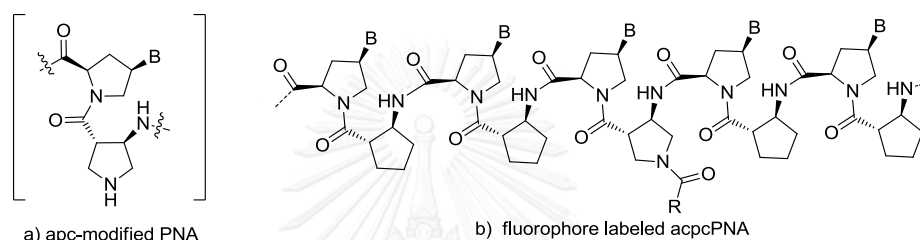
Figure 1.16 Structures of (a) apc-modified acpcPNA, (b) fluorophore-labeled apc/acpcPNA *via* an amide bond

More recently, Ditmanklo et al. [63] reported a new and general method for attachment of various fluorophores onto the backbone of APC-modified acpcPNA *via* a reductive alkylation and sequential reductive alkylation-Click reaction strategies. The thiazole orange was attached onto acpcPNA used to PNA probes. The method was empolyed to synthesize a thiazole orange-labeled acpcPNA probe that show large fluorescence enhancement upon hybridization with DNA. Unfortunately, some non-specific binding to unrelated DNA sequences were observed. The specificity was, however, greatly improved by digestion of the non-complementary DNA targets with S1 nucleases.
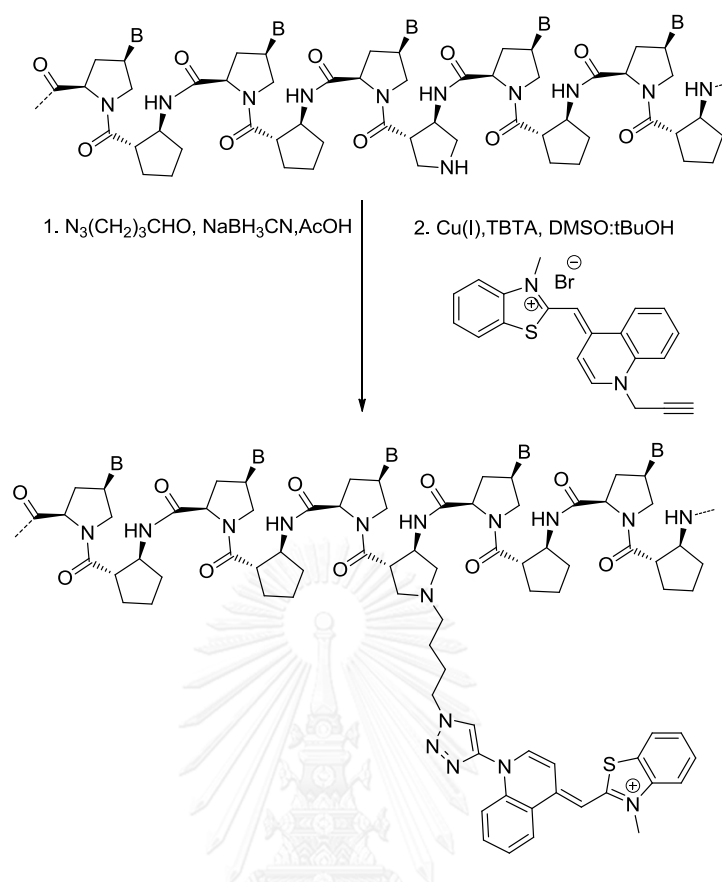
Figure 1.17 Synthesis of thizole orange-labeled acpcPNA probe via sequential reductive alkylation-click strategy

All fluorescence acpcPNA probes described so far carried only one dye. Such singly labeled probes are not ideal because they rely on fluorescence intensity change at just one wavelength. To improve the reliability of the detection, Maneeluan et al. [64] developed a dual pyrene-labeled acpcPNA probe that can switch between excimer (single stranded form) to monomer (double stranded form). The excimer-monomer switching acpcPNA probe was able to efficiently distinguish between complementary and single mismatched DNA targets.
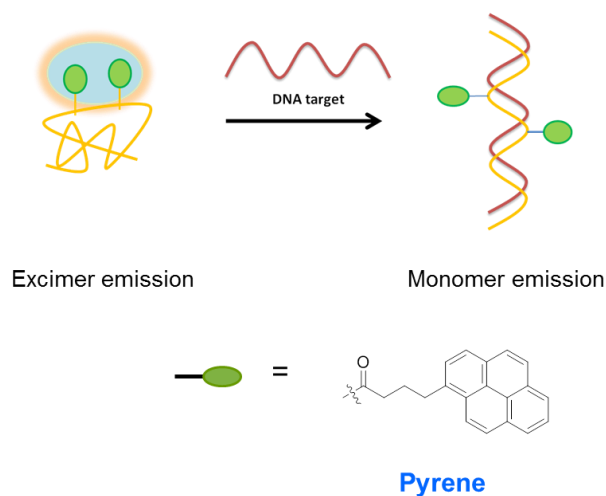
Figure 1.18 Eximer-monomer switching acpcPNA probes

1.5 Objectives of this research

The main objective of this research is to develop new fluorescence acpcPNA probes that can change the fluorescence properties in response to the presence of correct DNA target. The research is divided into three parts. The first part involves the development of new strategies for double labeling of acpcPNA backbones in an orthogonal fashion, and evaluation of the performance of such internally dual-labeled acpcPNA as a DNA probe. In the second part, a novel terminally dual-labeled acpcPNA probe is developed. The last part involves development of acpcPNA modified with a solvatochromic dye that can change not only fluorescence intensity, but also emission wavelength in response to the changing environment between the single stranded and hybridized states of the PNA.

CHAPTER II

EXPERIMENTAL SECTION

2.1 Materials

All chemical reagents and solvents were purchased form standard suppliers and were used as received. Tetrahydrofuran were dried with sodium metal and benzophenone under reflux prior to distillation. Nitrogen was obtained from Labgas Co.,Ltd with 99.995% purity. HPLC grade methanol and acetonitrile used for HPLC experiments were obtained from BDH and were filtered through a Nylon membrane filter (Φ 13 mm, 0.45 μm) before use. Anhydrous N,N-dimethylformamide (< 0.01% H_2O) for solid phase peptide synthesis was obtained from RCI Labscan (Thailand) and was dried with activated 4Å molecular sieves. The solid support for peptide synthesis (TentaGel S RAM Fmoc resin, 0.24 mmol/g) was obtained from Fluka. The protected amino acids, Fmoc-L-Lys(Boc)-OPfp was obtained from Calbiochem Novabiochem Co., Ltd. (USA). Fmoc-L-Lys(Tfa)-OH, piperidine, 1,8-diazabicyclo[5.4.0]undec-7-ene (DBU), trifluoroacetic acid (TFA), diisopropylethyl-amine (DIEA) were purchased from Fluka. 1-Hydroxy-7-azabenzotriazole (HOAt) and O-(7-azabenzotriazol-1-yl)-N,N,N',N'-tetramethyluronium hexafluorophosphate (HATU) were obtained from GLBiochem (Shanghai). Oligonucleotides were purchased from the Pacific Science Co., Ltd. (Thailand) or BioDesign Co., Ltd. (Thailand) and were used as received. All aqueous solutions were made with Milli Q water from Ultrapure water systems with a Millipak® 40 filter unit (0.22 μm, Millipore, USA).

2.2 Methods

Solvent removal was performed on Büchi Rotavapor R-124 with a water aspirator model B-490 or a Refco Vacuubrand pump or a diaphragm pump. ^{1}H and ^{13}C NMR spectra were recorded in deuterated solvents on a Bruker Avance 400 or Varian Mercury 400+ operating at 400 (^{1}H) and 100 MHz (^{13}C). IR spectra were recorded on Nicolet 6700 FT-IR spectrometer. HPLC experiments were carried out on Water Delta

600[TM] system and Water 996[TM] photodiode array detector. MALDI-TOF mass spectra were recorded on a Microflex MALDI-TOF mass spectrometer (Bruker Daltonik, Germany). Melting temperature (T_m) and UV-vis experiments were performed on a CARY 100 Bio UV-visible spectrophotometer (Varian, Australia). Fluorescence spectra were recorded on a Varian Cary Eclipse Fluorescence spectrometer (Varian, Australia). High resolution mass spectra were recorded in positive ion mode on a Micro-TOF mass spectrometer at Faculty of Science, Mahidol University.

2.3. Synthesis of modified APC spacer for selective labeling of acpcPNA

2.3.1 Synthesis of Fmoc/Teoc-protected APC spacer (2a)
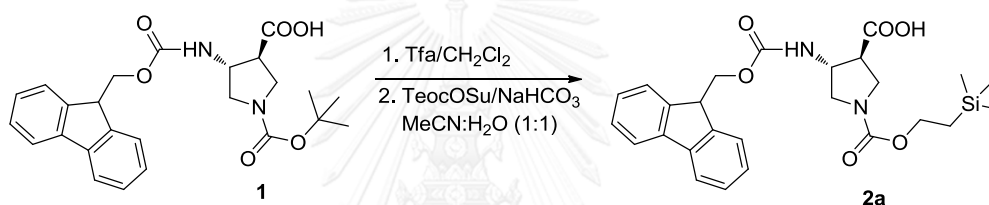
Figure 2.1 Synthesis of Fmoc/Teoc-protected APC spacer (**2a**)

Compound **1** (200 mg, 0.44 mmol) [13] was dissolved in 1:1 TFA:CH$_2$Cl$_2$ (2 mL) and stirred at room temperature for 60 min. The reaction mixture was evaporated to dryness under a stream of nitrogen gas and the residue was dissolved together with NaHCO$_3$ (170 mg, 2.02 mmol) in 1:1 CH$_3$CN:H$_2$O (2 mL). Next N-[2-(trimethylsilyl)ethoxycarbonyl-oxy]succinimide (TeocOSu, 140 mg, 1.20 mmol) was slowly added as a solid with stirring at room temperature. The reaction was stirred overnight at room temperature and the pH of the reaction was controlled at ~8 by periodical addition of solid NaHCO$_3$. The reaction mixture was diluted with 10 mL of water and was extracted with diethyl ether (3×10 mL). The aqueous phase was acidified with 10% HCl to pH 3. The precipitated crude product was filtered off and purified by column chromatograpy (10:90 MeOH:CH$_2$Cl$_2$) to give compound **2a** as a white solid (76.9 mg, 35%yield).

^{1}H NMR (400 MHz, CDCl$_3$): δ 0.00 (s, 9H), 0.96 (t, J=4.4 Hz, 2H), 2.95-3.15 (m, 1H), 3.15-3.40 (m, 1H), 3.45-3.95 (m, 6H), 4.14 (t, J= 4.8 Hz, 2H), 4.41 (s, 2H), 5.08 (s, 1H), 7.26 (t, J=7.6 Hz, 2H), 7.35 (t, J=7.6 Hz, 2H), 7.51 (t, J=7.6 Hz, 2H), 7.71 (t, J=7.6 Hz, 2H)

^{13}C NMR (100 MHz, CDCl$_3$): δ –0.2, 0.0, 0.25, 19.3, 47.9, 48.6, 49.3, 51.9, 54.6, 65.3, 68.4, 121.5, 126.3, 128.5, 129.2, 142.0, 145.0, 156.6, 157.4, 175.7

IR (ATR): $\mathbf{V}_{max}$ = 3307.86 3059.73 2950.9, 2885.6, 1714.6, 1688.5, 1623.22, 1540.5, 1449.0, 1348.9, 1244.5, 1157.4, 1039.9, 726.4 cm^{-1}

HRMS (ESI+) calcd. for C$_{26}$H$_{32}$N$_2$O$_6$SiNa [M+Na]$^+$ = 519. 1927, found = 519.1931.

2.3.2 Synthesis of Fmoc/o-Nosyl-protected APC spacer (2b)
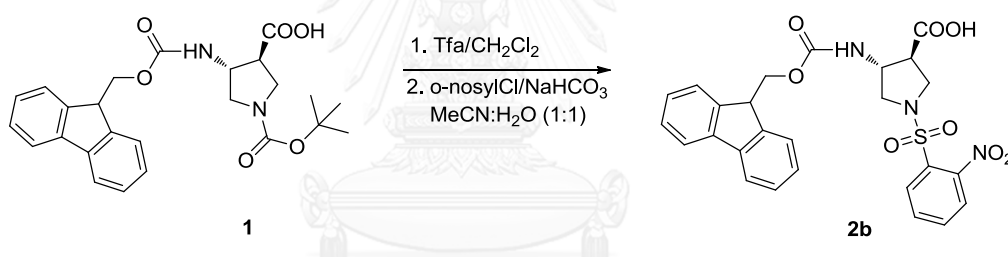
Figure 2.2 Synthetic of Fmoc/o-Nosyl-protected APC spacer (**2b**)

Compound **1** (200 mg, 0.44 mmol) was dissolved in 1:1 TFA:CH$_2$Cl$_2$ (2 mL) and stirred at room temperature for 60 min. The reaction mixture was evaporated to dryness under a stream of nitrogen gas, and the residue was dissolved together with NaHCO$_3$ (175 mg, 2.1 mmol) in 1:1 CH$_3$CN:H$_2$O (2 mL). Next, 2-nitrobenzylsulfonylchloride (o-NsCl, 110 mg, 0.5. mmol) was slowly added as a solid with stirring at room temperature. The reaction was stirred overnight at room temperature and the pH of the reaction was controlled at ~8 by periodical addition of solid NaHCO$_3$. The reaction mixture was diluted with 10 mL of water and was extracted with diethyl ether (3✕10 mL). The aqueous phase was acidified with 10% HCl to pH 3. The precipitated product was filtered off and the crude product was purified by

column chromatograpy (10:90 MeOH : CH$_2$Cl$_2$) to give compound **2b** as a white solid (55 mg, 30%yield).

^{1}H NMR (400 MHz, DMSO-d_6): δ 2.90-3.10 (m, 1H), 3.12-3.50 (m, 2H), 3.50-3.79 (m, 2H), 4.15-4.45 (m, 4H), 7.26 (m, 2H), 7.38 (m, 2H), 7.60-7.82 (m, 3H), 7.82-7.95 (m, 3H), 7.95-8.10 (m, 2H)

^{13}C NMR (100 MHz, DMSO-d_6): δ 46.6, 47.5, 48.6, 48.9 (rotamer), 52.0, 53.0, 53.4 (rotamer), 65.5, 120.1, 124.1, 125.0, 127.0, 127.6, 129.2, 130.2, 132.1, 134.6, 134.7, 140.7, 143.7, 147.9, 155.5, 172.0

IR (ATR): ν_{max} = 3316.5, 3059.7, 2955.2, 2889.9, 1688.5, 1631.9, 1536.1, 1453.4, 1348.9, 1166.1, 1144.3, 1039.9, 730.8

HRMS (ESI+) calcd for C$_{26}$H$_{23}$N$_3$O$_8$SNa [M+Na]$^+$ = 560.1104, found = 560.1103.

2.3.3 Synthesis of 4-propargylamino-7-nitrobenzofurazan [65]
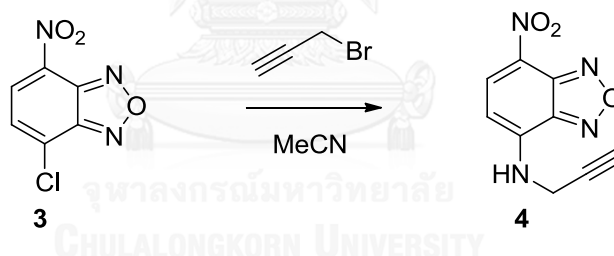
Figure 2.3 Synthesis of 4-pronpargylamine-7-nitrobenzofurazan (**4**)

A solution of compound **3** (500 mg, 2.5 mmol) in CH$_3$CN (5 mL) was added propagylamine (276 mg, 3 mmol), and the reaction mixture was stirred for 2 h at room temperatue. The solvent was removed and the residue was purified by column chromatrography, eluting with hexanes/EtOAc (2:1) to afford compound **4** as a brown solid (170 mg, 30% yield)

^{1}H NMR (400 MHz, CDCl$_3$) δ 2.31 (t, J= 2.4 Hz, 1H), 3.80 (s, 2H), 4.11 (d, J=2.4 Hz, 2H), 6.18 (d, J= 8.7 Hz, 1H), 8.34 (d, J=8.7 Hz, 1H)

2.3.4 Synthesis of 7-diethylamino-3-carboxy-coumarin[66]
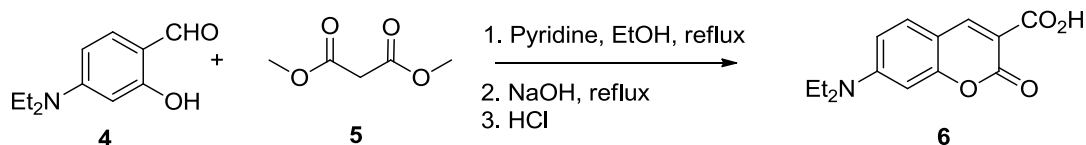
Figure 2.4 Synthesis of 7-diethylamino-3-carboxy-coumarin (**6**)

A solution of 4-diethylaminosalicyaldehyde (**5**) (386 mg, 2 mmol) in ethanol (20 mL) were added diethyl malonate (**6**) (640 mg, 4 mmol) and piperidine (1 mL). After stirring under reflux for 6 h, 10% aqueous NaOH (10 mL) was added and the mixture was continued to reflux for another 15 min. The reaction was cooled in an ice bath and acidified to pH 2 using conc. HCl under ice bath. The orange solid formed was filtered, washed with water, then recrystallized from ethanl to give compound 7 as a yellow crystalline solid (520 mg, 89% yield)

^{1}H NMR (400 MHz, CDCl$_3$): δ 1.28 (t, J=6.8 Hz, 6H), 3.51 (q, J= 6.8Hz, 4H), 6.54 (s, 1H), 6.73 (d, J=8.4 Hz, 1H), 7.46 (d, J=9.2 Hz, 1H), 8.65 (s, 1H), 12.36 (s, 1H)

2.3.5 Synthesis of phenoxazine red

Figure 2.5 Synthesis of propargyl phenoxazine red (**10**)

A mixture of compound **8** (80 mg, 0.5 mmol) [67] and compound **9** (85 mg, 0.5 mmol) in ethanol (5 mL) was stirred at 80 °C for 48 h. The solvent was removed by rotary evaporation and the residue was purified by column chromatrography, eluting with hexanes:EtOAc (1:1) to give propargyl phenoxazine red (**10**) as a dark purple solid (44.0 mg, 30 %yield)

^{1}H NMR (400 MHz, DMSO-d$_6$): δ 3.10 (s, 6H), 3.71 (s, 1H), 4.88 (s, 2H), 6.04 (s, 1H), 6.61 (s, 1H), 6.82 (d, J=8.0 Hz, 1H), 7.60 (d, J= 8.0 Hz, 1H)

2.4 PNA oligomer synthesis

2.4.1 General procedure for synthesis of acpcPNA

The four Pfp-activated, Fmoc-protected pyrrolidinyl PNA monomer (Fmoc-A^{Bz}-OPfp ,Fmoc-C^{Bz}-OPfp , Fmoc-G^{Ibu}-OH, Fmoc-T-OPfp), ACPC spacer and Tfa-APC spacer were synthesized by Dr. Chalotorn Boonlua, Dr. Woraluk Manaswat, Ms. Boonsong Ditmangklo, Ms. Duangrat Nim-anussornkul, Mr. Nattaporn Maneeluan and Mr. Chayan Charoenpakdee according to the literature protocol [13, 14].
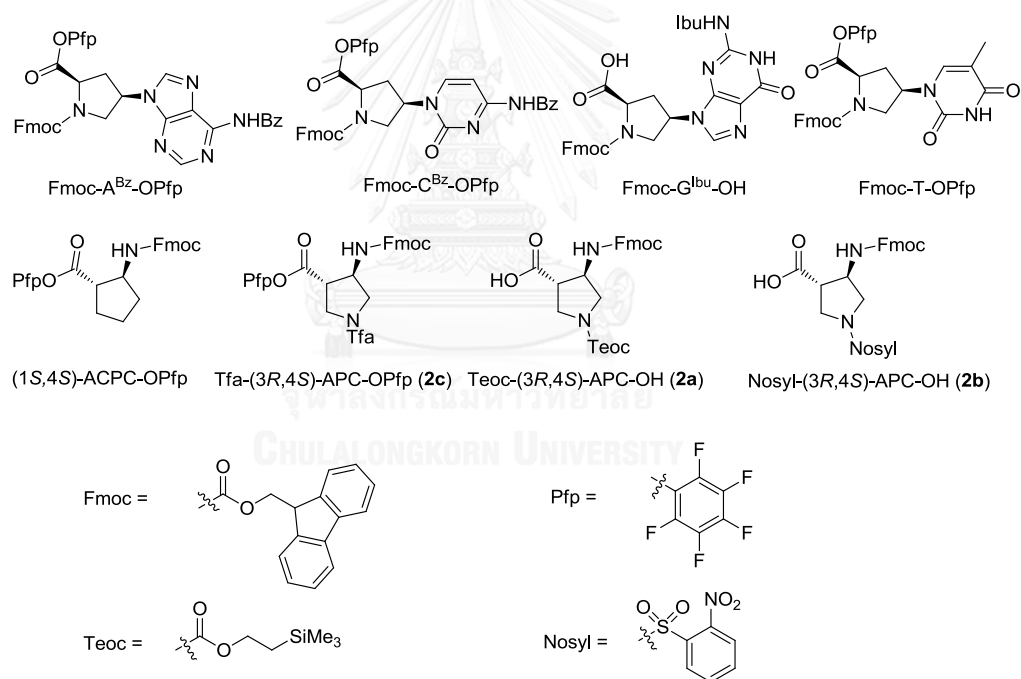
Figure 2.6 Structures of pyrrolidinyl PNA monomers and spacers used for the solid phase synthesis of modified acpcPNA.

All acpcPNA and APC-modified acpcPNA were synthesized by Fmoc-solid phase peptide synthesis at 1.5 µmol scale using Tentagel S-RAM resin (0.24 meq/g loading) as the solid support according to the literature procedure [68]. One lysine residue was

included at the C-termini [via Fmoc-Lys(Boc)-OPfp or Fmoc-Lys(Mtt)-OH] and another lysine was also included at the N-termini [via Fmoc-Lys(Boc)-OPfp or Fmoc-Lys(Tfa)-OH for internally modified PNA or Fmoc-Lys(Tfa)-OH for terminally modified PNA] to increase the solubility of the labeled-acpcPNA in water. The PNA synthesis cycle consists of three steps: Fmoc-deprotection (2% DBU + 20% piepridine in DMF, 100 µL, 5 min) coupling and capping (acetic anhydride 5 µL and 7% DIEA in DMF 30 µL). In the coupling step, the Pfp-activated monomers [Fmoc-Lys(Boc)-OPfp, Fmoc-ABz-OPfp, Fmoc-CBz-OPfp, Fmoc-T-OPfp, Fmoc-ACPC-OPfp and 2c] (6.0 µmol) were dissolved in 7% DIEA in DMF (15 µL) and 0.4 M HOAt solution (15 µL) was added and then the solution was coupled to the Fmoc-deprotected resin. For free acid, the monomers [Fmoc-Lys(Tfa)-OH, Fmoc-Lys(Mtt)-OH, Fmoc-GIbu-OH, **2a** and **2b**] (6.0 µmol) and HATU (2.2 mg, 6 µmol) was dissolved in 7%DIEA in DMF (30 µL) and shaken for a few minutes prior to the coupling. The PNA monomers and spacers were added one by one in an alternating manner until the desired sequence was obtained. After coupling of the last monomer, the resin-bound PNA was end-capped by acetylation, side-chain deprotected (1:1 aqueous NH$_3$:dioxane, 60 °C, overnight) and directly cleaved from the resin (TFA, 3 × 300 µL × 30 min) or further modified with the labels (see **2.4.2**).

2.4.2 Synthesis of labeled acpcPNA

2.4.2.1 General procedures for acpcPNA labeling

Prior to the labeling, a portion of the Tfa-APC-modified acpcPNA (0.5 µmol) that still attached on the solid support was placed in a small glass column for peptide synthesis and was treated with 20% piperidine and 2% DBU in DMF (100 µL, 5 min) to remove the N-terminal Fmoc group. The free amino group was acetylated by 15% Ac$_2$O and 7% DIEA in DMF (30 µL, 5 min). Next the Tfa and nucleobase protecting groups (Ibu for G, Bz for A and C) were removed by heating with 1:1 aqueous ammonia:dioxane in screw cap test tube at 60 °C for 16 h.

a) Coupling with fluorescence label via direct acylation

The fluorescence label carrying a carboxylic group was coupled to the N- or C-termini of the PNA or to the pyrrolidine nitrogen atom of the APC space after removal of the APC protecting group. The deprotected PNA resin (0.5 µmol) was swollen in DMF. The fluorescence label with a free carboxylic group (6 µmol, 12 equiv.) was activated with HATU (2.2 mg, 6 µmol) and 30 µL of 7% DIEA in DMF prior to the coupling reaction, which was allowed to proceeded for 1 hour at room temperature or until no unlabeled PNA was observed according to MALDI-TOF MS analysis after cleavage of a small portion of the PNA sample from the solid support with TFA. 5(6)-Carboxyfluorescein label was coupled via the commercially available N-hydroxysuccinimide (NHS) ester. The coupling was repeated if the reaction was not complete.

b) Coupling with fluorescence label via reductive amination (with C2 linker) and acylation

In some cases, an aminoethyl linker was installed at the pyrrolidine nitrogen atom of the APC spacer before attaching the label to compare the effect of the linker. The side-chain deprotected APC-modified acpcPNA was treated with N-Fmoc aminoacetaldehyde [69] (30 µmol, 60 equiv.), AcOH (2 µL, 30 µmol, 60 equiv.) and NaBH$_3$CN (2.0 mg, 30 µmol, 60 equiv.) in methanol (200 µL) for 16 h at room temperature. The Fmoc group was next removed by treatment with 20% piperidine and 2% DBU in DMF and further coupling with the fluorescence label was carried out as in a)

c) Coupling with fluorescence label via reductive alkylation and Click reaction

Attachment of terminal alkyne-containing fluorescence dyes was carried out on the acpcPNA that was previously modified with an azidobuyl linker according to the reductive alkylation-Click reaction protocol developed by Ditmangklo et al. [63]. The deprotected APC-modified PNA (0.5 µmol) was treated with 4-azidobutanal (15 µmol, 30 equiv.) in the presence of NaBH$_3$CN (30 µmol, 60 equiv.) and HOAc (30 µmol, 60 equiv.) in MeOH (200 µL) at room temperature overnight. The azidobutyl-modified

acpcPNA obtained was next treated, while still on the solid support, with the alkyne-modified fluorescence label (7.5 μmol, 15 equiv.) in the presence of tris[(benzyl-1*H*-1,2,3-triazol-4-yl)methyl]amine (TBTA, 30 μmol, 60 equiv.), tetrakis(acetonitrile) copper(I) hexafluorophosphate (15 μmol, 30 equiv.) and (+)-sodium-L-ascorbate (60 μmol, 120 equiv.) in 3:1 (v/v) DMSO:*t*BuOH (300 μL) at room temperature overnight. The progress of the reaction was monitored by MALDI-TOF mass spectrometry as described in **2.4.2.1**(a).

2.4.2.2 Synthesis of dual-labeled pyrrolidinyl peptide nucleic acid (internal modification)

a) Synthesis of orthogonally protected PNA

The orthogonally protected APC-modified acpcPNA was synthesized using the standard protocol for acpcPNA synthesis, except for the replacement of two ACPC spacers with the Tfa-protected APC spacer (**2c**) and the Teoc-protected APC spacer (**2a**) or Nosyl-protected APC spacer. In practice, the Teoc group could not be selectively removed therefore the combination of Tfa-APC and *o*-Nosyl-APC was the only possible option.

b) Selective deprotection and labeling of orthogonally protected PNA

A portion of the solid-supported APC-modified acpcPNA (0.5 μmol) was subjected to Fmoc group removal and end capping by acetylation as described in the general procedure above. The first labels were attached onto the acpcPNA backbone (see the general procedure for label attachment above) after removal of the Tfa protection on the APC spacer (1:1 aqueous ammonia:dioxane, 60 °C, 16 h, which also removes the nucleobase protecting groups). After attachment of the first label, the *o*-Ns remaining APC spacer was removed and the *o*-nosyl group (10% 2-mercaptoethanol + 5% DBU in DMF, room temperature, 1 h) before attachment of the second label. Which dyes are chosen as the first and second labels depend on their stability towards the conditions required for deprotecting the *o*-Ns group. The details of the dye attachment are summarized in Table 2.1.

Table 2.1. Details of dye attachment in internally labeled dual-labeled acpcPNA probes.

PNA	Sequence and modification position	x (first modification)			y (second modification)		
		APC protection	linker	label	APC protection	linker	label
T9(Cou1/Flu)	TTTyTTTxTTT	Tfa	none	Flu	o-Ns	none	Cou1
T9(C2Cou1/C2Flu)	TTTyTTTxTTT	Tfa	-NH(CH$_2$)$_2$-	Flu	o-Ns	-NH(CH$_2$)$_2$-	Cou1
T9(DNB/Pyr)	TTyTTTTTxTT	Tfa	none	Pyrene	o-Ns	o-Ns	DNB
T9(Cou2/Flu)	TTyTTTTTxTT	Tfa	none	Flu	o-Ns	none	Cou2
T9(Cou2/C2Flu)	TTyTTTTTxTT	Tfa	-NH(CH$_2$)$_2$-	Flu	o-Ns	none	Cou2
T9(C2Cou2/C2Flu)	TTyTTTTTxTT	Tfa	none	Flu	o-Ns	-NH(CH$_2$)$_2$-	Cou2
T9(C2Cou2/Flu)	TTyTTTTTxTT	Tfa	-NH(CH$_2$)$_2$-	Flu	o-Ns	-NH(CH$_2$)$_2$-	Cou2
T9(NBD/PheR)	TTyTTTTTxTT	Tfa	-Tz(CH$_2$)$_4$-	PheR	o-Ns	-Tz(CH$_2$)$_4$-	NBD
T9(NBD/Nr)	TTyTTTTTxTT	Tfa	-Tz(CH$_2$)$_4$-	Nile red	o-Ns	-Tz(CH$_2$)$_4$-	NBD
T9(Flu/TMR)1	TTyTTTTTxTT	Tfa	none	TMR	o-Ns	none	Flu
T9(Flu/TMR)2	TTTTyTxTTTT	Tfa	none	TMR	o-Ns	none	Flu
T9(Flu/TMR)3	yTTTTTTTTTx	Tfa	none	TMR	o-Ns	none	Flu
T9(Dns/Nr)	TTyTTTTTxTT	Tfa	none	Nile red	o-Ns	none	Dns
T9(Flu/AQ)	TTyTTTTTxTT	Tfa	none	AQ	o-Ns	none	Flu
T9(Flu/Dab)	TTyTTTTTxTT	Tfa	none	Dab	o-Ns	none	Flu
M12(Flu/TMR)	AGTTyATCCCxTGC	Tfa	-NH(CH$_2$)$_2$-	TMR	o-Ns	none	Flu
M12(C2Cou/Flu)	AGTTyATCCCxTGC	Tfa	none	Flu	o-Ns	-NH(CH$_2$)$_2$-	Cou2
M12(Dns/Nr)	AGTTyATCCCxTGC	Tfa	-Tz(CH$_2$)$_4$-	Nile red	o-Ns	none	Dns
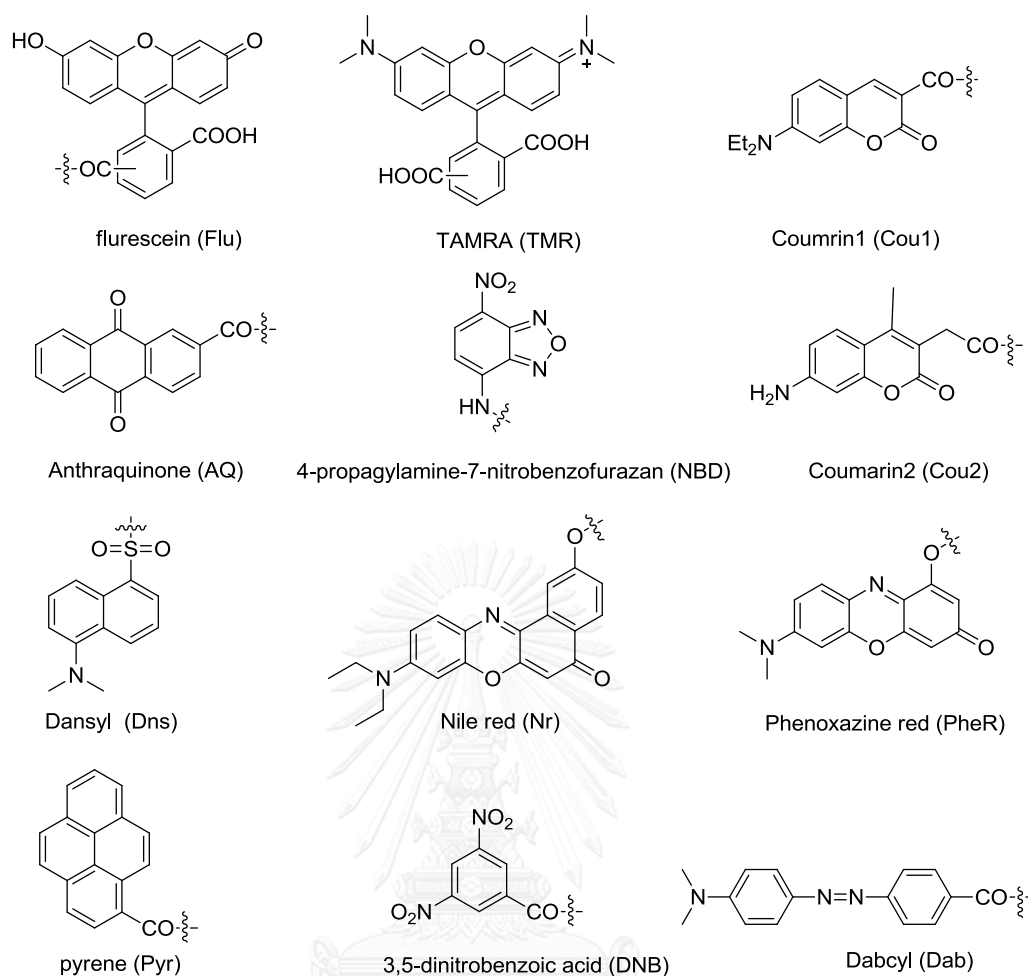
Figure 2.7 Structures of the dyes used for acpcPNA labeling

2.4.2.3 Synthesis of dual-labeled pyrrolidinyl peptide nucleic acid (terminal modification)

A portion of the solid-supported APC-modified acpcPNA (0.5 μmol) after end-capping with Fmoc-Lys(Tfa)-OH was placed in a small glass column for peptide synthesis and treated with 20% piperidine + 2% DBU in DMF (100 μL, 5 min) to remove the N-terminal Fmoc group. The first dye was coupled at the α-nitrogen atom of the lysine via amide bond formation following the general procedure a). Next, the protecting group of the ϵ-nitrogen atom of the lysine (Tfa) and the nucleobase protecting groups were simultaneously removed by heating with 1:1 aqueous ammonia:dioxane at 60 °C overnight. This treatment did not affect the N-Boc or N-Mtt

protecting group at the ε-nitrogen atom of the C-terminal lysine. The second dye was next coupled at the Nε of the N-terminal lysine as in the general procedure a).

2.4.2.4 Synthesis of pyrrolidinyl peptide nucleic acid carrying Nile red label

a) Synthesis propargyl-modified nile red (PNr)
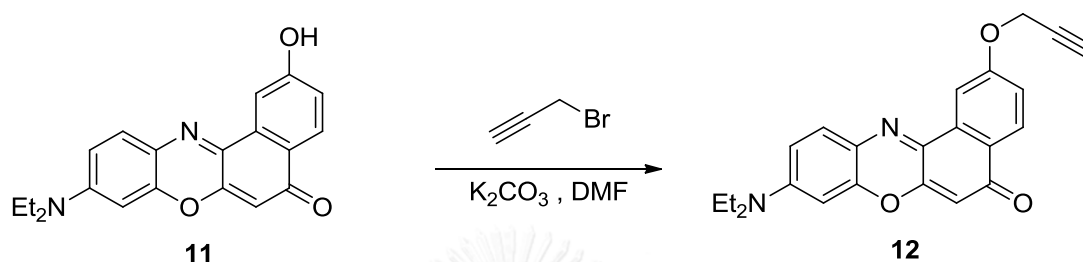
Figure 2.8 Synthesis of propargyl nile red (PNr) (**12**)

Compound (**11**) [70] (140.1 mg, 0.41 mmol) was reacted with propargyl bromide (0.1 mL, 1.2 mmol) in the presence of potassium carbonate (150 mg, 1.1 mmol) in anhydrous DMF at 70 °C. After completion, the solution was dried by nitrogen gas. The mixture was purified by column chromatrography (EtOAc:hexanes; 1:4) to give the product as a dark purple solid (108 mg, 70%).

^{1}H NMR (400 MHz, DMSO-d_6): δ 1.17 (t J = 6.9 Hz, 6H), 3.51 (, q J = 6.9 Hz, 4H), 3.67 (t J = 2.2 Hz, 1H), 5.03 (d J = 2.2 Hz, 2H), 6.20 (s,1H), 6.65 (d J = 2.6 Hz, 1H), 6.83 (dd J = 9.1 and 2.6 Hz, 1H), 7.32 (dd, J = 8.7 and 2.5 Hz, 1H), 7.64 (d J = 9.1 Hz, 1H), 8.04 (d J = 2.5 Hz, 1H), 8.08 (d J = 8.7 Hz, 2H)

^{13}C NMR (100 MHz, DMSO-d_6): δ 181.3, 159.8, 151.8, 150.9, 146.5, 138.1, 133.5, 131.0, 127.2, 125.5, 124.0, 118.2, 110.1, 107.0, 104.1, 96.0, 78.8, 78.7, 55.9, 44.4, 12.4

IR (ATR): ν_{max} =3281.7, 3190.3, 2968.3, 2920.4, 2846.4, 1675.4, 1584.0, 1405.6 cm^{-1}

HRMS(ESI+): calcd for $C_{23}H_{21}N_2O_3$ [M+Na]$^+$: 373.1552; found: 373.1581

UV(MeOH): λ_{max} (ε) = 553 (3.2×10^4).

b) Synthesis of nile red-modified acpcPNA

A portion of the APC-modified acpcPNA (0.5 µmol) on the solid support was placed in a small glass column for peptide synthesis and was treated as described in the general procedure in 2.4.2.1. The deprotected PNA was modified successively with azidobutanal (15 µmol, 30 equiv.) and propargyl nile red (**12**) (7.5 µmol, 15 equiv.) following the general procedure **2.4.2.1** (c).

2.5 Purification and characterization of PNA oligomers

2.5.1 Cleavage of PNA from the solid support

The PNA was cleaved from the solid support resin by TFA (3 × 300 µL × 30 min). The acid was removed under a stream of nitrogen gas and the residue was centrifugally washed with diethyl ether.

2.5.2 MALDI-TOF mass spectrometry

The identity of acpcPNA oligomer was verified by MALDI-TOF mass spectrometry. The samples were prepared by mixing of 2 µL of aqueous solution of the sample with 10 µL of containing saturated solution of α-cyano-4-hydroxy cinnamic acid (CCA) in 1:1 mixture of 0.1% TFA in acetonitrile and 0.1% TFA in MilliQ water and deposited on the MALDL-TOF target. The mass spectra were recorded in linear positive ion mode with accelerating voltage of 25 kV.

2.5.3 Reversed phase HPLC purificaion

An ACE M8–AR HPLC column (4.6 × 150 mm, 5 µm particle size) was used for preparative and analytical purposes. The crude acpcPNA was prepared for reversed phase HPLC purification by dissolving in 120 µL of MilliQ water. The HPLC purification and analysis were performed, monitoring by UV absorbance at 310 nm and eluting with a gradient system of 0.1% TFA in methanol/water at a flow rate of 0.5 mL/min. The HPLC gradient consists of two solvent systems which are solvent A (0.1% TFA in MilliQ water) and solvent B (0.1% TFA in methanol). The elution began with A:B (90:10) for 5 min followed by a linear gradient to A:B (10:90) over period of 60 min, with a

holding time for 10 min before reverting back to A:B (90:10). Fractions from HPLC were collected manually and were assisted by real-time HPLC chromatogram monitoring.

2.5.4 Reversed phase HPLC analysis

A Vertical UPS C18 HPLC column (4.6 ✕ 50 mm, 3 µm particle size) was used for analytical purposes. The analysis used a gradient system of 0.1% TFA in methanol/water at a flow rate 0.5 mL/min. The gradient consists of two solvent systems: A (0.1% TFA in MilliQ water) and B (0.1% TFA in methanol). The elution started with 90:10 A:B followed by a linear gradient to 10:90 A:B over period of 30 min, and reverting back to 90:10 A:B. Peak monitoring and data processing were performed using the Empower software associated with the HPLC system.

2.5.5 Determination of PNA concentration

The concentrations of modified-PNA were determined by UV-absorption measurements at 260 nm. A portion of the PNA solution was diluted to 1000 µL with 10 mM sodium phosphate buffer pH 7.0 and the UV absorbance at 260 nm was measured. This value was used for calculation of the PNA concentrations. Extinction coefficients of PNA was calculated from the sum of individual extinction coefficients (ε) of the corresponding nucleobases and fluorophores [71]. The individual extinction coefficients at 260 nm used in the calculation, ε(Flu) = 20.9 µM^{-1}.cm^{-1}[72] and ε(TMR) = 32.2 µM^{-1}.cm^{-1} [72]. The extinction coefficients at 260 nm (ε_{260}) of other dyes were obtained by measuring the UV-vis absorption at varying concentrations. The ε_{260} was obtained from the slope of the calibration plot between concentration (x) and absorbtion (y). The following values were obtained: ε(Cou1) = 13.0 µM^{-1}.cm^{-1}, ε(Cou2) = 10.1 µM^{-1}.cm^{-1}, ε(Nile red) = 18.0 µM^{-1}.cm^{-1}, ε(PheR) = 4.6 µM^{-1}.cm^{-1}, ε(Pyrene) = 13.3 µM^{-1}.cm^{-1}

2.6 Experimental procedures for studying of PNA properties

2.6.1 UV melting experiments

UV-melting temperatue (T_m) were measured at 260 nm. The T_m experiment was carried out at the specified concentrations of PNA and DNA in 10 mM sodium

phosphate buffer (pH 7.0) (1000 μL) in a 10 mm quartz cell with a Teflon stopper and equilibrated at the starting temperature for 10 min. The A_{260} was recorded in heating from 20-90 $^\circ$C (temperature) with a temperature ramp of 1 $^\circ$C /min. The temperature recorded was the block temperature and was corrected by the linear equation (1) obtained from the block temperature and the actual temperature obtained from a built-in temperature probe

Corrected Temperature $=$ $(0.9696 \times T_{block}) - 0.8396$ (1)

The absorbance was normalized by divigng the value each temperauture with the initial absorbance. The melting temperature was determined from the maximum of the first derivative after smoothing using KaliedaGraph 4.0 (Synergy Software). Data analysis was performed on a PC compatible computer using Microsoft Excel XP (Microsoft Crop.).

2.6.2 UV/Vis experiments

All UV/Vis experiments were carried out at the specified concentrations of PNA and DNA in 10 mM sodium phosphate buffer (pH 7.0) (1000 μL) in a 10 mm quartz cell at room temperature (20 $^\circ$C).

2.6.3 Fluorescence experiments

All fluorescence experiments were carried out at the specified concentrations of PNA and DNA in 10 mM sodium phosphate buffer (pH 7.0) (1000 μL) or 10 mM β-cyclodextrin in a 10 mm quartz cell with a Teflon stopper at room temperature (20 $^\circ$C). The excitation and emission slits were set to 5 nm, and the photomultiplier tube (PMT) voltage set to a appropriate value (to give the fluorescence read-out not exceeding 1000 a.u.).

2.6.4 Fluorescence melting experiments

Fluorescence melting experiments were carried out by preparing the sample as in normal fluorescence experiments. The fluorescence emission was recorded from

20 to 90 °C at 5 °C intervals with temperature ramp of 1 °C /min. The temperature recoded was the block temperature and was uncorrected.

2.6.5 Photographing

The samples for photographing were prepared at the specified concentrations of PNA and DNA in 10 mM sodium phosphate buffer (pH 7.0) (1000 µL) in a 10 µL polypropylene tube for PCR. The photograph was taken under black light (365 nm) in the dark room using a digital camera (Canon PowerShot SX 110 IS) in manual mode (ISO 100, F2.8, shutter speed 1 sec.)

CHAPTER III

RESULTS AND DISCUSSION

The work described in this dissertation involves development of fluorescence PNA probe that can change the fluorescence signal in response to the presence of correct DNA target. More specifically, the acpcPNA probes modified with one or more fluorophores were developed, by attachment of the fluorophores to the PNA terminus or backbone. This chapter is divided into three parts. The first part consists of the synthesis and optical properties of doubly-labeled acpcPNA as well as its hybrids with DNA. The second part involves synthesis and fluorescence properties of doubly end-labeled acpcPNA and its hybrids with DNA. The third part involves synthesis and optical properties of acpcPNA modified with Nile red (a solvatochromic dye) and its hybrid with DNA. In all cases, it is expected that these doubly- or singly-labeled PNA would change its fluorescence properties in response to the presence of correct DNA target with high specificity.

3.1 Dual-labeled acpcPNA probes

This part of the dissertation dedicated to the design and performance evaluation of dual-labeled acpcPNA. Two fluorescence labels were covalently incorporated onto the backbone of pyrrolidinyl acpcPNA that was previously modified at pre-defined positions with 3-aminopyrrolidine-4-carboxylic acid (APC) spacer to provide a secondary amine functionality that would allow fluorophore attachement. The APC spacer was incorporated into the acpcPNA following the strategy introduced by Reenabthue *et al.* [61] . The dual-labeled acpcPNAs were expected to form a compact structure in single-stranded state similar to other PNA [44] which forced the two fluorophores to be in close proximity. The two fluorophores should therefore interact by various mechanisms such as quenching or FRET. In the presence of the correct DNA target, the increased the rigidity of the duplex structure as a result of base pairing induced separation of the two fluorophores, resulting in a different level of quenching or FRET.
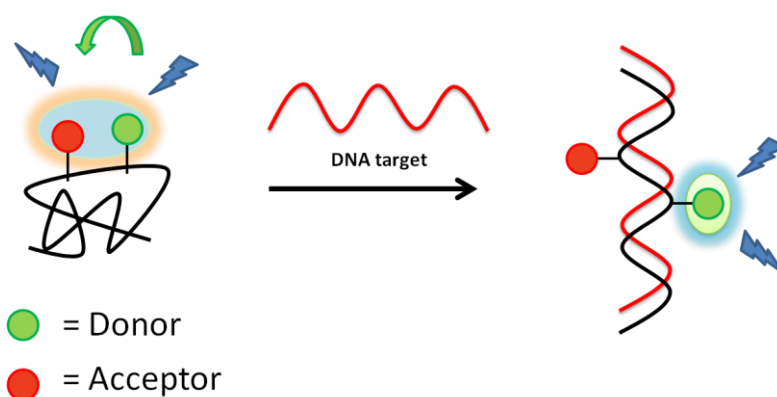
Figure 3.1 A schematic diagram showing the concept of doubly-labeld PNA beacons in this work

3.1.1 Synthesis of N^3-Fmoc-N^1-(Teoc) protected and N^1-(*o*-nosyl) protected APC derivatives

To synthesize the dual-labeled acpcPNA, two orthogonally protected APC spacers must be site-specifically incorporated into the acpcPNA backbone. In the strategy of Reenabthue et al. [61], the base labile trifluoroacetyl (Tfa) group was used as the APC protecting group. If Tfa-protected APC is used as the first APC modification, another APC protecting group that is orthogonal to the Tfa, i.e. stable to base and should be removable under the conditions that did not affect the Tfa group is required. Furthermore, the protecting group should also be compatible with the non-aqueous basic conditions used for removal of the Fmoc group during the PNA synthesis. In addition, since one or more Lys(Boc) or Lys(Mtt) residues are usually included in the PNA to increase the solubility, it is important that the condition for removal of the APC protecting group should not affect these acid-labile lysine protecting groups. Two potential candidates are *o*-nosyl (*o*Ns) (base stable, removable by thiolysis) [73] and Teoc (base stable, removable by fluoride) [74]. The required N^3-Fmoc-N^1-Teoc-protected APC and N^3-Fmoc-N^1-(*o*-Ns)-derivatives **2a** and **2b** were synthesized according to the procedure shown in **Figure 3.2**. The known compound **1**[61] was treated with trifluoroacetic acid (TFA) to remove the Boc group from the N^1-position

(the pyrrolidine nitrogen atom). The deprotected Fmoc-acid was further reacted with TeocCl or *o*-NsCl under basic conditions (aqueous NaHCO₃) to give the expected products **2a** and **2b** in 35% and 30% yield, respectively.
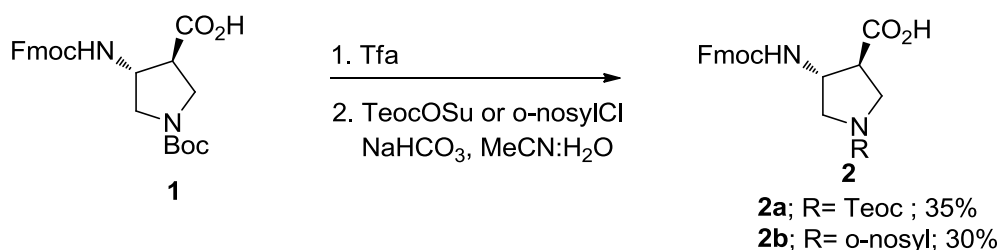
Figure 3.2 Synthesis of the modified APC spacers **2a** and **2b**

3.1.2 Synthesis of orthogonally protected acpcPNA

To demonstrate the orthogonality of the N^1-Teoc-/N^1-*o*Ns- protected APC and the N^1-Tfa-protectedAPC spacers [61], a model experiment was carried out by synthesizing a simple acpcPNA sequence (TT) in which one of the two ACPC spacers was replaced with the N^1-Tfa-APC spacer and the remaining one was replaced with either the N^1-Teoc or N^1-*o*Ns-APC spacers. The stability of these protecting groups under the acpcPNA synthesis conditions and the ability to selectively remove any of these protection groups without affecting the other were then studied. (**Figure 3.3**)
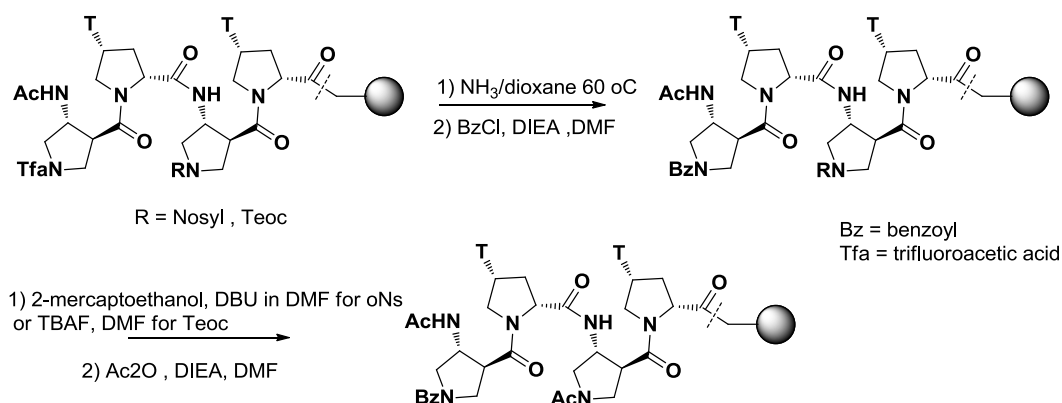
Figure 3.3 Evaluation of orthogonality of APC protecting groups (Tfa vs *o*-Ns/Teoc) in synthesis of a model doubly-modified acpcPNA (T2)

The synthesis of the protected doubly modified acpcPNA proceeded smoothly for both oNs/Tfa and Teoc/Tfa combinations as confirmed by MALDI-TOF MS analyses after cleavage from the resin. This suggests that all protecting groups are compatible with the Fmoc-solid phase peptide synthesis (**Figure 3.4**). It should be noted that the Teoc group is Tfa-labile, the mass observed corresponded to the free-APC spacer. Next, the orthogonality between N^1-Tfa-protection and N^1-Teoc or N^1-oNs protections was explored. While the N^1-Tfa group can be selectively removed in the presence of both N^1-Teoc and N^1-oNs by treatment with aqueous ammonia, treatment of the N^1-Teoc-PNA with fluoride ion under various conditions (TBAF in THF at room temperature 16 h, CsF in DMF at room temperature 1 h) failed to selectively remove the N^1-Teoc group. Apparently, the N^1-Teoc group was quite resistant to the cleavage by fluoride ion. All attempts to completely remove the N^1-Teoc group failed. In all cases, complete or partial cleavage of the N^1-Tfa group presumably due to the high basicity of the fluoride ion was always observed. On the other hand, the N^1-oNs group is completely stable under the basic conditions required for N^1-Tfa deprotection, yet could be selectively removed by 2-mercaptoethanol in the presence of DBU. This was demonstrated by the following reaction sequence (**Figure 3.4**): 1) starting from the model PNA carrying the APC modifications (m/z = 1135.7 with a smaller peak at m/z = 1120.4 attributed to the deoxygenated product derived from removal of one oxygen atom from the nitro group under the MALDI-TOF analysis conditions) 2) selective removal of N^1-Tfa by treatment with aq NH_3 at 60 ^{o}C overnight (m/z = 1038.8) 3) acetylation with Ac_2O (m/z = 1081.8) 4) removal of N^1-oNs (m/z = 895.9) (the deoxygenated product peak disappeared, confirming the association of this peak with the presence of nitro group) and 5) benzoylation with Bz_2O (m/z = 1001.0). The two conditions for the deprotection of N^1-Teoc-APC and N^1-oNs-APC spacers are completely orthogonal and the deprotection sequences could be reversed, therefore the N^1-oNs protected APC spacer **2b** was selected for further used in combination with the N^1-Tfa protected APC spacer for PNA labeling studies.
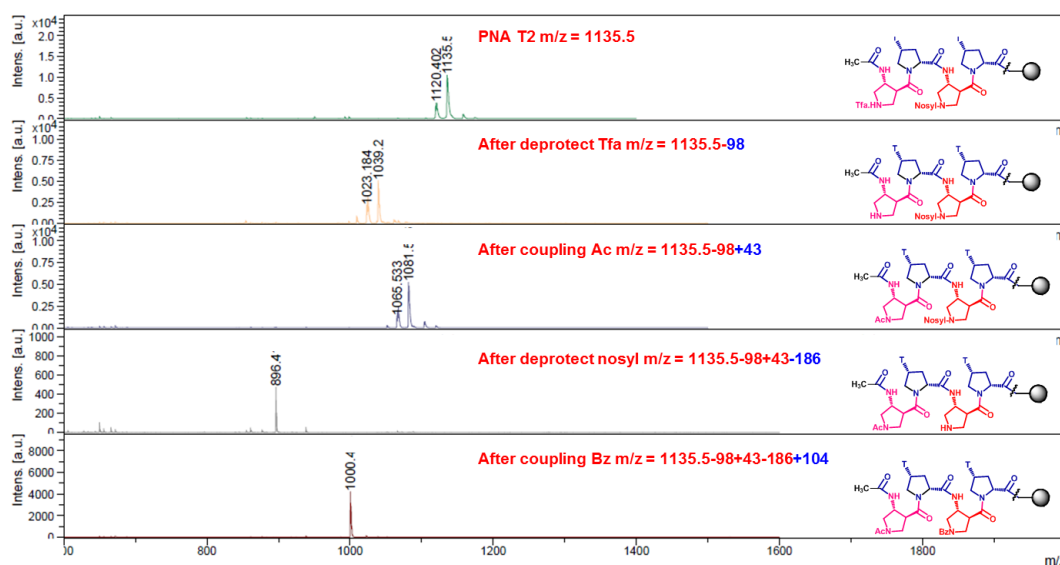
Figure 3.4 MALDI-TOF mass spectra of the model doubly-labeling experiments of acpcPNA (T2). More explanation can be found in the text.

3.1.3 Orthogonal fluorophore labeling onto acpcPNA
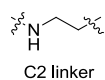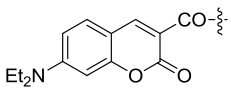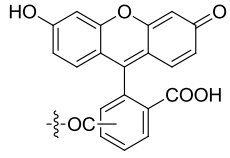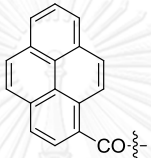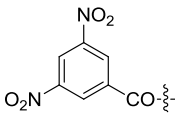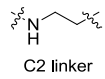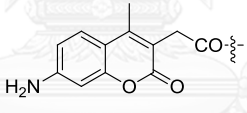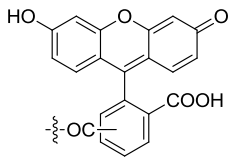
To demonstrate the applicability of the two orthogonally protected APC spacers (Tfa and N^1-oNs) for the synthesis of acpcPNA carrying two different labels, acpcPNA with a homothymine (T9) and mix-base (M12) sequences were synthesized. The N^1-Tfa- and N^1-oNs -protected APC spacers were incorporated at various positions in the sequence **(Table 3.1)**. In most sequences, the two modified spacers were placed 5 bases apart because it was shown earlier in a pyrene excimer/monomer switching acpcPNA probe that this is the distance that gave maximum fluorescence change due to placement of the labels on the opposite sides of the helix.[64] After the synthesis of the acpcPNA was completed, the N-terminal Fmoc group was removed and capped by $N\alpha$-acetylated lysine (to improve water solubility). The N^1-Tfa protecting group on one of the APC residue was removed by treatment with hot aqueous ammonia. This condition removed the Tfa as well as all nucleobase protecting groups (Bz and Ibu) but would not affect the other protecting groups (Boc or Mtt on lysine and oNs on another APC residue). The partially deprotected acpcPNA was next modified with the first dye, either through standard amide coupling chemistry or the newly developed

reductive alkylation-click strategy [63] while the PNA was still on the solid support. In some cases an amino-C2 linker (aminoethyl, $H_2NCH_2CH_2$-) was first attached to the ring nitrogen atom of the APC spacer to separate the dye from the PNA backbone. After completing the attachment of the first dye, the *o*Ns protecting group on the second APC spacer was removed and the second dye was added in the same way as the first dye. The structures of the dyes/fluorophores used, as well as the PNA sequences and the positions of dye attachment are shown in **Table 3.1**. The doubly-labeled acpcPNA probes were cleaved from the solid support using trifluoroacetic acid (TFA) and the crude labeled acpcPNA probes were purified by reversed phase HPLC.

3.1.4 Purification and identification of the synthesized acpcPNA oligomers
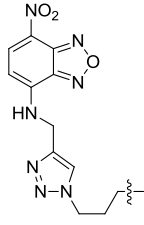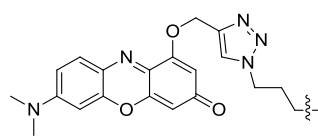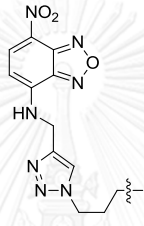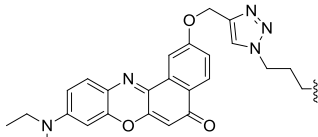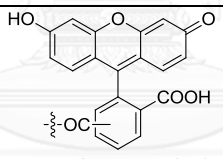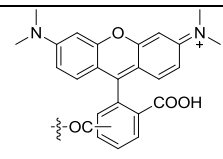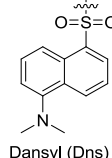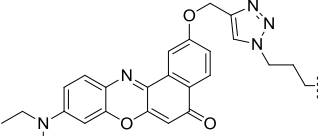
After completing the synthesis, the modified acpcPNA was cleaved by TFA. The crude PNA oligomers were purified by C-18 reversed phase HPLC, monitoring by UV-absorbance at 300 nm and eluting with a gradient system of 0.1% TFA in methanol/water. Fractions containing the pure PNA as determined by MALDI-TOF MS were combined and lyophilized. The residues were re-dissolved in 120 μL of water and the concentration of the PNA was determined by UV/Vis spectrophotometry. The identities of the PNA oligomers were verified by MALDI-TOF mass spectrometry. The *m/z* data obtained from MALDI-TOF analysis for each PNA are illustrated in **Table 3.2**. The purities of all modified PNA were determined to be >90% by reversed phase HPLC analyses.

Table 3.1 Structure of donor fluorophores, acceptor fluorophores and quenchers used in internally dual-labeled acpcPNA

PNA	Linker	Donor Fluorophore[a]	Acceptor Fluorophore/ Quencher[a]
T9(Cou1/Flu) T9(C2Cou1/C2Flu)	none or N H C2 linker	coumarin1 (Cou1) λ_{max} (abs = 425, em = 485 nm)	fluorescein (Flu) λ_{max} (abs = 480, em = 520 nm)
T9(DNB/Pyr)	none	pyrene, (Pyr) λ_{max} (abs = 340, em = 400 nm)	3,5-dinitrobenzoic acid (DNB) λ_{max} (abs = 340)
T9(Cou2/Flu) T9(Cou2/C2Flu) T9(C2Cou2/C2Flu) T9(C2Cou2/Flu)	none or N H C2 linker	coumarin2 (Cou2) λ_{max} (abs = 330, em = 425 nm)	fluorescein (Flu) λ_{max} (abs = 480, em = 520 nm)
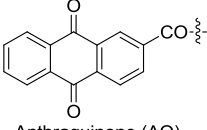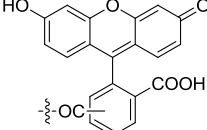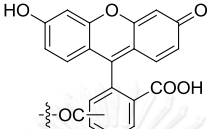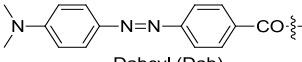
[a]All λ_{max} values were experimentally determined by UV-vis and fluorescence spectroscopy.

Table 3.1 Structure of donor fluorophores, acceptor fluorophores and quenchers used in internally dual-labeled acpcPNA (continued)

PNA	Linker	Donor Fluorophore[a]	Acceptor Fluorophore/ Quencher[a]
T9(NBD/PheR)	none	4-propagylamine-7-nitrobenzofurazan (NBD) λ_{max} (abs = 475, em = 540 nm)	Phenoxazine red (PheR) λ_{max} (abs = 600, em = 640 nm)
T9(NBD/Nr)	none	4-propagylamine-7-nitrobenzofurazan (NBD) λ_{max} (abs = 480, em = 525 nm)	Nile red (Nr) λ_{max} (abs = 600, em = 650 nm)
T9(Flu/TMR)1, T9(Flu/TMR)2 T9(Flu/TMR)3	none	fluorescein (Flu) λ_{max} (abs = 480, em = 520 nm)	TAMRA (TMR) λ_{max} (abs = 560 , em = 580 nm)
T9(Dns/Nr)	none	Dansyl (Dns) λ_{max} (abs = 335, em = 500 nm)	Nile red (Nr) λ_{max} (abs = 600, em = 650 nm)

[a]All λ_{max} values were experimentally determined by UV-vis and fluorescence spectroscopy.

Table 3.1 Structure of donor fluorophores, acceptor fluorophores and quenchers used in internally dual-labeled acpcPNA (continued)

PNA	Linker	Donor Fluorophore[a]	Acceptor Fluorophore/ Quencher[a]
T9(Flu/AQ)	none	Anthraquinone (AQ) λ_{max} (abs = 330 nm)	fluorescein (Flu) λ_{max} (abs = 490, em = 520 nm)
T9(Flu/Dab)	none or C2 linker	flurescein (Flu) λ_{max} (abs = 480, em = 520 nm)	Dabcyl (Dab) λ_{max} (abs = 490, em = 520 nm)

[a]All λ_{max} values were experimentally determined by UV-vis and fluorescence spectroscopy.

Table 3.2 Sequences and yield of modified PNA obtained after HPLC purification.

PNA	Sequence (N to C)	t_R (min)	*m/z* (calcd)	*m/z* (found)	%yield
T9(Cou1/Flu)	TTT(Cou1)TTT(Flu)TTT	30.8	3911.1	3913.0	5.5
T9(C2Cou1/C2Flu)	TTT(C2Cou1)TTT(C2Flu)TTT	30.8	3998.3	3998.8	2.3
T9(DNB/Pyr)	TT(DNB)TTTTT(Pyr)TT	35.2	3719.1	3717.7	2.0
T9(Cou2/Flu)	TT(Cou2)TTTTT(Flu)TT	29.1	3882.6	3883.9	5.8
T9(Cou2/C2Flu)	TT(Cou2)TTTTT(C2Flu)TT	30.2	3911.3	3911.9	1.8
T9(C2Cou2/C2Flu)	TT(C2Cou2)TTTTT(C2Flu)TT	30.8	3973.1	3976.5	1.4
T9(C2Cou2/Flu)	TT(C2Cou2)TTTTT(Flu)TT	29.3	3911.3	3911.9	5.1
T9(NBD/PheR)	TT(NBD)TTTTT(PheR)TT	32.4	4018.1	4017.7	5.8
T9(NBD/Nr)	TT(NBD)TTTTT(Nr)TT	32.4	4078.3	4077.1	7.9
T9(Flu/TMR)1	TT(Flu)TTTTT(TMR)TT	34.2	4075.6	4076.7	3.0
T9(Flu/TMR)2	TTTT(Flu)T(TMR)TTTT	34.2	4077.5	4077.5	3.4
T9(Flu/TMR)3	(Flu)TTTTTTTTT(TMR)	34.2	4188.5	4188.7	4.2
T9(Dns/Nr)	TT(Dns)TTTTT(Nr)TT	31.6	4011.2	4010.9	2.9
T9(Flu/AQ)	TT(Flu)TTTTT(AQ)TT	34.0	3901.9	3901.1	3.4

Table 3.2 Sequences and yield of modified PNA obtained after HPLC purification (continued).

PNA	Sequence (N to C)	t_R (min)	m/z (calcd)	m/z (found)	%yield
T9(Flu/Dab)	TT(Flu)TTTTT(Dab)TT	39.6	3919.2	3918.9	2.8
M12(Flu/TMR)	AGTT(Flu)ATCCC(TMR)TGC	36.0	5065.2	5064.8	1.9
M12(C2Cou/Flu)	AGTT(C2Cou)ATCCC(Flu)TGC	30.8	4932.6	4931.5	1.3
M12(Dns/Nr)	AGTT(Dns)ATCCC(Nr)TGC	30.0	5017.4	5016.6	1.4

3.1.5 Thermal stability of dual-pyrene-labeled acpcPNA probes

Thermal stability was studied by measurement of melting temperature (T_m) using UV-vis spectrophotometry. In this technique, the maximum absorption of the duplex at 260 nm was monitored at different temperatures from 20–90 °C. When the temperature is increased, the duplex separates into two random coiled strands that exhibited around 10–20% hyperchromicity relative to the duplex. The intensity at 260 nm is plotted against temperature to give a sigmoidal curve called melting curve. The melting temperature (T_m) is defined as the temperature at which an equilibrium between double-stranded and single-stranded of oligonucleotide take place.

In practice, this can be determined from the maximum of the first derivative of the melting curve. T_m values can be used to estimate the binding affinity and specificity of the probe to the target. T_m values of all doubly-labeled acpcPNA are shown in **Table 3.3**. It should also be noted that due to the hydrophobic nature of the dye-labeled PNA, some sequences do not give well-defined melting curves and thus the T_m values presented in **Table 3.3** are only approximation.

Table 3.3 T_m of the dual labeled acpcPNA probes

PNA	DNA sequences 5'→3'	T_m (°C)[a]
T9(Cou1/Flu)	dAAAAAAAAA	37.0
	dAAAACAAAA	26.0
	dAGTGCTGAT	<20
T9(C2Cou1/C2Flu)	dAAAAAAAAA	51.1
	dAAAACAAAA	29.1
	dAGTGCTGAT	<20
T9(DNB/Pyr)	dAAAAAAAAA	50.1
	dAAAACAAAA	30.0
	dAGTGCTGAT	<20
T9(Cou2/Flu)	dAAAAAAAAA	49.6
	dAAAACAAAA	30
	dAGTGCTGAT	<20
T9(Cou2/C2Flu)	dAAAAAAAAA	48.4
	dAAAACAAAA	32.6
	dAGTGCTGAT	<20
T9(C2Cou2/C2Flu)	dAAAAAAAAA	51.7
	dAAAACAAAA	31.0
	dAGTGCTGAT	<20
T9(C2Cou2/Flu)	dAAAAAAAAA	53.4
	dAAAACAAAA	25.0
	dAGTGCTGAT	<20
T9(NBD/PheR)	dAAAAAAAAA	66.0
	dAAAACAAAA	36.0
	dAGTGCTGAT	<20
T9(NBD/Nr)	dAAAAAAAAA	62.0
	dAAAACAAAA	34.5
	dAGTGCTGAT	<20

[a][PNA] = 1μM and [DNA] = 1.2 μM in 10 mM sodium phosphate buffer pH 7.

Table 3.3 T_m of the dual labeled acpcPNA probes (continued)

PNA	DNA sequences 5'→3'	T_m (°C)[a]
T9(Flu/TMR)1	dAAAAAAAAA	44.7
	dAAAACAAAA	37.5
	dAGTGCTGAT	<20
T9(Flu/TMR)2	dAAAAAAAAA	34.0
	dAAAACAAAA	23.0
	dAGTGCTGAT	<20
T9(Flu/TMR)3	dAAAAAAAAA	66.0
	dAAAACAAAA	50
	dAGTGCTGAT	<20
T9(Dns/Nr)	dAAAAAAAAA	54.4
	dAAAACAAAA	32.1
	dAGTGCTGAT	<20
T9(Flu/AQ)	dAAAAAAAAA	42.8
	dAAAACAAAA	21.3
	dAGTGCTGAT	<20

[a][PNA] = 1μM and [DNA] = 1.2 μM in 10 mM sodium phosphate buffer pH 7.

Table 3.3 T_m of the dual labeled acpcPNA probes (continued)

PNA	DNA sequences 5'→3'	T_m (°C)[a]
T9(Flu/Dab)	dAAAAAAAAA	36.0
	dAAAACAAAA	31.0
	dAGTGCTGAT	<20
M12(Flu/TMR)	dGCAGGGATAACT	47.6
	dGCAGCGATAACT	30.0
	dGCATTAAGATAC	<20
M12(C2Cou/Flu)	dGCAGGGATAACT	58.3
	dGCAGCGATAACT	37.0
	dGCATTAAGATAC	< 20
M12(Dns/Nr)	dGCAGGGATAACT	65.1
	dGCAGCGATAACT	31.0
	dGCATTAAGATAC	<20

[a][PNA] = 1.0 μM and [DNA] = 1.2 μM in 10 mM sodium phosphate buffer pH 7.

The nine bases homothymine acpcPNA (T9) was selected as a model system for optimization of the type of fluorophore labels in all experiments because it is the simplest and shortest sequence that can exhibit a good thermal stability (T_m = 80.0 °C) upon hybridization with complementary DNA (dA9) [63]. All dual-labeled acpcPNA probes were investigated for the duplex stability and specificity by melting temperature experiments. The results showed that all T9 acpcPNA probes were able to hybridize with their complementary targets. The T_m values (with complementary DNA) in range of 34–66 °C were obtained, depending on type of labels and linkage. In all cases, the presence of the labels decreased the T_m quite substantially relative to the unmodified T9 (T_m = 80.0 °C). Nevertheless, single base mismatch PNA·DNA duplexes gave much lower T_m than the complementary PNA·DNA duplexes as shown in **Table 3.3**, indicating that the specificity was retained in these dual-labeled acpcPNA probes.

In addition, three mix-base 12 mers acpcPNA probes were designed for studying of the more general behavior of the dual-labeled acpcPNA probes. All mix-base

acpcPNA probes were able to hybridize with their complementary targets as shown by the T_m values of 47.6, 58.3 and 65.1 $^\circ$C for **M12(Flu/TMR)**, **M12(C2Cou/Flu)** and **M12(Dns/Nr)**, respectively. Single base mismatch PNA·DNA duplexes gave much lower T_m than the complementary PNA·DNA duplexes as shown in **Table 3.3**. The higher T_m of perfectly matched PNA·DNA also indicated the high specificity of the dual-labeled mix-base acpcPNA probes.

3.1.6 Optical properties of homothymine dual-labeled acpcPNA probes

UV-vis absorption spectra of all acpcPNA incorporating two fluorophore labels were firstly investigated in both single-stranded forms and as duplexes with complementary, single base mismatched and non-complementary DNAs. The UV-vis spectra of all single-stranded doubly-labeled acpcPNA showed the absorption maxima of the two fluorophores. In most cases, the presence of DNA induced a small change in the absorption spectra from the single stranded acpcPNA. The absorption change between single and double strand suggests ground state interactions between the two fluorophores. Raw UV-vis spectra are included in the appendices. (Figure A76-93)

A series of hybridization experiments was performed with the aim to identify one or more suitable FRET pairs and donor-acceptor distances that provide the maximum change of fluorescence intensities upon target binding. To search for the suitable FRET pairs, the distance between the two labels was fixed at five bases apart with the hypothesis that for the duplex with a pitch of 10-11 base pairs per turn like in normal DNA duplexes, the maximum separation of the two labels should be obtained when they are on the opposite sides of the same duplex.[64] For FRET pairs, the fluorophore pairs were chosen in such a way that the emission spectrum of the donor fluorophore overlaps with the absorption spectrum of the acceptor fluorophore (**Figure 3.5**).[75] Some of these fluorophore-quencher pairs were chosen based on literature reports (Flu-Dab, Flu-AQ, Pyr-DNB) [76-78] .
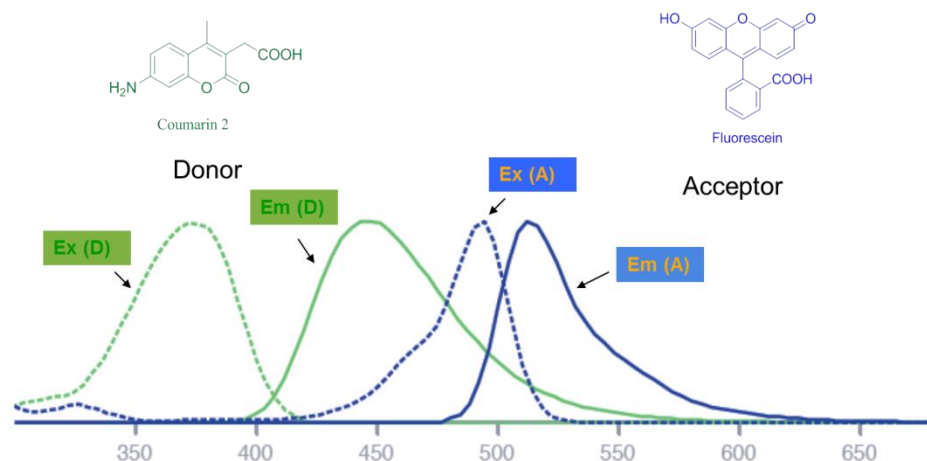
Figure 3.5 Example of absorption and emission profiles of an ideal FRET pair (coumarin ad donor and fluorescein as acceptor). λ_{max} of donor: abs= 380; em = 440 nm; λ_{max} of acceptor: abs = 490; em = 520 nm [75].

The investigation started with labeling of the acpcPNA with a fluorophore-quencher pair **T9(DNB/Pyr)**. The **T9(DNB/Pyr)** was labeled with pyrene-1-carboxylic acid (fluorophore) and 3,5-dinitrobenzoic acid (quencher). In the single stranded form, **T9(DNB/Pyr)** exhibited a relatively weak fluorescence with maxima at 390, 410 and 435 nm (41 a.u.). The shape of the fluorescence spectra is characteristic of the pyrene. In the presence of complementary DNA target, the fluorescence was increased from 41 to 280 a.u. which is approximately 6.6 folds. The significant increase in the fluorescence intensity upon PNA-DNA binding is most likely due to the separation of the fluorophore-quencher pairs. Although Reenabthue et al. [61] has shown that the fluorescence of singly pyrene-labeled T9 acpcPNA was increased when hybridized with target DNA (from 180 to 430 a.u.), the fluorescence increase was lower than the present study (2.4 vs 6.6 folds). This can be attributed to the better quenching efficiency of the DNB, which decrease the fluorescence background of the single stranded PNA. In the mismatched PNA-DNA hybrid, the fluorescence intensity was lower than complementary DNA (**Figure 3.6** and **Figure 3.7**) indicating that the interaction was specific. This is also supported by a much higher T_m of the complementary duplex (50.1 °C) when compared to the single mismatched duplex (T_m <20 °C). The results

suggest that it is possible to design a hybridization responsive acpcPNA probe based on this strategy.
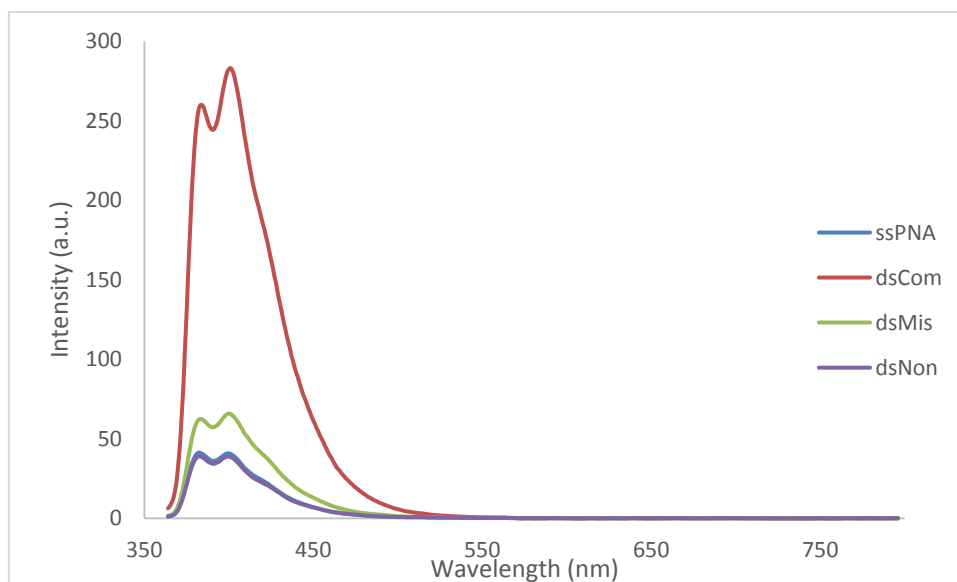
Figure 3.6 Fluorescence spectra of **T9(DNB/Pyr)** with complementary, mismatch and non-complementary DNA (comp DNA = dA9, mismatched DNA = dAAAACAAAA, non-comp DNA = AGTGCTGAT); Conditions: [PNA] = 1.0 µM and [DNA] = 1.2 µM in 10 mM sodium phosphate buffer pH 7, excitation wavelength = 330 nm, PMT voltage = medium
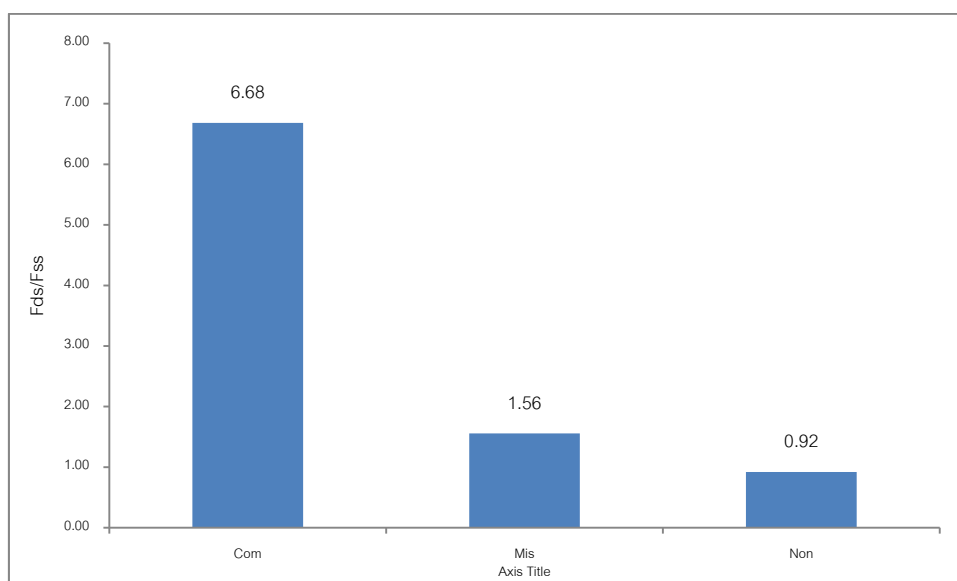
Figure 3.7 F_{ds}/F_{ss} of **T9(DNB/Pyr)** hybrids with complementary, mismatch and non-complementary DNA. The conditions are the same as in **Figure 3.6**.

In addition to Pyr-DNB, other fluorophore-quencher pairs were also investigated. The **T9(Flu/AQ)** probe was labeled with fluorescein (fluorophore) and anthraquinone-2-carboxylic acid (quencher). In the single stranded form, the **T9(Flu/AQ)** probe exhibited a rather high fluorescence emission of the fluorescein at 520 nm (619 a.u.). In the presence of the complementary DNA target, the fluorescence was increased by 40% from 619 to 886 a.u. (F_{ds}/F_{ss} of **T9(Flu/AQ)**) Non-complementary and single mismatched DNA showed virtually no change in the emission. However, the quenching efficiency in this case is not good so only small fluorescence change was observed upon hybrid formation (**Figure 3.8** and **Figure 3.9**).
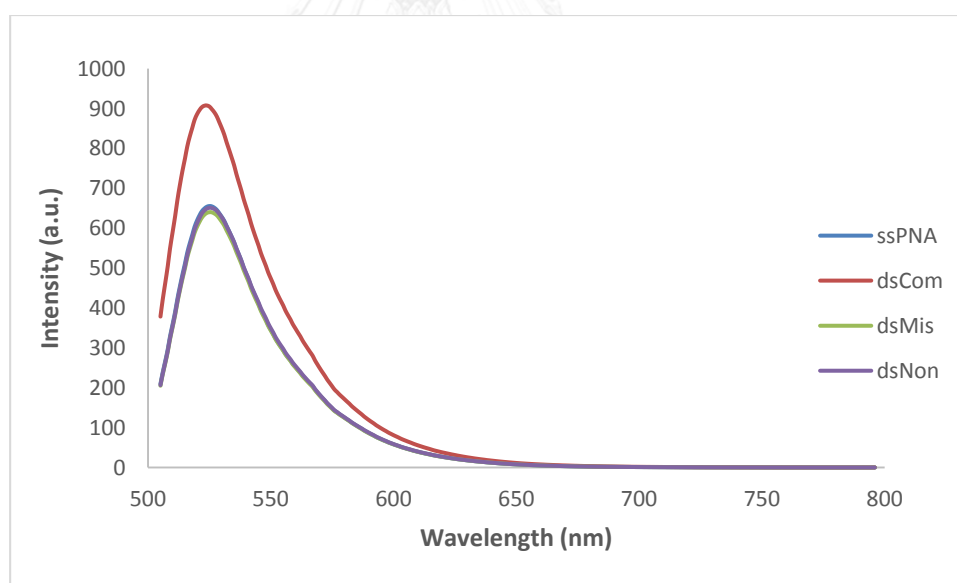
Figure 3.8 Fluorescence spectra of **T9(Flu/AQ)** with complementary, mismatch and non-complementary DNA (comp DNA = dA9, mismatched DNA = dAAAACAAAA, non-comp DNA = AGTGCTGAT); Conditions: [PNA] = 1.0 µM and [DNA] = 1.2 µM in 10 mM sodium phosphate buffer pH 7, excitation wavelength = 490 nm, PMT voltage = high
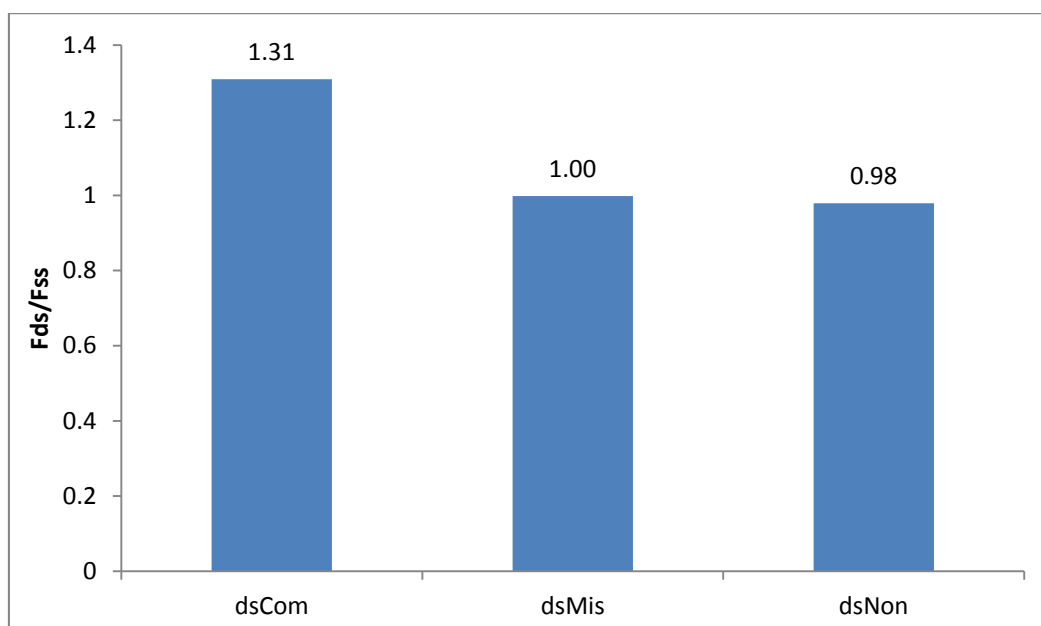
Figure 3.9 F_{ds}/F_{ss} of T9(Flu/AQ) hybrids with complementary, mismatch and non-complementary DNA. The conditions are the same as in **Figure 3.8.**

Next we turned to another fluorophore-quencher pair consisting of fluorescein and dabcyl in **T9(Flu/Dab)** probe. In single-stranded form, the **T9(Flu/Dab)** probe showed considerably lower emission at 520 nm (210 a.u) compared to the **T9(Flu/AQ)** probe. After hybridization with complementary DNA target, the emission increased by almost 3 folds (from 210 to 610 a.u.). Again, no fluorescence changes were observed with non-complementary DNA (**Figure 3.10**). The F_{ds}/F_{ss} of PNA-DNA hybrids of **T9(Flu/Dab)** with complementary is higher than mismatched and non-complementary (2.8, 1.0 and 0.9 respectively), indicating that the binding and the fluorescence change are specific **(Figure 3.11)**. Although the **T9(Flu/Dab)** exhibit much better fluorescence change than the **T9(Flu/AQ)** probes, the single-strandedprobe still exhibited a relatively high fluorescence. As a result, we turned our attention to a FRET pairs instead of fluorophore-quencher pairs.

,
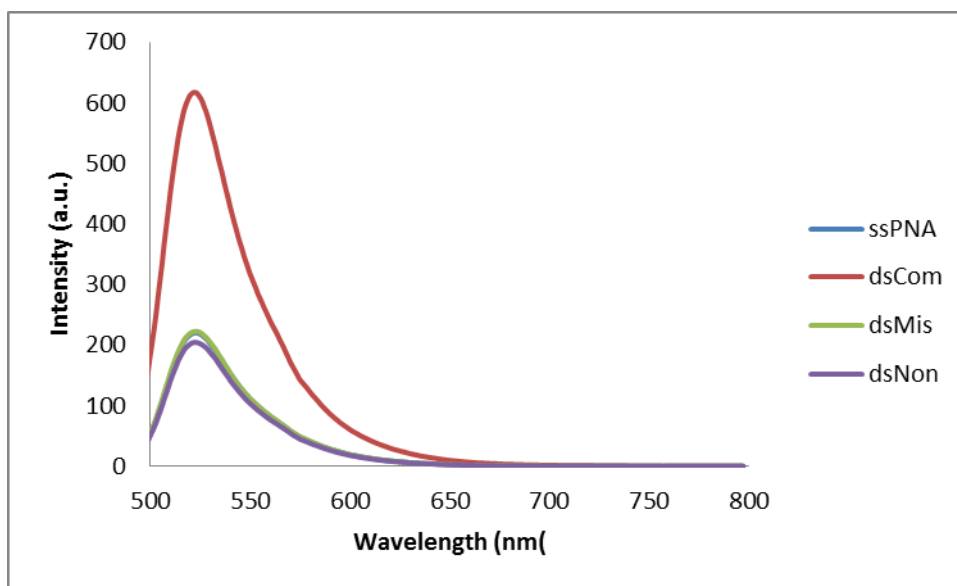
Figure 3.10 Fluorescence spectra of **T9(Flu/Dab)** with complementary, mismatch and non-complementary DNA (comp DNA = dA9, mismatched DNA = dAAAACAAAA, non-comp DNA = AGTGCTGAT); Conditions: [PNA] = 1.0 µM and [DNA] = 1.2 µM in 10 mM sodium phosphate buffer pH 7, excitation wavelength = 490 nm, PMT voltage = high
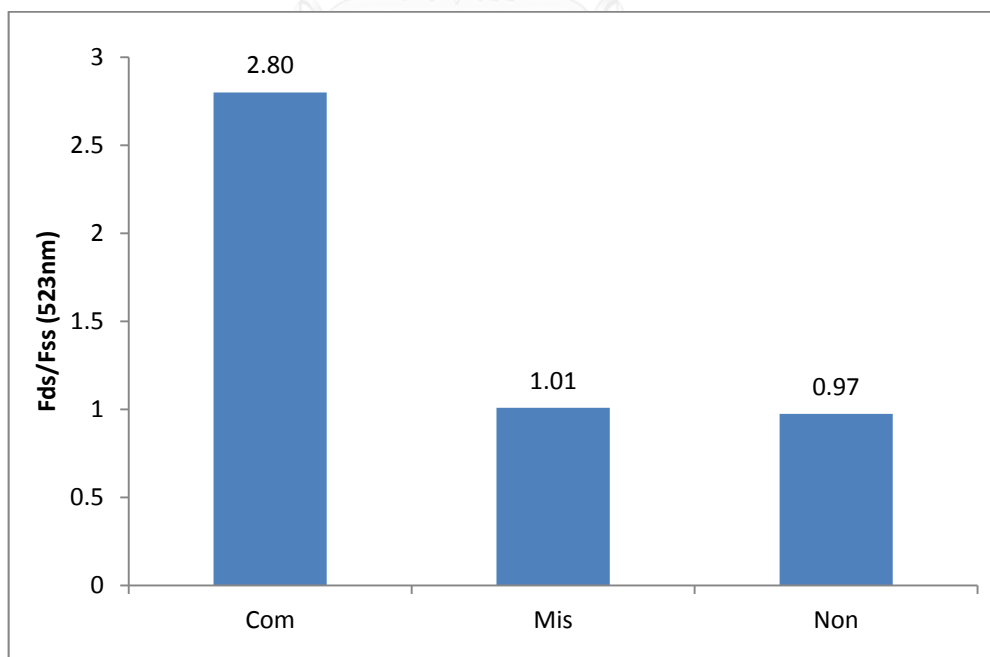
Figure 3.11 F_{ds}/F_{ss} of **T9(Flu/Dab)** with with complementary, mismatch and non-complementary DNA. The conditions are the same as in **Figure 3.9**.

The use of a fluorophore-quencher pair as in the previous examples has one important limitation that is the intensity change relies on the measurement at only one specific wavelength. Since the fluorescence intensity is concentration dependent, and since fluorescence can be quenched in various ways that may not involve the desired pathway, such single wavelength measurement are prone to errors. It should be much better to detect at two different wavelengths because although the fluorescence intensity at each wavelength is sensitive to concentration, but the ratio of the two should not. As a result, the acpcPNA probes containing coumarin-fluorescein FRET pairs **T9(Cou1/Flu)**, **T9(C2Cou1/C2Flu)**, **T9(Cou2/Flu)**, **T9(Cou2/C2Flu)**, **T9(C2Cou2/C2Flu)** and **T9(C2Cou2/Flu)** were next studied. In this series, two different coumarin derivatives (Cou1 have a more extended conjugation thus the absorption and emission maxima were at slightly longer wavelengths than Cou2) were used as the donor and fluorescein was used as the acceptor. The dyes were attached onto acpcPNA using standard amide coupling, optionally with an aminoethyl (C2) linker inserted between the dyes and the PNA backbone in **T9(Cou2/C2Flu)**, **T9(C2Cou2/C2Flu)** and **T9(C2Cou2/Flu)**. Fluorescence spectra of all coumarin-fluorescein labeled probes showed two emission maxima corresponding to coumarin and fluorescein, respectively. After addition of complementary DNA, the fluorescence intensity should change. Unfortunately, the absorption of the **Cou1** label at a rather long wavelength (425 nm) resulted in a direct excitation of the acceptor dye (fluorescein), therefore **T9(Cou1/Flu)** and **T9(C2Cou1/C2Flu)** showed only modest fluorescence change upon hybridization with the complementary DNA target. For the **T9(Cou1/Flu)**, the emission of donor (at 480 nm) was not changed but the emission of acceptor (520 nm) was slightly decreased. Insertion of an aminoethyl linker between the labels and the PNA backbone, as in **T9(C2Cou1/C2Flu)**, did not help much. The donor emission was only slightly increased and the emission of acceptor was increased. The Cou2 labels having less extensive conjugation could be excited at much shorter wavelengths (330 nm) therefore the direct excitation of the fluorescein, which may complicate the analysis of the results, are minimal. For **T9(Cou2/Flu)**,

T9(Cou2/C2Flu), T9(C2Cou2/C2Flu) and **T9(C2Cou2/Flu)**, the fluorescence was observed at 424 nm (emission of coumarin) and 524 nm (emission of fluorescein) after excitation at 330 nm (maximum absorption of the Cou2 label). In all cases, the presence of complementary DNA resulted in an increase in the donor (Cou2) emission at 445 nm. However, the acceptor (fluorescein) emission was not significantly changed. According to our proposed model (**Figure 3.12**), the emission of the donor fluorophore should decrease and that of the acceptor fluorophore should increase upon hybridization because of the less effective FRET. This suggests that FRET may not be the principal interaction between the Cou2/Flu pair. The most likely situation is that the coumarin is quenched by the fluorescein dye as a result of close contact between the two dyes in the single stranded PNA. Hybridization with DNA separated the two dyes, and restored the fluorescence of the coumarin. This hypothesis is supported by the significant difference between UV spectra of the dye in the single stranded vs double stranded form of the PNA (see below). Nevertheless, the Cou2/Flu labeled acpcPNA showed enhancement factor [$f = F_D(ds)/F_D(ss)/ F_A(ds)/F_A(ss)$] in the range of 2.1, 4.5, 2.6 and 2.2 for **T9(Cou2/Flu), T9(Cou2/C2Flu), T9(C2Cou2/C2Flu)** and **T9(C2Cou2/Flu)** respectively (see **Table 3.4**). The **T9(CCou2/C2Flu)** with a more flexible linker at the Flu label but not at the Cou2 label gave the highest enhancement factor of 4.5. In all cases, the fluorescence intensity change is specific as much lower fluorescence enhancements were observed with mismatched DNA targets (see **Table 3.4**). Melting temperature analyses confirmed the specificity of the PNA-DNA binding [**T9(Cou2/Flu)**:T_m = 49.6 $^\circ$C, **T9(Cou2/C2Flu)**: T_m = 48.4 $^\circ$C, **T9(C2Cou2/C2Flu)**: T_m = 51.7 $^\circ$C **T9(C2Cou2/Flu)**: T_m = 53.4 $^\circ$C].
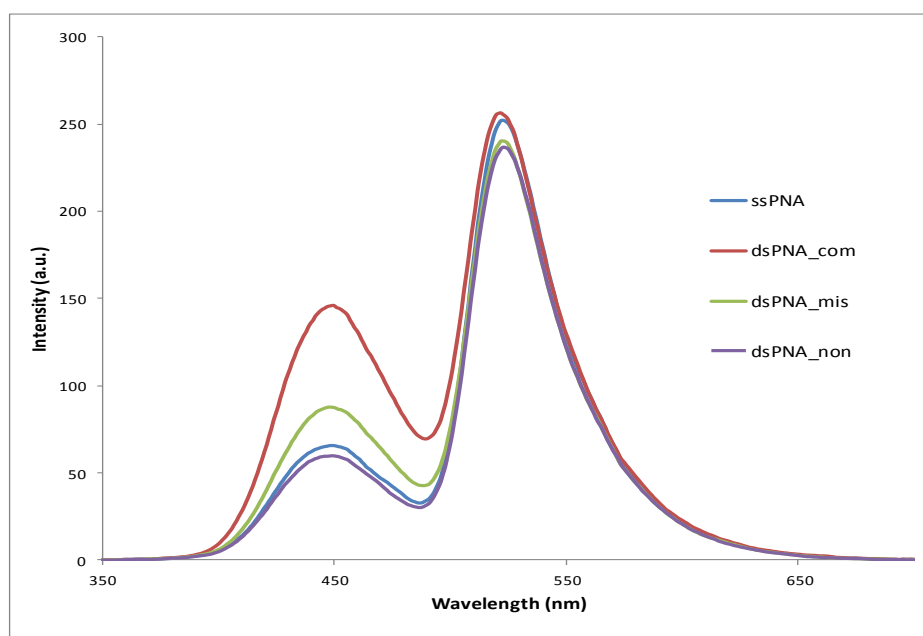
Figure 3.12 Fluorescence spectra of **T9(C2Cou2/Flu)** in the absence and presence of various DNA (comp DNA = dA9, mismatch DNA = dAAAACAAAA, noncomp DNA = dAGTGCTGAT); Conditions: [PNA] = 1.0 µM and [DNA] = 1.2 µM in 10 mM sodium phosphate buffer pH 7, excitation wavelength = 330 nm, PMT voltage = medium
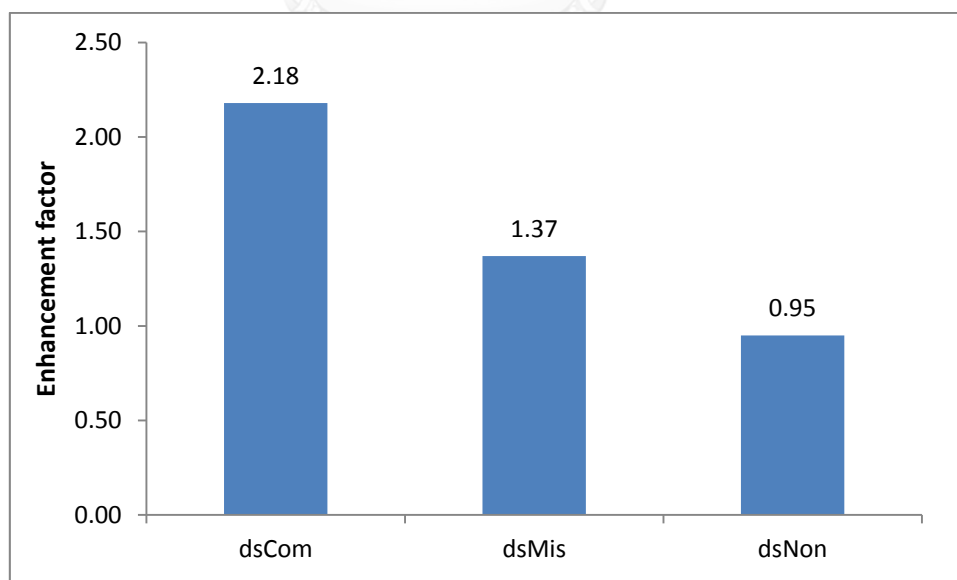
Figure 3.13 F_{ds}/F_{ss} of **T9(C2Cou/Flu)** with complementary, mismatch and non-complementary DNA. The conditions are the same as in **Figure 3.12.**
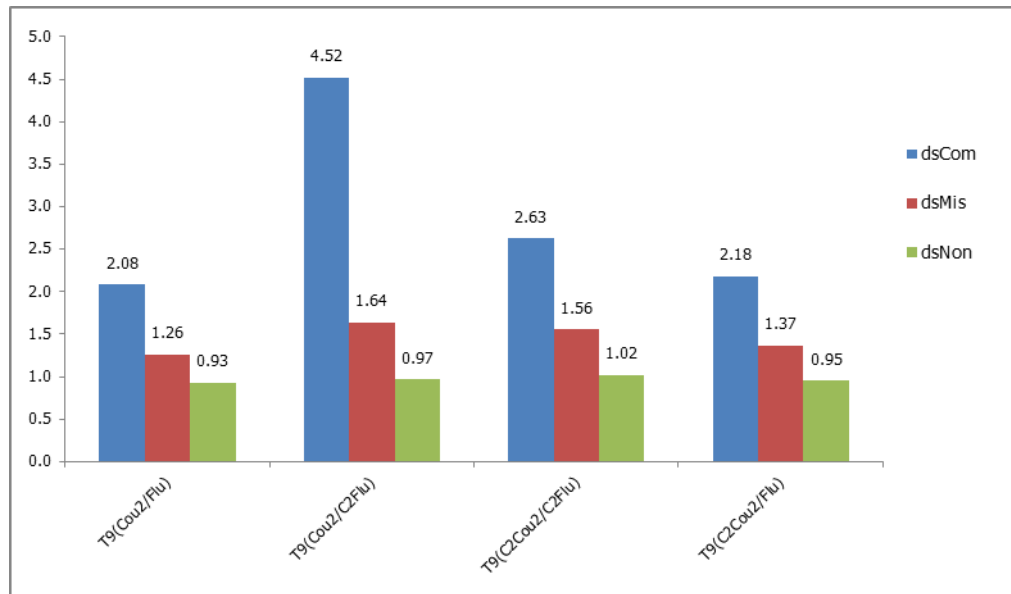
Figure 3.14 Enhancement factors (*f*) of **T9(Cou2/Flu)**, **T9(Cou2/C2Flu)**, **T9(C2Cou2/C2Flu)** and **T9(C2Cou2/Flu)** with various DNA

Table 3.4 Summary of fluorescence data of internally dual-labeled FRET acpcPNA probes

PNA	DNA	F_D(ss) (a.u.)	F_A(ss) (a.u.)	F_D(ds) (a.u.)	F_A(ds) (a.u.)	F_D(ds)/ F_D(ss)	F_A(ds)/ F_A(ss)	$f =$ [F_D(ds)/F_D(ss)/ F_A(ds)/F_A(ss)]
T9(Cou2/Flu)	Com	57.10	194.90	128.20	210.60	2.24	1.08	2.08
	Mis	57.20	192.10	73.10	194.10	1.28	1.01	1.26
	Non	54.70	181.00	50.90	181.50	0.93	1.00	0.93
T9(Cou2/C2Flu)	Com	11.60	276.01	55.70	292.00	4.78	1.06	4.52
	Mis	12.00	287.00	19.60	286.00	1.64	1.00	1.64
	Non	12.80	302.20	12.30	296.90	0.95	0.98	0.97
T9(C2Cou2/C2Flu)	Com	14.60	203.90	33.30	176.70	2.28	0.87	2.63
	Mis	14.70	204.60	20.00	178.30	1.36	0.87	1.56
	Non	14.60	203.50	14.80	200.70	1.01	0.99	1.02
T9(C2Cou2/Flu)	Com	64.80	251.80	143.60	256.20	2.22	1.02	2.18
	Mis	63.70	241.40	86.70	240.30	1.36	1.00	1.37
	Non	63.40	239.10	59.40	235.80	0.94	0.99	0.95
T9(NBD/PheR)	Com	57.46	81.82	55.58	40.10	0.70	1.39	0.51
	Mis	51.17	83.84	51.17	41.58	0.69	1.23	0.56
	Non	69.40	74.77	32.84	37.34	0.93	0.88	1.06
T9(NBD/Nr)	Com	10.00	44.10	30.80	207.80	3.06	4.71	0.65
	Mis	10.30	45.20	17.60	212.50	1.71	4.69	0.36
	Non	10.40	41.10	9.40	32.50	0.89	0.79	1.12
T9(Flu/TMR)1	Com	260.40	128.50	290.00	261.00	1.11	2.03	0.55
	Mis	248.70	124.90	254.00	132.10	1.02	1.06	0.97
	Non	276.50	139.50	274.30	137.20	0.99	0.98	1.01
T9(Flu/TMR)2	Com	513.80	211.80	465.90	186.80	0.91	0.88	1.03
	Mis	473.50	190.20	464.10	184.60	0.98	0.97	1.01
	Non	476.20	192.10	470.70	188.40	0.99	0.98	1.01
T9(Flu/TMR)3	Com	264.10	98.60	272.80	142.50	1.03	1.45	0.71
	Mis	247.50	92.40	271.50	135.40	1.10	1.46	0.75
	Non	256.15	95.90	246.60	91.80	0.96	0.96	1.01

Table 3.4 Summary of fluorescence data of internally dual-labeled FRET acpcPNA probes

PNA	DNA	F_D(ss) (a.u.)	F_A(ss) (a.u.)	F_D(ds) (a.u.)	F_A(ds) (a.u.)	F_D(ds)/ F_D(ss)	F_A(ds)/ F_A(ss)	$f =$ [F_D(ds)/F_D(ss)/ F_A(ds)/F_A(ss)]
T9(Dns/Nr)	Com	3.91	8.29	9.27	150.41	2.37	16.23	0.15
	Mis	3.87	11.88	5.64	45.85	1.46	8.13	0.18
	Non	3.69	10.77	3.41	8.99	0.92	2.63	0.35
Mix12(Flu/TMR)	Com	127.00	52.50	158.90	100.20	1.25	1.91	0.66
	Mis	131.10	54.20	141.70	70.00	1.08	1.29	0.84
	Non	132.10	54.50	124.80	49.50	0.94	0.91	1.04
Mix12(C2Cou2/Flu)	Com	53.80	79.50	106.30	110.20	1.98	1.39	1.43
	Mis	56.10	78.40	107.69	101.42	1.92	1.29	1.48
	Non	57.50	83.70	49.95	80.15	0.87	0.96	0.91
Mix12(Dns/Nr)	Com	5.57	15.53	6.12	30.19	1.10	1.94	0.57
	Mis	5.57	14.96	5.73	37.11	1.03	2.48	0.41
	Non	5.80	14.21	3.64	7.01	0.61	0.49	1.25

Next, a different combination of FRET pair was used, namely fluorescein (Flu) as the donor and tetramethylrhodamine (TMR) as the acceptor. The T9 acpcPNA was again labeled at the backbone with the two dyes at different distances (1, 5 and 9 bases). The fluorescence spectra of all single-stranded **T9** with Flu/TMR labels showed two emissions at 520 nm (Flu) and 578 nm (TMR). Addition of complementary DNA resulted in a small increase in the Flu emission but a large increase in the TMR emission (**Figure 3.15**). The probe **T9(Flu/TMR)1** with the Flu/TMR at 5 base separation gave larger fluorescence change than the **T9(Flu/TMR)2** and **T9(Flu/TMR)3** probes carrying the same FRET pairs at 1 and 9 base separation, respectively. The results confirmed that 5-base is the most suitable distance for dye attachment to achieve maximum fluorescence change (**Figure 3.16**). In all cases, T_m showed specificity for PNA-DNA binding: **T9(Flu/TMR)1** = 44.7 $^{\circ}$C, **T9(Flu/TMR)2** = 34 $^{\circ}$C, **T9(Flu/TMR)3** = 70.0 $^{\circ}$C. The almost negligible fluorescence change observed in the case of **T9(Flu/TMR)2** probe carrying two adjacent labels may be explained by the low stability of the hybrid.

In any cases, the fluorescence increase was observed only at the acceptor fluorophore (TMR, 578 nm) but not at the other donor fluorophore (Flu, 520 nm) upon hybridization with DNA. Moreover, the fluorescence increase is opposite to the proposed model whereby the fluorescence of TMR (acceptor) should decrease and that of Flu (donor) should increase after the hybridization. The likely explanation is that the TMR label was quenched by the Flu as a result of close contact between the two dyes. Hybridization caused separation of the two dyes and increment of the fluorescence. The enhancement factors (f) of all **T9(Flu/TMR)** hybrids are summarized in **Table 3.4**. The value of f less than unity means that the fluorescence change is in the opposite direction to the proposed model.
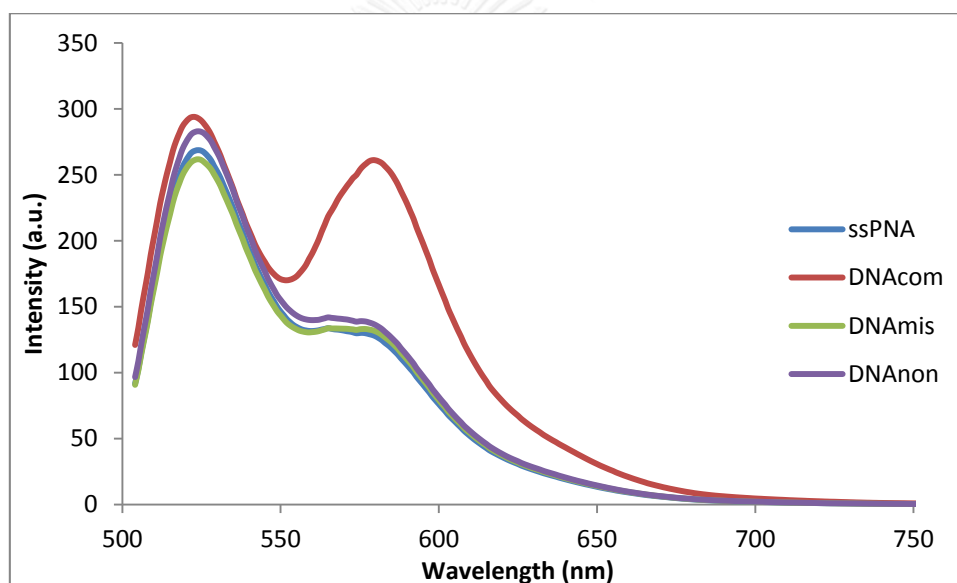
Figure 3.15 Fluorescence spectra of **T9(Flu/TMR)1** at 5 base distance with complementary, mismatch and non-complementary DNA (comp DNA = dA9, mismatched DNA = dAAAACAAAA, non-comp DNA = AGTGCTGAT); Conditions: [PNA] = 1.0 µM and [DNA] = 1.2 µM in 10 mM sodium phosphate buffer pH 7, excitation wavelength = 490 nm, PMT voltage = medium

64
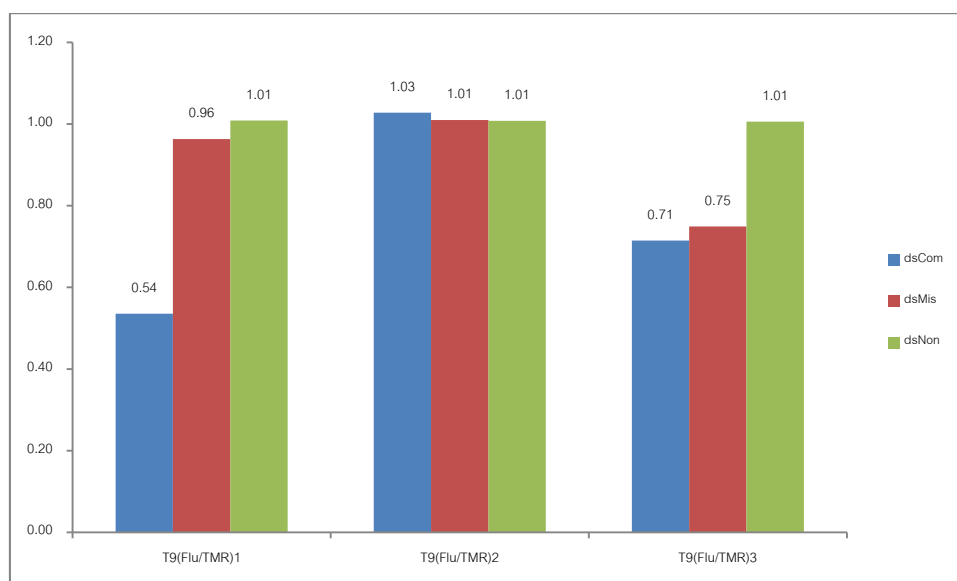
Figure 3.16 Enhancement factor of **T9(Flu/TMR)1**, **T9(Flu/TMR)2** and **T9(Flu/TMR)3** with various DNA. The conditions are the same as in **Figure 3.15**.

In another series of dual-labeled acpcPNA probe, the FRET pair consisting of 4-amino-7-nitrobenzofurazan (NBD) as the donor and benzophenoxazine dyes (7-(dimethylamino)-1-hydroxy-3H-phenoxazin-3-one (Phenoxazine red, PheR) [79], or 9-diethylamino-5-benzo[α]phenoxazinone (Nile red, Nr) [80] as the acceptor were used. The fluorescence spectra of the **T9(NBD/PheR)** probe in the absence of the DNA target showed two emissions at 539 nm (NBD; 80 a.u) and 629 nm (PheR; 40 a.u). In the presence of complementary DNA, the fluorescence intensity of NBD was slightly decreased (80 to 55 a.u) while the fluorecscence intensity of **PheR** was slightly increased (40 to 55 a.u). Unfortunately, the fluorescence spectra of the same PNA in the presence of mismatched DNA were similar to complementary DNA (**Figure 3.17**). Again, the results of **T9(NBD/PheR)** contradicted our design, which predicted an increase in NBD (donor) and decrease in PheR (acceptor) fluorescences. These results suggest that the two labels are mutually quenched in the single stranded state similar to the Flu-TMR pair discussed above. For comparison, PNA T9 with single NBD label was synthesized. The fluorescence of this **T9(NBD)** PNA is much higher in the single stranded form (325 a.u.). Quenching of the NBD was observed in the hybrids with complementary or mismatched DNA (325 to 130 a.u. and 325 to 156 a.u., respectively)

but not as large as when the PheR was also present. This confirms that there are some interactions between NBD and PheR labels. The enhancement factors of **T9(NBD/PheR)** are in the range of 0.51, 0.56 and 1.06 for complementary, mismatched and non-complementary DNA (**Table 3.3**). Again, the value of f less than unity means that the fluorescence change is in the opposite direction to the expected model. Quite surprisingly, the complementary and mismatched hybrids gave almost identical fluorescence change despite of the large T_m difference (66 vs 36 °C).
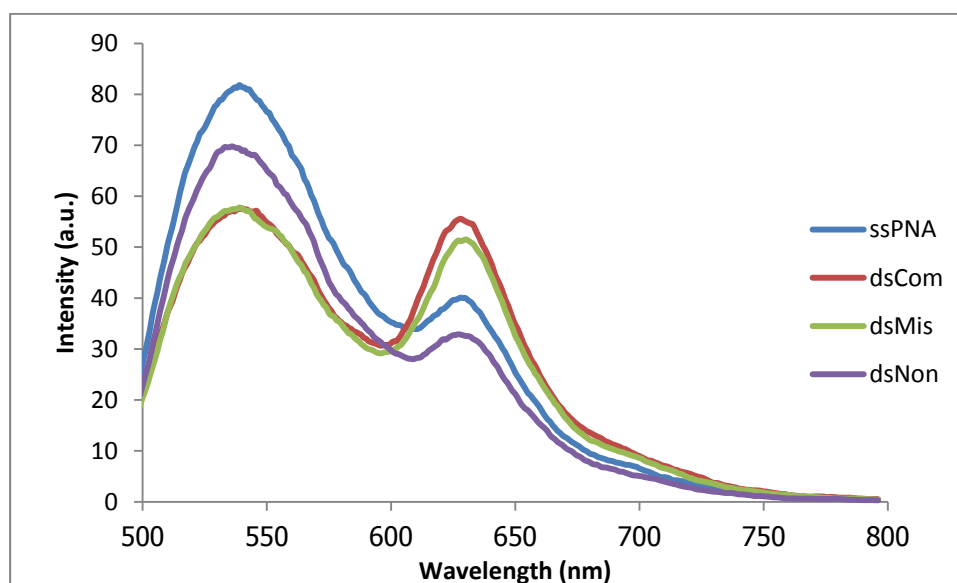
Figure 3.17 Fluorescence spectra of **T9(NBD/PheR)** in the absence and presence of various DNA (comp DNA = dA9, mismatch DNA = dAAAACAAAA, noncomp DNA = dAGTGCTGAT); Conditions: [PNA] = 1.0 μM and [DNA] = 1.2 μM in 10 mM sodium phosphate buffer pH 7, excitation wavelength = 490 nm, PMT voltage = medium
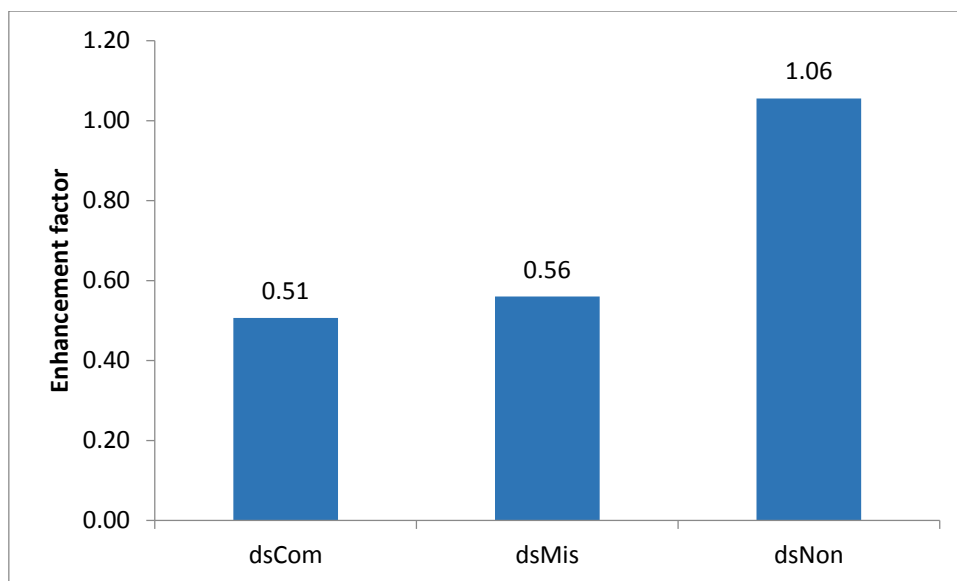
Figure 3.18 Enhancement factor **of T9(NBD/PheR)** with various DNA. The conditions are the same as in **Figure 3.17**.

A new FRET pair, NBD (donor) and Nile red (acceptor) was used in another PNA probe **T9(NBD/Nr)** because the emission spectra of NBD nicely overlaps with absorption spectra of Nile red. The fluorescence spectra of single stranded **T9(NBD/Nr)** exhibited two emissions at 539 nm (NBD; 10 a.u) and 630 nm (Nr, 50 a.u) (**Figure 3.19**). When complementary and mismatched DNAs were added, the fluorescence intensity of both the donor and acceptor were increased. The fluorescence increase of the NBD was more pronounced in the complementary pairs. Thus **T9(NBD/Nr)** showed enhancement factor [$f = (F_{ds}/F_{ss})_{539}/((F_{ds}/F_{ss})_{649}$] in the range of 0.65, 0.36 and 1.12 for DNAcom, DNAmis and DNAnon respectively (**Figure 3.20**). Again, the value of f less than unity means that the fluorescence change is still in the opposite direction to the expected model. The mismatch discrimination was also not good.
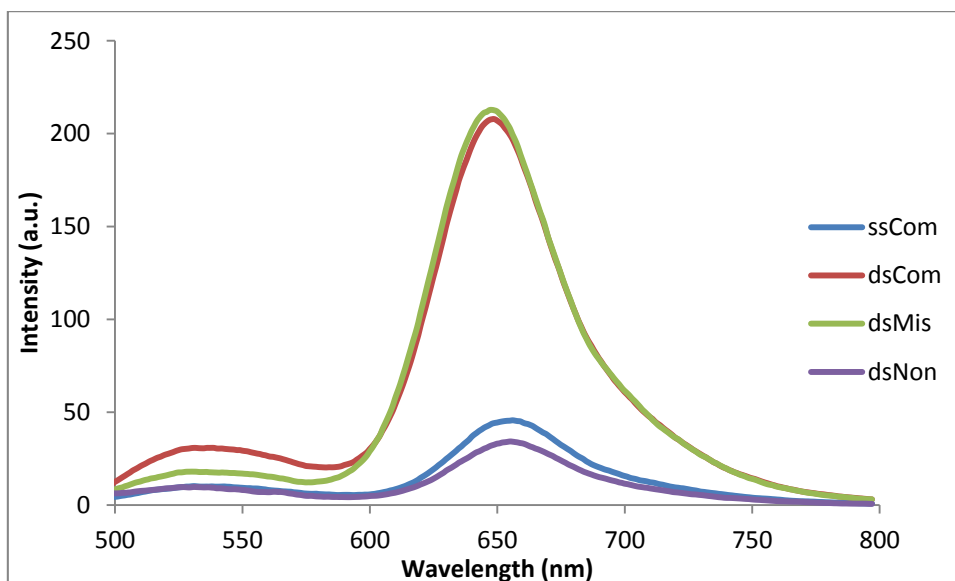
Figure 3.19 Fluorescence spectra of **T9(NBD/Nr)** with complementary, mismatch and non-complementary DNA (comp DNA = dA$_9$, mismatched DNA = dAAAACAAAA, non-comp DNA = AGTGCTGAT); Conditions [PNA] = 1.0 μM and [DNA] = 1.2 μM in 10 mM sodium phosphate buffer pH 7, excitation wavelength = 490 nm, PMT voltage = high
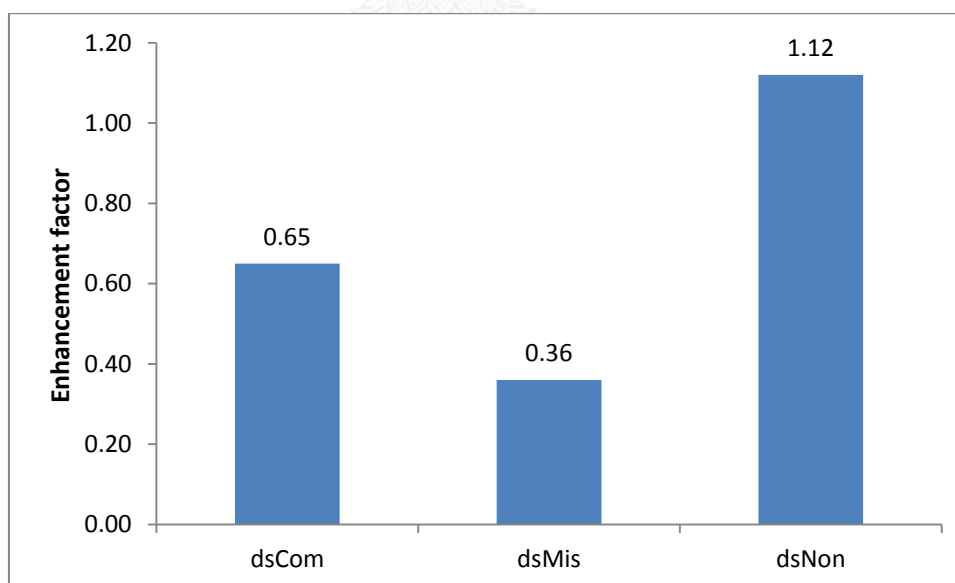
Figure 3.20 Enhancement factor of **T9(NBD/Nr)** with various DNA. The conditions are the same as in **Figure 3.19**.

The dansyl (Dns) and Nile red (Nr) were also used as another potential FRET pair. The fluorescence spectrum of single stranded **T9(Dns/Nr)** showed weak emissions of both dansyl at 548 nm (4 a.u) and Nile red at 649 nm (9 a.u) upon excitation at 330 nm (absorption of dansyl) (**Figure 3.21**). The presence of complementary DNA resulted in a slight increase in the donor (Dns) emission at 548 nm (2.4 folds) and a large increase in the Nile red acceptor emission at 649 nm from 9 to 153 a.u. (17 folds). For mismatch DNA, the emission of the donor was almost unchanged and the acceptor emission increased from 6 to 48 a.u. (5 folds). No change in both the emissions of the donor and acceptor was observed in the presence of non-complementary DNA, indicating the high specificity. The f ratios of complementary, mismatched and non-complementary DNA hybrids were 0.50, 0.18 and 0.35, respectively (**Table 3.4**). Melting temperature also comfirmed specificity of PNA-DNA hybrid (dsCom = 54.4 $^{\circ}$C, dsMis = 32.0 $^{\circ}$C and dsNon <20 $^{\circ}$C). Moreover, we compared the fluorescence of **T9(Dns/Nr)** with **T9(Dns)** acpcPNA. The fluorescence at 548 nm of the single stranded **T9(Dns)** was 60 a.u., and does not change much in the presence of DNA (complementary: 80 a.u., mismatch: no change). The results confirmed the Dns label was strongly quenched by energy transfer to the Nr label.
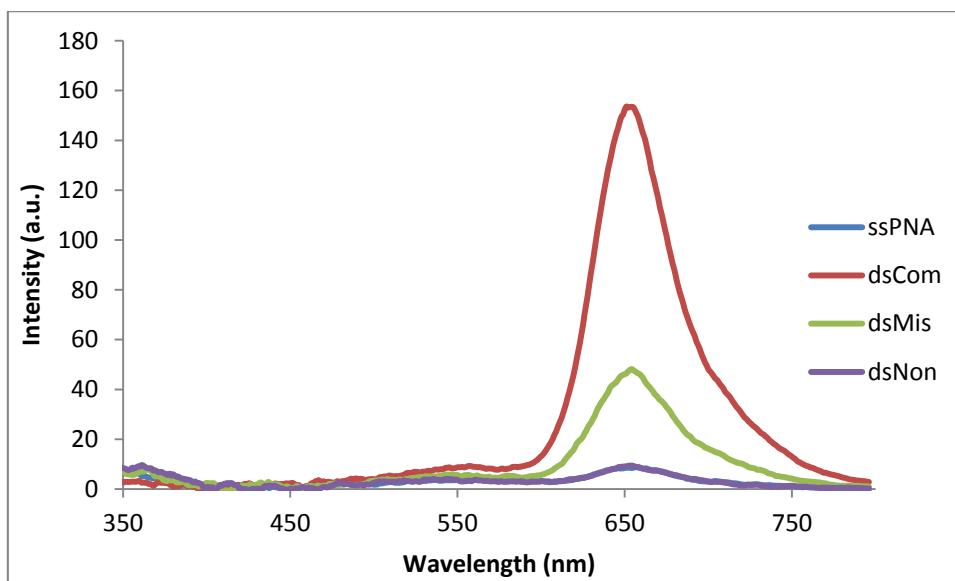
Figure 3.21 Fluorescence spectra of **T9(Dns/Nr)** with complementary, mismatch and non-complementary DNA (comp DNA = dA9, mismatched DNA = dAAAACAAAA, non-comp DNA = AGTGCTGAT); Conditions: [PNA] = 1.0 μM and [DNA] = 1.2 μM in 10 mM sodium phosphate buffer pH 7, excitation wavelength = 340 nm, PMT voltage = high
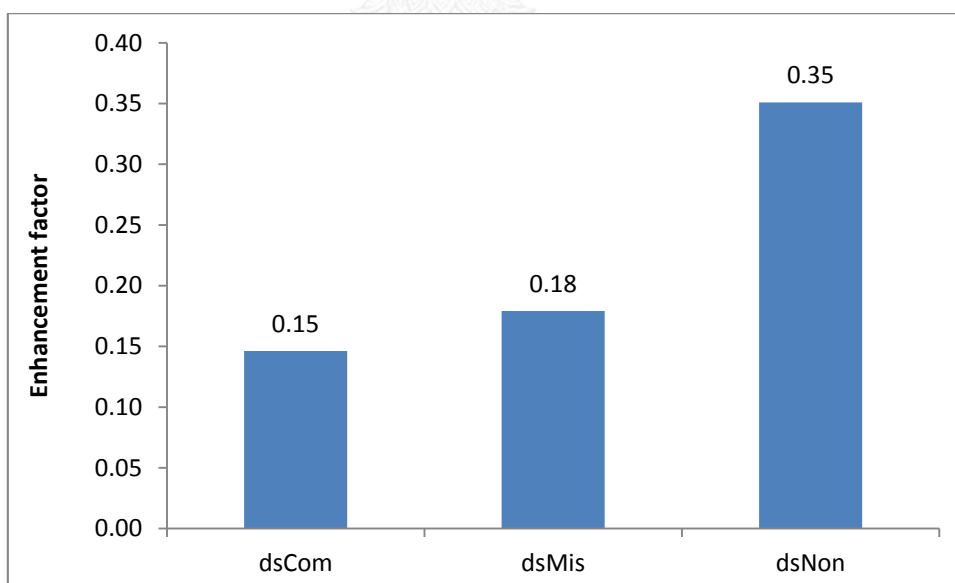
**Figure 3.22** Enhancement factor of **T9(Dns/Nr)** with various DNA. The conditions are the same as in **Figure 3.21.**

The above results suggest that none of the proposed FRET pairs worked according to the design in **Figure 3.1**. In most cases, the UV-vis spectra of the doubly-labeled PNA and their hybrids with complementary DNA showed significant difference in the shape and extinction coefficient of either or both the donors and acceptors (**Figure 3.23**). This suggests that there are ground state interactions between the two dyes in single stranded probe. This leads to quenching of the dyes, which invalidates our design. Nevertheless, in several dyes combinations, significant fluorescence change were observed when compared single stranded PNA and their DNA hybrids. In some cases, the change is sufficient to discriminate between complementary and single mismatched DNA targets. A few combinations of dyes including Flu/TMR, Cou2/Flu and Dns/Nr were selected for further experiments with mix-sequence PNA/DNA.
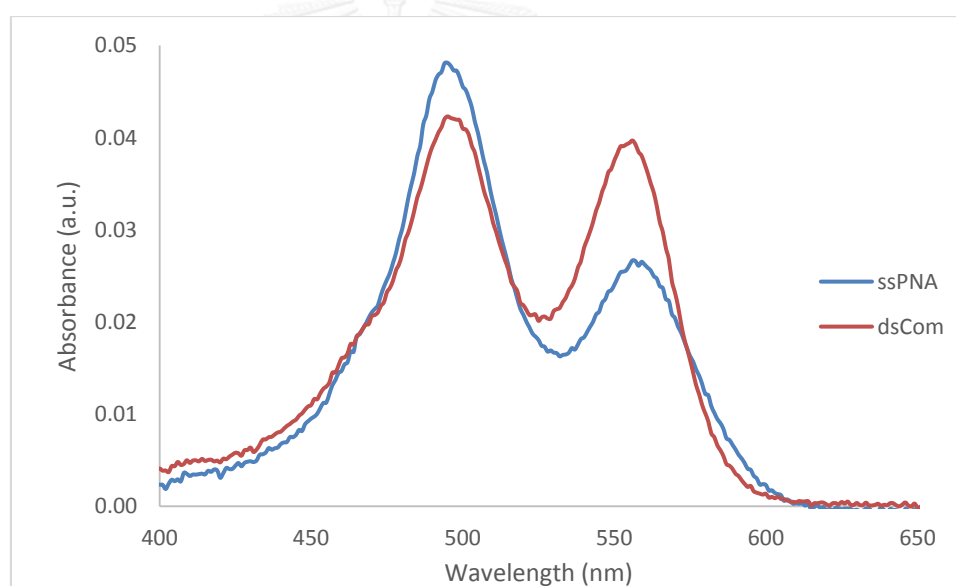
Figure 3.23 Uv-vis spectrua of **T9(Flu/TMR)1** (ssPNA) and its hybrid with dA9 (dsCom); Conditions: [PNA] = 1.0 µM and [DNA] = 1.2 µM in 10 mM sodium phosphate buffer pH 7.

3.1.7 Optical properties of mix-sequence doubly-labeled acpcPNA probe

Three FRET pairs from the above experiments with T9 sequences were chosen for further studies with mix-sequence acpcPNA. The arbitrarily chosen PNA sequence was AGT<u>TA</u>TCC<u>CT</u>GC (**M12**). The two dyes were placed between the underlined bores

to keep them at 5 bases apart. The fluorescence properties of the **M12(Flu/TMR)** were first investigated. Two fluorescence emission peaks were observed at 520 nm (Flu) and 573 mn (TMR) after excited at 490 nm (absorption of Flu). The single stranded PNA exhibited a high fluorescence emission of Flu (122 a.u.) and low fluorescence emission of TMR (50 a.u.). In the prescence of complementary and mismatched DNA, the fluorescence of both the donor and acceptor were increased (**Figure 3.24**). Enhancement factor (*f*) in the range of 0.66, 0.84 and 1.04 were achieved for complementary, mismatched and non-complementary DNA respectively (**Figure 3.25**). The fluorescence change in the complementary case was less than the **T9(Flu/TMR)** probe, and the specificity was not as good. Melting temperature analyses confirmed the specificity of the PNA-DNA binding (complementary: T_m = 47.6 $^{\circ}$C, mismatched: T_m = 30.0 $^{\circ}$C, non-complementary: T_m <20 $^{\circ}$C).
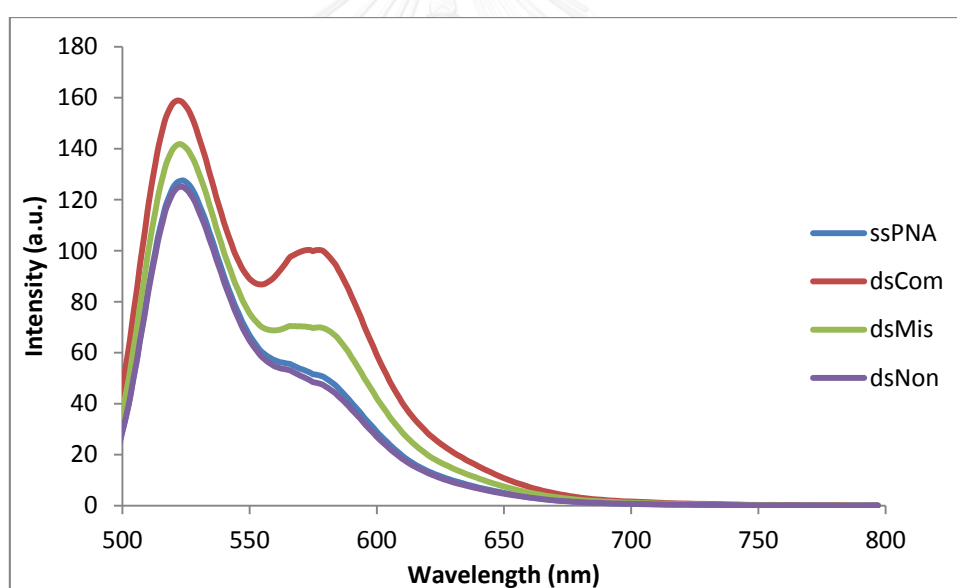
Figure 3.24 Fluorescence spectra of **Mix12(Flu/TMR)1** with complementary, mismatch and non-complementary DNA (comp DNA = GCAGGGATAACT, mismatched DNA = GCAGCGATAACT, non-comp DNA = AGTGCTGAT); Conditions: [PNA] = 1.0 μM and [DNA] = 1.2 μM in 10 mM sodium phosphate buffer pH 7, excitation wavelength = 490 nm, PMT voltage = medium.
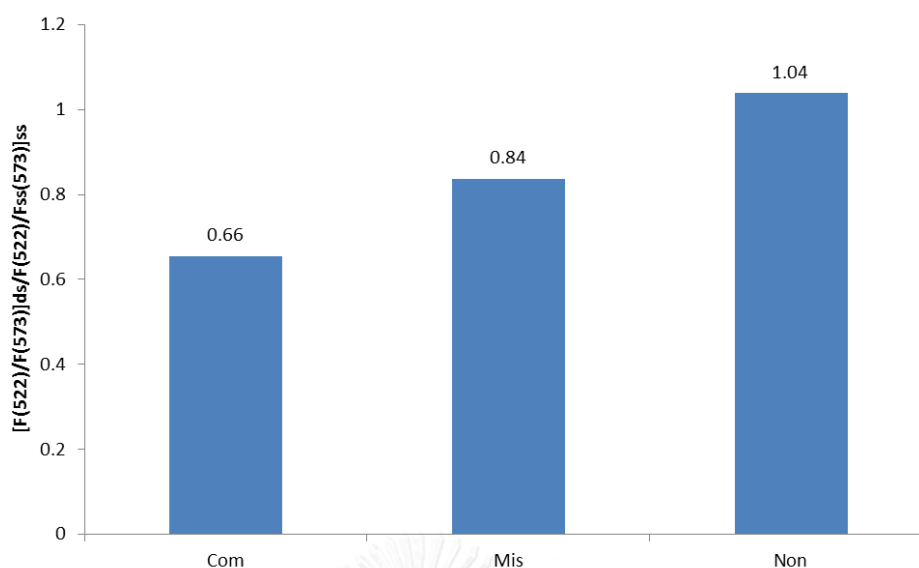
Figure 3.25 Enhancement factors (*f*) of **Mix12(Flu/TMR)** with various DNA. The conditions are the same as in **Figure 3.24.**

In addition, the Cou2 donor (attached via a C2 linker) and fluorescein acceptor pairs were also attached onto the **M12** acpcPNA probe. In single stranded form, two fluorescence emissions were observed at 448 nm (coumarin) and 520 nm (fluorescein) upon excitation at 330 nm. In the duplex form, the fluorescence emissions of both the donor and acceptor were increased relative to the single-stranded form. The enhancement factor (*f*) values are shown in **Figure 3.27**. In this case the single mismatch DNA gave similar change to the complementary DNA hybrid. This can be explained by the relatively high melting temperature of the single mismatched hybrid. The specificity could conceivably be improved by increasing the temperature or by the use of S1 nuclease to digest the mismatched DNA [63].
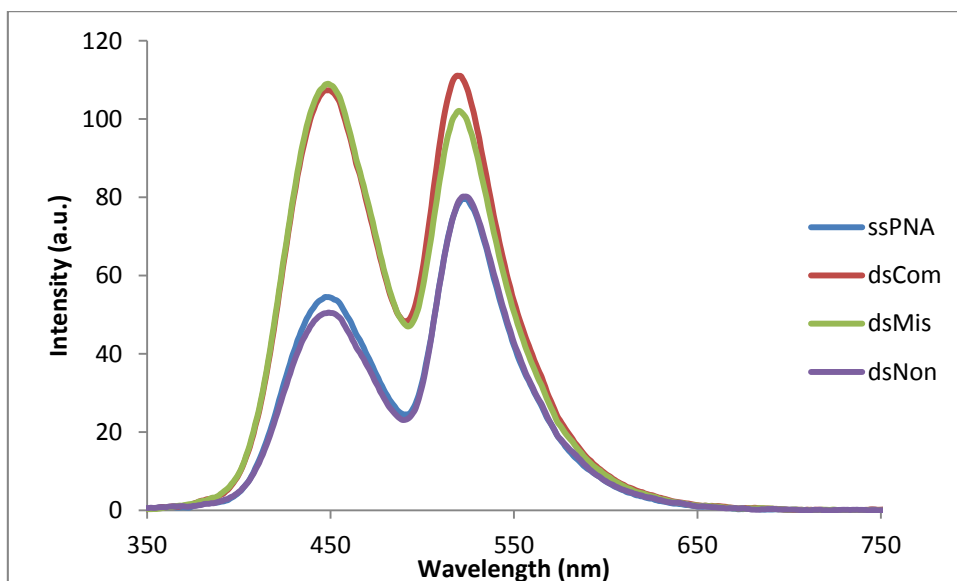
Figure 3.26 Fluorescence spectra of **Mix12(C2Cou2/Flu)** with complementary, mismatch and non-complementary DNA (comp DNA = dA9, mismatched DNA = dAAAACAAAA, non-comp DNA = AGTGCTGAT); Conditions: [PNA] = 1.0 μM and [DNA] = 1.2 μM in 10 mM sodium phosphate buffer pH 7, excitation wavelength = 340 nm, PMT voltage = medium
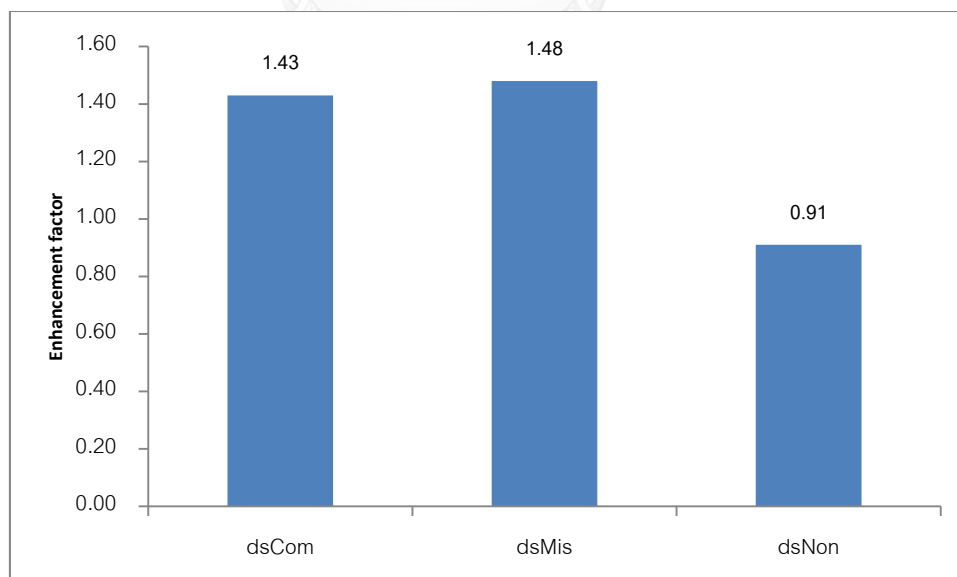

Figure 3.27 Enhancement factors (*f*) of **Mix12(C2Cou2/Flu)** with various DNA. The conditions are the same as in **Figure 3.26.**

Finally, the dansyl (donor) and Nile red (acceptor) pair was attached onto another **M12** acpcPNA probe. The fluorescence studies of the resulting **M12(Dns/Nr)** also showed that the Nile red label is quenched by the Dns similar to the **T9(Dns/Nr)**. In the single stranded form, **M12(Dns/Nr)** exhibited a weak fluorescence at 650 nm. (6 a.u.) and almost negligible fluorescence at the Dns emission. In the presence of complementary DNA, the fluorescence of Nile red was increased from 6 to 30 a.u. (5.0 folds). No significant change was observed in the Dns fluorescence. However, mismatched DNA also caused fluorescence change. In fact, the change was more pronounced than complementary DNA.
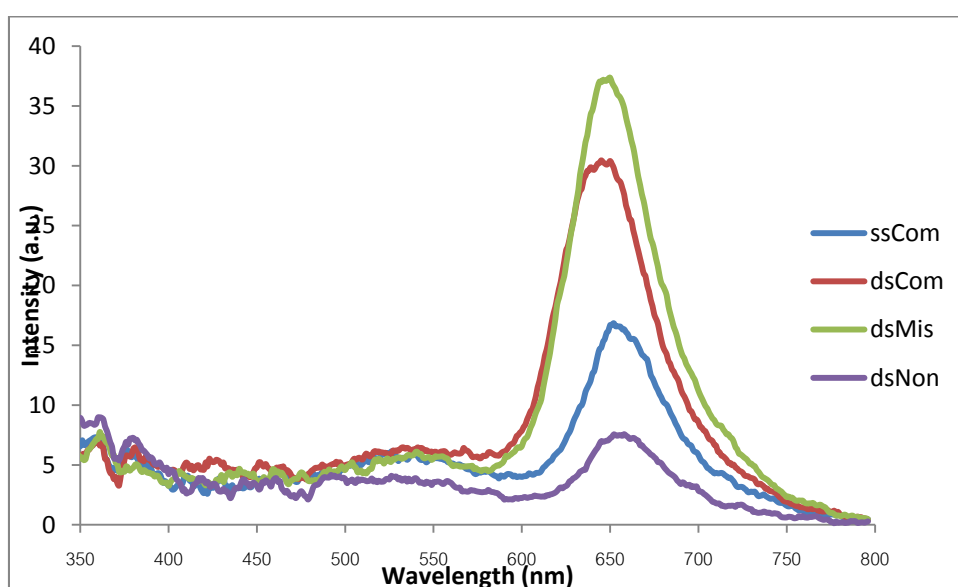
Figure 3.28 Fluorescence spectra of **Mix12(Dns/Nr)** with complementary, mismatch and non-complementary DNA (comp DNA = dA9, mismatched DNA = dAAAACAAAA, non-comp DNA = AGTGCTGAT); Conditions: [PNA] = 1.0 µM and [DNA] = 1.2 µM in 10 mM sodium phosphate buffer pH 7, excitation wavelength = 340 nm, PMT voltage = high
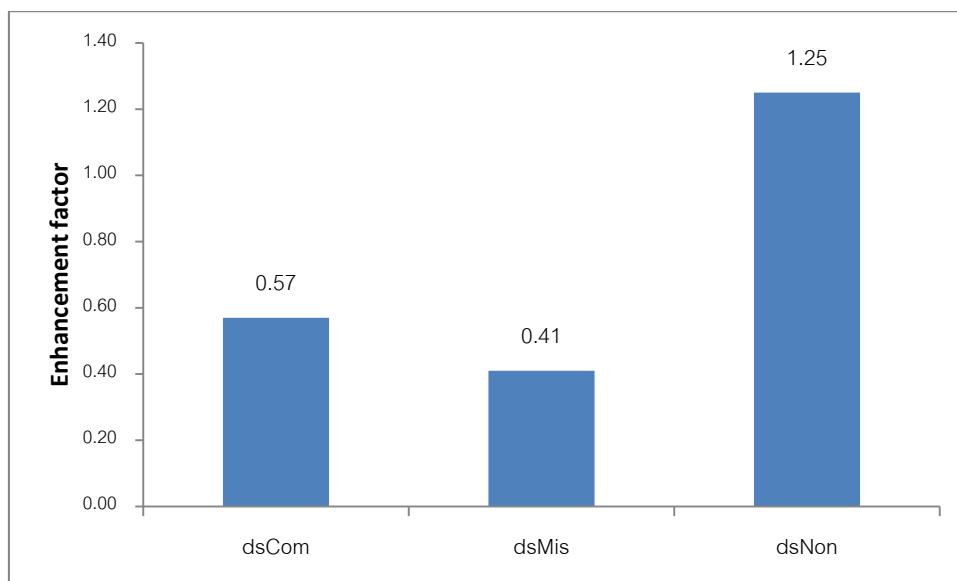
Figure 3.29 Enhancement factors (*f*) of **Mix12(Dns/Nr)** with various DNA. The conditions are the same as in **Figure 3.28**.

In this section, we successfully synthesized several internally dual-labeled acpcPNA probes by the combined use of *o*-Ns and Tfa-protected APC monomer. Various dyes were attached onto the acpcPNA backbone via acylation or reductive alkylation-Click stategy. Unfortunately, the fluorophore-quencher pair gave only modest quenching efficiency and therefore the fluorescence changes upon hybridization with DNA were not large. The FRET probes showed significant quenching as a result of ground state interactions between the dyes due to a close contact. None of them showed the fluorescence change patterns that are in agreement with the model. In addition, the degree of fluorescence change as well as the specificity was quite modest and very sensitive to the sequence. As a result, we decided to abandon this approach in order to seek for a better probe design. The results will be discussed in the next two sections.

3.2 Doubly end-labeled pyrrolidinyl PNA probes

Many research groups had reported fluorescence oligonucleotide probes that were labeled with two or more dyes, most commonly a fluorophore and a quencher,

at both ends of the probes[21, 40]. The fluorescence change relies on the change of the secondary structure of the probe upon hybridization which results in different interactions between the two dyes when compared to the free probes. A classic example is molecular beacon developed by Tyagi and Kramer [21] which is a long piece of DNA that is partially self-complementary at the ends and thus can form a stem-loop structure. A fluorophore and a quencher were attached at each end of the molecular beacon. In the free probe, the stem-loop structure force the two dyes in close proximity, resulting in efficient quenching of the fluorophore. Hybridization in the loop region causes dissociation of the stem, which separates the two dyes and therefore the fluorescence increases. (**Figure 3.30**) Many variations of the same concept had been reported over the past 20 years. Despite the beauty of the concept, the design of molecular beacons is not a simple task because the stem part must be strong enough to make efficient quenching. On the other hand, too strong interaction will result in inefficient un-quenching due to unfavorable thermodynamics and/or slow kinetics of the DNA hybridization. Therefore there are needs to develop a new molecular beacon probe that does not require the stem-loop structure to operate. It has been reported for some times that PNA beacons do not require the stem-loop structure because PNA tends to form a compact structure in the solution [52]. The PNA beacon can carry two dyes or just one environment sensitive fluorophore that can change its fluorescence in response to hybridization with DNA.[53, 54] However, quenching in these linear probes are often inefficient and are highly sequence-dependent. Moreover, specificity is generally not high due to the ability of the linear probes to form hybrid with mismatched target.
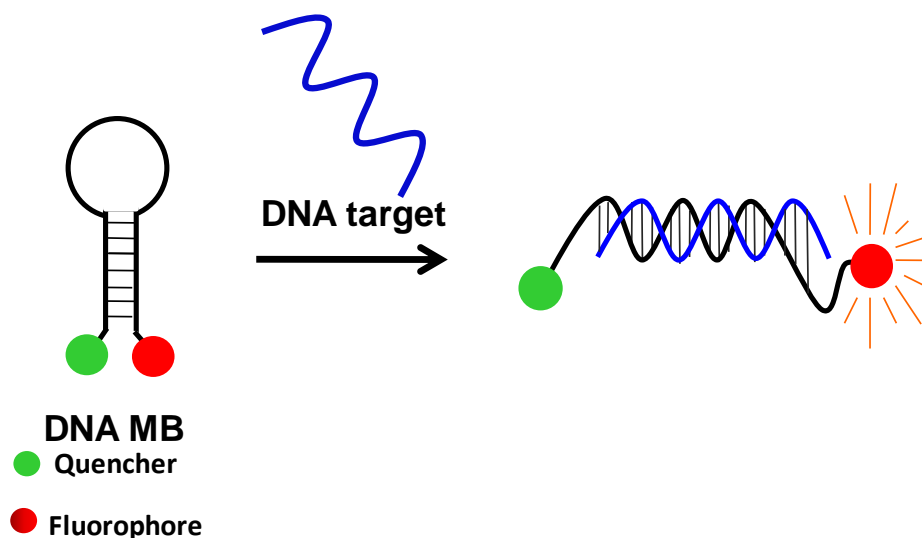
Figure 3.30 The concept of molecular beacons

In this work, a new doubly end-labeled pyrrolidinyl PNA probe is proposed. In most other PNA beacons, the two fluorophores are placed at the two ends of the molecules [50], or one at the end and the other within the PNA strand [62, 63]. We propose that a more efficient quenching should be possible if the two labels are placed very close to each other at one end of the PNA probe. If the labels are chosen so that one of them can intercalate between the base stacks (internal labeling) or stack to the terminal base pair (terminal labeling) of the PNA-DNA hybrids, the interactions between the two dyes in the free and hybridized probes should be sufficiently different to allow discrimination between the two states (**Figure 3.31**). A similar concept had been previously applied to DNA, but the fluorescence change was not large, and the mismatch discrimination was not perfect [77, 81-83]. It was hoped that the acpcPNA version of such doubly end-labeled probe should give a superior performance than the corresponding DNA probes.

= Fluorophore ▮ = Quencher
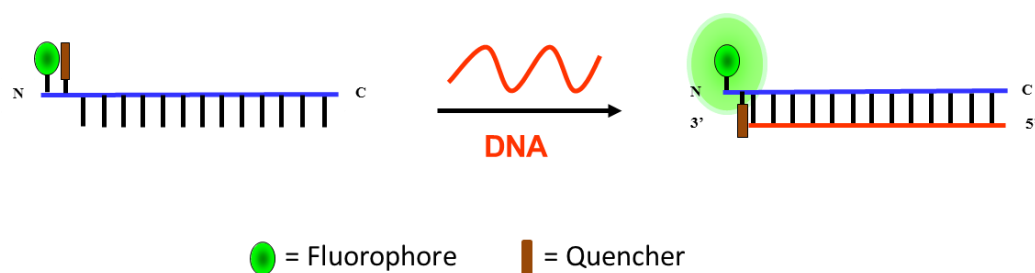
Figure 3.31 Schematic diagram showing the concept of doubly end-labeled PNA beacon

3.2.1 Attachment of the fluorophore-quencher pair onto acpcPNA

Fluorescein was chosen as the fluorophore because this dye doesn't interact with DNA bases, and anthraquinone was chosen as the quencher because our previous T_m studies indicated that it can stabilize the PNA-DNA duplex by end-stacking [84]. The fluorophore/quencher pair was attached to the N-terinal of acpcPNA via simple acylation on the solid support.

The strategy for end-labeling of acpcPNA with the fluorophore-quencher pair involves initial attachment of Fmoc-Lys(Tfa)-OH at the N-terminal of the PNA. The Fmoc group was removed and the free N_α-position was modified with 5(6)-carboxyfluorescein. Next the Tfa protecting group of lysine N_ε-position was removed by aqueous ammonia:dioxane at 60 °C followed by attachment with anthraquinone-2-carboxylic acid. The reaction progess was monitored by MALDI-TOF mass spectrometry. (**Figure 3.32**)
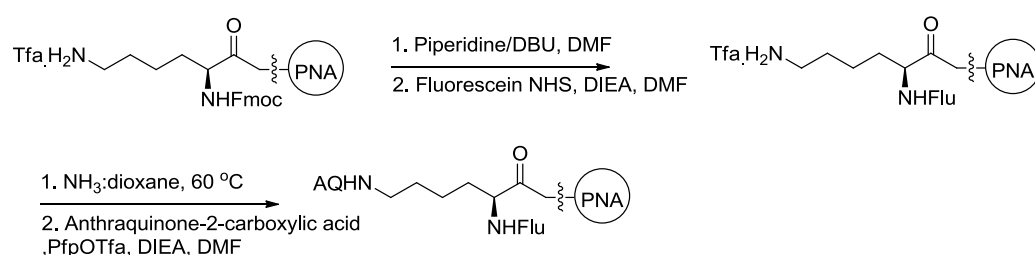
Figure 3.32 Synthesis doubly end-labeled acpcPNA probes

When the coupling reaction was complete, the labeled acpcPNA probe was cleaved from the solid support using trifluoroacetic acid (TFA) and was purified by reverse phase HPLC and characterized by MALDI-TOF mass spectrometry. In all case, the acpcPNA probes were obtained in purity >90%. The sequence, retention time calculated mass, observed mass and isolated yield of doubly end-labeled acpcPNA probes successfully synthesized are shown in **Table 3.5**. Some variations of the chemistry, dyes and linkers have been made for comparison purposes. For example, the more rigid APC was used as a scaffold in **(AQ/Flu)apcM10G** to compare with the more flexible lysine scaffold in **(AQ/Flu)LysM10G**. The positions of the dye attachement were reversed (i.e. Flu to Nϵ and AQ to Nα) in **(Flu/AQ)LysM10G**. To study the effect of different quenchers, the anthraquinone label was omitted in **(Flu)LysM10G** or changed to dabcyl in **(Dab/Flu)LysM10G**. The effect of distance from the terminal base pairs was studied by removing the last spacer before adding the dye in **(AQ/Flu)Lys(-acpc)M10G**. Finally, other (AQ/Flu)-labeled acpcPNA sequences with different terminal bases were synthesized to compare the effect of terminal base pairs.

Table 3.5 Sequences and yield of modified PNA obtained after HPLC purification

PNA	Sequence (N$\rightarrow$C)	t_R (min)[a]	m/z (calcd)[b]	m/z (found)[c]	%yield
(AQ/Flu)LysM10G	Nε-AQ-Nα-Flu-Lys-GTAGATCACT-LysNH$_2$	31.2	4239.5	4237.6	3.0
(AQ/Flu)apcM10G	Nδ-AQ-Nα-Flu-apc-GTAGATCACT-LysNH$_2$	30.5	4111.3	4111.1	6.9
(Flu/AQ)LysM10G	Nε-Flu-Nα-AQ-Lys GTAGATCACT-LysNH$_2$	30.8	4239.5	4237.6	6.8
(Flu)LysM10G	Nα-Flu-Lys GTAGATCACT-LysNH$_2$	31.5	4004.2	4002.5	12.0
(Dab/Flu)LysM10G	Nε-Dab-Nα-Flu-Lys GTAGATCACT-LysNH$_2$	31.2	4256.5	4253.6	5.5
(AQ/Flu)Lys(-acpc)M10G	Nε-AQ-Nα-Flu-Lys (x)GTAGATCACT-LysNH$_2$	35.8	4128.5	4126.9	9.5
(AQ/Flu)LysM11-C	Nε-AQ-Nα-Flu-Lys CTAAATTCAGA-LysNH$_2$	34.5	4564.8	4564.1	3.8
(AQ/Flu)LysM12-A	Nε-AQ-Nα-Flu-Lys AGTTATCCCTGC-LysNH$_2$	34.8	4865.1	4863.6	4.1
(AQ/Flu)LysM10-T	Nε-AQ-Nα-Flu-Lys TACAGACATC-LysNH$_2$	34.3	4208.4	4205.9	9.1
(AQ/TMR)LysM10-G	Nε-AQ-Nα-TMR-Lys TACAGACATC-LysNH$_2$	N.D.[d]	4293.6	4294.6	8.3

[a]hplc condition: reverse phase analysis used: flow rate 0.5 mL/min., The gradient consists of two solvent systems: A (0.1% TFA in MilliQ water) and B (0.1% TFA in methanol). The elution started with 90:10 A:B followed by a linear gradient to 10:90 A:B (90:10) for 5 min followed by a linear gradient to A:B (10:90) over period of 60 min, with a holding time for 10 min before reverting back to A:B (90:10).

[b]Average mass (M+H$^+$)

[c]MALDI-TOF

[d]Not determined

3.2.2 Fluorescence properties of doubly end-labeled acpcPNA probes

The fluorescence properties of the acpcPNA probes before and after hybridization with DNA targe were next studied. The fluorescence intensity ratio and its DNA hybrids are summarized in **Table3.6**. When excited at 490 nm, the single strand **(AQ/Flu)LysM10G** probe (1 μM) exhibited a weak fluorescence emission of fluorescein at 520 nm (F_{ss} = 19 a.u.)(**Figure 3.33**). This value is much lower than the corresponding fluorescein-labeled probe without the anthraquinone **(Flu)LysM10G** (F_{ss} = 400 a.u.) (**Figure 3.34**). This indicates an efficient quenching of the fluorescein by the anthraquinone.

Remarkably, when the complementary DNA was added, the fluorescence intensity of the duplex at 520 nm was increased by a factor of 18.8 relative to the single strand **(AQ/Flu)LysM10G** probe (**Table 3.6** and **Figure 3.33**). This is in accordance with the design shown in **Figure 3.31**. However, it is important to confirm that the fluorescence increase is specific to only the complementary DNA target.

Next, the fluorescence properties of the hybrids between complementary and various single base mismatched DNA targets of the **(AQ/Flu)LysM10G** probe were next investigated. When the DNA strands contained a mismatched base, the fluorescence intensities were also increase relative to the single strand probe, but to a much smaller extent when compared to the complementary DNA. The fluorescence intensity ratios (F_{ds}/F_{ss}) of the duplexes of **(AQ/Flu)LysM10G** and internal dC-pT mismatched (**Mis**), terminal pG-dA mismatched (**MisA**) and non-complementary (**Non**) DNA were increased by 6.0, 7.0 and 1.1 folds, respectively (**Table 3.6**). These values are much smaller that the increase of 18.8 fold observed with complementary DNA (**Com**). This translates to a relative fluorescence change between complementary and single mismatched (internal and terminal) hybrids of between 2.7 to 3.1 folds. From the results, it can be concluded that the fluorescence of the **(AQ/Flu)LysM10G** is highly sensitive to its hybridization state and specific to the DNA hybridization event. It is important to note that even terminal mismatches, which are generally difficult to detect due to the similar stabilities of the complementary and terminal mismatched duplexes, can be readily distinguished from complementary DNA with this probe. The

fluorescence increase after complementary DNA hybridization is much larger than linear DNA probes [77, 81] and singly-labeled acpcPNA probes that we had previously reported [60, 62, 63] as well as the internal doubly labeled acpcPNA probes reported in **Section 3.1**. The only acpcPNA probe that showed higher fluorescence change is the thiazole orange (TO) labeled probe which gave up to 22 folds fluorescence increase with the same sequence [63]. However, the TO dye tends to bind to DNA non-specifically and large fluorescence are occasionally observed even with completely unrelated DNA sequences [63]. This present end-labeled probe is much better than such TO-labeled acpcPNA probe in terms of specificity.

Figure 3.33 Fluorescence spectra of **(AQ/Flu)LysM10G** with complementary (dsCom), internal mismatch (dsMis), mismatched (dsMisA) and non-complementary (dsNon). Fluorescence were measured in 10 mM sodium phosphate buffer pH 7.0, [PNA] = 1.0 µM and [DNA] = 1.2 µM, excitation wavelength = 490 nm, PMT voltage = medium.

The fluorescene increase after hybridization with complementary DNA of **(AQ/Flu)LysM10G** was almost the same at that of single stranded **(Flu)LysM10G**. This suggests that the un-quenching was almost prefect. Interestingly, the fluorescence of **(Flu)LysM10G** in the presence of various DNA, except the non-complementary one, showed slightly decreased fluorescence as shown in **Figure 3.34** and **Table 3.6.** This effect had been previously observed in fluorescein labeled PNA with terminal G or C,

and was explained by quenching of the fluorescein label by the terminal G-C base pair [85]. However, stacking of the anthraquinone on top of the terminal G-C pair appears to block this quenching process and therefore a large fluorescence increase was observed in **(AQ/Flu)LysM10G** hybrids.

Figure 3.34 Fluorescence spectra of **(Flu)LysM10G** with complementary (dsCom), internal mismatch (dsMis), mismatched (dsMisA) and non-complementary (dsNon). Fluorescence were measured in 10 mM sodium phosphate buffer pH 7.0, [PNA] = 1.0 μM and [DNA] = 1.2 μM, excitation wavelength = 490 nm, PMT voltage = medium.

3.2.3 Effects of chemistry for dye attachment to form doubly end-labeled acpcPNA probes

The interaction between the fluorescein and anthraquinone that lead to quenching can occurs by several means. To understand the mechanism of the quenching, the effect of rigid linker on the fluorescence properties of AQFlu-end labeled PNA probe was investigated by changing the flexible lysine to a more rigid APC spacer. The fluorescein was attached to the N_α and the anthraquinone was attached to the N_ε of the APC linker. According to this design, the two dyes cannot efficiently interact by contact quenching because of the rigid nature of the APC linker. Single stranded **(AQ/Flu)apcM10G** showed relatively higher fluorescence than

(AQ/Flu)LysM10G (88 vs 19 a.u.). This suggests that the major pathway for quenching in the AQ/Flu labeled probe through a flexible lysine linker is due to contact quenching. This proposal is supported by the significant change of the UV spectra of the fluorescein dye before and after hybridization with the DNA (**Figure 3.35**).
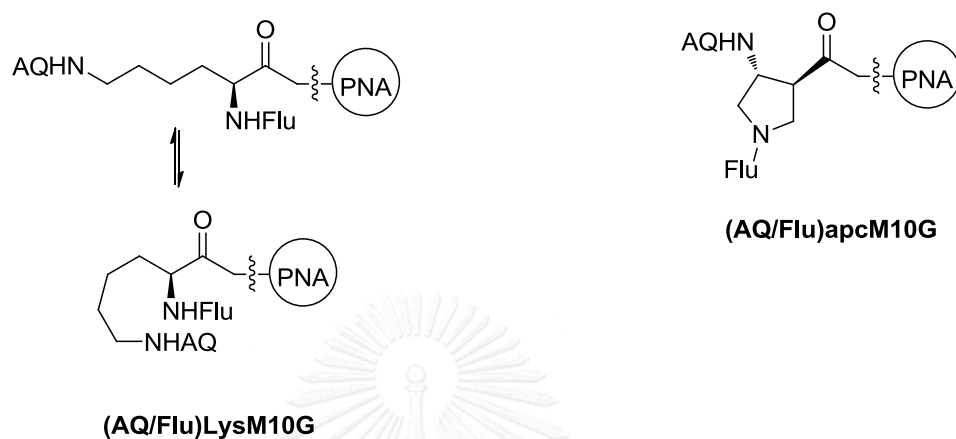
Figure 3.35 Chemical structures of **(AQ/Flu)LysM10G** and **(AQ/Flu)apcM10G**
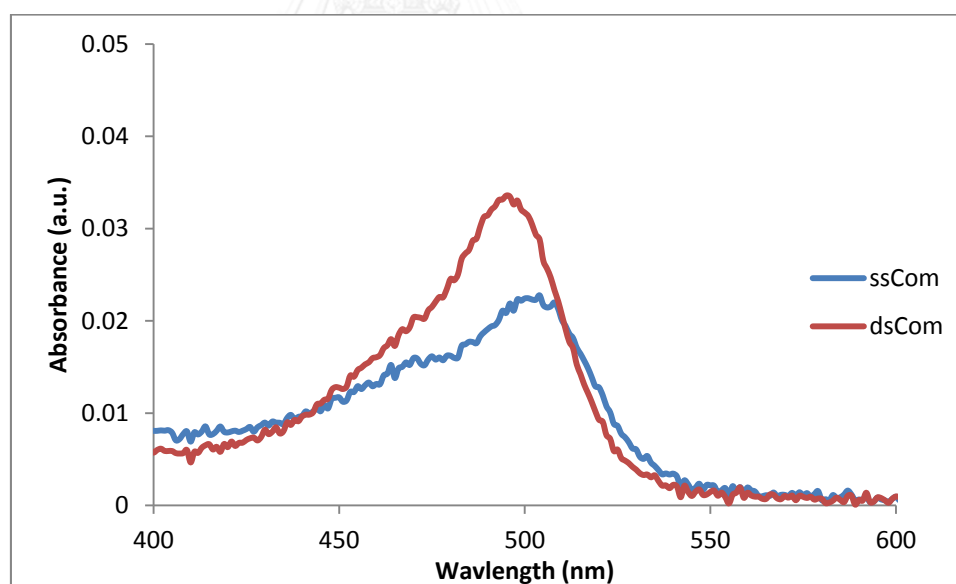
Figure 3.36 UV-vis spectrum of **(AQ/Flu)LysM10G** with complementary (dsCom), Conditions: 10 mM sodium phosphate buffer pH 7.0, [PNA] = 1. µM and [DNA] = 1.2 µM

The presence of the rigid APC linker may also interfere with the stacking of the anthraquinone to the terminal base pair of the duplex, and therefore the fluorescence

increase after addition of the complementary DNA was only marginal (2.4 folds). Incidentally, the fluorescence was similar to the complementary DNA hybrid of **(Flu)LysM10G** (ca. 200 a.u.). Negligible fluorescence increases were observed with internally mismatched and non-complementary DNA (2.0 and 1.1 folds, respectively). However, the terminally mismatched DNA gave almost as large fluorescence increase (2.0 fold) as the complementary DNA target. These results suggest that the fluorescence change may not involve stacking of the anthraquinone, which is clearly different from the **(AQ/Flu)LysM10G** probe (**Figure 3.37** and **Table 3.6**).

Figure 3.37 Fluorescence spectra of **(AQ/Flu)apcM10G** with complementary (dsCom), internal mismatch (dsMis), mismatched (dsMisA) and non-complementary (dsNon) Fluorescence were measured in 10 mM sodium phosphate buffer pH 7.0, [PNA] = 1.0 µM and [DNA] = 1.2 µM, excitation wavelength = 490 nm, PMT voltage = medium.

When acpcPNA was synthesized, an ACPC linker was always present at the N-terminus. This will increase the extra distance between the dye on the lysine scaffold and the terminal base pair of the PNA-DNA hybrid. Since the working principle of the present double end-labeled probe relies on stacking interaction, the presence or absence of this linker may have significant effects on the performance of the probe.

To investigate this problem, another double end-labeled probe **(AQ/Flu)(-acpc)LysM10G** without the extra ACPC spacer at the N-terminus (before the lysine scaffold) of acpcPNA was synthesized to compare fluorescence properties with the original AQ/Flu probe **(AQ/Flu)LysM10G** that have the ACPC linker.

As shown by the fluorescence spectra in **Figure 3.38**, single stranded **(AQ/Flu)(-acpc)LysM10G** exhibited low fluorescence intensity (36 a.u.). After addition of complementary DNA, the fluorescence was increased from 30 to 177 a.u. (approximately 5.8 folds). The fluorescence of hybrids with internal single mismatched and non-complementary DNA was much lower than with complementary DNA (55 and 36 a.u. respectively). The fluorescence of the terminal mismatched hybrid was also much higher (140 a.u.) than the internal mismatched hybrid. When compared to **(AQ/Flu)LysM10G**, the fluorescence increases of **(AQ/Flu)(-acpc)LysM10G** hybrids were much smaller in all cases. This suggests that the un-quenching is not perfect. The specificity of the **(AQ/Flu)(-acpc)LysM10G** is also lower than the **(AQ/Flu)LysM10G** probe. It is therefore important to have the ACPC spacer before the lysine scaffold. This may keep the proper distance between the terminal base pairs and the anthraquinone to allow efficient stacking.
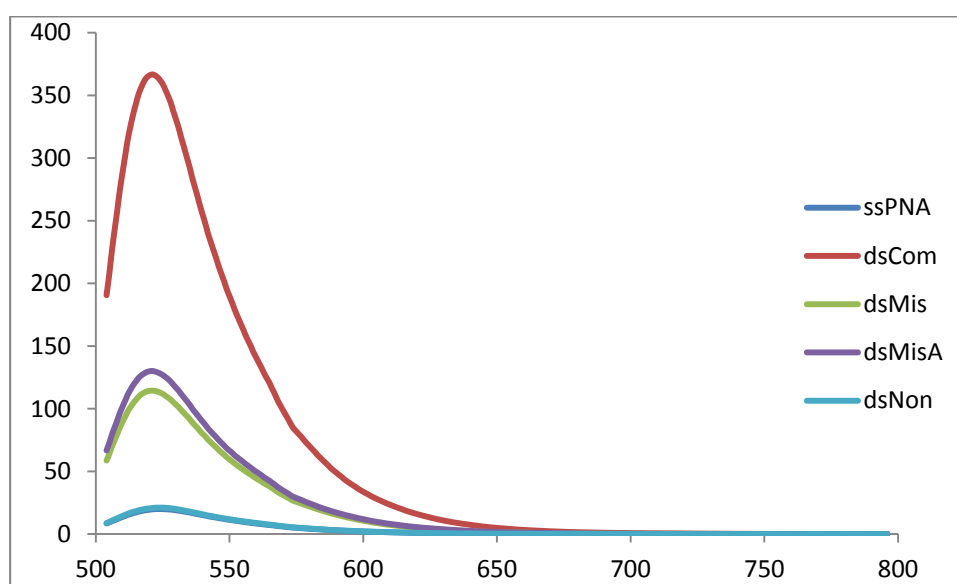
Figure 3.38 Fluorescence spectra of **(AQ/Flu)Lys(-acpc)M10G** with complementary (dsCom), internal mismatch (dsMis), mismatched (dsMisA) and non-complementary (dsNon). Fluorescence were measured in 10 mM sodium phosphate buffer pH 7.0, [PNA] = 1.0 µM and [DNA] = 1.2 µM, excitation wavelength = 490 nm, PMT voltage = medium.

.

The effect of switching the position of the fluorescein and anthraquinone label on the lysine scaffold from N_ε-AQ and N_α-Flu in **(AQ/Flu)LysM10G** to N_ε-Flu and N_α-AQ in **(Flu/AQ)LysM10G** was next investigated. The fluorescence spectra are shown in **Figure 3.3**9 and the fluorescence ratios are summarized in **Table 3.6**. In the single strand state, **(Flu/AQ)LysM10G** exhibited low fluorescence emission (60 a.u.). The duplexes with DNA showed fluorescence ratios of 2.1, 1.6, 1.6 and 1.1 for complementary, internal mismatched, terminal mismatched and non-complementary DNA, respectively. The results confirmed that position of the two labels have significant effects to the fluorescence properties. In this case, the low fluorescence increase can be explained by the less efficient stacking of the anthraquinone label linked to the more rigid N_α position. The higher fluorescence background of the single stranded DNA is more difficult to explain, but it may indicate less efficient contact between the two dyes.
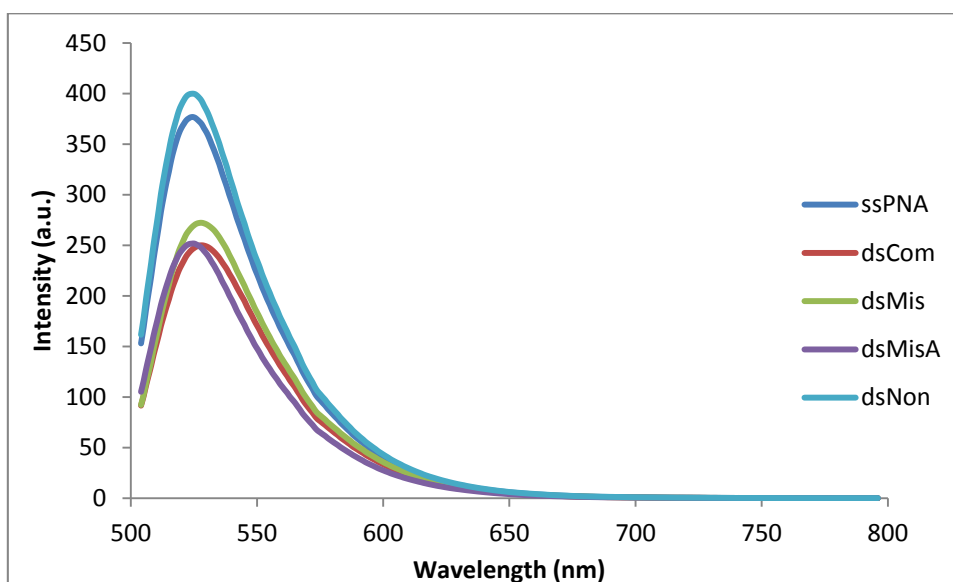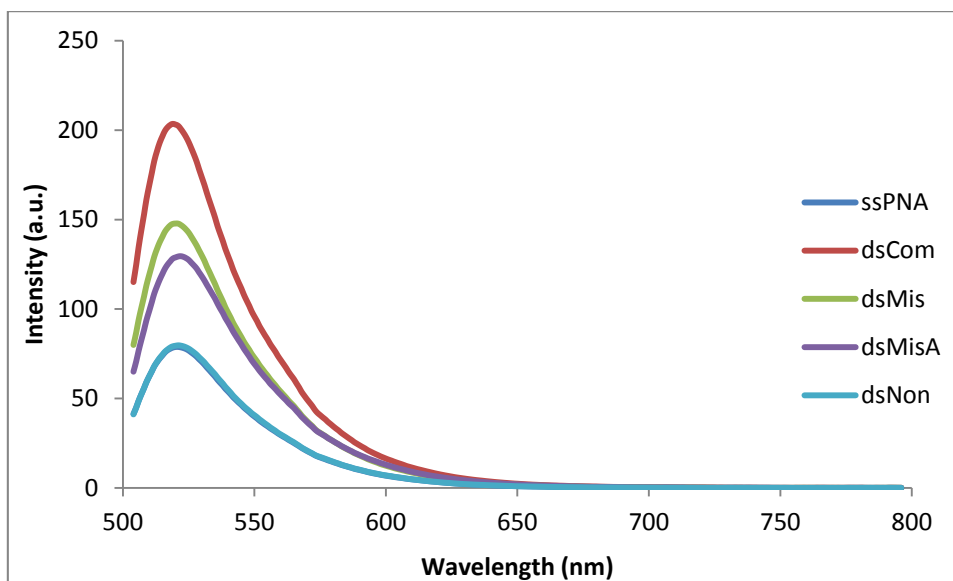
Figure 3.39 Fluorescence spectra of **(Flu/AQ)LysM10G** with complementary (dsCom), internal mismatch (dsMis), mismatched (dsMisA) and non-complementary (dsNon). Fluorescence were measured in 10 mM sodium phosphate buffer pH 7.0, [PNA] = 1.0 µM and [DNA] = 1.2 µM, excitation wavelength = 490 nm, PMT voltage = medium.

3.2.4 Effects of different dye combinations in doubly end-labeled acpcPNA probes

Finally, different combinations of fluorophore and quencher pairs were compared. The **(Dab/Flu)LysM10G** and **(AQ/Flu)LysM10G** have the same design, except that the AQ was replaced with dabcyl as a quencher. Single stranded **(Dab/Flu)LysM10G** showed very low fluorescence (ca. 3 a.u.) as compared to **(AQ/Flu)LysM10G** (ca. 20 a.u.). This indicates that dabcyl is a more efficient quencher than AQ. Addition of DNA resulted in fluorescence increases, (**Figure 3.40**) but the maximum fluorescence observed was only 12 a.u. in the presence of complementary DNA (4.7 folds). Mismatched and non-complementary DNA gave lower fluorescence. This suggests that the un-quenching process was not complete after the hybridization. Therefore AQ is a superior quencher for this purpose.
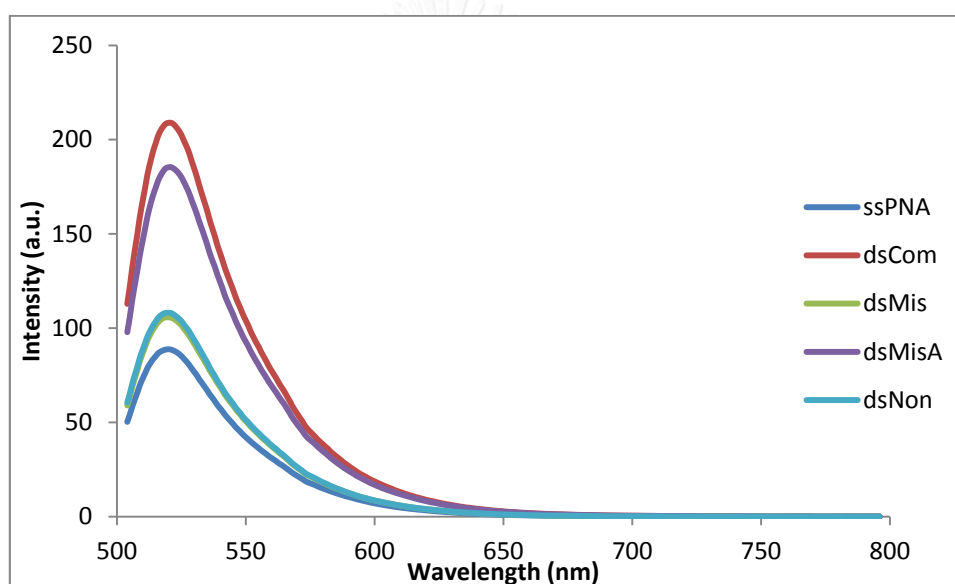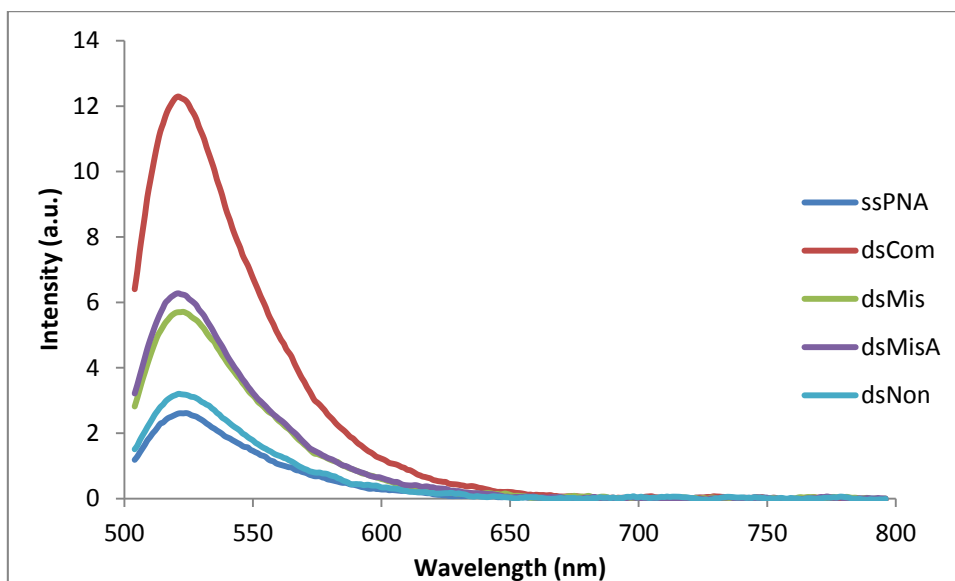
Figure 3.40 Fluorescence spectra of **(Dab/Flu)LysM10G** with complementary (dsCom), internal mismatch (dsMis), mismatched (dsMisA) and non-complementary (dsNon). Fluorescence were measured in 10 mM sodium phosphate buffer pH 7.0, [PNA] = 1.0 µM and [DNA] = 1.2 µM, excitation wavelength = 490 nm, PMT voltage = medium.

To investigate the possibility of using other fluorophores, the fluorescein label in **(AQ/Flu)LysM10G** was replaced with tetramethylrhodamine (TMR). Gratifyingly, the fluorescence of single stranded **(AQ/TMR)LysM10G** was also very low (17 a.u.). Such high quenching efficiency of TMR by AQ despite the poor spectral overlap confirmed that the quenching occurred by contact quenching rather than by FRET mechanism. In the presence of complementary DNA, the fluorescence emission showed a large increase to 307 a.u. (18 folds). Similar to the **(AQ/Flu)LysM10G** probe, the fluorescence of complementary PNA-DNA hybrids was higher than all mismatched DNA hybrids (84 and 52 a.u., which correspond to 4.9 and 3.0 folds of fluorescence increase) (**Figure 3.41**). Surprisingly, non-complementary lowered the fluorescence further to ca. 5 a.u. This unexpected results require further studies to understand, but doesn't negatively affect the performance of the present dual end-labeled probes. The results indicate that the design should be general for many combinations of fluorophore and quencher.
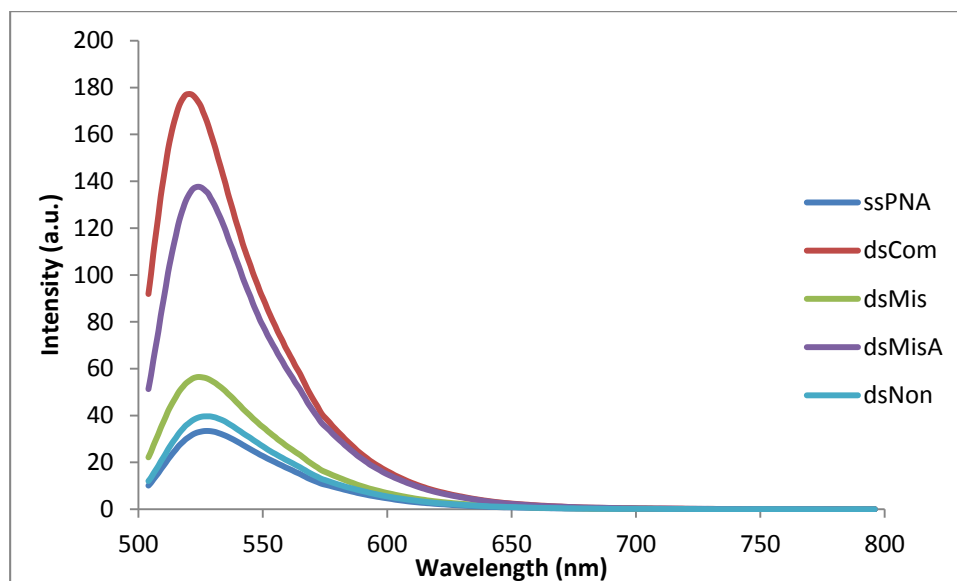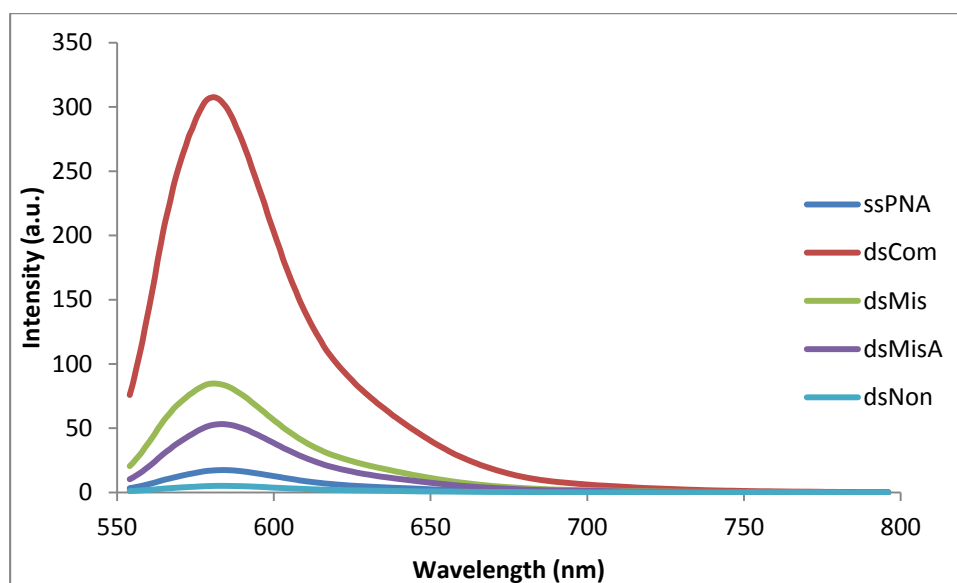
Figure 3.41 Fluorescence spectra of **(AQ/TMR)LysM10G** with complementary (dsCom), internal mismatch (dsMis), mismatched (dsMisA) and non-complementary (dsNon). Fluorescence were measured in 10 mM sodium phosphate buffer pH 7.0, [PNA] = 1.0 µM and [DNA] = 1.2 µM, excitation wavelength = 490 nm, PMT voltage = medium.

3.2.5 Comparison of performances of doubly end-labeled acpcPNA probes

To allow comparison between different probes, all results are summarized in **Table 3.6** and the performances of selected probes **(AQ/Flu)LysM10G**, **(AQ/Flu)apcM10G**, **(Flu/AQ)LysM10G**, **(AQ/Flu)Lys(-acpc)M10G** and **(Dab/Flu)LysM10G)** are compared in **Figure 3.42**. It becomes apparent that the **(AQ/Flu)LysM10G** and **(AQ/TMR)LysM10G** probes offer the best performance due to the largest difference between single stranded and hybridized states. They also exhibit good specificity for complementary over internal and terminal mismatched DNA targets.

Table 3.6 Fluorescence intensity of doubly end-labeled acpcPNAs and their hybrids with DNA (Conditions: 10 mM sodium phosphate buffer pH 7.0, [PNA] = 1.0 μM and [DNA] = 1.2 μM, excitation wavelength = 490 nm, PMT voltage = high)

PNA	DNA	DNA sequences(5′⟶3′)	F_{ss} (a.u)	F_{ds} (a.u)	F_{ds}/F_{ss}
(AQ/Flu)LysM10G	Com	AGTGATCTAC	19.4	365.9	18.8
	Mis	AGTGCTCTAC	19.0	114.3	6.0
	MisA	AGTGATCTAA	18.5	129.8	7.0
	Non	TCTGCATTTAG	19.0	20.5	1.1
(AQ/Flu)apcM10G	Com	AGTGATCTAC	88.8	208.9	2.4
	Mis	AGTGCTCTAC	90.7	105.7	1.2
	MisA	AGTGATCTAA	92.6	185.3	2.0
	Non	TCTGCATTTAG	97.4	108.2	1.1
(AQ/Flu)Lys(-acpc)M10G	Com	AGTGATCTAC	30.6	177.2	5.8
	Mis	AGTGCTCTAC	31.0	54.5	1.8
	MisA	AGTGATCTAA	31.9	133.7	4.2
	Non	TCTGCATTTAG	32.5	36.5	1.1
(Flu/AQ)LysM10G	Com	AGTGATCTAC	78.8	203.1	2.6
	Mis	AGTGCTCTAC	93.2	147.8	1.6
	MisA	AGTGATCTAA	80.5	128.9	1.6
	Non	TCTGCATTTAG	72.0	79.5	1.1
(Dab/Flu)LysM10G	Com	AGTGATCTAC	2.6	12.	4.8
	Mis	AGTGCTCTAC	2.5	5.7	2.3
	MisA	AGTGATCTAA	2.8	6.3	2.2
	Non	TCTGCATTTAG	3.0	3.2	1.1
(Flu)LysM10G	Com	AGTGATCTAC	366.0	230.2	0.6
	Mis	AGTGCTCTAC	377.6	250.2	0.7
	MisA	AGTGATCTAA	386.7	244.5	0.6
	Non	TCTGCATTTAG	402.5	388.7	1.0
(AQ/TMR)LysM10G	Com	AGTGATCTAC	17.0	307.2	18.1
	Mis	AGTGCTCTAC	17.4	84.7	4.9
	MisA	AGTGATCTAA	17.6	52.3	3.0
	Non	TCTGCATTTAG	18.0	5.0	0.3
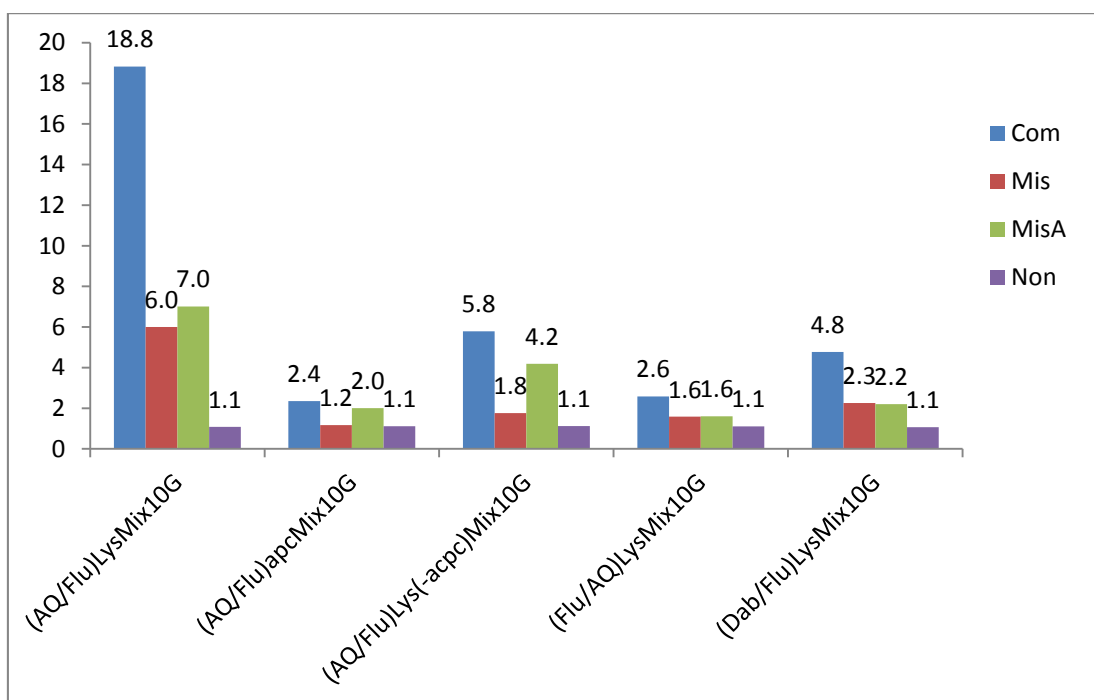
Figure 3.42 Comparison of F_{ds}/F_{ss} values of various Flu/AQ dual end-labeled acpcpPNA in the presence of complementary (Com), internal mismatched (Mis), terminal mismatched (MisA) and non-complementary (Non) DNAs. Fluorescence were measured in 10 mM sodium phosphate buffer pH 7.0, [PNA] = 1.0 µM and [DNA] = 1.2 µM, excitation wavelength = 490 nm, PMT voltage = medium.

3.2.6 Fluorescence properties of PNA probe hybridization at low concentrations

In this study, the fluorescence properties of the **(AQ/Flu)LysM10G** probe were investigated with a more extensive set of DNA targets. Due to the limited amounts of PNA probe available, the study was carried out at 0.1 µM, which was ten folds lower than the previous experiments. The results are summarized in **Figure 3.43** and **Table 3.7**. In the absence of DNA, the fluorescence emission was still low, but was rather high relative to the value at 1 µM. This may imply that some additional intermolecular processes may involve in the quenching at high concentrations. In the presence of complementary DNA, the fluorescence intensity of the duplex at 520 nm was increased by a factor of 12.3 relative to the single strand probe. This fluorescence increase is

smaller than the fluorescence ratio obtained at 1 µM, which may be attributed to the high fluorescence background and slow kinetics of the hybridization. Nevertheless, it confirms that the un-quenching effect can be reproduced in dilute solution, which should be more relevant for detection of real DNA samples.
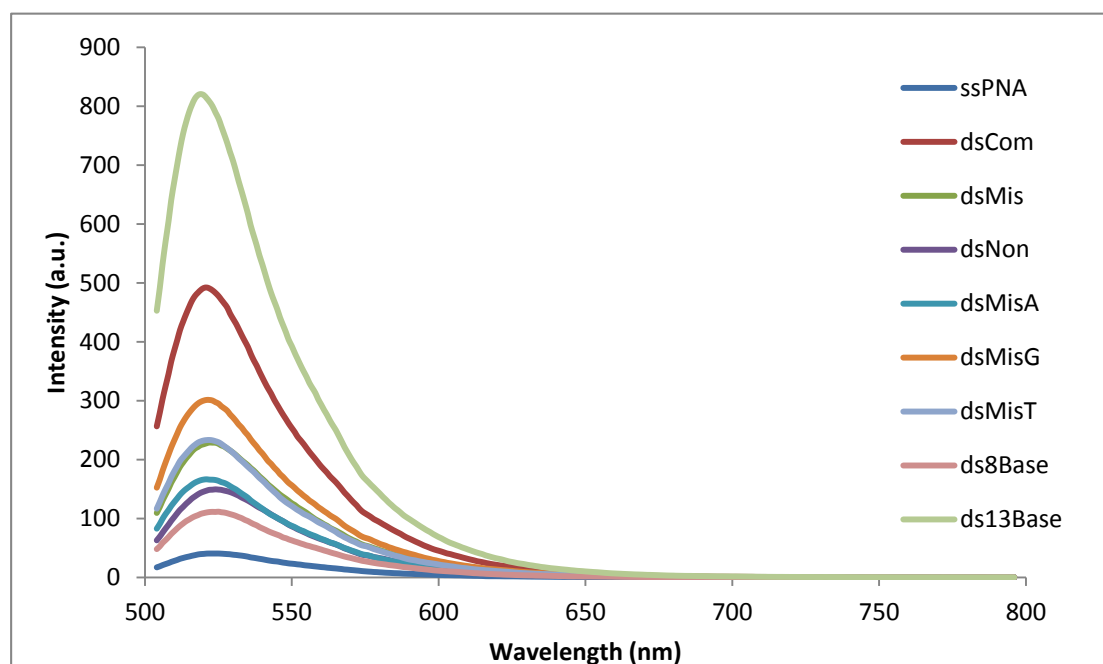
Figure 3.43 Fluorescence spectra of **(AQ/Flu)LysM10G** with various DNA, DNAcom: AGTGATCTAC, DNAmis: AGT GCT CTAC, DNAnon: TCTGCATTTAG, DNAmisA: AGTGATCTAA, DNAmisG: AGTGCTCTAG, DNAmisT: AGTGATCTAT, DNA8bases: AGTGCTCT, DNA13bases: AGTGATCTACTAC. Conditions: 10 mM sodium phosphate buffer pH 7.0, [PNA] = 0.10 µM and [DNA] = 0.12 µM, excitation wavelength 490 nm, PMT voltage = high

The fluorescence properties of **(AQ/Flu)LysM10G** in the presence of various other DNA targets were next investigated. When the DNA strand contained a mismatched base, the fluorescence intensities were increased relative to the single strand probe, but to a much smaller extent when compared to the complementary hybrid. When **(AQ/Flu)LysM10G)** was hybridized with an internal mismatched (**Mis**) and various terminal mismatched DNAs (**MisA**, **MisG** and **MisT**), the fluorescence

intensities of the duplex were increased by 3.4, 9.7 and 7.1 folds, respectively, as opposed to the increase of 12.3 fold with complementary DNA. This translates to discriminations between complementary and single mismatched (internal and terminal) hybrids of between 1.3 to 4.1 folds. In addition, when **(AQ/Flu)LysM10G** was hybridized with terminal deletion (**8base**) and long complementary DNA with extra hanging bases from the 3'-end (**13base**), the fluorescence intensities of duplex was increased by 3.3 and 18.3 folds, respectively. Although the terminal deletion DNA still gave some fluorescence increase, the much higher fluorescence increase of the long DNA is completely consistent with the probe design.

Table 3.7 Fluorescence intensity of doubly end-labeled acpcPNA hybrid with DNA (Conditions: 10 mM sodium phosphate buffer pH 7.0, [PNA] = 0.1 µM and [DNA] = 0.12 µM, excitation wavelength = 490 nm, PMT voltage = high)

PNA	DNA	DNA sequences(5′⟶3′)	F_{ds}/F_{ss}
(AQ/Flu)LysM10G	Com	AGTGATCTAC	12.3
	Mis	AGTGCTCTAC	5.80
	MisA	AGTGATCTAA	3.40
	MisT	AGTGATCTAT	7.06
	MisG	AGTGATCTAG	9.75
	Non	TCTGCATTTAG	3.00
	8base	AGTGATCT	3.31
	13base	AGTGATCTATAC	18.3

3.2.7 Effects of terminal nucleobase in the doubly end-labeled acpcPNA probes

More doubly end-labeled acpcPNA probes were designed for studying of the behavior of the probes in a broader context. All acpcPNA probes synthesized carried the anthraquinone/fluorescein labels at N_ε and $N\alpha$ of lysine at the N-termini. To investigate the effects of different neighboring nucleobases to the fluorescence properties of the dual end-labeled PNA probes and its duplexes with DNA, the AQ/Flu labeled acpcPNA probes **(AQ/Flu)LysM10T**, **(AQ/Flu)LysM11C** and **(AQ/Flu)LysM12A**,

which carried the base T, C and G at the N-termini were synthesized and their fluorescence properties studied and compared with the **(AQ/Flu)LysM10G** probe used in previously experiments as summarized in **Table 3.8**. The single stranded **(AQ/Flu)LysM10T**, **(AQ/Flu)LysM11C** and **(AQ/Flu)LysM12A** probes showed fluorescence intensity of 97, 33 and 153 respectively at 0.1 µM. The single stranded **(AQ/Flu)LysM10G** showed fluorescence intensity of 39 a.u. at the same concentration. In all cases, hybridization with complementary DNA resulted in fluorescence increases relative to single stranded probe. Except for the **(AQ/Flu)LysM11C** probe, the F_{ds}/F_{ss} values of complementary DNA hybrids of all other probes were smaller than that of the **(AQ/Flu)LysM10G** probe. In the worst case, only 4.4 fold increase was observed in the **(AQ/Flu)LysM10T** probe carrying the base T at the N-terminus. This suggests that the un-quenching is more efficient with G or C as terminal bases, which could be explained by the more efficient stacking interactions between anthraquinone and G-C pairs. In all cases, the fluorescence intensity ratios of hybrids with complementary DNAs were larger than with internal and terminal mismatched DNAs. However, the ratios are not as good as in the case of **(AQ/Flu)LysM10G** probe discussed earlier. However, since all experiments were carried out at a low concentration (0.1 µM), the fluorescence ratios as well as the mismatch selectivity may not be optimal due to the strong background fluorescence.

Table 3.8 Fluorescence intensity of doubly end-labeled acpcPNA hybrid with DNA (Conditions: 10 mM sodium phosphate buffer pH 7.0, [PNA] = 0.1 µM and [DNA] = 0.12 µM, excitation wavelength = 490 nm, PMT voltage = high)

| PNA	DNA	DNA sequences(5′→3′)	F_{ss} (a.u.)	F_{ds} (a.u.)	F_{ds}/F_{ss}
(AQ/Flu)LysM10T	Com	GATGTCTGTA	153.8	675.5	4.39
	Mis(int)	GATGACTGTA	161.4	320.9	1.98
	Mis(ter)	GATGTCTGTC	146.9	417.5	2.84
(AQ/Flu)LysM11C	Com	TCTGAATTTAG	33.1	433.1	13.08
	Mis(int)	TCTGAGTTTAG	34.7	314.7	9.07
	Mis(ter)	TCTGAATTTAA	37.4	274.2	7.33
(AQ/Flu)LysM12A	Com	GCAGGGATAACT	97.1	717.0	7.38
	Mis(int)	GCAGGAATAACT	107.1	541.5	5.05
	Mis(ter)	GCAGGGATAACA	118.1	417.6	3.53
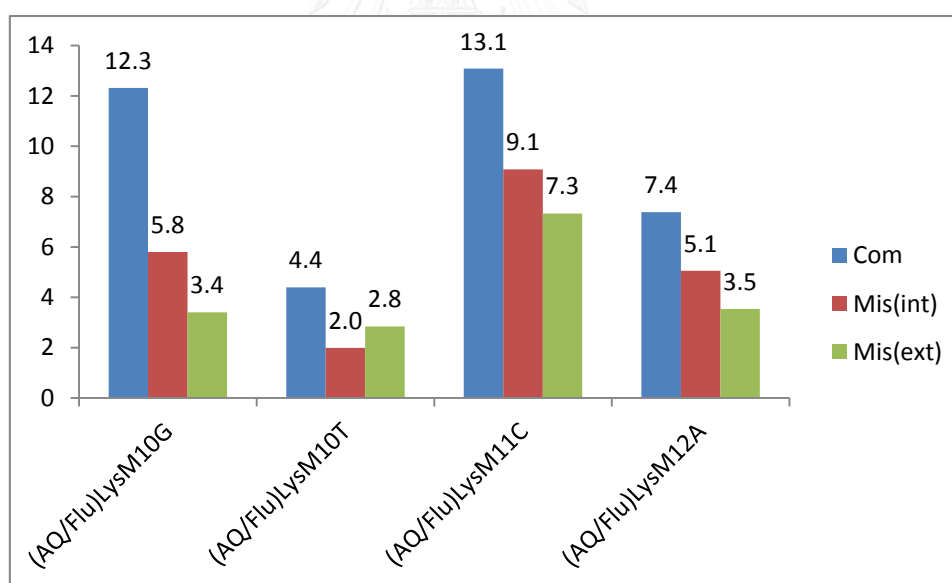
Figure 3.44 F_{ds}/F_{ss} of **(AQ/Flu)LysM10G**, **(AQ/Flu)LysM10T**, **(AQ/Flu)LysM11C**, **(AQ/Flu)LysM12A** and their hybrids with complementary (Com), internal mismatched [Mis(int)] and terminal mismatched [Mis(ext)] DNA. Conditions: 10 mM sodium phosphate buffer pH 7.0, [PNA] = 0.10 µM and [DNA] = 0.12 µM, excitation wavelength 490 nm, PMT voltage = high.

3.2.8 Attempts to improve the mismatch specificity by strand displacement

Although the aforementioned doubly end-labeled acpcPNA probes exhibited a large fluorescence increase when hybridized to the complementary DNA, the mismatch discrimination is less than satisfactory, especially at low concentrations. In order to improve the mismatch discrimination, the strand displacement concept was applied.[86] In classical displacement probes, two complementary oligonucleotide probes of different lengths are required. The longer strand is labeled at one end with a fluorophore and the shorter strand is labeled at the complementary end with a quencher. The hybrid between the two strands exhibits low fluorescence because the fluorophore is quenched by the quencher. The DNA target can displaced the short quencher strand because it can form more stable hybrid with the long fluorescence probe. After displacement of the quencher strand, the probe becomes fluorescent.[86-88]   The strand displacement should in principle be more specific than simple hybridization because the DNA target must form a sufficiently stable hybrid with the probe to initiate and sustain the displacement reaction. The thermodynamics and kinetics of the displacement should be readily controlled by adjusting the sequence and length of the probe to be displaced.

Following this concept, we proposed a displacement probe based on dual end-labeled acpcPNA by first forming a hybrid with a short, unlabeled DNA with truncated 3'-end. The resulting hybrid should be non-fluorescent similar to the single stranded probe because there is no terminal base pair for the anthraquinone to stack on top. Complementary DNA will displace the short DNA since it can form more stable hybrid. The displacement process should be accompanied by a fluorescence increase because the anthraquinone can now stack with the terminal base pairs. On the other hand, DNA with single base mismatch should form much less stable hybrid and therefore the displacement should be kinetically unfavorable.
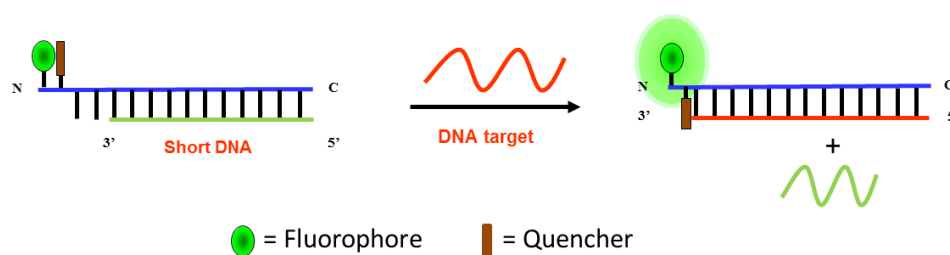
Figure 3.45 The concept of strand displacement reaction applied to the present dual end-labeled PNA probe.

The concept was prove by first forming a duplex between **(AQ/Flu)LysM10G** and a short complementary DNA with 3'-deletion (**8base**). The fluorescence of this probe is twice as high as the single stranded probe but still relatively low ($F_{ds}/F_{ss} \sim 2$) (**Figure 3.46**). Addition of DNA resulted in a slow increase of the fluorescence. A stable signal was observed after about 1 h at room temperature. The F/F_0 (F = fluorescence after the displacement reaction, F_0 = original fluorescence of the displacement probe before the displacement reaction) ratio reach a high value of ~11, which is comparable to the value obtained for the free probe (12.3 fold). The selectivity ratio $[(F_{ds}/F_{ss})_{comp}/(F_{ds}/F_{ss})_{mm}]$ improved from 2.1 (without displacement) to 5.5 (with displacement). This is quite different from the F/F_0 value of ~2 constantly observed with the internally mismatched DNA target. This experiment showed that the specificity of the dual end-labeled PNA probe can be further improved by the strand displacement concept.

Figure 3.46 PNA-DNA displacement of **(AQ/Flu)LysMix10G**-dAGTGATAT (8base) hybrids with complementary (dAGTGATCTAC, blue) and mismatched DNA (dAGTG$\underline{C}$TCTAC, red). Conditions: 10 mM sodium phosphate buffer pH 7.0, [PNA] = 0.1 μM and [DNA] = 0.12 μM, excitation wavelength 490 nm, PMT voltage = high.

In another experiment, the displacement probe deriving from **(AQ/Flu)LysMix11C** showed similar results to **(AQ/Flu)LysMix10G**. In the presence of short DNA, the fluorescence was low. Addition of complementary DNA caused displacement of the short DNA strand, resulting in a fluorescence increase. In contrast, single-base mismatched DNA caused only slightly increased fluorescence because the mismatched DNA could not effectively compete with the short but complementary DNA strand in binding to the probe. The selectivity ratio [$(F_{ds}/F_{ss})_{comp}/(F_{ds}/F_{ss})_{mm}$] in the displacement reaction was 6.2 which was considerably better than only 1.4 obtained without displacement.
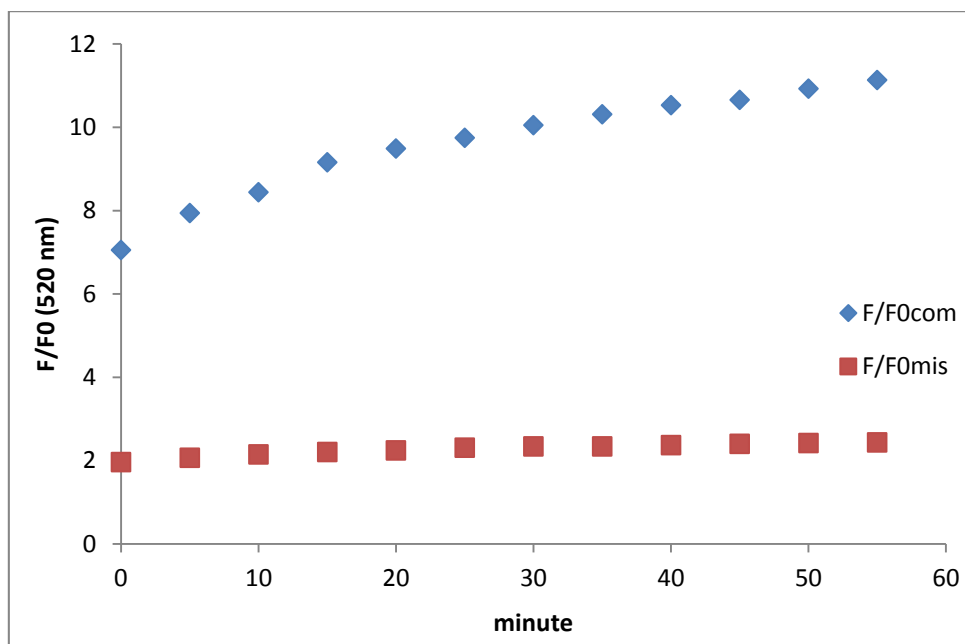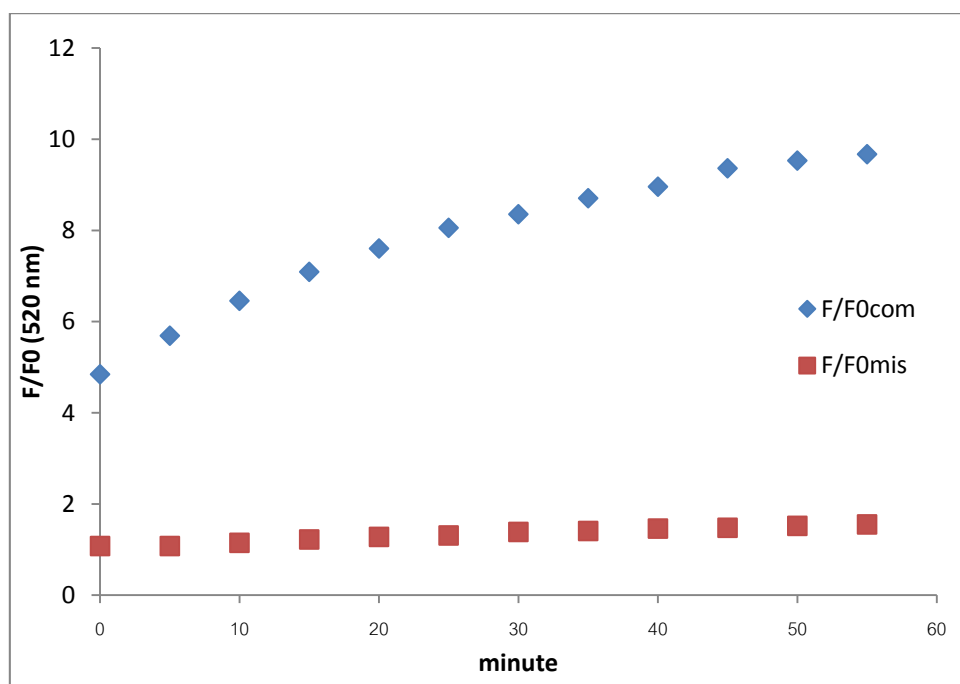
Figure 3.47 PNA-DNA displacement **of (AQ/Flu)LysMix11C**-dTCTGAA (6base) hybrids with complementary (dTCTGAATTTAG, blue) and mismatched DNA (dTCTGA<u>G</u>TTTAG, red). Conditions: 10 mM sodium phosphate buffer pH 7.0, [PNA] = 0.1 µM and [DNA] = 0.12 µM, excitation wavelength 490 nm, PMT voltage = high

3.2.9 Attempts to improve the mismatch specificity by varying the temperature

The high fluorescence of hybrids between dual end-labeled acpcPNA probe and mismatched DNA is not surprising considering that these single mismatched hybrids are stable enough to form a duplex at room temperature. However, since mismatched hybrids should be much less thermally stable than the complementary hybrid, it should be possible to find a temperature at which the mismatched hybrid is completely dissociated and the complementary hybrid is still intact. This is perhaps the only way that can discriminate between complementary and mismatched hybrids in DNA-based probesThe same concept was adapted to the present study by measuring the fluorescence T_m of various DNA hybrids of dual end-labeled acpcPNA probes. Some typical T_m curves are shown in **Figure 3.48**. The fluorescence T_m values

of 42.6, 43.3, 65.0 and 65.5 °C were obtained for **(AQ/Flu)LysM10G**, **(AQ/Flu)LysM10T**, **(AQ/Flu)LysM11C** and **(AQ/Flu)LysM12A** respectively.   All single base mismatch hybrids gave much lower T_m than the complementary hybrids as shown in **Table 3.9**. The large T_m difference confirmed the high specificity of the doubly end-labeled acpcPNA probes, at least in the internal mismatched cases. At temperatures sufficiently high to dissociate the mismatched, but not too high to dissociate the complementary, duplexes (around 45 °C for the **(AQ/Flu)LysM10G** and **(AQ/Flu)LysM10C** probes), the complementary and single mismatched DNA could be readily distinguished (**Figure 3.48**).

Table 3.9 Fluorescence T_m data of dual end-labeled acpcPNA. Conditions: 10 mM sodium phosphate buffer pH 7.0, [PNA] = 0.1 µM and [DNA] = 0.12 µM, excitation wavelength = 490 nm, PMT voltage = high

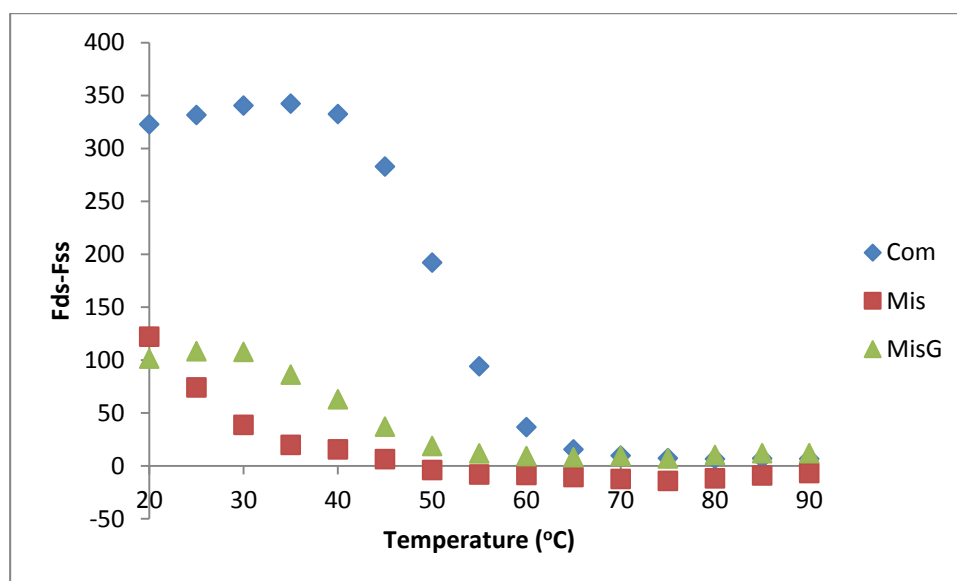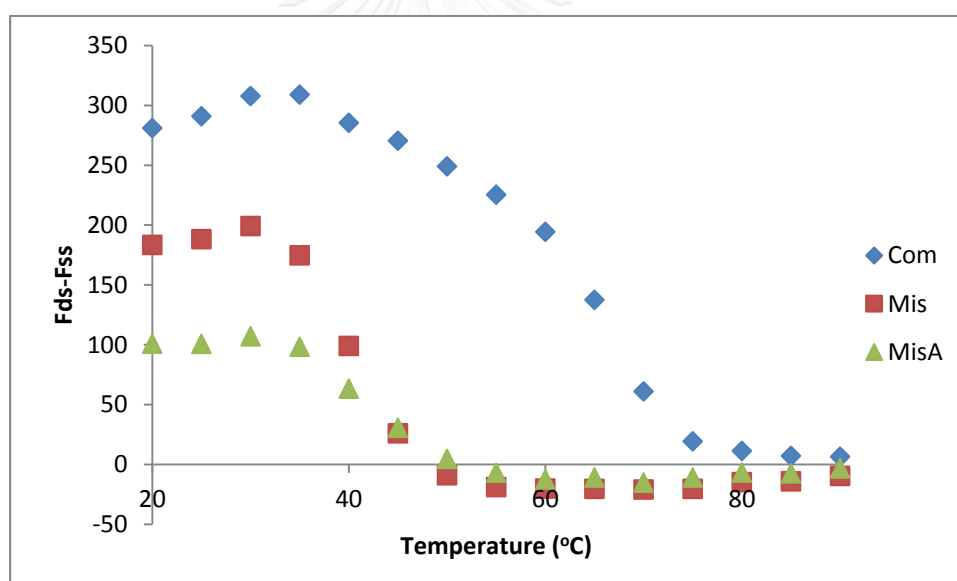| PNA	DNA sequences 5' $\longrightarrow$ 3'	T_m (°C)
(AQ/Flu)LysM10G	AGTGATATAC	50.4
	AGTGCTATAC	<20
	AGTGATATAA	36.2
(AQ/Flu)LysM10-T	GATGTCTGTA	43.3
	GATGACTGTA	<20
	GATGTCTGTC	35
(AQ/Flu)LysM11-C	TCTGAATTTAG	65.0
	TCTGAGTTTAG	39.0
	TCTGAATTTAA	40.0
(AQ/Flu)LysM12-A	GCA GGGATAACT	65.6
	GCA GGAATAACT	42.3
	GCAGGGATAACA	60.5

(a)

(b)

Figure 3.48 Fluorescence T_m curves with complementary (dsCom), internal mismatch (dsMis), mismatched (dsMisA) and non-complementary (dsNon) DNA of a) **(AQ/Flu)LysM10G** and b) **(AQ/Flu)LysM11C**. Conditions: 10 mM sodium phosphate buffer pH 7.0, [PNA] = 0.1 μM and [DNA] = 0.12 μM, excitation wavelength = 490 nm, PMT voltage = high
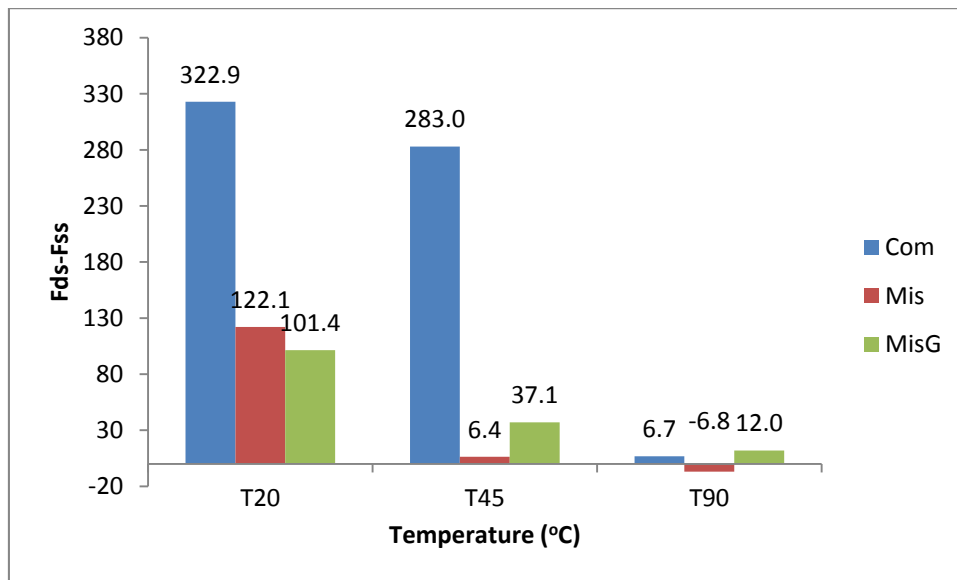
(a)
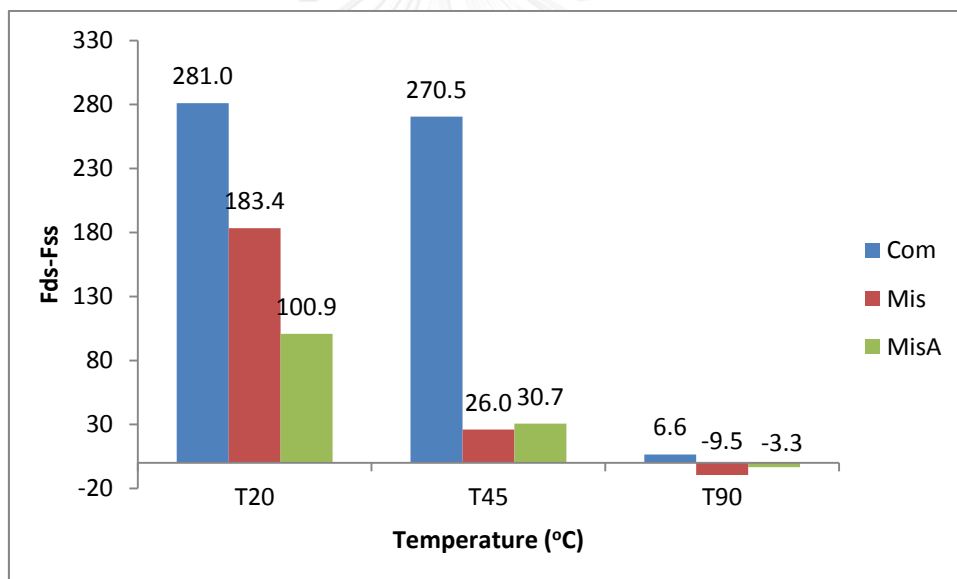
(b)

Figure 3.49 F_{ds}/F_{ss} of **(AQ/Flu)LysM10G** (a) and **(AQ/Flu)LysM11C** (b) at 20, 45 and 90 °C with dCom, dMis and dMisG. Conditions are the same as in **Figure 3.48**.

3.2.10 Naked eyes visualization of PNA-DNA hybridization

The difference between the fluorescence of the single stranded **(AQ/Flu)LysM10G** probe as well as its hybrids with complementary and mismatched DNAs could be visualized by the naked eye under UV light irradiation at 365 nm. As shown in **Figure 3.50**, the single stranded probe and non-complementary DNA hybrid was almost non-fluorescence. The complementary DNA hybrid showed the most intense green fluorescence while the internal single mismatched hybrid showed much less fluorescence.

ssPNA   dsCom   dsMis   dsNon

(a)
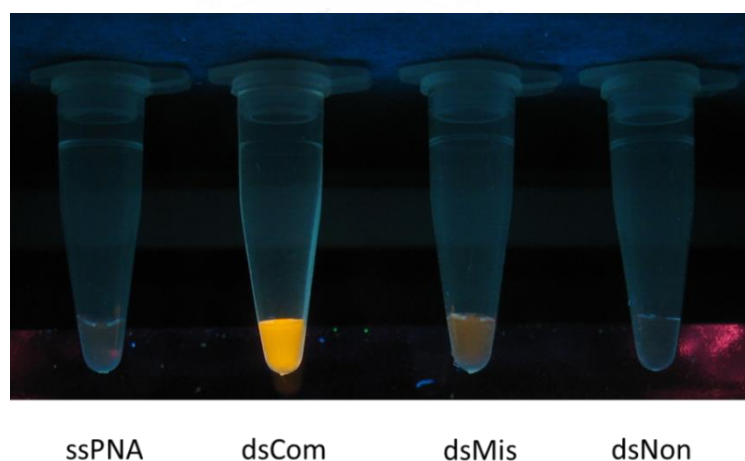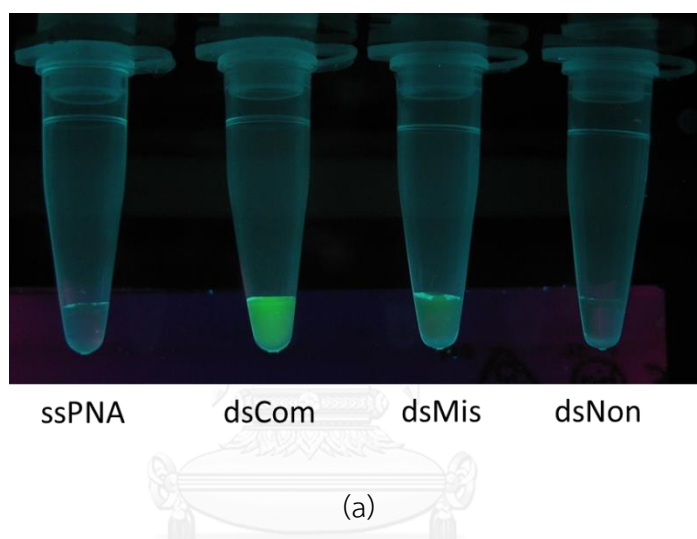

ssPNA   dsCom   dsMis   dsNon

(b)

Figure 3.50 Photographs of (a) **(AQ/Flu)LysM10G** (b) **(AQ/TMR)LysM10G** and their hybids with various DNA (dsCom = AGTGATATAC, dsMis = AGTGCTATAC, dsNon = :

TCTGCATTTAG) in 10 mM sodium phosphate buffer pH 7.0, [PNA] = 10 µM and [DNA] = 12 µM underblack light (365 nm)

In addition, hybrids of **(AQ/Flu)LysM10G** with various mismatched DNA showed small fluorescence increases similar to the internally mismatched DNA. These can be readily observed by naked eyes (**Figure 3.51**).

ssPNA   dsCom   dsMis   dsMisA   dsMisT   dsMisG
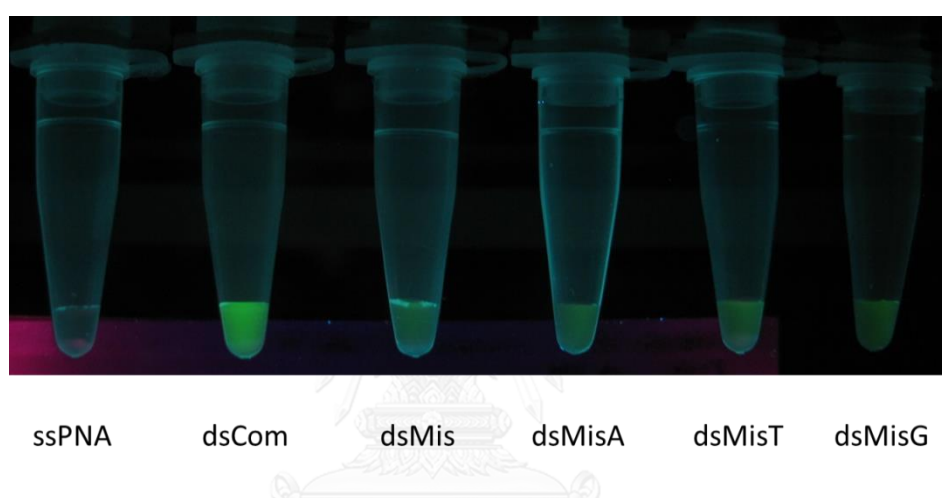
Figure 3.51 Photographs of **(AQ/Flu)LysM10G** and its hybids with DNA (dsCom =AGT GAT CTAC, dMis: AGTGCTCTAC, dMisA : AGTGATCTAA, dMisG: AGTGCTCTAG, dMisT: AGTGATCTAT) in 10 mM sodium phosphate buffer pH 7.0, [PNA] = 10 µM and [DNA] = 12 µM under black light (365 nm).

Moreover, the fluorescence change of **(AQ/Flu)LysM10G** hybrids in the presence of shorter and longer DNA targets (8base and 13base) were in agreement with the 3.3 and 18.3 fold increment obtained from fluorescence measurement (**Figure 3.29**).
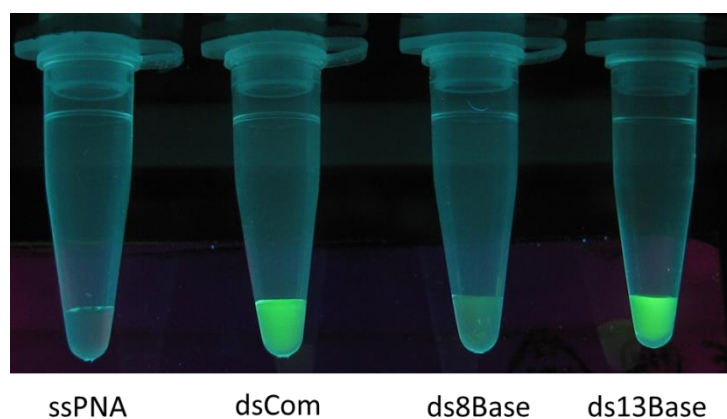
Figure 3.52 Photographs of **(AQ/Flu)LysM10G** and its hybrids with short and long complementary DNA (dCom = AGT GAT CTAC, d8base = AGT GCT CT, d13base = AGT GATCTACTAC) in 10 mM sodium phosphate buffer pH 7.0, [PNA] = 10 µM and [DNA] = 12 µM under black light (365 nm).

Figure 3.53 Photographs of strand displacement of **(AQ/Flu)LysM10G** (dCom = AGT GAT CTAC, dMis = AGT GCT CTAC, d8base = AGT GCT CT, d13base = AGT GATCTACTAC) in 10 mM sodium phosphate buffer pH 7.0, [PNA] = 10 µM and [DNA] = 12 µM under black light (365 nm)

3.3 Synthesis of Nile-red labeled peptide nucleic acid

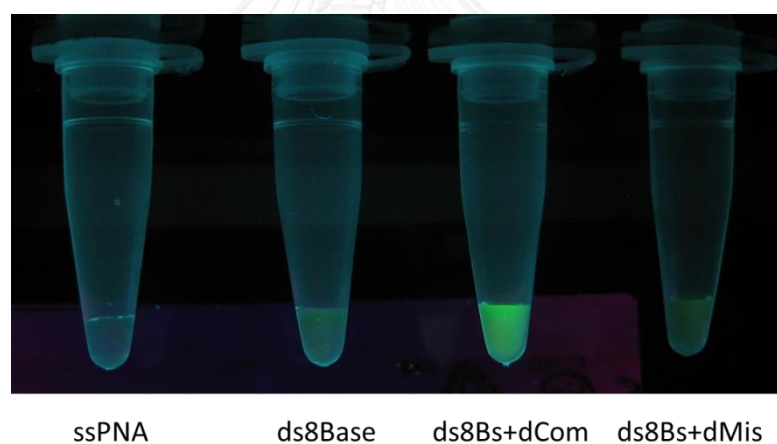In this part, acpcPNA probe was modified with an environment sensitive label that can change fluorescence properties in response to its environment [89-91]. It was hypothesized that the label in single stranded and duplex PNA should be placed in distinct environments and should result in different fluorescence and can be used as hybridization-responsive DNA probes. Nile red is an example of such environment sensitive dye that showed significant variation of fluorescence properties in different solvents (so-called solvatochromic dye) [92]. It is a member of the benzophenoxazine dye family that exhibits interesting properties including a high quantum yield, good photostability, long excitation and emission wavelengths [92].


Nile red   benzophenoxazine dye

Figure 3.54 Structure of Nile red and benzophenoxazine dyes

Nile red had been attached to DNA in several ways, such as by base replacement [93], as a base modifier [94, 95], or by backbone labeling. However, in most cases formation of DNA duplexes does not generally yield significant fluorescence change of the Nile red. Following a promising preliminary study [96], we synthesized acpcPNA probes that are modified with Nile red at the backbone using Click chemistry and studied the change in optical properties in response to DNA hybridization.

3.3.1 Synthesis of internally Nile red-modified acpcPNA

In order to click the Nile red lable onto acpcPNA backbone, the previously reported sequential reductive alkylation-click chemistry strategy was employed [63]. The acpcPNA was site-specifically modified with a Tfa-protected APC residue to provide a handle for the post-synthetic modification [61]. After removal of the Tfa and nucleobase protecting groups by treatment with ammonia, the PNA was reductively alkylated with 4-azidobutanal to install an azide group [63, 97]. Next the alkyne-modified Nile red label (PNr, **12**), which was synthesized in 70% yield from alkylation of 2-hydroxyNile red (**11**) [98] by propargyl bromide in the presence of K_2CO_3, was clicked onto the PNA backbone under copper(I) catalysis conditions following our previously reported protocol.[63] (**Figure 3.55**) The success of both the reductive alkylation and click steps were monitored by MALDI-TOF mass spectrometry (**Figure 3.56**).
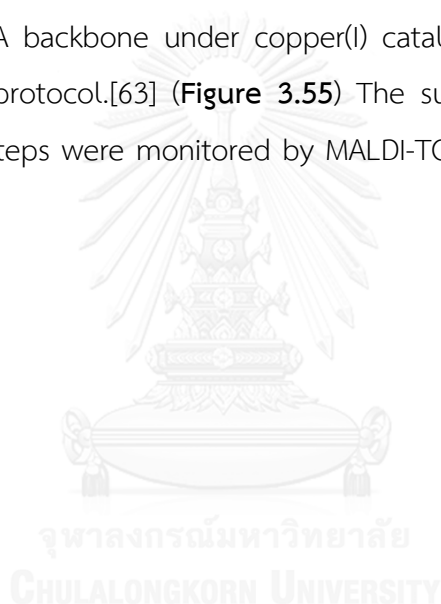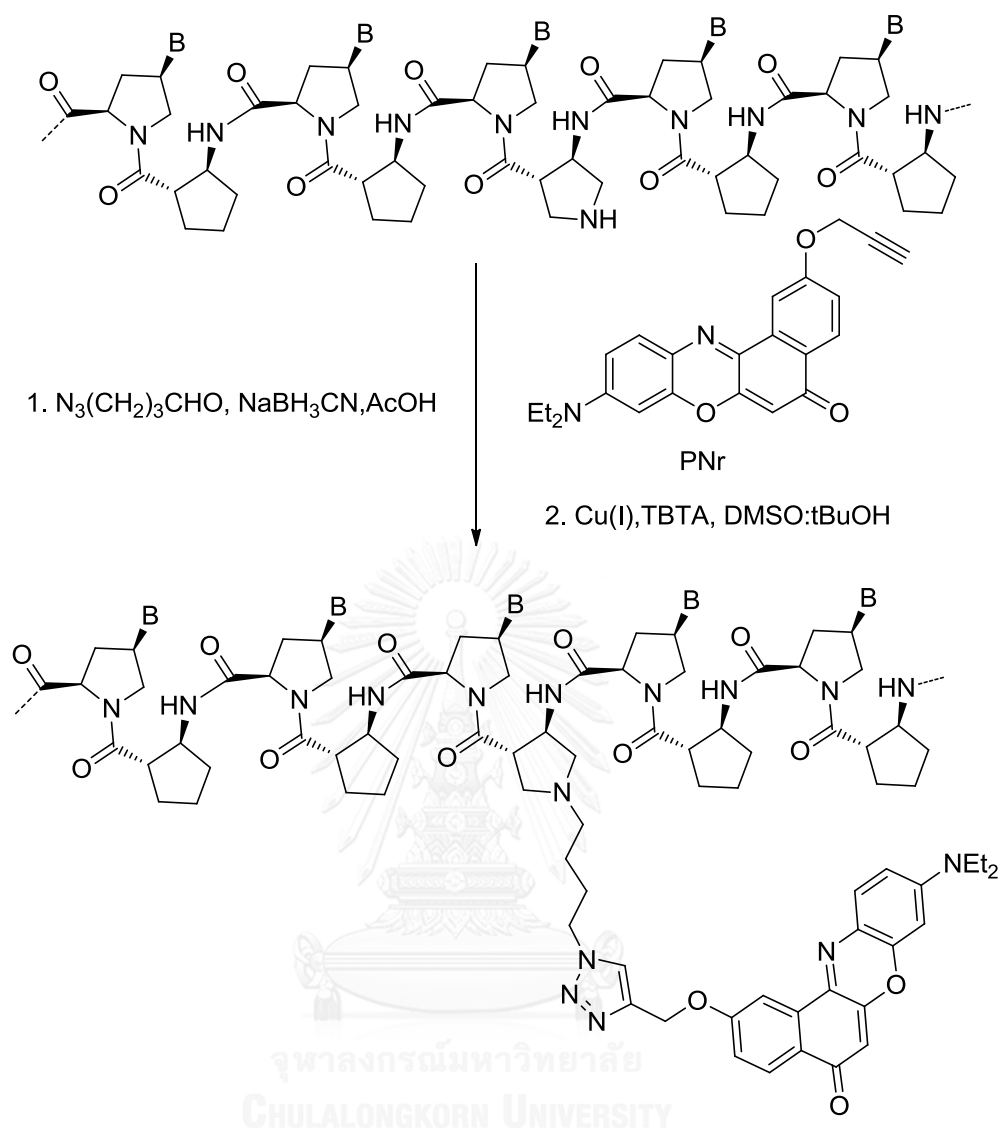
Figure 3.55 A synthetic strategy for internal labeling of acpcPNA via acylation of APC-modified acpcPNA by propargyl nile red
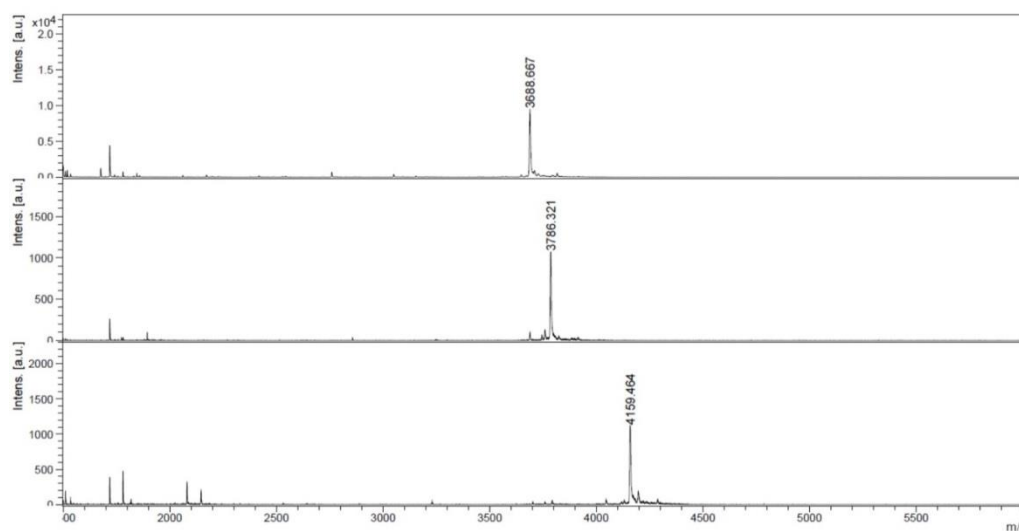
Figure 3.56 MALDI-TOF mass spectra of crude 10mer acpcPNA before (top) (calcd *m/z* 3688.0) and after functionalizing with azidobutyl (middle) (calcd *m/z* 3785.1) followed by clicking with Nile red (bottom) (calcd *m/z* 4157.5)

After completion of the synthesis, cleavage and purification were performed as described for other PNAs. The identity of the PNA oligomers was confirmed by MALDI-TOF mass spectrometry (**Table 3.10**) and the purities determined to be >90% by reversed phase HPLC analyses.

Table 3.10 Sequences and characterization data of modified PNA obtained after HPLC purification.

PNA	sequence (N to C)[a]	t_R (min)	m/z (calcd)	m/z (found)	%yield
M10(Nr)	GTAGA(Nr)TCACT	33.6	4157.5	4155.1	6.3
M11AA(Nr)	CATAA(Nr)AATACG	34.2	4491.9	4491.1	18.5
M11CC(Nr)	CATAC(Nr)CATACG	34.6	4443.9	4441.8	11.4
M11GG(Nr)	CATAG(Nr)GATACG	32.8	4523.9	4523.2	15.2
M11TT(Nr)	CATAT(Nr)TATACG	34.3	4473.9	4473.0	8.4

[a]All PNA sequences were capped at the N-termini by N-Ac-Lys and at the C-termini by Lys-NH$_2$.

3.3.2 Optical properties of free Nile red and single stranded Nile red-labeled acpcPNA

UV-vis spectrum of the free propargyl Nile red (**12**) in acetonitrile showed absorption maxima at 538 nm. The polarity of the solvent was adjusted by varying the composition of acetonitrile and aqueous phosphate buffer. The absorption maxima were red-shifted when the polarity was increased with increasing amounts of the buffer (**Figure 3.57**). UV-vis spectrum of Nile red-labeled acpcPNA **M10(Nr)** in aqueous phosphate buffer exhibited an absorption peak at 575 nm. A similar trend to the free Nile red label (**12**) was observed upon changing the solvent.
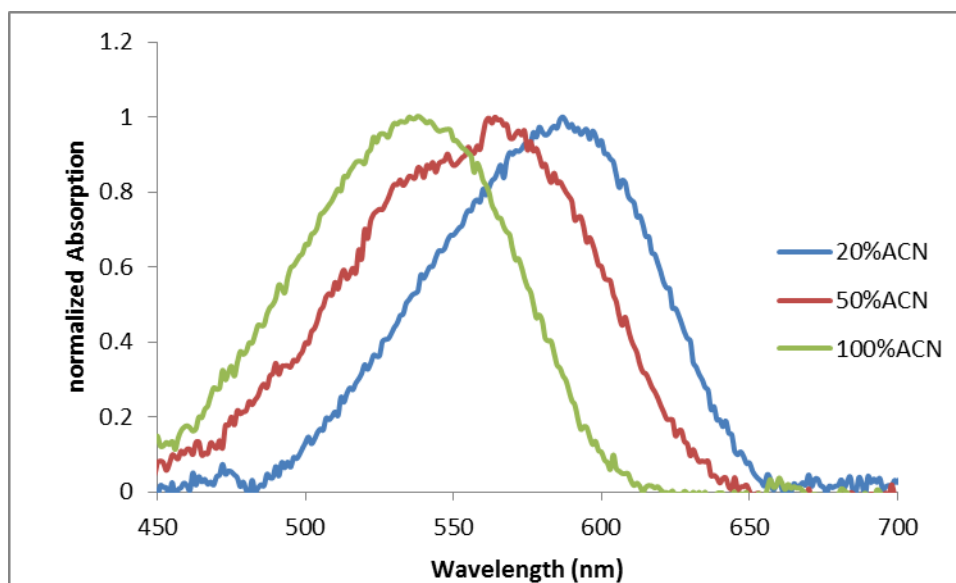
Figure 3.57 UV-vis spectra of propargyl Nile red (1.0 µM) in various solvents (blue = 20% MeCN, red = 50% MeCN, green = 100% MeCN)
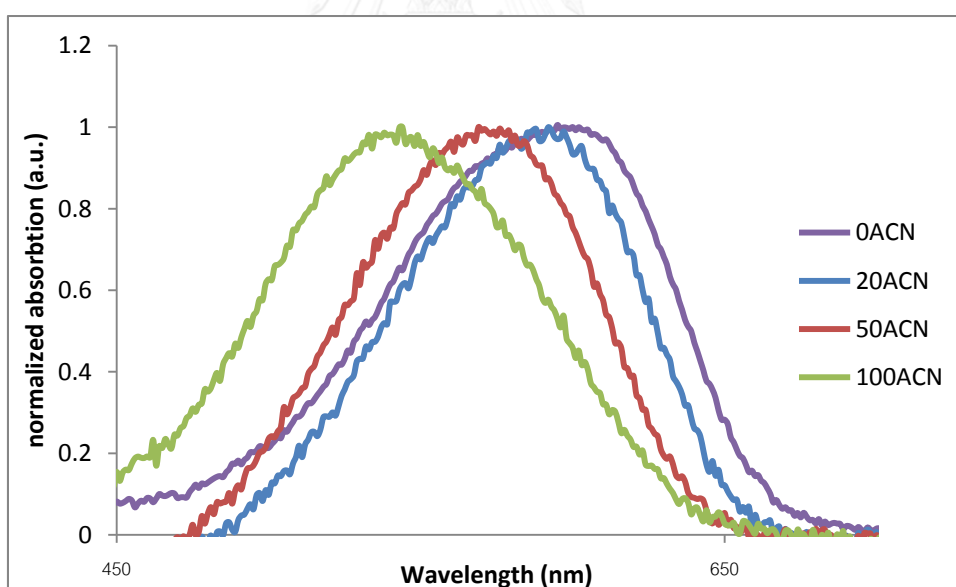

Figure 3.58 UV-vis spectra of M10(Nr) (1.0 µM) in various solvents (purple = 0% MeCN, blue = 20% MeCN, red = 50% MeCN, green = 100% MeCN

The fluorescence spectrum of **12** in acetonitrile showed a fluorescence emission at 620 nm with a fluorescence quantum yield (Φ_F) of 0.65, which was

comparable to Nile red derivative report in literature [92]. The fluorescence maxima were red-shifted when the polarity was increased with increasing amounts of the buffer. On the other hand, The fluorescence quantum yield was decreased (50% acetonitrile = 0.29; 20% acetonitrile = 0.14). Due to the insolubility of **12** in water, the absorption and fluorescence could not be measured in pure aqueous phosphate buffer without acetonitrile.

The Nile red-labeled acpcPNA **M10(Nr)** in aqueous phosphate buffer exhibited fluorescence emission at 656 nm. The fluorescence emission maxima were blue-shifted in less polar solvents (**Figure 3.59**). When compared in the same solvent, the Nile red in PNA and as the free label (**12**) showed similar quantum yields (20% acetonitrile: PNA Φ_F = 0.16, free Nile red = 0.14; 50% acetonitrile: PNA Φ_F = 0.23, free Nile red = 0.29). This suggests that the Nile red label was not significantly quenched in single stranded PNA, at least in this particular sequence context.
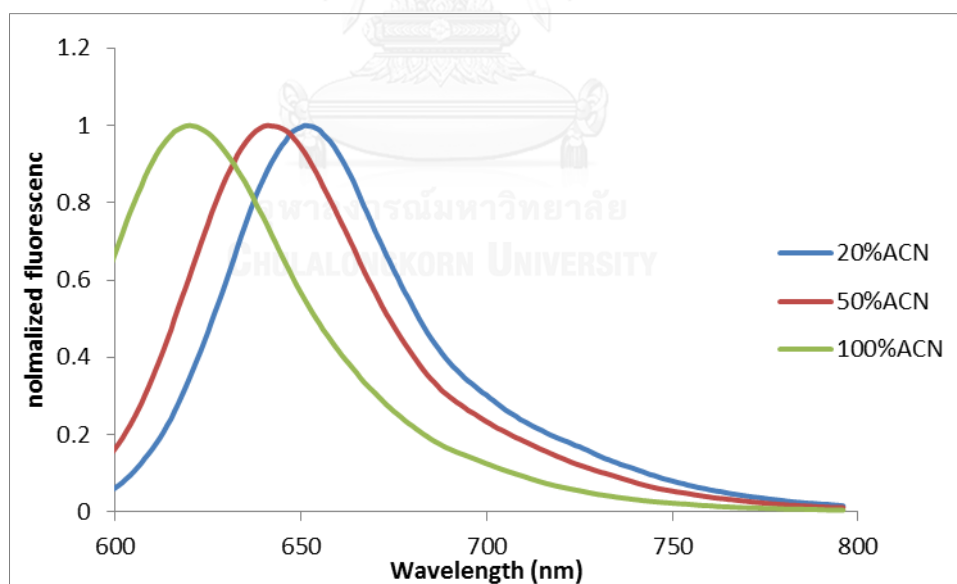

Figure 3.59 Normalized fluorescence of propargyl Nile red (1.0 µM) in various solvents (blue = 20% MeCN, red = 50% MeCN, green = 100% MeCN)
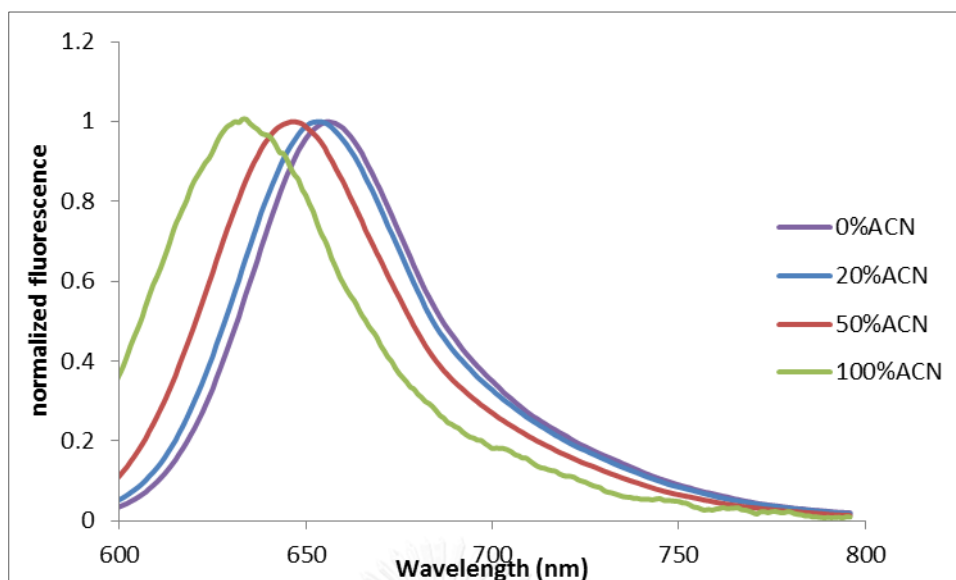
Figure 3.60 Normalized fluorescence of **M10(Nr)** (1.0 µM) in various solvents (purple = 0% MeCN, blue = 20% MeCN, red = 50% MeCN, green = 100% MeCN)

Absorption spectra of **M10(Nr)** and its complementary DNA duplex are significantly different from the single stranded in the Nile red region as shown by the sharpening and red-shifting of the absorption maxima (λ_{max} = 575 and 598 nm in single stranded and duplex, respectively) (**Figure 3.61**). Moreover, the mismatched DNA was showed red-shift absorbtion similarly complementary DNA
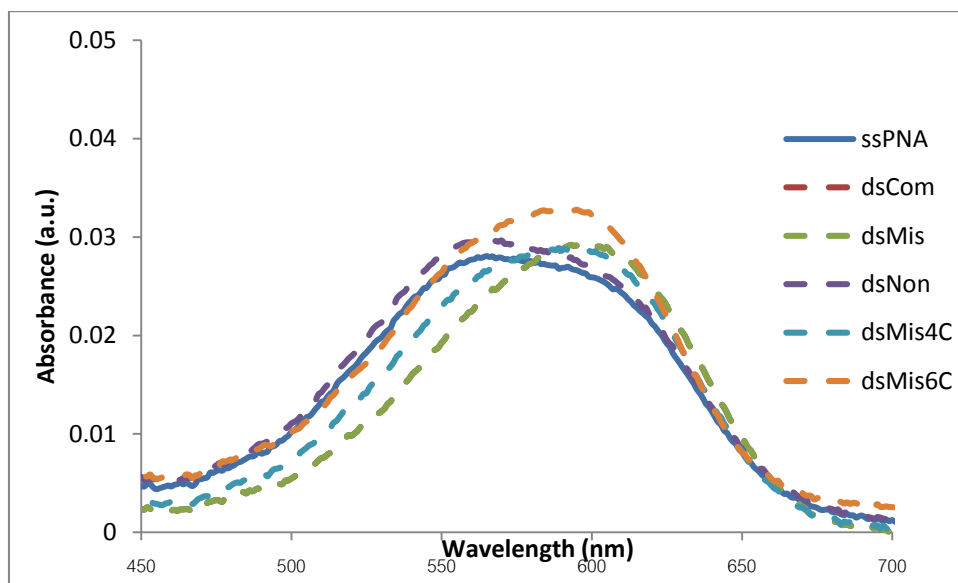
Figure 3.61 UV-vis spectra of **M10(Nr)** in the single stranded form (ssPNA) and hybrids with various DNA (dsCom: dAGTGATATAC; dsMis: dAGTG<u>C</u>TATAC; dsNon: dTCTGCATTTAG , dsMis4C: AGTG<u>C</u>TCTAC; dsMis6C: dAGTGA<u>C</u>ATAC.). Conditions: 10 mM phosphate buffer pH 7.0, [PNA] = 1.0 μM , [DNA] = 1.2 μM.

3.3.3 Optical properties of Nile red-labeled acpcPNA duplexes

Thermal denaturation experiments suggest that the Nile red-labeled acpcPNA forms a stable hybrid with complementary DNA (**Table 3.11**). The T_m of the complementary DNA hybrid of **M10(Nr)** (58.8 °C by UV or 56.9 °C by fluorescence) was comparable to that of unlabeled acpcPNA (57.6 °C) [63]. In the presence of a mismatched base in the DNA strand, the T_m of the duplex was decreased to the range of 37–41 °C. Hybrids with DNA carrying an inserted base also showed slightly decreased T_m values.

Table 3.11 T_m and optical properties of Nile red-labeled acpcPNA **M10(Nr)**[a]

DNA (5' to 3')[b]	T_m (°C)[c]	λ_{abs}	λ_{em}[d]	Φ_F[e]	F/F_0[f]
none (ssPNA)	-	575	656	0.11	-
+AGTGATCTAC (dsCom)	58.8 (56.9)	598	647	0.15	1.36
+ AGTG<u>C</u>TCTAC (dsMis)	37.5 (36.7)	585	648	0.17	1.72
+AGT<u>C</u>ATCTAC (dsMis4C)	37.7 (37.5)	589	649	0.14	1.43
+AGTGA<u>C</u>CTAC (dsMis6C)	40.8 (41.3)	592	652	0.15	1.70
+AGTGA**C**TCTAC (dsBLC)	46.9 (52.0)	589	643	0.29	2.91
+AGTGA**A**TCTAC (dsBLA)	40.1 (46.7)	588	648	0.20	2.60
+AGTGA**T**TCTAC (dsBLT)	54.7 (52.7)	591	649	0.22	2.65
+AGTGA**G**TCTAC (dsBLG)	42.2 (46.0)	593	645	0.20	3.31

[a]All measurements were carried out in 10 mM sodium phosphate buffer pH 7.0, [PNA] = 1.0 µM; [DNA] = 1.2 µM at 20 °C.

[b]Underlined and boldface letters in DNA sequences indicate the position of mismatch and base insertion, respectively.

[c]Determined by UV-vis (260 nm) and/or fluorescence spectrophotometry (643 nm, shown in parentheses)

[d]λ_{ex} = 580 nm

[e]Cresyl violet was used as a standard (Φ = 0.54 in MeOH)[99]

[f]F/F_0 was calculated from the ratio of fluorescence of duplex divided by the single stranded PNA at 643 nm.

[g]Not determined

Table 3.11 T_m and optical properties of Nile red-labeled acpcPNA **M10(Nr)**[a]

DNA (5' to 3')[b]	T_m (°C)[c]	λ_{abs}	λ_{em}[d]	Φ_F[e]	F/F_0[f]
+AGTCGATCTAC(dsBL4C)	N.D.[g]	591	648	0.14	1.16
+AGTGATCCTAC(dsBL8C)	N.D.[g]	597	653	0.10	0.87
+AGTGCCTCTAC(dsBLsm5)	N.D.[g]	585	648	0.17	1.45
+AGTGACCCTAC(dsBLsm7)	N.D.[g]	593	652	0.13	1.23
+AGTGACTCCAC(dsBLsm9)	N.D.[g]	585	647	0.13	1.24

[a]All measurements were carried out in 10 mM sodium phosphate buffer pH 7.0, [PNA] = 1.0 µM; [DNA] = 1.2 µM at 20 °C.

[b]Underlined and boldface letters in DNA sequences indicate the position of mismatch and base insertion, respectively.

[c]Determined by UV-vis (260 nm) and/or fluorescence spectrophotometry (643 nm, shown in parentheses)

[d]λ_{ex} = 580 nm

[e]Cresyl violet was used as a standard (Φ = 0.54 in MeOH)[99]

[f]F/F_0 was calculated from the ratio of fluorescence of duplex divided by the single stranded PNA at 643 nm.

[g]Not determined

UV-vis spectra of all Nile red-labeled acpcPNA showed a slight blue shift relative to the single strand form after hybridized with DNA (**Figure 3.62**).
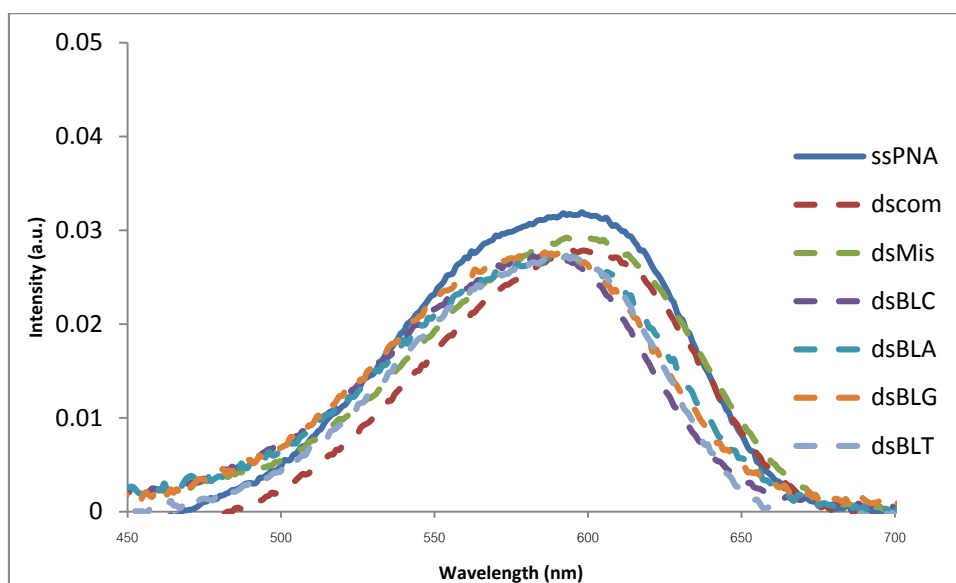
Figure 3.62 UV-vis spectraof **M10(Nr)** and its hybrids with DNA (dsCom: dAGTGATATAC.; dsMis: dAGTG<u>C</u>TATAC; dsNon: dTCTGCATTTAG , dsMis4C: AGTG<u>C</u>TCTAC; dsMis6C: dAGTGA<u>C</u>ATAC.). Conditions: 10 mM phosphate buffer pH 7.0, [PNA] = 1.0 μM , [DNA] = 1.2 μM

Fluorescence spectra of all Nile red-labeled acpcPNA and their DNA hybrids were studied in 10 mM phosphate buffer pH 7 with an excitation wavelength of 580 nm (**Table 3.11**, **Figure 3.63**). The single stranded acpcPNA **M10(Nr)** showed the emission maxima at 656 nm. In the presence of complementary DNA, a significant blue shift of the emission maxima to 647 nm was observed. This was also accompanied by ca 30% increase of quantum yield (Φ_F = 0.15). The blue shift and fluorescence increase suggest that the Nile red label in the complementary PNA-DNA hybrid was placed in a less polar environment than when it was in single stranded PNA.[100] The hybrids of **M10(Nr)** with DNA carrying a mismatched base in close proximity of the Nile red label showed blue-shifted fluorescence spectra similar to complementary duplex, with fluorescence increases ranging from 1.4 to 1.7 folds relative to the single stranded Nile red-labeled acpcPNA. The results suggest that the Nile red label in the mismatched PNA-DNA hybrids was placed in less polar environment compared to single strand similar to the complementary hybrids.
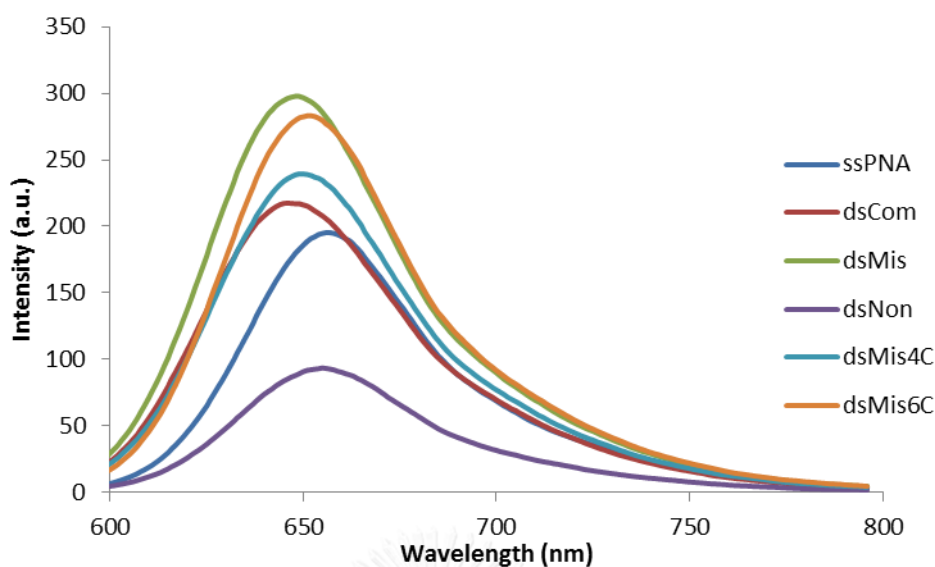
Figure 3.63 Fluorescence spectra of **M10(Nr)** (ssPNA) and its hybrids with complementary (dsCom), direct mismatch (dsMis), indirect mismatch (dsMis4C, dsMis6C) and non-complementary (dsNon) DNA; Conditions: 10 mM phosphate buffer, [PNA] = 1.0 µM, [DNA] = 1.2 µM, excitation wavelength = 580 nm, PMT voltage = high

Interestingly, the Nile red-labeled acpcPNA showed a relatively large fluorescence increase after hybridization with DNA carrying a base insertion in close proximity of the Nile red label. The relatively high Tm values suggest that the extra inserted base formed a bulge so that the remaining base pairs between PNA and DNA could still form. These bulged duplexes showed fluorescence increase in the range of 2.6–3.3 folds, depending on the type of the inserted base. Base C gave the highest fluorescence increase. The fluorescence spectra were also considerably more blue-shifted relative to the single strand and complementary hybrids (**Table 3.11** and **Figures 3.64** and **3.65**). When the inserted base was misplaced or when a mismatched base was incorporated in the DNA strand, the fluorescence of the hybrids became small. All of these results suggest that the Nile red label was buried in the hydrophobic pocket formed by the looped out base, thus resulting in a large fluorescence increase. A similar binding mode had been proposed to explain the monomer-excimer switching in bis-pyrene labeled DNA before [101].
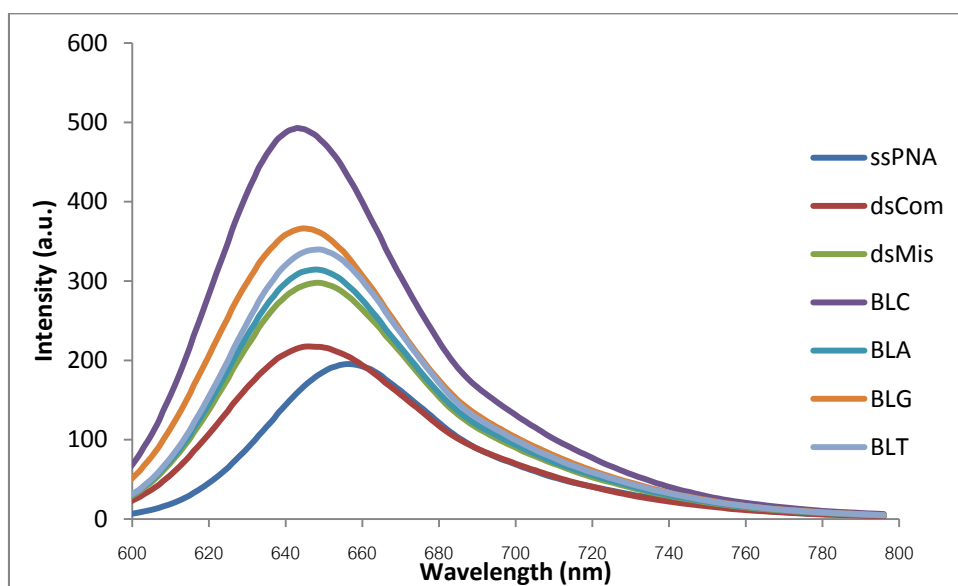
Figure 3.64 Fluorescence spectra of **M10(Nr)** (ssPNA) and its hybrids with various DNA (dsCom: dAGTGATCTAC; dsMis: dAGTG<u>C</u>TCTAC; BLC: dAGTGACTCTAC; BLA: dAGTGA<u>A</u>TCTAC. BLG: dAGTGA<u>G</u>TCTAC; BLT: dAGTGA<u>T</u>TCTAC); Conditions: 10 mM sodium phosphate buffer pH 7.0, [PNA] = 1.0 µM and [DNA] = 1.2 µM, excitation wavelength = 580 nm, PMT voltage = 700
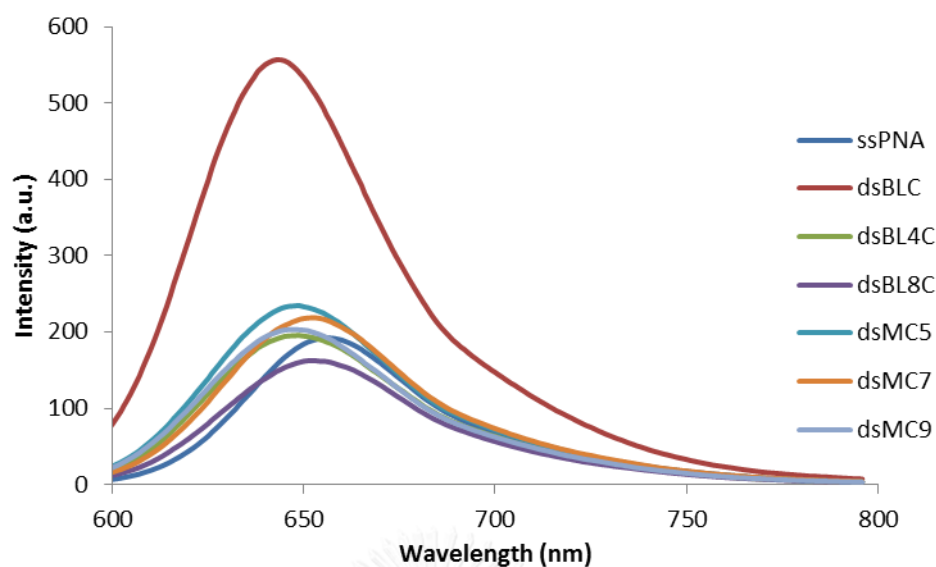
Figure 3.65 Fluorescence spectra of **M10(Nr)** (ssPNA) and its hybrids with various bulge-forming DNA containing a mismatch or misplaced bulge (dsBLC : dAGTGACTCTAC ; dsBL4C: dAGTCGATCTAC ; dsBL8C: dAGTGATACTAC; dsMC5: dAGTG<u>C</u>CTCTAC; dsMC7: dAGTGAC<u>C</u>CTAC; dsMC9: dAGTGACTC<u>C</u>AC; Conditions: 10 mM sodium phosphate buffer pH 7.0, [PNA] = 1.0 µM and [DNA] = 1.2 µM, excitation wavelength = 580 nm, PMT voltage = 700

To confirm this hypothesis, the effects of β-cyclodextrin to the fluorescence of Nile red label were studied. It was known that β-cyclodextrin could form an inclusion complex with Nile red and shifted its fluorescence spectra to shorter wavelengths [93]. As shown in **Figure 3.66**, a pronounced blue shift was observed in the cases of single stranded PNA. Smaller blue shifts were observed in complementary or mismatched duplexes (2 nm and 4 nm respectively), indicating some interactions between Nile red and cyclodextrin. This also suggest that the Nile red label in complementary and mismatched PNA-DNA duplexes was quite accessible to the cyclodextrin, and the most likely binding mode of the Nile red in these duplexes is more likely to be groove binding rather than intercalation. Interaction of the Nile red with the PNA-DNA groove will place it in a hydrophobic environment, which should increase the fluorescence as observed experimentally. No change in the fluorescence spectra was observed in the bulged duplex. This indicates that the Nile red label in the bulged duplex is unavailable

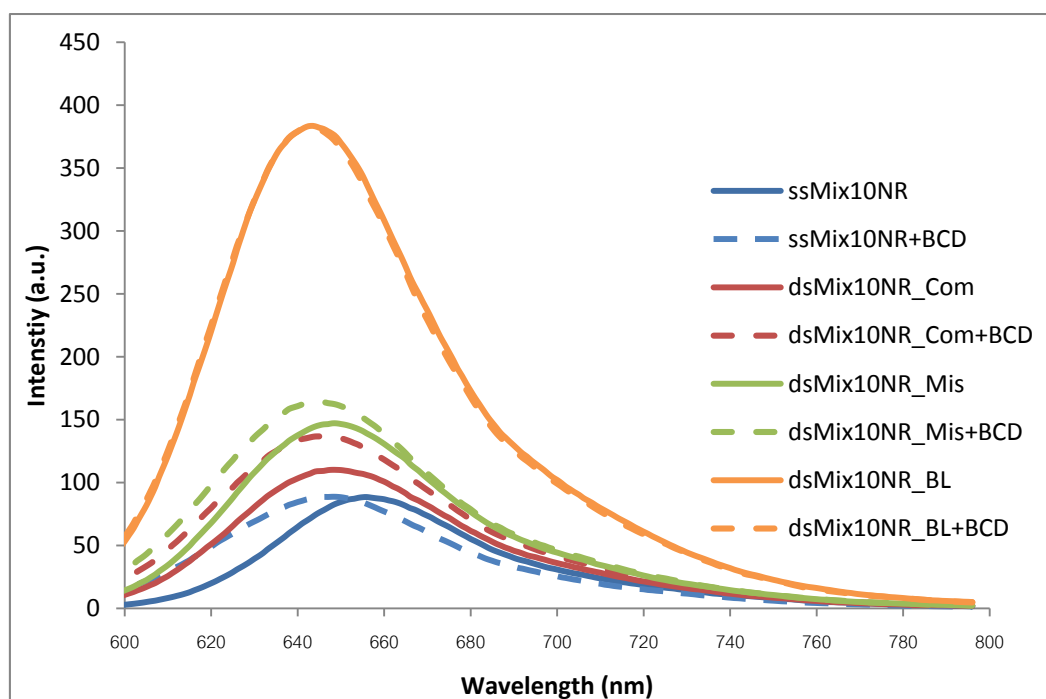to form the inclusion complex, which is in good agreement to the proposed binding mode.

Figure 3.66 Fluorescence spectra of single stranded PNA M10(Nr) and its duplexes in the absence (solid lines) and presence of β-cyclodextrin (dotted lines). Conditions: 10 mM sodium phosphate buffer pH 7.0, [PNA] = 1.0 µM and [DNA] = 1.2 µM, excitation wavelength = 580 nm, PMT voltage = 700

The difference between the fluorescence of single-stranded **M10(Nr)** and its complementary, mismatched and bulged duplexes, could be visualized by naked eyes under UV light at 365 nm (**Figure 3.67**).
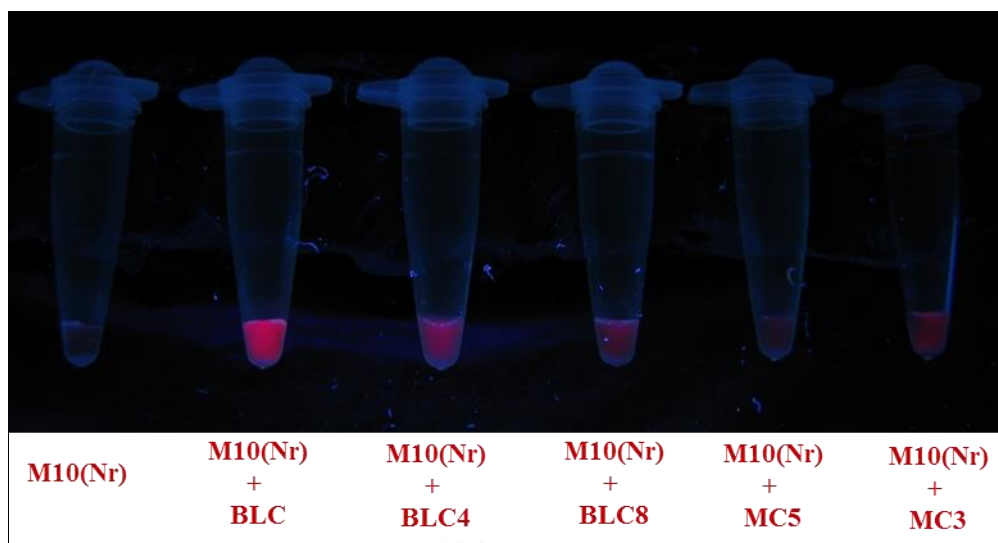
Figure 3.67 Photographs of **M10(Nr)** and its hybrids with mismatched DNA in 10 mM sodium phosphate buffer pH 7.0, [PNA] = 10 µM and [DNA] = 12 µM under black light (365 nm)

3.3.4 Effects of neighboring base on fluorescence properties of Nile red-labeled acpcPNA

To investigate the effect of neighboring nucleobases on the fluorescence properties of Nile red labeled acpcPNA, fluorescence properties of four PNA sequences with different neighboring bases adjacent to the Nile red were compared. The quantum yield and fluorescence intensity ratio are summarized in **Table 3.12.**

Table 3.12 T_m and optical properties of Nile red-labeled acpcPNA

PNA	DNA (5' to 3')[b]	T_m (°C)[c]	λ_{abs}	λ_{em}[d]	Φ_F[e]	F/F_0[f]
M11AA(Nr)	none	-	598	657	0.15	-
	CGTATTTTATG	76.0	600	651	0.23	1.55
	CGTATTCTTATG	74.7	593	645	0.33	2.34
M11CC(Nr)	none	-	594	656	0.08	-
	CGTATGGTATG	67.4	594	646	0.19	2.49
	CGTATGCGTATG	71.2	598	644	0.13	1.79
M11GG(Nr)	none	-	599	660	0.04	-
	CGTATCCTATG	(62.3)	599	655	0.15	3.27
	CGTATCCCTATG	(62.3)	599	652	0.10	2.46
M11TT(Nr)	none	-	588	655	0.09	-
	CGTATAATATG	76.6	602	654	0.19	2.05
	CGTATACATATG	76.0	590	646	0.29	3.44

[a]All measurements were carried out in 10 mM sodium phosphate buffer pH 7.0, [PNA] = 1.0 μM; [DNA] = 1.2 μM at 20 °C.

[b]Underlined and boldface letters in DNA sequences indicate the position of mismatch and base insertion, respectively.

[c]Determined by UV-vis (260 nm) and/or fluorescence spectrophotometry (643 nm, shown in parentheses)

[d]λ_{ex} = 580 nm

[e]Cresyl violet was used as a standard (Φ = 0.54 in MeOH)[99]

[f]F/F_0 was calculated from the ratio of fluorescence of duplex divided by the single stranded PNA at 643 nm.

[g]Not determined

The quantum yields of single stranded PNA **M10AA(Nr)**, **M10AA(Nr)**, **M10AA(Nr)** and **M10AA(Nr)** were in the order of AA>TT~CC>GG . The results show that the Nile red label is quenched to different extents by neighboring nucleobases. G exerts the highest quenching effect than other nucleobases, while A is almost non-quenching as shown by high quantum yield (Φ_F = 0.15). In all cases, when hybridized

with complementary DNA, the fluorescence intensities of duplexes were enhanced in the range from 1.55 to 3.27 folds. Hybridization with DNA with an inserted base to form bulged duplexes also resulted in fluorescence increase in the range from 1.79 to 3.44 folds. In the case of complementary duplexes, the presence of neighboring G/C gave more pronounced fluorescence increase relative to the single stranded PNA. On the other hand, larger fluorescence increases were observed in in the bulged duplexes with neighboring A/T than G/C. This may be due to quenching of the Nile red label by the neighboring G-C pairs. In all cases, the fluorescence emissions of the bulged duplexes were at shorter wavelengths than complementary duplexes and single stranded PNA, which is in good agreement with previous experiments.

CHAPTER IV

CONCLUSION

The objective of this work is to synthesize dual-labeled fluorescence acpcPNA probes that can change their fluorescence in response to the presence of correct DNA target. The research divided into three parts. The first part involves acpcPNA carrying two labels onto acpcPNA by APC-modifed derivative. The second part concerns with acpcPNA modified with a fluorophore-quencher pair at terminal positions. The last part explores acpcPNAs with a solvochromic dye attached onto the backbone.

In the first part, the internally dual-labeled acpcPNA was successfully synthesized by a combination of two orthogonally-protected APC spacers. The Tfa- and o-nosyl groups were found to be an ideal protecting group combination as one can be selectively removed without affecting the other. The fluorophore/quencher or FRET pairs were covalently attached onto the acpcPNA backbone via acylation or reductive alkylation followed by acylation (aminoethyl modifier) or Click reaction (azidobutyl modifier). The probes bearing flurophore-quencher pairs, **T9(Pyr/DNB)**, **T9(Flu/Dab)** and **T9(Flu/AQ)**, exhibited low quenching efficiency and the fluorescence increased only slightly after hybridization with DNA. None of the probe with FRET pairs worked according to the design because of the ground state interactions between the donor and acceptor fluorophores that leads to quenching instead of FRET.

In the second part of the study, the fluorescence properties of terminally dual labeled acpcPNA with a fluorophore/end-stacking quencher pair were investigated in the absence and presence of target DNA. The fluorophore/quencher pair was covalently attached to a lysine at the N-terminal positions of acpcPNA. The fluorescence of AQ/Flu or AQ/TMR labeled acpcPNA in single stranded form exhibited very low fluorescence emission. On the other hand, the fluorescence was enhanced upon hybridization with complementary DNA because the quencher was stacked with the terminal base pairs of the PNA-DNA duplex. The AQ/Flu and AQ/TMR labeled

acpcPNA probe showed high specificity and could distinguish complementary from single base-mismatched (internal and terminal) in the DNA strand. The specificity could be further improved by using a strand displacement reaction, or by increasing temperature. Moreover, the effects of fluorophore/quencher attachment, types of fluorophore/quencher pairs and the effect of base at the end of the PNA and DNA strands to the fluorescence properties were investigated.

In the third part, we succesfully synthesized acpcPNAs modified with the solvatochromic dye Nile red. The fluorescence of Nile red-modified acpcPNA in the presence of complementary DNA and complementary DNA with an extra base insertion that could form a bulge in the vicinity of the Nile red label were blue-shifted and noticeably enhanced. This indicated that the Nile red label in acpcPNA-DNA duplex is located in a more hydrophobic environment than the Nile red label in single-stranded acpcPNA. Based on spectroscopic data, the Nile red was proposed to interact with the groove in complementary PNA-DNA hybrid, or the hydrophobic pocket formed by the bulged duplex rather than intercalated within the base stacks. Moreover, the effects of neighboring base to the fluorescence change in Nile red-modified acpcPNA were investigated. The quenching is in the order to $G > C \sim T > A$.

The studies had provided several new potential designs of fluorescence hybridization probes for DNA sequence determination. They also advanced the understanding of dye-interactions in PNA that may not always follow the same rules as in DNA. Finally, the new probes that were developed – especially the dual end-labeled probe – show a great potential as a tool for DNA sequence analysis due to their high responsiveness and specificity.

REFERENCES

[1]   Nielsen, P.E., and Egholm, M., Berg, R. H., Buchardt. Sequence-selective recognition of DNA by strand displacement with a thymine-substituted polyamide. Science 254 (1991): 1497-1500

[2]   Hyrup, B., and Nielsen, P.E. Peptide Nucleic Acids (PNA): Synthesis, properties and potential applications. Bioorganic & Medicinal Chemistry 4(1) (1996): 5-23.

[3]   Uhlmann, E., Peyman, A., Breipohl, G., and Will, D.W. PNA: Synthetic polyamide nucleic acids with unusual binding properties. Angewandte Chemie International Edition 37(20) (1998): 2796-2823.

[4]   Ray, A., and Norden, B. Peptide nucleic acid (PNA): its medical and biotechnical applications and promise for the future. The FASEB Journal 14(9) (2000): 1041-1060.

[5]   Wang, J. DNA biosensors based on peptide nucleic acid (PNA) recognition layers. a review. Biosensors and Bioelectronics 13(7–8) (1998): 757-762.

[6]   Briones, C., and Moreno, M. Applications of peptide nucleic acids (PNAs) and locked nucleic acids (LNAs) in biosensor development. Analytical and Bioanalytical Chemistry 402(10) (2012): 3071-3089.

[7]   Lundin, K.E., Good, L., Stro¨mberg, R., Graslund, A., and Smith, C.I.E. Biological activity and biotechnological aspects of peptide nucleic acid. Advances in Genetics 56: 1-51.

[8]   Wang, G. and Xu, X.S. Peptide nucleic acid (PNA) binding-mediated gene regulation. Cell Res 14(2) (2004): 111-116.

[9]   Braasch, D.A., and Corey, D.R. Novel antisense and peptide nucleic acid strategies for controlling gene expression. Biochemistry 41(14) (2002): 4503-4510.

[10]   Ito, K., Katada, H., Shigi, N., and Komiyama, M. Site-selective scission of human genome by artificial restriction DNA cutter. Chemical Communications (43) (2009): 6542-6544.

[11]   Bonifazi, D., Carloni, L.-E., Corvaglia, V., and Delforgem, A. Peptide nucleic acids in materials science. Artificial DNA: PNA & XNA 3(3) (2012): 112-122.

[12]   Ackermann, D. and Famulok, M. Pseudo-complementary PNA actuators as reversible switches in dynamic DNA nanotechnology. Nucleic Acids Research 41(8) (2013): 4729-4739.

[13]   Suparpprom, C., Srisuwannaket, C., Sangvanich, P., and Vilaivan, T. Synthesis and oligodeoxynucleotide binding properties of pyrrolidinyl peptide nucleic acids bearing prolyl-2-aminocyclopentanecarboxylic acid (ACPC) backbones. Tetrahedron Letters 46(16) (2005): 2833-2837.

[14]   Vilaivan, T. and Srisuwannaket, C. Hybridization of pyrrolidinyl peptide nucleic acids and DNA: Selectivity, base-pairing specificity, and direction of binding. Organic Letters 8(9) (2006): 1897-1900.

[15]   Vilaivan, C., et al. Pyrrolidinyl peptide nucleic acid with α/β-peptide backbone. Artificial DNA: PNA & XNA 2(2) (2011): 50-59.

[16]   Mansawat, W., Vilaivan, C., Balázs, Á., Aitken, D.J., and Vilaivan, T. Pyrrolidinyl peptide nucleic acid homologues: Effect of ring size on hybridization properties. Organic Letters 14(6) (2012): 1440-1443.

[17]   Siriwong, K., Chuichay, P., Saen-oon, S., Suparpprom, C., Vilaivan, T., and Hannongbua, S. Insight into why pyrrolidinyl peptide nucleic acid binding to DNA is more stable than the DNA·DNA duplex. Biochemical and Biophysical Research Communications 372(4) (2008): 765-771.

[18]   Sahu, B., et al. Synthesis and characterization of conformationally preorganized, (R)-fiethylene glycol-containing γ-peptide nucleic acids with superior hybridization properties and water solubility. The Journal of Organic Chemistry 76(14) (2011): 5614-5627.

[19]   Rapireddy, S., He, G., Roy, S., Armitage, B.A., and Ly, D.H. Strand invasion of mixed-sequence B-DNA by acridine-linked, γ-peptide nucleic acid (γ-PNA). Journal of the American Chemical Society 129(50) (2007): 15596-15600.

[20]   Englund, E.A. and Appella, D.H. γ-Substituted peptide nucleic acids constructed from L-lysine are a versatile scaffold for multifunctional display. Angewandte Chemie International Edition 46(9) (2007): 1414-1418.

[21]   Tyagi, S. and Kramer, F.R. Molecular beacons: probes that fluoresce upon hybridization. <u>Nat Biotech</u> 14(3) (1996): 303-308.

[22]   Tyagi, S., Bratu, D.P., and Kramer, F.R. Multicolor molecular beacons for allele discrimination. <u>Nat Biotech</u> 16(1) (1998): 49-53.

[23]   Nitin, N., Santangelo, P. J., Kim, G., Nie S., and Bao, G. Peptide‐linked molecular beacons for efficient delivery and rapid mRNA detection in living cells. <u>Nucleic Acids Research</u> 32 (2004): e58.

[24]   Bonnet G., T.S., Libchaber A., and Kramer F.R. Thermodynamic basis of the enhanced specificity of structured.<u>Proceedings of the National Academic of Sciences of the United States of Amarica.</u> 96 (1999): 6171-6176.

[25]   Li, X., Huang, Y., Guan, Y., Zhao, M., and Li, Y. A novel one cycle allele specific primer extension—molecular beacon displacement method for DNA point mutation detection with improved specificity. <u>Analytica Chimica Acta</u> 584(1) (2007): 12-18.

[26]   http://www.lifetechnologies.com/th/en/home/references/molecular-probes-the-handbook/technical-notes-and-product-highlights/fluorescence-resonance-energy-transfer-fret.html.

[27]   Jockusch, S., et al. Spectroscopic investigation of a FRET molecular beacon containing two fluorophores for probing DNA/RNA sequences. <u>Photochemical & Photobiological Sciences</u> 5(5) (2006): 493-498.

[28]   Varghese, R. and Wagenknecht, H.-A. Red-white-blue emission switching molecular beacons: ratiometric multicolour DNA hybridization probes. <u>Organic & Biomolecular Chemistry</u> 8(3) (2010): 526-528.

[29]   Saito, Y., et al. Dual-labeled oligonucleotide probe for sensing adenosinevia FRET: A novel alternative to SNPs genotyping. <u>Chemical Communications</u> (21) (2007): 2133-2135.

[30]   Holzhauser, C. and Wagenknecht, H.A. In-stem-labeled molecular beacons for distinct fluorescent color readout. <u>Angewandte Chemie International Edition</u> 50(32) (2011): 7268-72.

[31] Venkatesan, N., Jun S.Y., and Hyean K.B. Quencher-free molecular beacons: a new strategy in fluorescence based nucleic acid analysis. <u>Chemical Society Reviews</u> 37(4) (2008): 648-663.

[32] Okamoto, A., Saito, Y., and Saito, I. Design of base-discriminating fluorescent nucleosides. <u>Journal of Photochemistry and Photobiology C: Photochemistry Reviews</u> 6(2–3) (2005): 108-122.

[33] Ryu, J.H., Seo, Y.J., Hwang, G.T., Lee, J.Y., and Kim, B.H. Triad base pairs containing fluorene unit for quencher-free SNP typing. <u>Tetrahedron</u> 63(17) (2007): 3538-3547.

[34] Heinlein, T., Knemeyer, J.-P., Piestert, O., and Sauer, M. Photoinduced electron transfer between fluorescent dyes and guanosine residues in DNA-hairpins. <u>The Journal of Physical Chemistry B</u> 107(31) (2003): 7957-7964.

[35] Dioubankova, N.N., et al. Pyrenemethyl ara-Uridine-2′-carbamate: A Strong Interstrand Excimer in the Major Groove of a DNA Duplex. <u>ChemBioChem</u> 4(9) (2003): 841-847.

[36] Fujimoto, K., Shimizu, H., and Inouye, M. Unambiguous detection of target DNAs by excimer–monomer switching molecular beacons. <u>The Journal of Organic Chemistry</u> 69(10) (2004): 3271-3275.

[37] Matsumoto, K., et al. Pyrene-labeled deoxyguanosine as a fluorescence sensor to discriminate single and double stranded DNA structures: Design of ends free molecular beacons. <u>Bioorganic & Medicinal Chemistry Letters</u> 19(22) (2009): 6392-6395.

[38] Häner, R., Biner, S.M., Langenegger, S.M., Meng, T., and Malinovskii, V.L. A highly sensitive, excimer-controlled molecular beacon. <u>Angewandte Chemie International Edition</u> 49(7) (2010): 1227-1230.

[39] Kumar, T.S., Wengel, J., and Hrdlicka, P.J. 2′-N-(Pyren-1-yl)acetyl-2′-amino-α-L-LNA: Synthesis and detection of single nucleotide mismatches in DNA and RNA targets. <u>ChemBioChem</u> 8(10) (2007): 1122-1125.

[40] Tyagi, S., Marras, S.A.E., and Kramer, F.R. Wavelength-shifting molecular beacons. <u>Nat Biotech</u> 18(11) (2000): 1191-1196.

[41]   Conlon, P., et al. Pyrene excimer signaling molecular beacons for probing
         nucleic acids. Journal of the American Chemical Society 130(1) (2007): 336-
         342.

[42]   Tong, A.K., et al. Triple fluorescence energy transfer in covalently
         trichromophore-labeled DNA. Journal of the American Chemical Society
         123(51) (2001): 12923-12924.

[43]   Wang, Q., Chen, L., Tian, H., and Wu, J. Molecular beacons of xeno-nucleic
         acid for detecting nucleic acid. Theranostics 3 (2013): 395-408.

[44]   Svanvik, N., Westman, G., Wang, D., and Kubista, M. Light-up probes: Thiazole
         orange-conjugated peptide nucleic acid for detection of target nucleic acid in
         homogeneous solution. Analytical Biochemistry 281(1) (2000): 26-35.

[45]   Socher, E., Jarikote, D.V., Knoll, A., Röglin, L., Burmeister, J., and Seitz, O. FIT
         probes: Peptide nucleic acid probes with a fluorescent base surrogate enable
         real-time DNA quantification and single nucleotide polymorphism discovery.
         Analytical Biochemistry 375(2) (2008): 318-330.

[46]   Englund, E.A. and Appella, D.H. Synthesis of γ-substituted peptide nucleic
         acids: A new place to attach fluorophores without affecting DNA binding.
         Organic Letters 7(16) (2005): 3465-3467.

[47]   Seitz, O. Solid-phase synthesis of doubly labeled peptide nucleic acids as
         probes for the real-time detection of hybridization. Angewandte Chemie
         International Edition 39(18) (2000): 3249-3252.

[48]   Svanvik, N., Nygren, J., Westman, G., and Kubista, M. Free-probe fluorescence
         of light-up probes. Journal of the American Chemical Society 123(5) (2001):
         803-809.

[49]   Köhler, O., Jarikote, D.V., and Seitz, O. Forced intercalation probes (FIT
         Probes): thiazole orange as a fluorescent base in peptide nucleic acids for
         homogeneous single-nucleotide-polymorphism detection. ChemBioChem 6(1)
         (2005): 69-77.

[50]   Kuhn, H., Demidov, V.V., Coull, J.M., Fiandaca, M.J., Gildea, B.D., and Frank-
         Kamenetskii, M.D. Hybridization of DNA and PNA molecular beacons to single-

stranded and double-stranded DNA targets. Journal of the American Chemical Society 124(6) (2002): 1097-1103.

[51] Kuhn, H., Demidov, V.V., Gildea, B.D., Fiandaca, M.J., Coull, J.C., and Frank-Kamenetskii, M.D. PNA beacons for duplex DNA. Antisense and Nucleic Acid Drug Development 11(4) (2001): 265-270.

[52] Socher, E., Bethge, L., Knoll, A., Jungnick, N., Herrmann, A., and Seitz, O. Low-noise stemless PNA beacons for sensitive DNA and RNA detection. Angewandte Chemie International Edition 47(49) (2008): 9555-9559.

[53] Socher, E., Knoll, A., and Seitz, O. Dual fluorophore PNA FIT-probes - extremely responsive and bright hybridization probes for the sensitive detection of DNA and RNA. Organic & Biomolecular Chemistry 10(36) (2012): 7363-7371.

[54] Hövelmann, F., et al. Brightness through local constraint—LNA-enhanced FIT hybridization probes for In vivo ribonucleotide particle tracking. Angewandte Chemie International Edition 53(42) (2014): 11370-11375.

[55] Hövelmann, F., Gaspar, I., Ephrussi, A., and Seitz, O. Brightness enhanced DNA FIT-probes for wash-free RNA imaging in tissue. Journal of the American Chemical Society 135(50) (2013): 19025-19032.

[56] Boontha, B., Nakkuntod, J., Hirankarn, N., Chaumpluk, P., and Vilaivan, T. Multiplex mass spectrometric genotyping of single nucleotide polymorphisms employing pyrrolidinyl peptide nucleic acid in combination with ion-exchange capture. Analytical Chemistry 80(21) (2008): 8178-8186.

[57] Theppaleak, T., Rutnakornpituk, M., Wichai, U., Vilaivan, T., and Rutnakornpituk, B. Anion-exchanged nanosolid support of magnetic nanoparticle in combination with PNA probes for DNA sequence analysis. Journal of Nanoparticle Research 15(12) (2013): 1-12.

[58] Theppaleak, T., Rutnakornpituk, B., Wichai, U., Vilaivan, T., and Rutnakornpituk, M. Magnetite nanoparticle with positively charged surface for immobilization of peptide nucleic acid and deoxyribonucleic acid. Journal of Biomedical Nanotechnology 9(9) (2013): 1509-1520.

[59]   Ananthanawat, C., Vilaivan, T., Hoven, V.P., and Su, X.D. Comparison of DNA, aminoethylglycyl PNA and pyrrolidinyl PNA as probes for detection of DNA hybridization using surface plasmon resonance technique. <u>Biosensors & Bioelectronics</u> 25(5) (2010): 1064-1069.

[60]   Boonlua, C., Vilaivan, C., Wagenknecht, H.-A., and Vilaivan, T. 5-(Pyren-1-yl)uracil as a base-discriminating fluorescent nucleobase in pyrrolidinyl peptide nucleic acids. <u>Chemistry – An Asian Journal</u> 6(12) (2011): 3251-3259.

[61]   Reenabthue, N., Boonlua, C., Vilaivan, C., Vilaivan, T., and Suparpprom, C. 3-Aminopyrrolidine-4-carboxylic acid as versatile handle for internal labeling of pyrrolidinyl PNA. <u>Bioorganic & Medicinal Chemistry Letters</u> 21(21) (2011): 6465-6469.

[62]   Boonlua, C., et al. Pyrene-labeled pyrrolidinyl peptide nucleic acid as a hybridization-responsive DNA probe: comparison between internal and terminal labeling. <u>RSC Advances</u> 4(17) (2014): 8817-8827.

[63]   Ditmangklo, B., Boonlua, C., Suparpprom, C., and Vilaivan, T. Reductive alkylation and sequential reductive alkylation-Click chemistry for on-solid-support modification of pyrrolidinyl peptide nucleic acid. <u>Bioconjugate Chemistry</u> 24(4) (2013): 614-625.

[64]   Maneelun, N. and Vilaivan, T. Dual pyrene-labeled pyrrolidinyl peptide nucleic acid as an excimer-to-monomer switching probe for DNA sequence detection. <u>Tetrahedron</u> 69(51) (2013): 10805-10810.

[65]   Berchel, M., et al. Modular Construction of fluorescent lipophosphoramidates by Click chemistry. <u>European Journal of Organic Chemistry</u> 2011(31) (2011): 6294-6303.

[66]   Li, Y., Schaffer, P., and Perrin, D.M. Dual isotope labeling: Conjugation of 32P-oligonucleotides with 18F-aryltrifluoroborate via copper(I) catalyzed cycloaddition. <u>Bioorganic & Medicinal Chemistry Letters</u> 23(23) (2013): 6313-6316.

[67]   Kele, P., et al. Clickable fluorophores for biological labeling-with or without copper. <u>Organic & Biomolecular Chemistry</u> 7(17) (2009): 3486-3490.

[68] Srisuwannaket, C. Synthesis and DNA-binding properties of novel peptide nucleic acids bearing (1S,2S)-2-aminocyclopentane carboxylic acid spacer. Doctoral Dissertation, Department of Chemistry, Chulalongkorn University (2005).

[69] Ngamwiriyawong, P. and Vilaivan, T. Synthesis and nucleic acids binding properties of diastereomeric aminoethylprolyl peptide nucleic acids (aepPNA). Nucleosides, Nucleotides and Nucleic Acids 30(2) (2011): 97-112.

[70] Berchel, M., et al. Functionalized phospholipid molecular platform: Use for production of cationic fluorescent lipids. European Journal of Organic Chemistry 2014(5) (2014): 1076-1083.

[71] Vilaivan, T. chemistry.sc.chula.ac.th. Avaialbe from: http://www.chemistry.sc.chula.ac.th/pna.

[72] glenresearch.com. [cited 2013 Aug 25] Avaiable from: http://www.glenresearch.com/Technical/Extinctions.html.

[73] Pak, J.K. and Hesse, M. Regioselective deprotection and acylation of penta-N-protected thermopentamine. Helvetica Chimica Acta 81(12) (1998): 2300-2313.

[74] Scheidt, K.A., Chen, H., Follows, B.C., Chemler, S.R., Coffey, D.S., and Roush, W.R. Tris(dimethylamino)sulfonium difluorotrimethylsilicate, a mild reagent for the removal of silicon protecting groups. The Journal of Organic Chemistry 63(19) (1998): 6436-6437.

[75] micro-shop.zeiss.com [cited 2013 July 20] Availble from: https://www.micro-shop.zeiss.com/?s=141775055866fe1&l=en&p=us&f=f&a=i.

[76] Kovaliov, M., Wachtel, C., Yavin, E., and Fischer, B. Synthesis and evaluation of a photoresponsive quencher for fluorescent hybridization probes. Organic & Biomolecular Chemistry 12(39) (2014): 7844-7858.

[77] Kodama, S., Asano, S., Moriguchi, T., Sawai, H., and Shinozuka, K. Novel fluorescent oligoDNA probe bearing a multi-conjugated nucleoside with a fluorophore and a non-fluorescent intercalator as a quencher. Bioorganic & Medicinal Chemistry Letters 16(10) (2006): 2685-2688.

[78] Lange, N. and Campo, M.A. Compounds for fluorescence imaging. 2010, Google Patents.

[79]   Lavis, L.D. and Raines, R.T. Bright building blocks for chemical biology. <u>ACS Chemical Biology</u> 9(4) (2014): 855-866.

[80]   Faletrov, Y.V., et al. Evaluation of the fluorescent probes Nile red and 25-NBD-cholesterol as substrates for steroid-converting oxidoreductases using pure enzymes and microorganisms. <u>FEBS Journal</u> 280(13) (2013): 3109-3119.

[81]   Yamane, A. MagiProbe: a novel fluorescence quenching-based oligonucleotide probe carrying a fluorophore and an intercalator. <u>Nucleic Acids Research</u> 30(19) (2002): e97.

[82]   Ranasinghe, R.T., Brown, L.J., and Brown, T. Linear fluorescent oligonucleotide probes with an acridine quencher generate a signal upon hybridisation. <u>Chemical Communications</u> (16) (2001): 1480-1481.

[83]   Shinozuka, K., Seto, Y., and Sawai, H. A novel multifunctionally labelled DNA probe bearing an intercalator and a fluorophore. <u>Journal of the Chemical Society, Chemical Communications</u> (11) (1994): 1377-1378.

[84]   Kongphet, J. Electrochemically active peptide nucleic acid probes <u>Dissertation, Department of Chemistry, Chulalongkorn University </u>(2014).

[85]   Boonlua, C. Development of fluorescencde pyrrolidinyl peptide nucleic acid as probes for determination of DNA sequences. <u>Dissertation, Department of Chemistry, Chulalongkorn University </u> (2012).

[86]   Barrois, S. and Wagenknecht, H.-A. In-stem labelling allows visualization of DNA strand displacements by distinct fluorescent colour change. <u>Organic & Biomolecular Chemistry</u> 11(19) (2013): 3085-3088.

[87]   Vary, C.P.H. A homogeneous nucleic acid hybridization assay based on stand displacement. <u>Nucleic Acids Research</u> 15(17) (1987): 6883-6897.

[88]   Little, M.C., et al. Strand displacement amplification and homogeneous real-time detection incorporated in a second-generation DNA probe system, BDProbeTecET. <u>Clinical Chemistry</u> 45(6) (1999): 777-784.

[89]   Lavis, L.D. and Raines, R.T. Bright ideas for chemical biology. <u>ACS Chemical Biology</u> 3(3) (2008): 142-155.

[90]   Waegele, M.M., Culik, R.M., and Gai, F. Site-specific spectroscopic reporters of the local rlectric field, hydration, structure, and dynamics of biomolecules. <u>The Journal of Physical Chemistry Letters</u> 2(20) (2011): 2598-2609.

[91]   Dziuba, D., et al. A universal nucleoside with strong two-band switchable fluorescence and sensitivity to the environment for investigating DNA interactions. <u>Journal of the American Chemical Society</u> 134(24) (2012): 10209-10213.

[92]   Jose, J. and Burgess, K. Benzophenoxazine-based fluorescent dyes for labeling biomolecules. <u>Tetrahedron</u> 62(48) (2006): 11021-11037.

[93]   Okamoto, A., Tainaka, K., and Fujiwara, Y. Nile Red nucleoside: design of a solvatofluorochromic nucleoside as an indicator of micropolarity around DNA. <u>The Journal of Organic Chemistry</u> 71(9) (2006): 3592-3598.

[94]   Varghese, R. and Wagenknecht, H.-A. Non-covalent versus covalent control of self-assembly and chirality of Nile Red-modified nucleoside and DNA. <u>Chemistry – A European Journal</u> 16(30) (2010): 9040-9046.

[95]   Beyer, C. and Wagenknecht, H.-A. In situ azide formation and "click" reaction of nile red with DNA as an alternative postsynthetic route. <u>Chemical Communications</u> 46(13) (2010): 2230-2231.

[96]   Charoenpakdee, C. and Wathanathavorn, P. Synthesis and optical properties of Nile Blue and Nile Red labeled pyrrolidinyl peptide nucleic acid. <u>Senior-Project, Department of Chemistry, Chulalongkorn University</u> (2012).

[97]   Drummond, T.G., Hill, Michael G, Barton, Jacqueline K. Electrochemical DNA sensors. <u>Nat Biotech</u> 21(10) (2003/10//print).

[98]   Briggs S.J.M., Bruce, I.,. Miller, J.N., Moody, C.J., Simmonds, A.C., and Swann, E. Synthesis of functionalised fluorescent dyes and their coupling to amines and amino acids. <u>Journal of the Chemical Society, Perkin Transactions 1</u> (7) (1997): 1051-1058.

[99]   Magde, D., Brannon, J.H., Cremers, T.L., and Olmsted, J. Absolute luminescence yield of cresyl violet. A standard for the red. <u>The Journal of Physical Chemistry</u> 83(6) (1979): 696-699.

[100] Varghese, R., Gajula, P.K., Chakraborty, T.K., and Wagenknecht, H.A. Synthesis and opitcal properties of Nile red modified 2'-deoxyuridine and 7-Deaza-2'-deoxyadenosine: Highly emissive solvatochromic nucleotides. <u>SYNLETT</u> 20 (2009): 3252-3257.

[101] Okamoto, A., Ichiba, T., and Saito, I. Pyrene-labeled oligodeoxynucleotide probe for detecting base insertion by excimer fluorescence emission. <u>Journal of the American Chemical Society</u> 126(27) (2004): 8364-8365.

APPENDIX
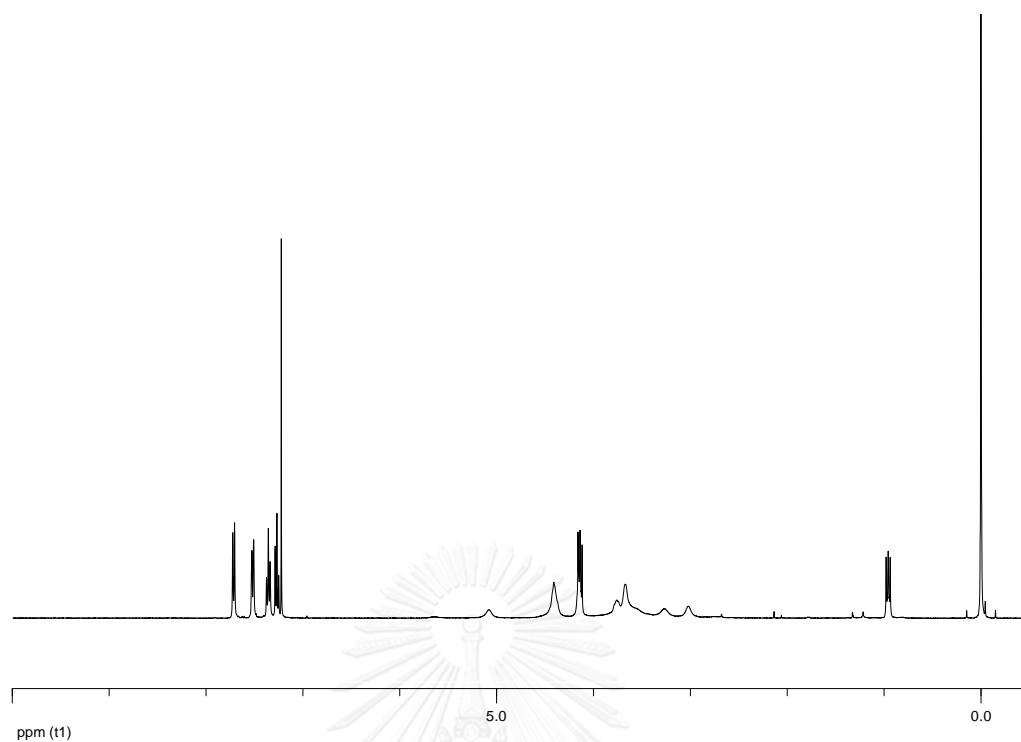
Figure A1. ^{1}H NMR spectrum (400 MHz, CDCl$_3$) of Teoc-protected APC spacer(**2a**)
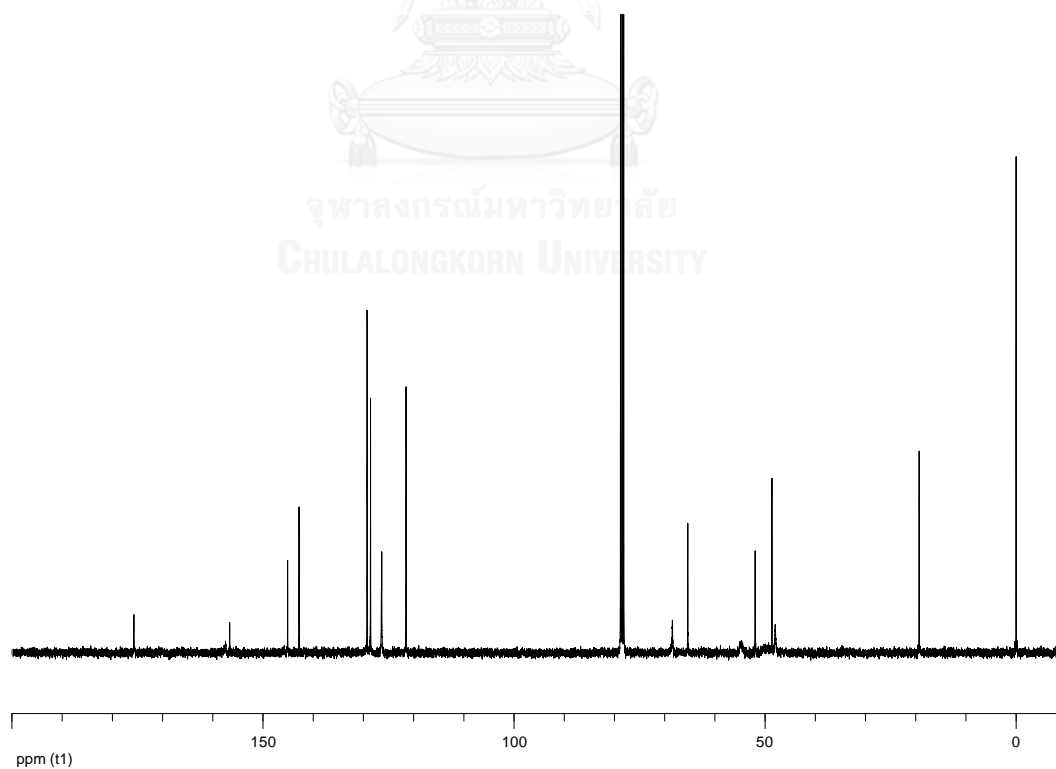
Figure A2. ^{13}C NMR spectrum (100 MHz, CDCl$_3$) of Teoc-protected APC spacer(**2a**)
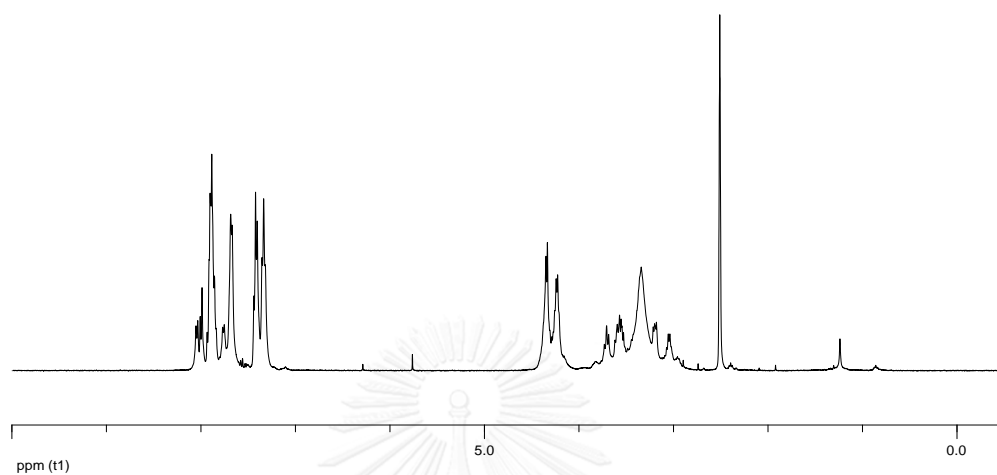
Figure A3. ^{1}H NMR spectrum (400 MHz, DMSO-d6) of of o-Nosyl-protected APC space (2b)
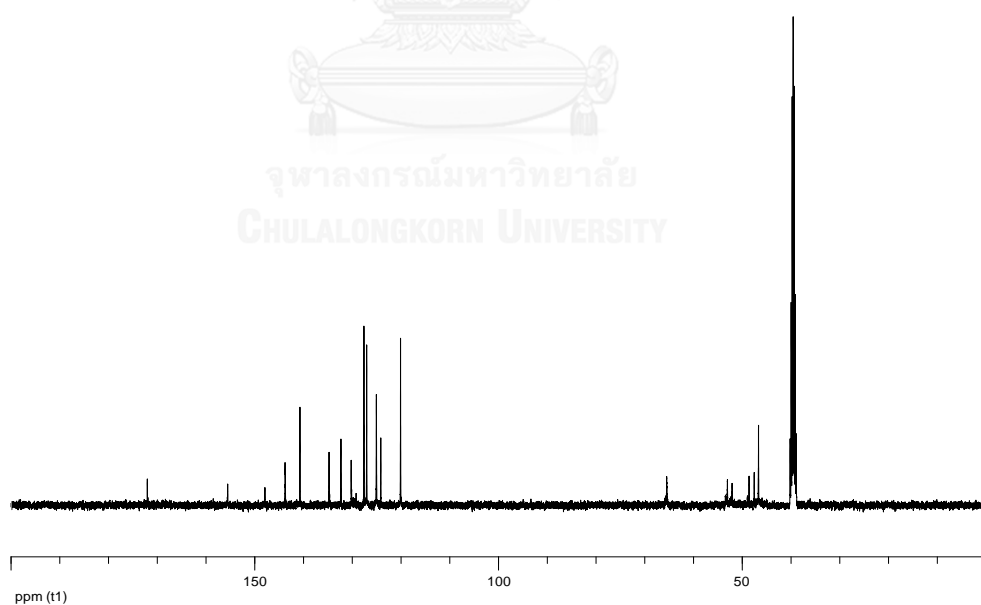
Figure A4. ^{13}C NMR spectrum (100 MHz, DMSO-d6) of o-Nosyl-protected APC space (**2b**)
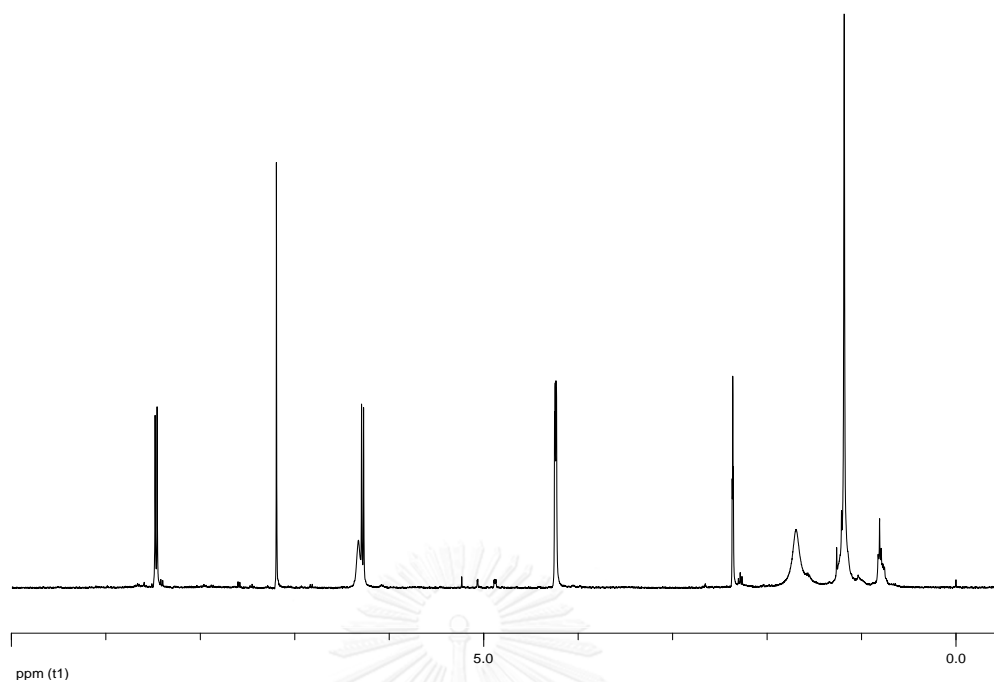
Figure A5. ^{1}H NMR spectrum (400 MHz, CDCl$_3$) of 4-propargylamino-7-nitrobenzofurazan (**4**)
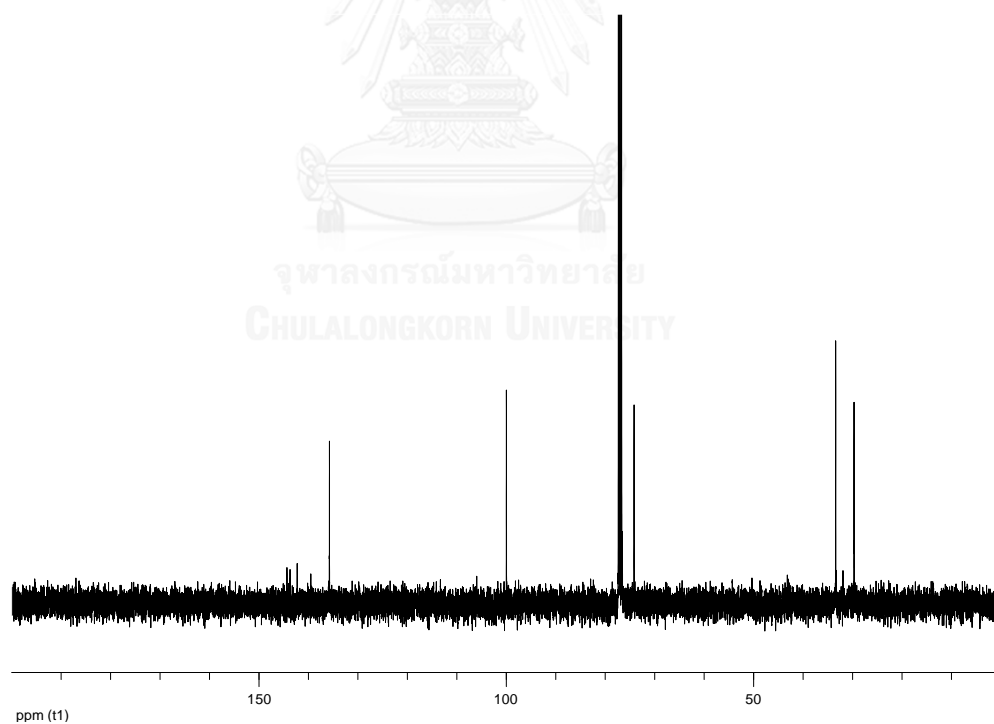
Figure A6. ^{13}C NMR spectrum (100 MHz, CDCl$_3$) of 4-propargylamino-7-nitrobenzofurazan (**4**)

ppm (t1)
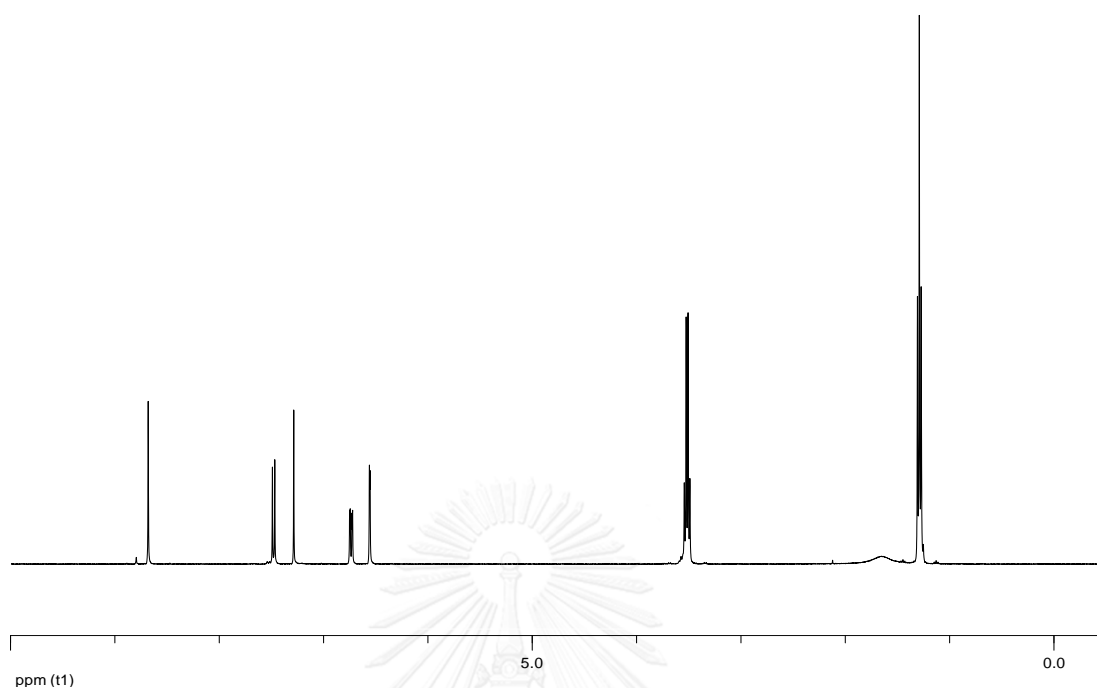
Figure A7. ^{1}H NMR spectrum (400 MHz, CDCl3) of 7-diethylamino-3-carboxy-coumarin (7)

ppm (t1)
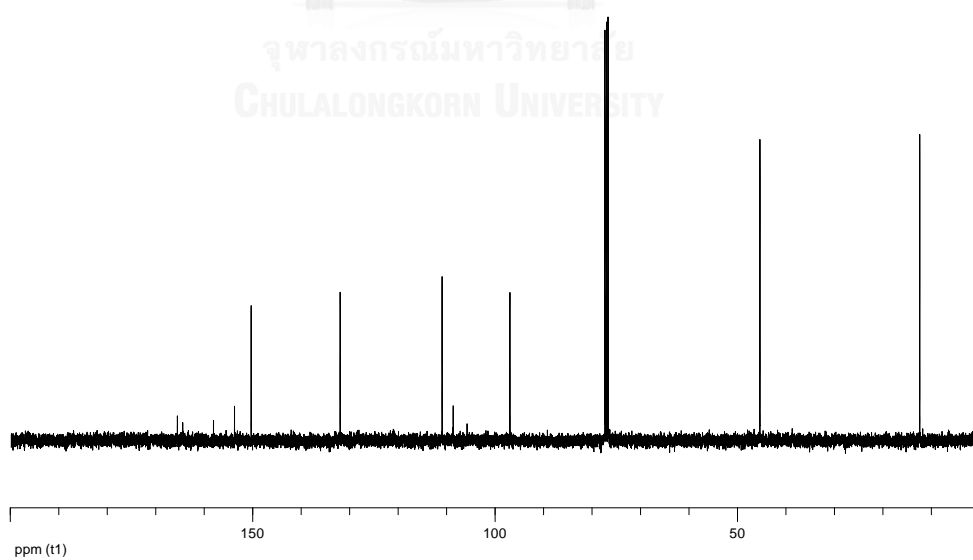
Figure A8. ^{13}C NMR spectrum (100 MHz, CDCl$_3$) of 7-diethylamino-3-carboxy-coumarin **(7)**
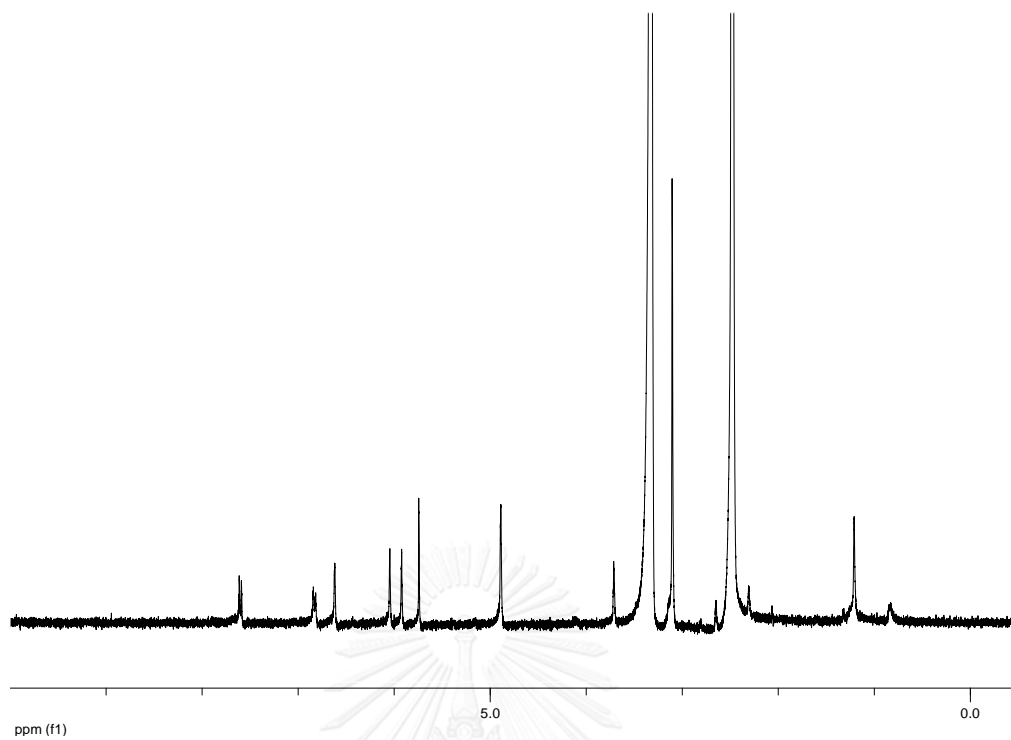
Figure A9. ^{1}H NMR spectrum (400 MHz, DMSO-d6) of Phenoxazine Red (**10**)
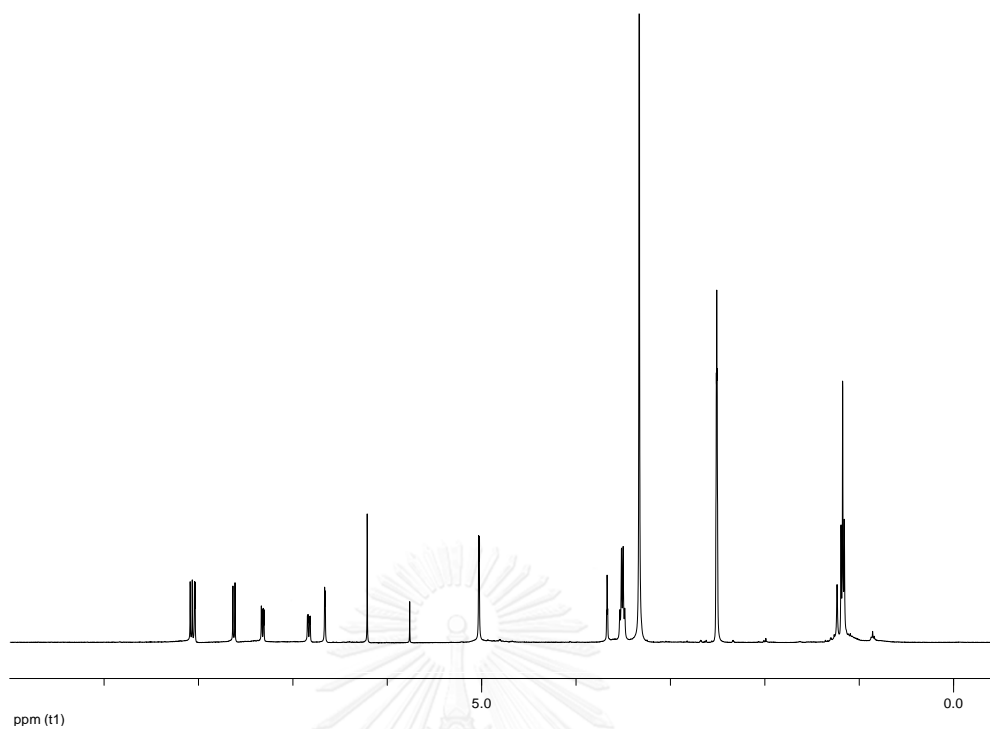
Figure A10. ^{1}H NMR spectrum (400 MHz, DMSO-d6) of Nile red (**12**)
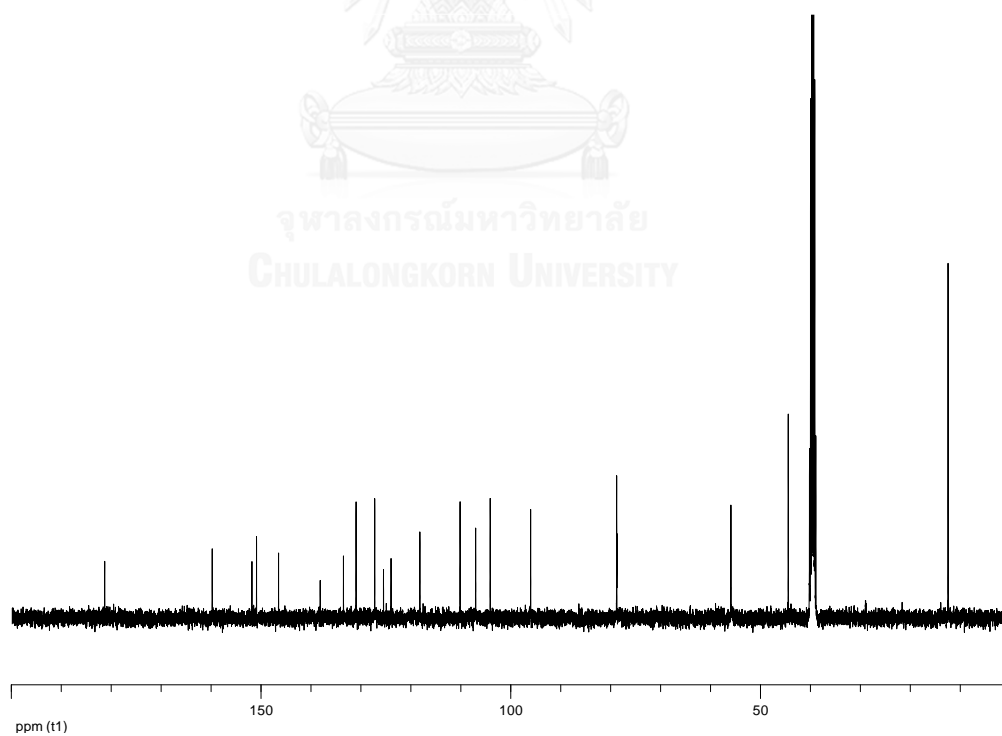
Figure A11. ^{13}C NMR spectrum (100 MHz, DMSO-d6) of Nile red (**12**)
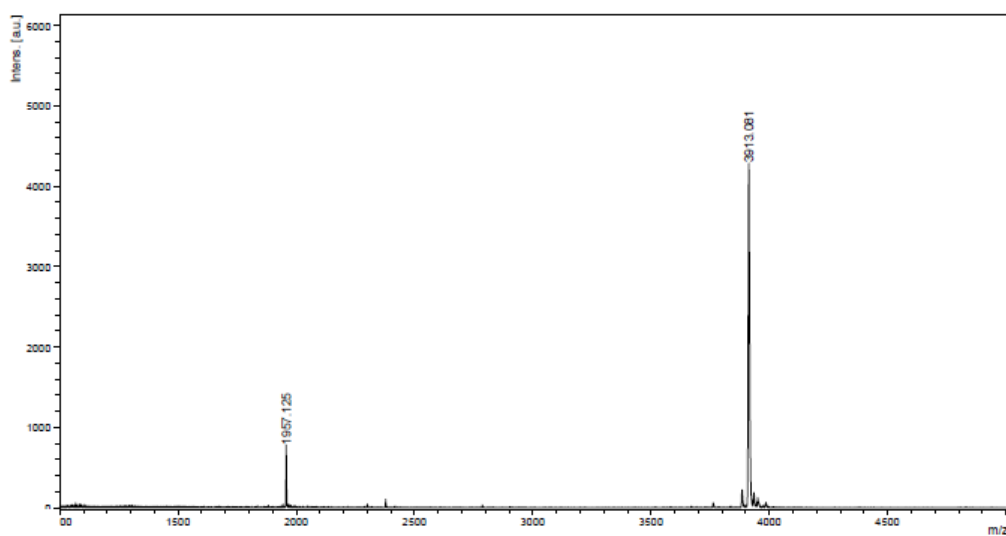
Figure A12. MALDI-TOF mass spectrum of AcLys-TTT(Cou1)TTT(Flu)TTT-LysNH$_2$

[**T9(Cou1/Flu)**] (calcd for [M+H]$^+$: m/z=3913.06)
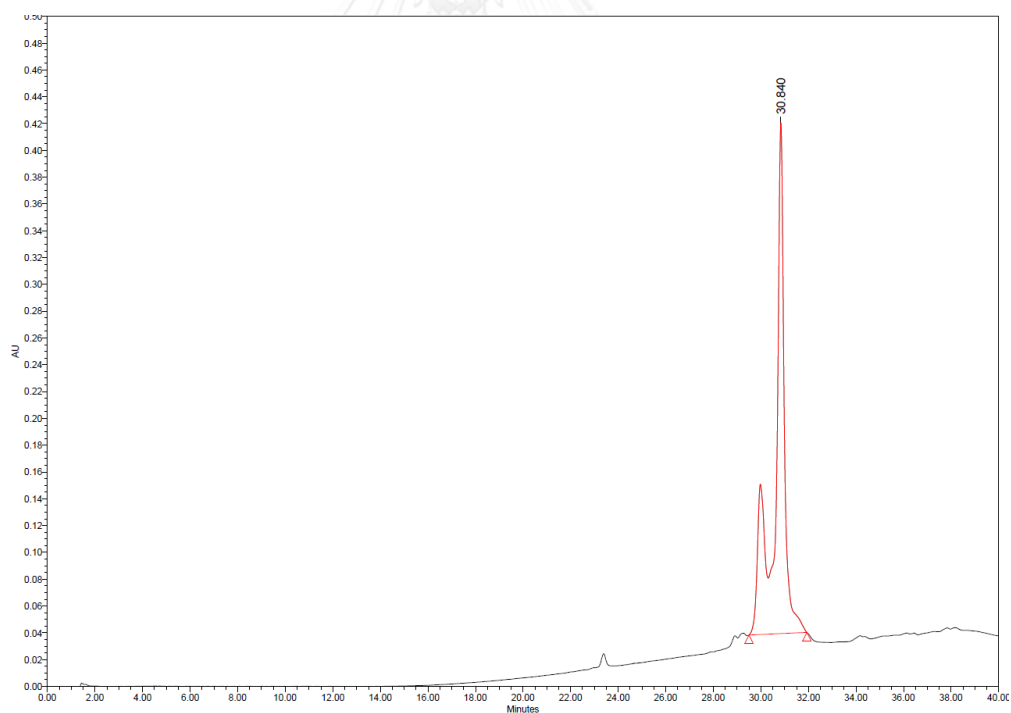
Figure A13. HPLC chromatogram of AcLys-TTT(Cou1)TTT(Flu)TTT-LysNH$_2$

[**T9(Cou1/Flu)**]
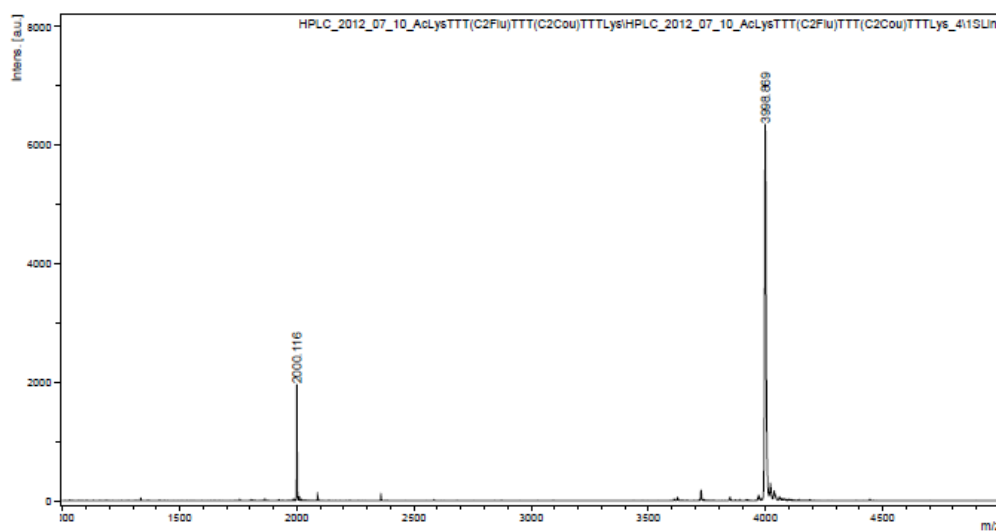
Figure A14. MALDI-TOF mass spectrum of AcLys-TTT(C2Cou1)TTT(C2Flu)TTT-LysNH$_2$ [**T9(C2Cou1/C2Flu)**] (calcd for [M+H]$^+$: m/z=3998.86)
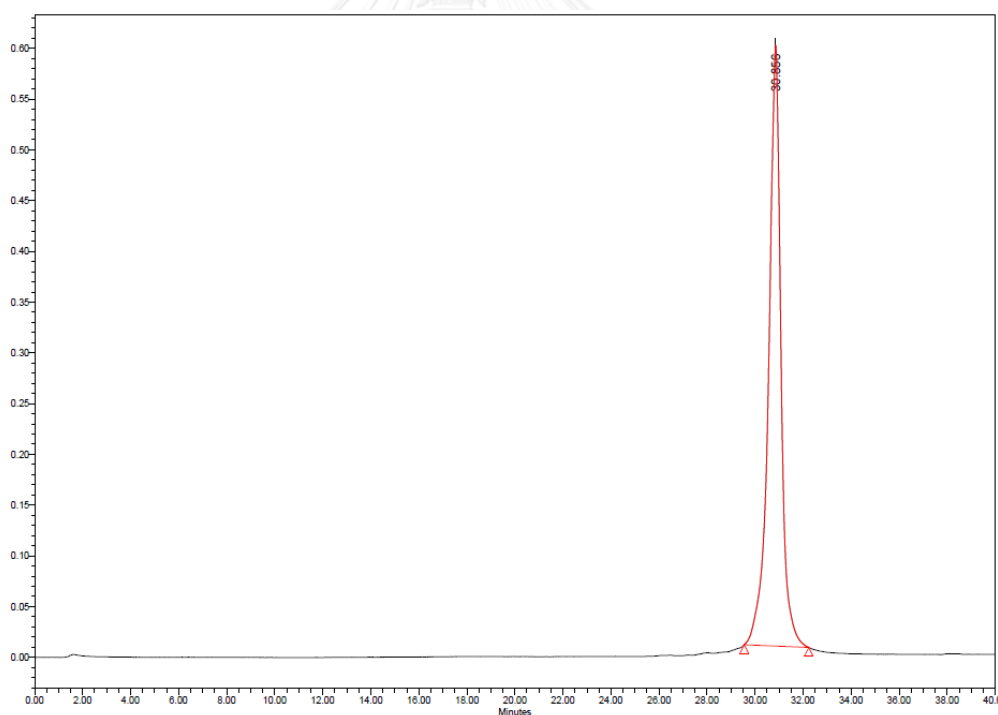
Figure A15. HPLC chromatogram of AcLys--TTT(C2Cou1)TTT(C2Flu)TTT-LysNH$_2$ [**T9(C2Cou1/C2Flu)**]
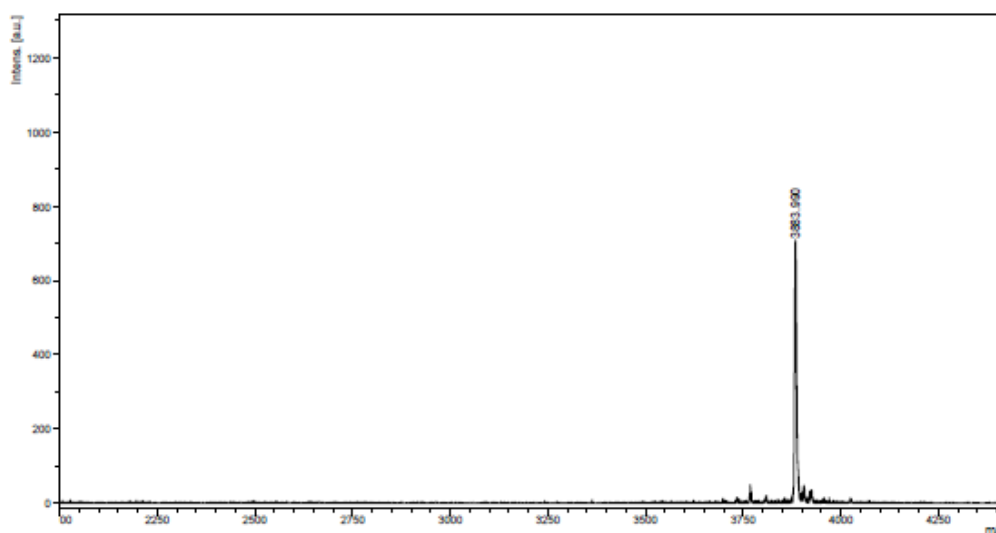
Figure A16. MALDI-TOF mass spectrum of AcLys--TT(Cou2)TTTTT(Flu)TT-LysNH$_2$ [**T9(Cou2/Flu)**] (calcd for [M+H]$^+$: m/z=3883.99)
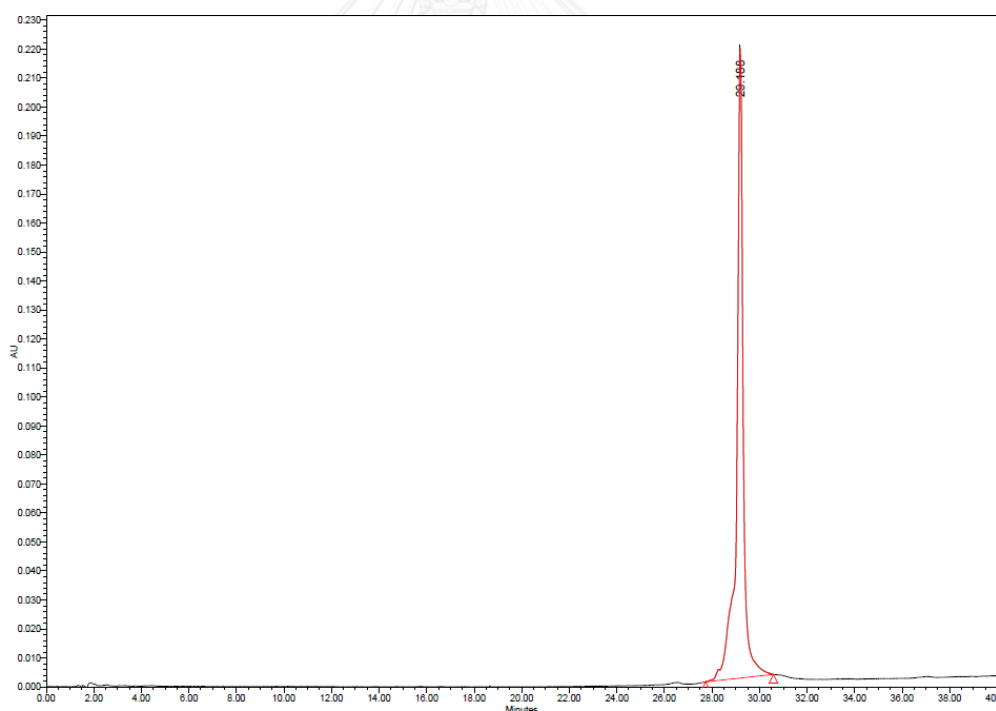
Figure A17. HPLC chromatogram of AcLys-TT(Cou2)TTTTT(Flu)TT-LysNH$_2$ [**T9(Cou2/Flu)**]
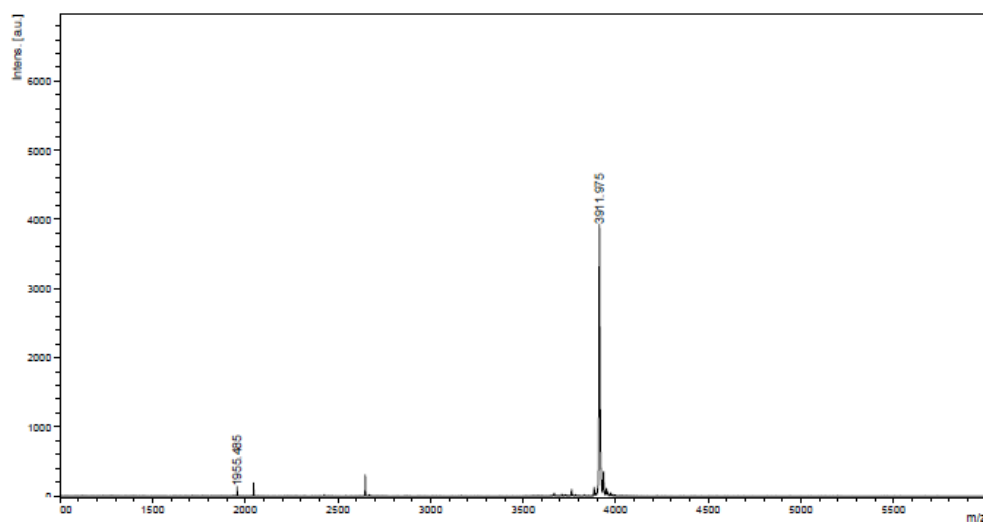
Figure A18. MALDI-TOF mass spectrum of AcLys-TT(Cou2)TTTTT(C2Flu)TT-LysNH$_2$ [**T9(Cou/C2Flu)**] (calcd for [*M*+H]$^+$: m/z=3911.97)
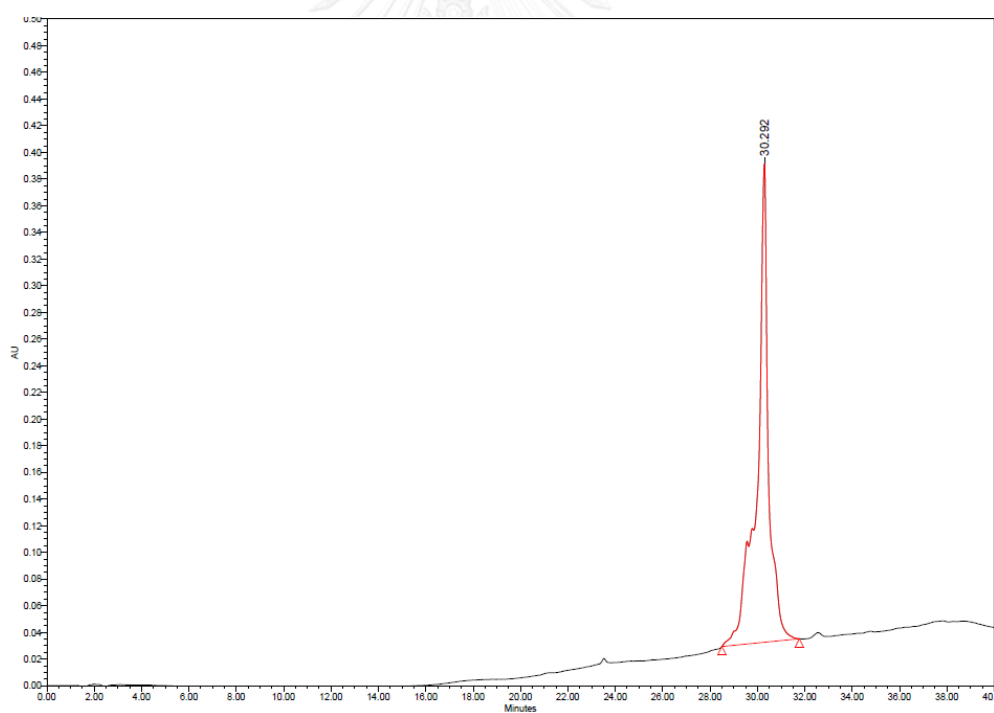
Figure A19. HPLC chromatogram of AcLys-TT(Cou2)TTTTT(C2Flu)TT-LysNH$_2$ [**T9(Cou2/C2Flu)**]
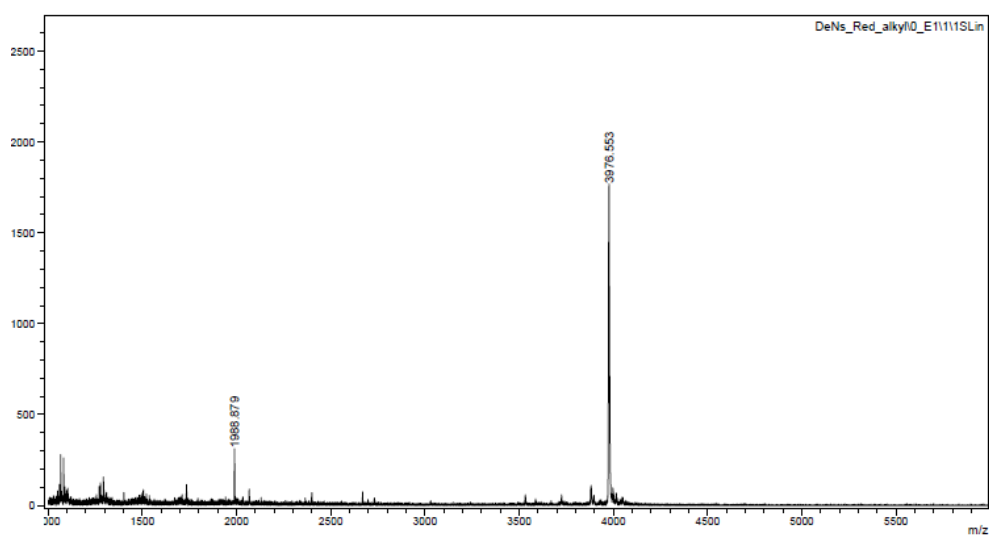
Figure A20. MALDI-TOF mass spectrum of AcLys-TT(C2Cou2)TTTTT(C2Flu)TT-LysNH$_2$ [**T9(C2Cou2/C2Flu)**] (calcd for [*M*+H]$^+$: m/z=3976.55)
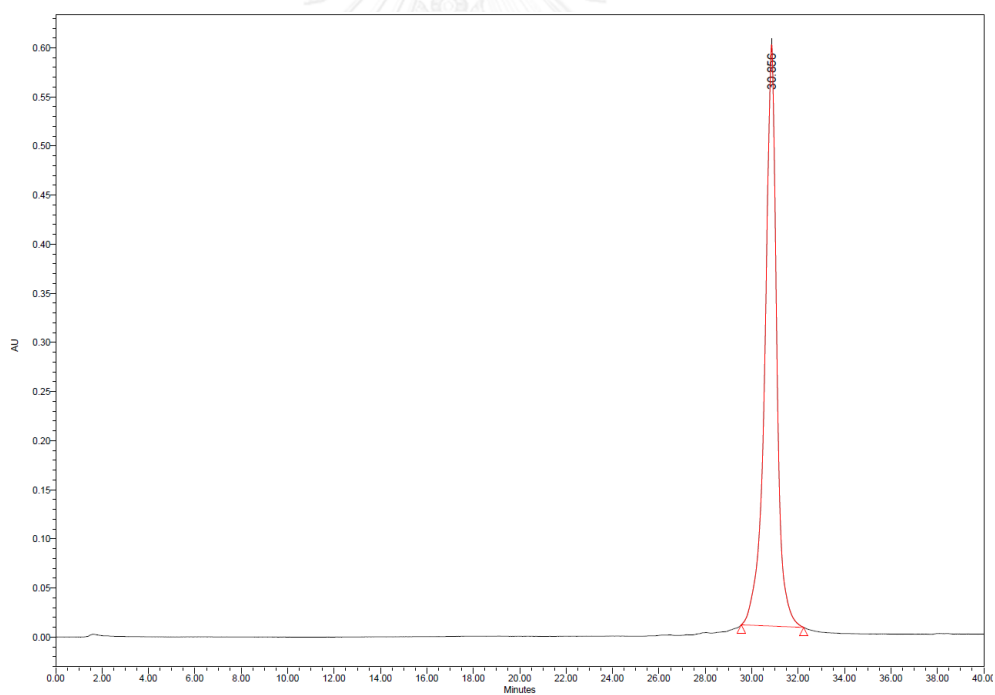
Figure A21. HPLC chromatogram of AcLys-TT(C2Cou2)TTTTT(C2Flu)TT-LysNH$_2$ [**T9(C2Cou2/C2Flu)**]
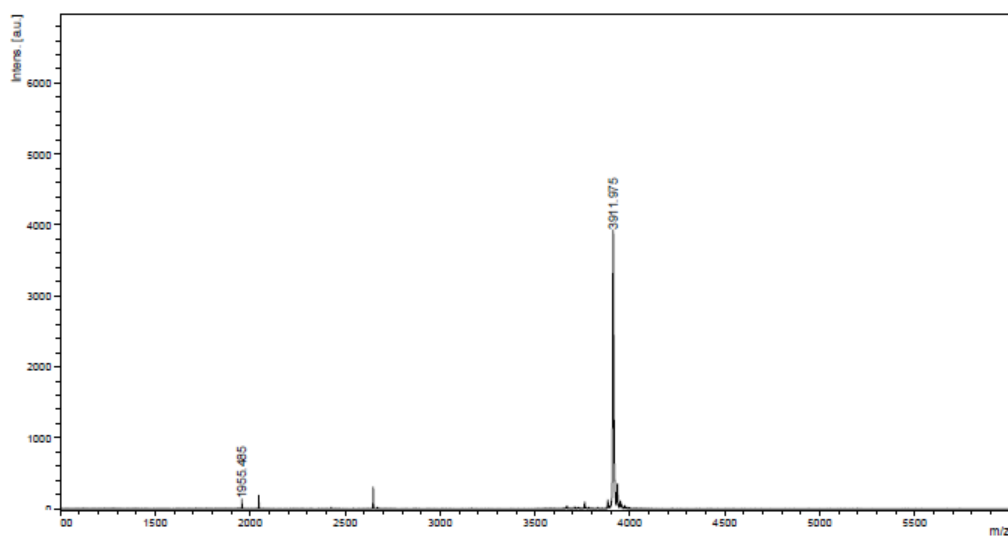
Figure A22. MALDI-TOF mass spectrum of AcLys-TT(C2Cou2)TTTTT(Flu)TT-LysNH$_2$ [**T9(C2Cou2/Flu)**] (calcd for [M+H]$^+$: m/z=3911.97)
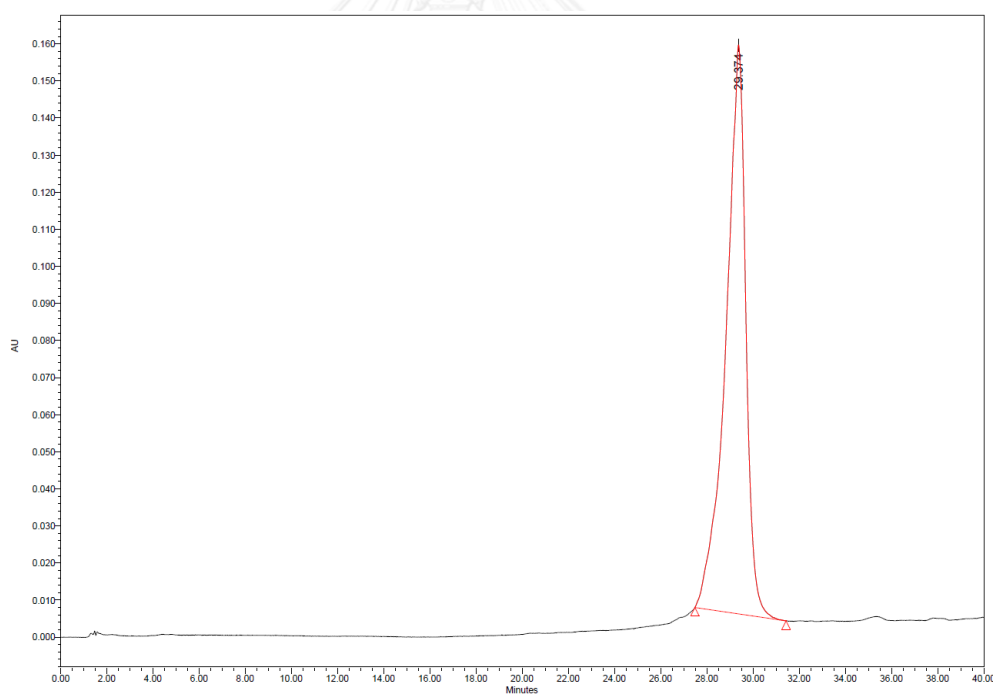
Figure A23. HPLC chromatogram of AcLys-TT(C2Cou2)TTTTT(Flu)TT-LysNH$_2$ [**T9(C2Cou2/Flu)**]
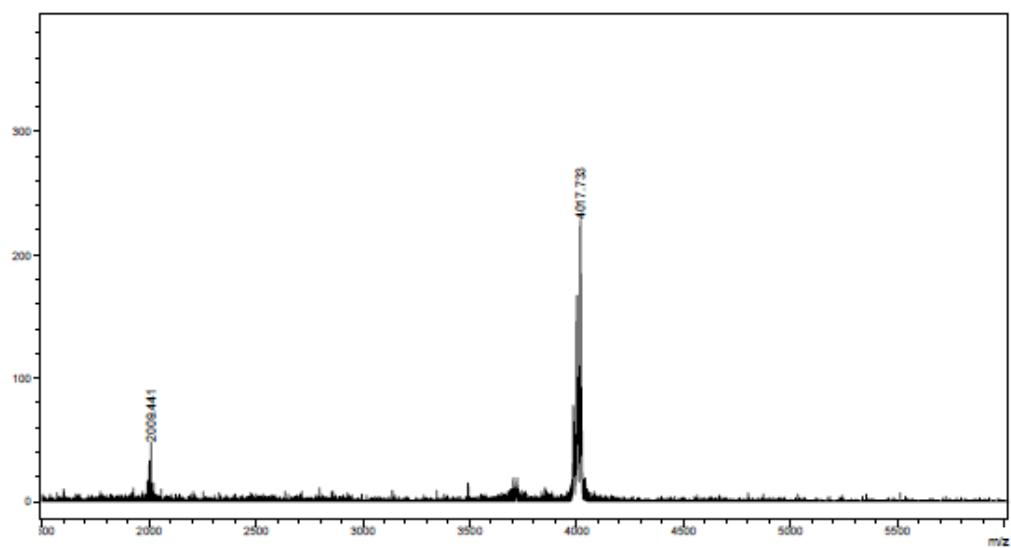
Figure A24. MALDI-TOF mass spectrum of AcLys-TT(NBD)TTTTT(PheR)TT-LysNH$_2$

[**T9(NBD/PheR)**] (calcd for [M+H]$^+$: m/z=4017.73)
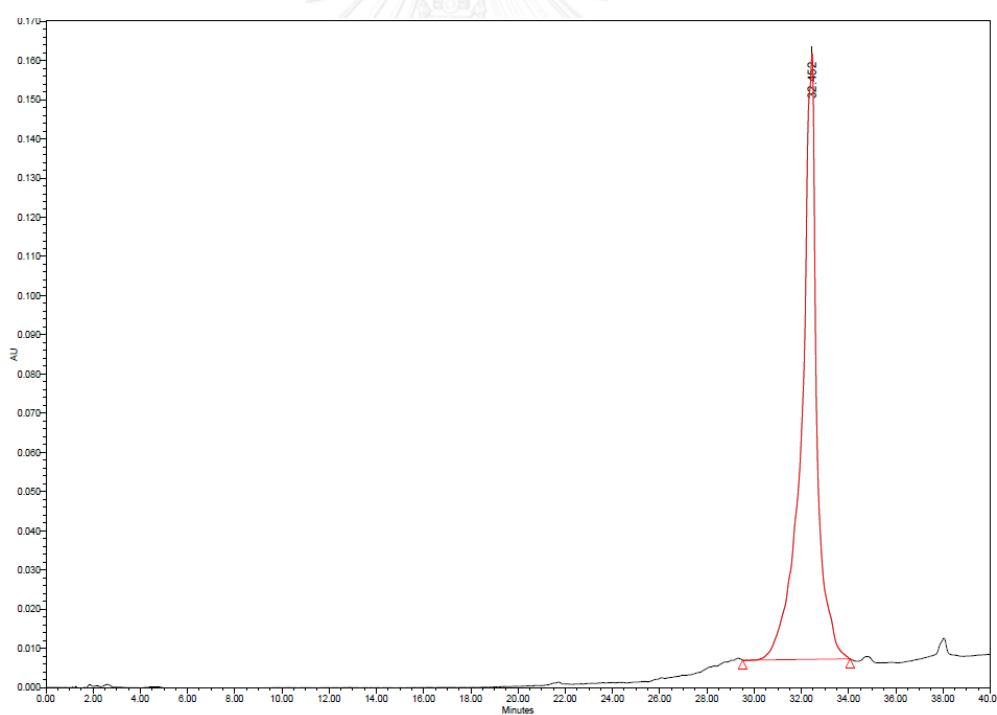
Figure A25. HPLC chromatogram of AcLys-TT(NBD)TTTTT(PheR)TT-LysNH$_2$

[**T9(NBD/PheR)**]
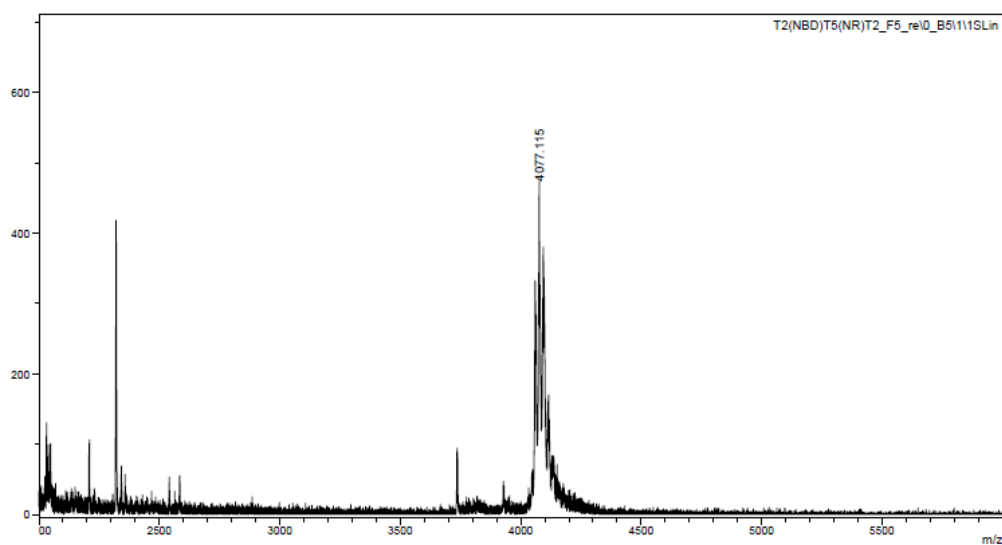
Figure A26. MALDI-TOF mass spectrum of AcLys-TT(NBD)TTTTT(Nr)TT-LysNH$_2$ [**T9(Cou2/Flu)**] (calcd for [M+H]$^+$: m/z=4077.11)
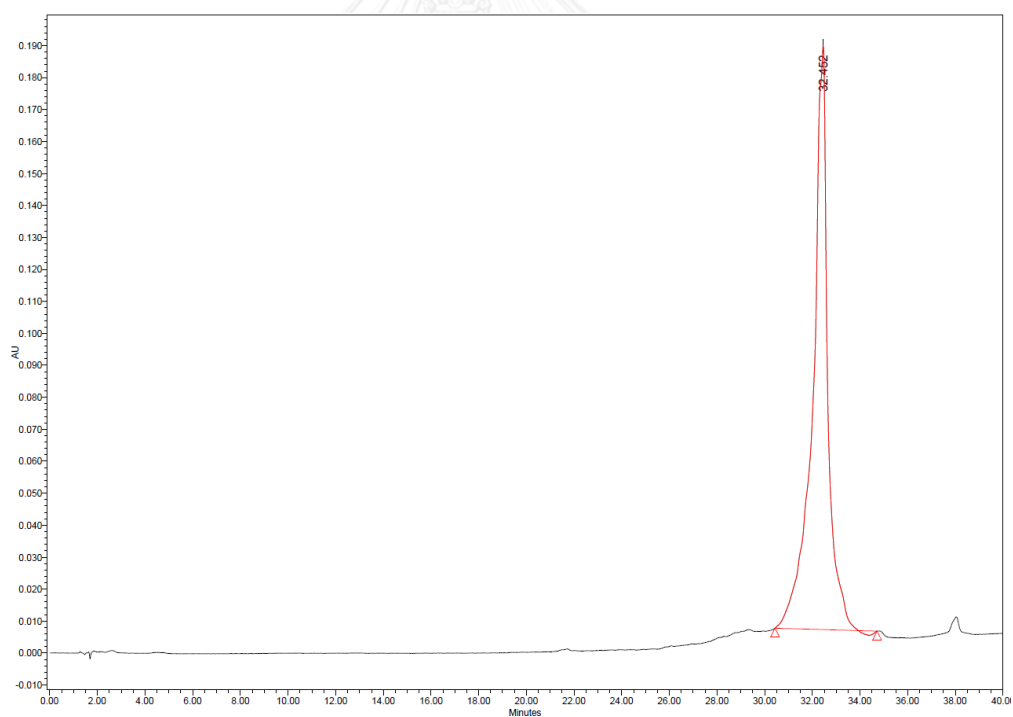
Figure A27. HPLC chromatogram of AcLys-TT(NBD)TTTTT(Nr)TT-LysNH$_2$ [**T9(NBD/Nr)**]
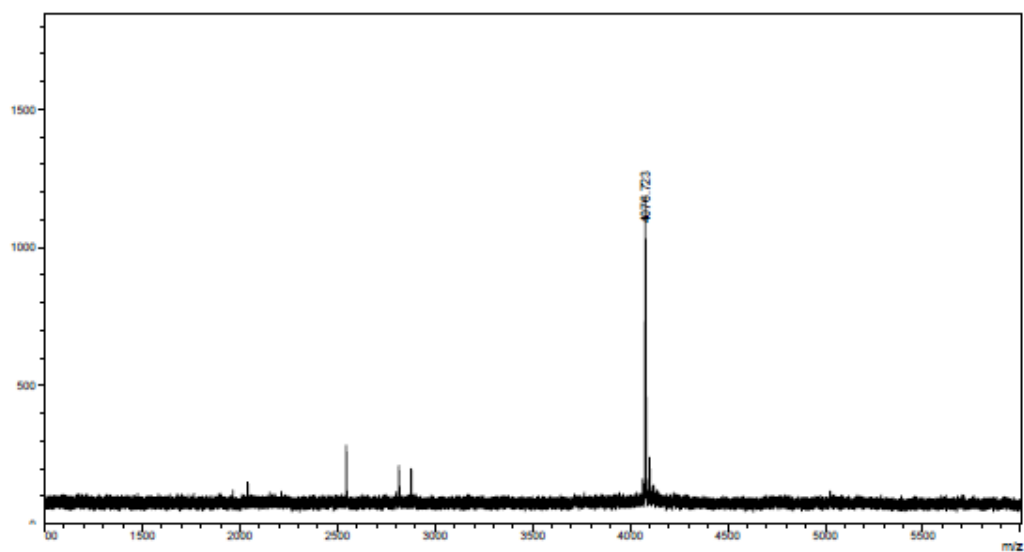
Figure A28. MALDI-TOF mass spectrum of AcLys-TT(Flu)TTTTT(TMR)TT-LysNH$_2$ [**T9(Flu/TMR)1**] (calcd for [M+H]$^+$: m/z=4076.72)
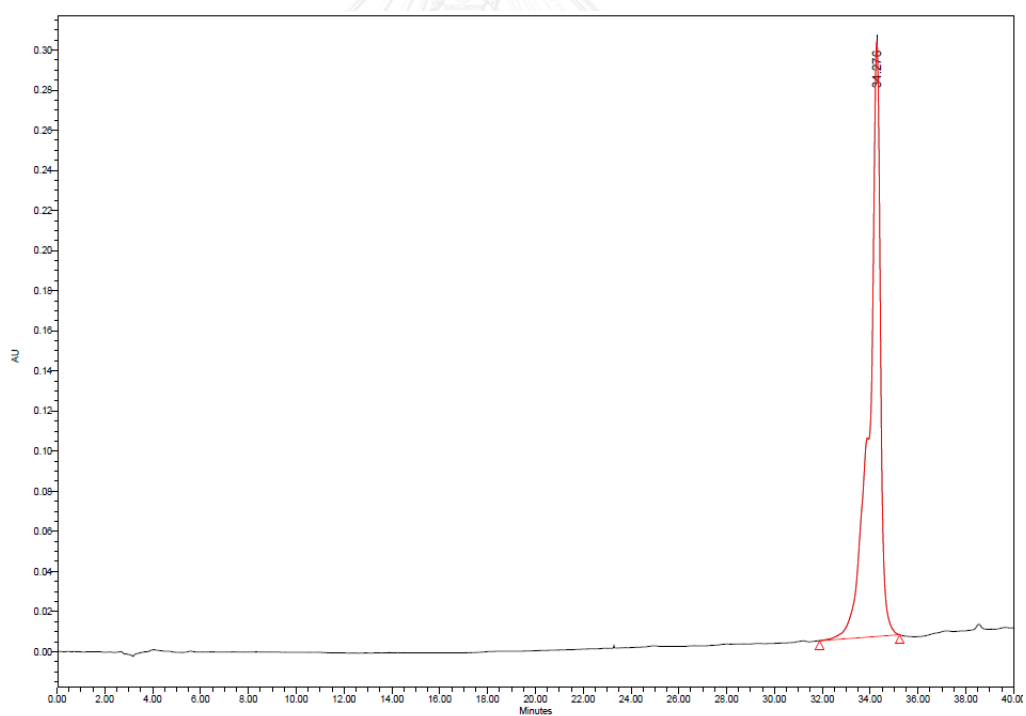
Figure A29. HPLC chromatogram of AcLys-TT(Flu)TTTTT(TMR)TT-LysNH$_2$ [**T9(Flu/TMR)1**]
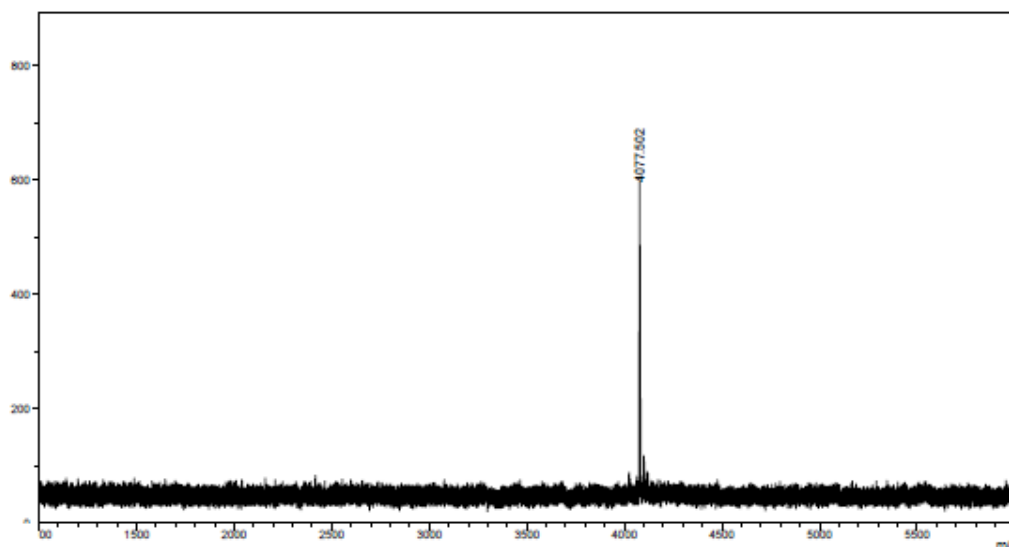
Figure A30. MALDI-TOF mass spectrum of AcLys-TTTT(Flu)T(TMR)TTTT-LysNH$_2$ [**T9(Flu/TMR)2**] (calcd for [*M*+H]$^+$: m/z=4077.50)
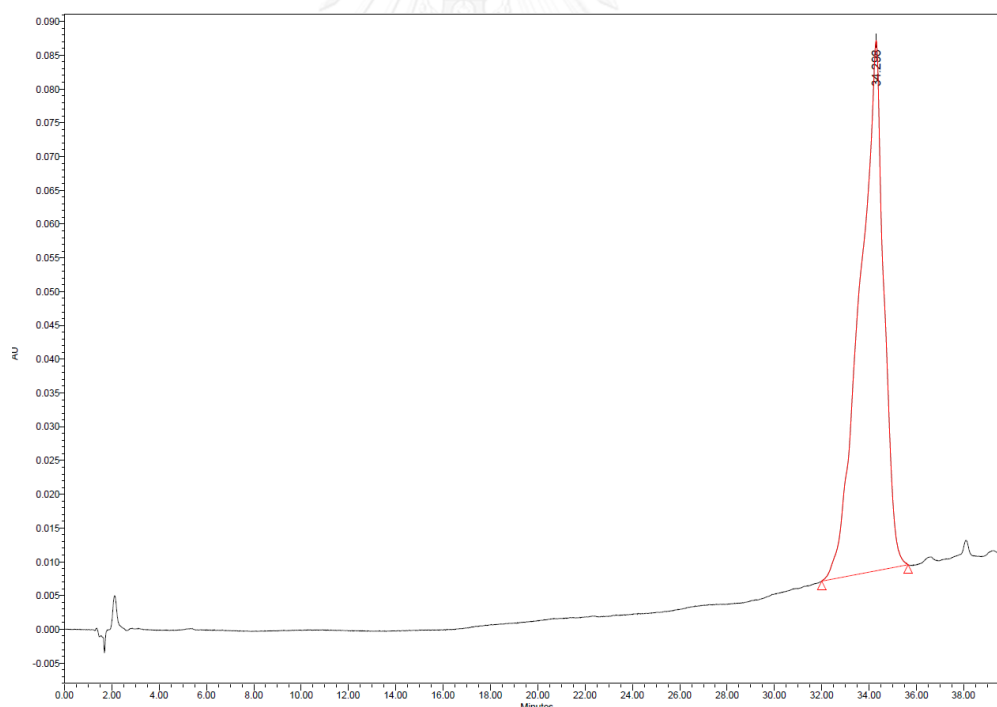
Figure A31. HPLC chromatogram of AcLys-TTTT(Flu)T(TMR)TTTT-LysNH$_2$ [**T9(Flu/TMR)2**]
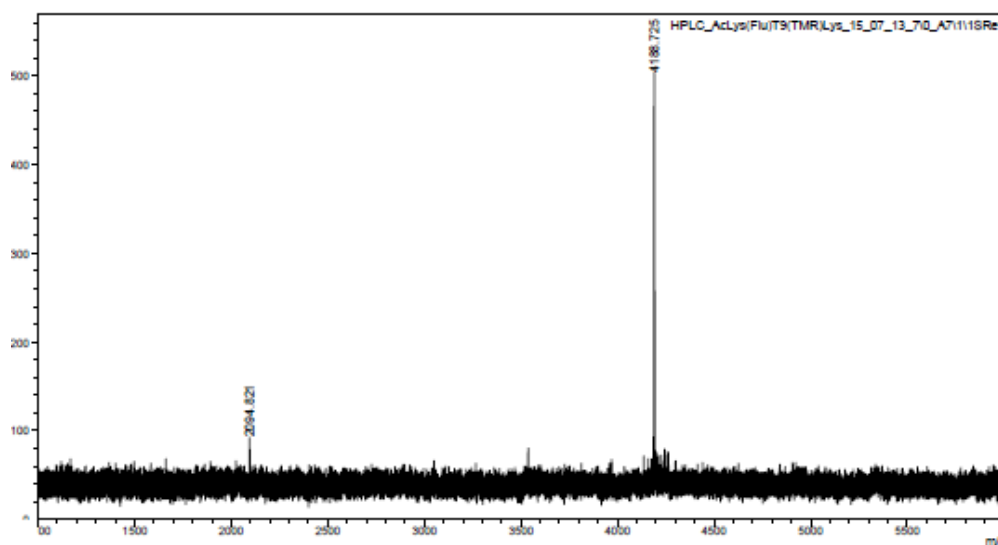
Figure A32. MALDI-TOF mass spectrum of AcLys--(Flu)TTTTTTTTT(TMR)-LysNH$_2$
[**T9(Flu/TMR)3**] (calcd for [M+H]$^+$: m/z=4188.72)
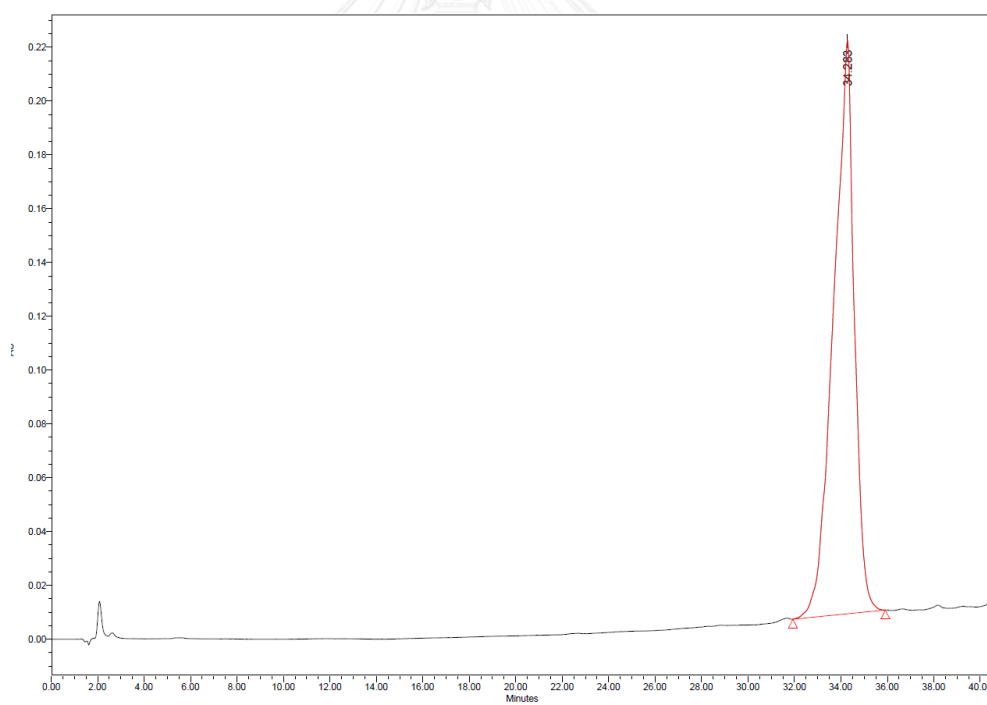
Figure A33. HPLC chromatogram of AcLys- (Flu)TTTTTTTTT(TMR) -LysNH$_2$
[**T9(Flu/TMR)3**]
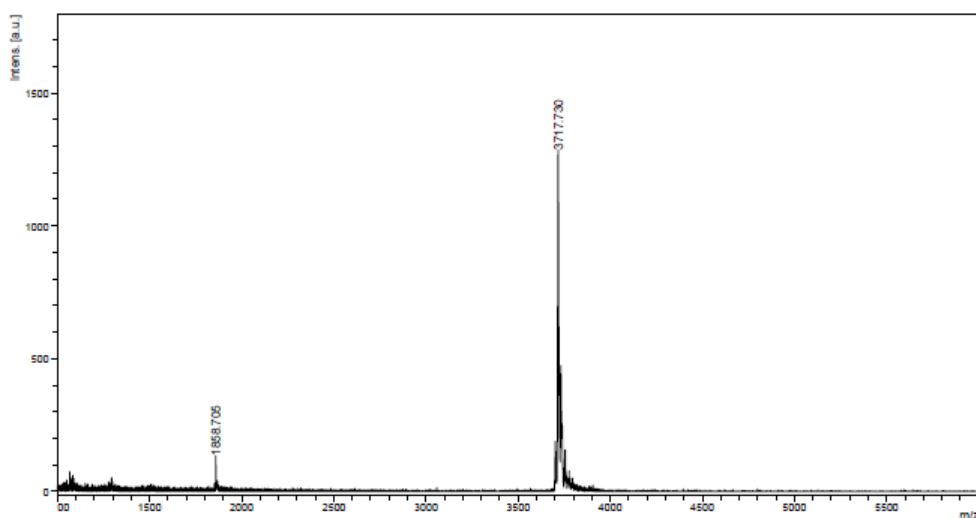
Figure A34. MALDI-TOF mass spectrum of AcLys-TT(DNB)TTTTT(Pyr)TT-LysNH$_2$
[**T9(DNB/Pyr)**] (calcd for [M+H]$^+$: m/z=3717.73)
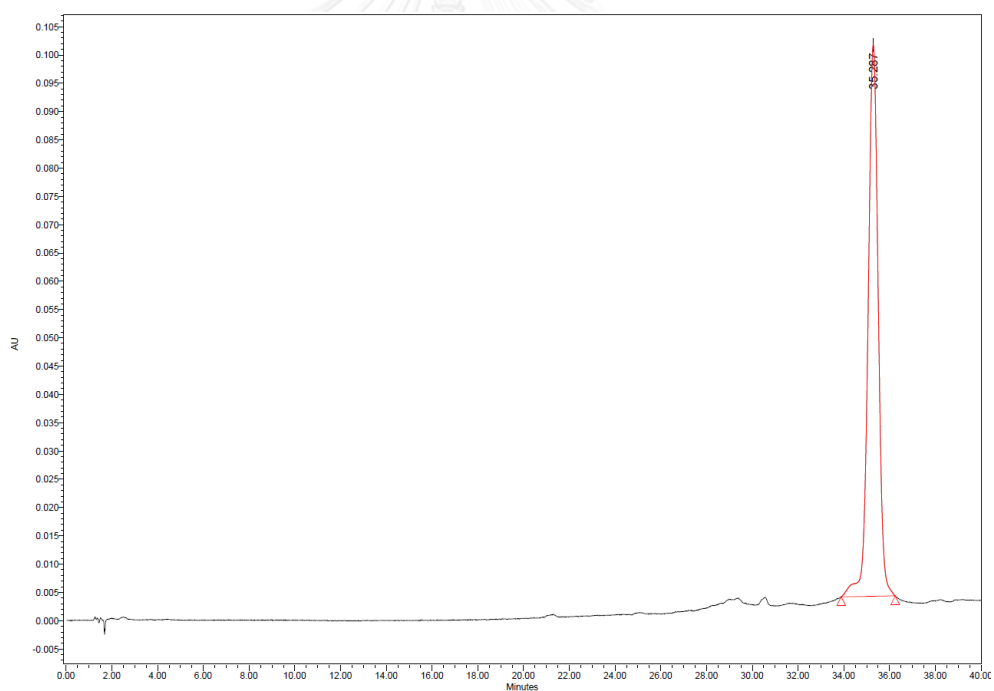
Figure A35. HPLC chromatogram of AcLys-TT(DNB)TTTTT(Pyr)TT-LysNH$_2$
[**T9(DNB/Pyr)**]
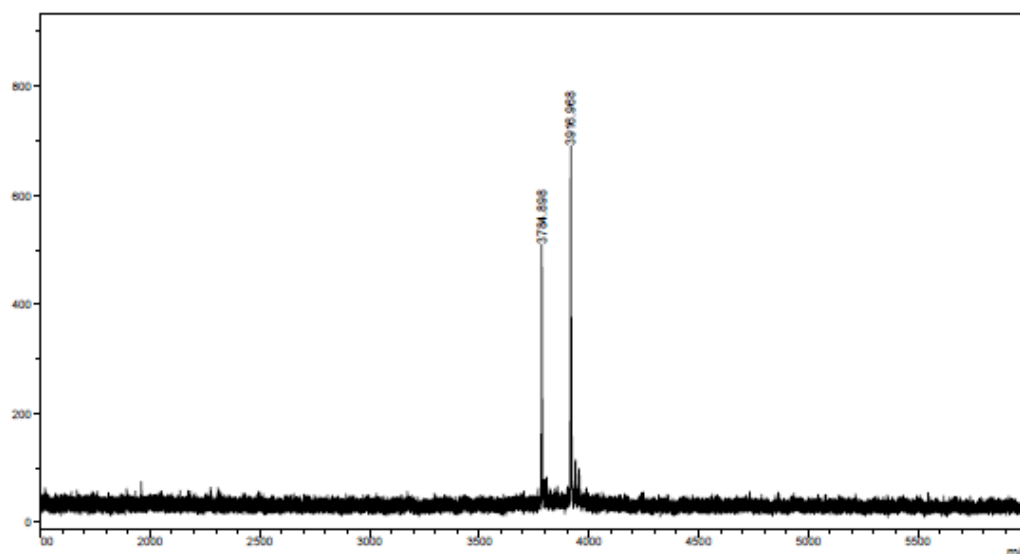
Figure A36. MALDI-TOF mass spectrum of AcLys-TT(Flu)TTTTT(Dab)TT-LysNH$_2$ [**T9(Flu/Dab)**] (calcd for [M+H]$^+$: m/z=3918.96)
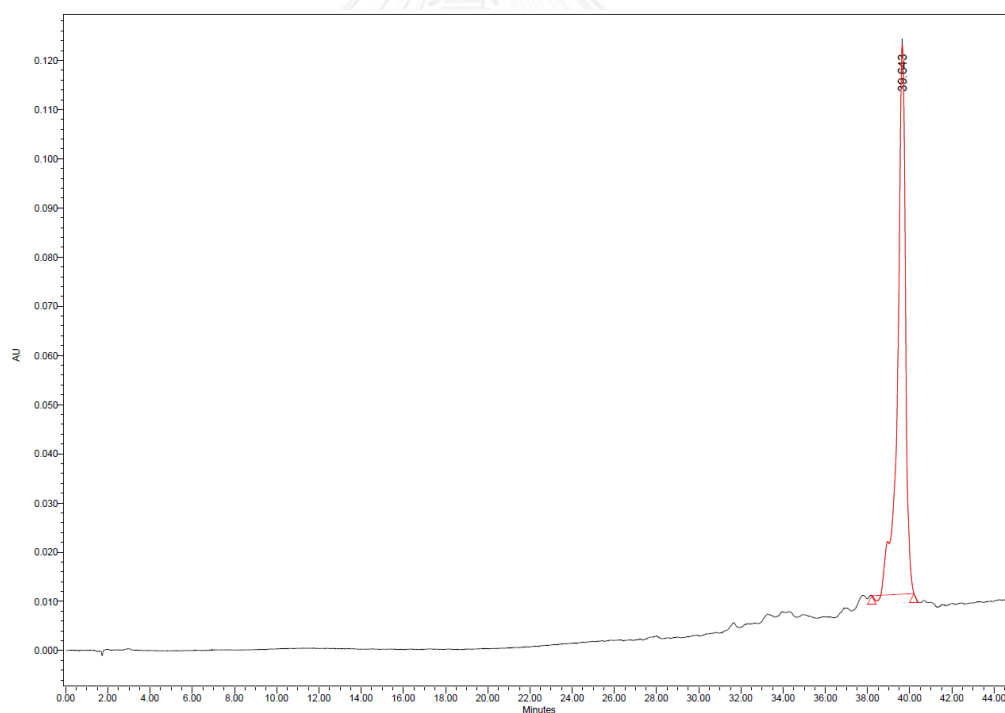
Figure A37. HPLC chromatogram of AcLys-TT(Flu)TTTTT(Dab)TT-LysNH$_2$ [**T9(Flu/Dab)**]
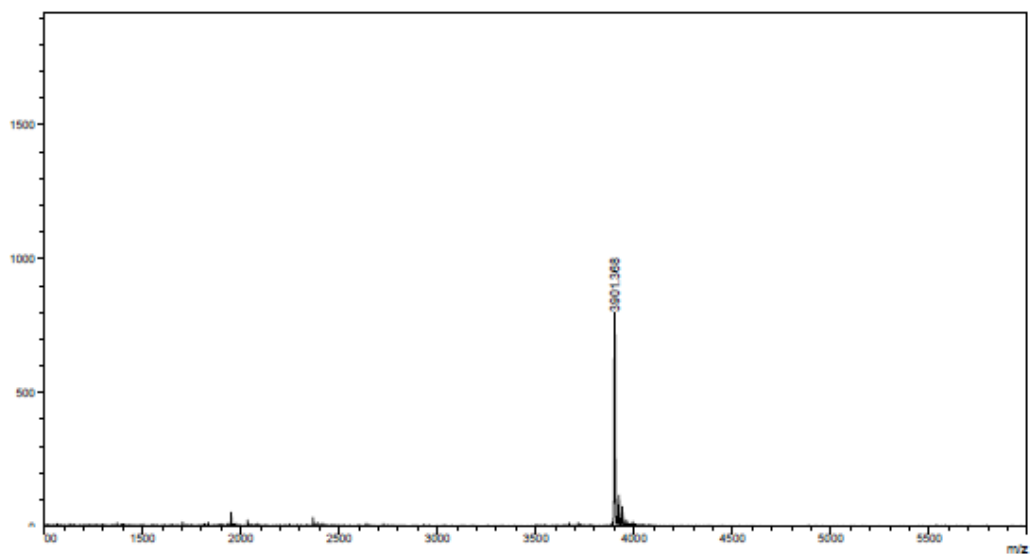
Figure A38. MALDI-TOF mass spectrum of AcLys-TT(Flu)TTTTT(AQ)TT-LysNH$_2$ [**T9(Flu/AQ)**] (calcd for [M+H]$^+$: m/z=3901.13)
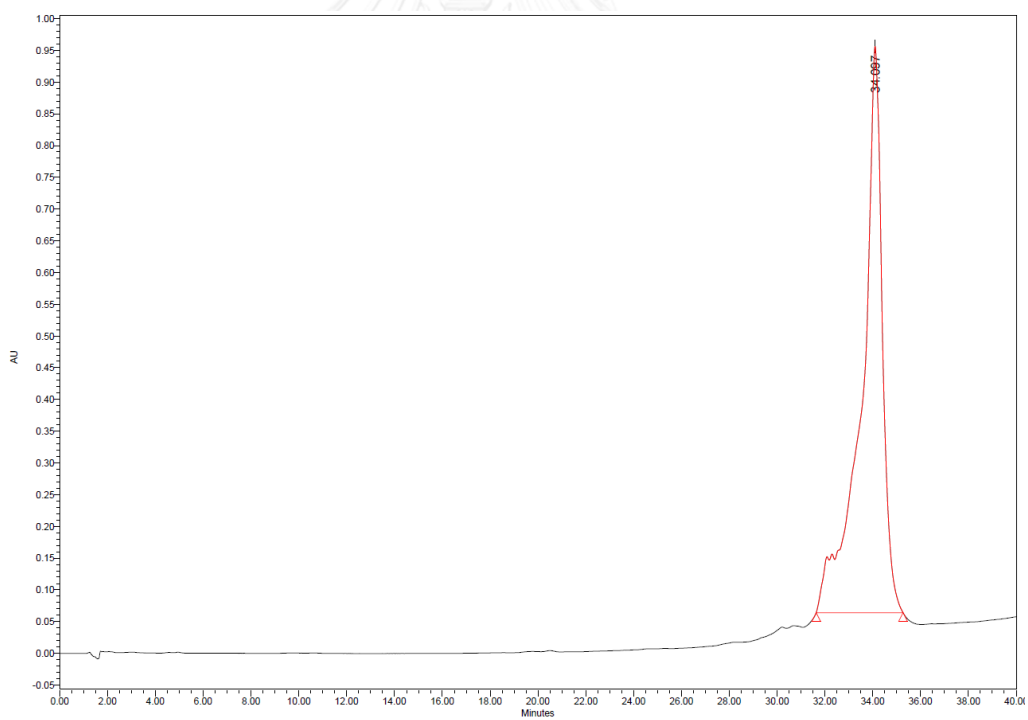
Figure A39. HPLC chromatogram of AcLys-TT(Flu)TTTTT(AQ)TT-LysNH$_2$ [**T9(Flu/AQ)**]
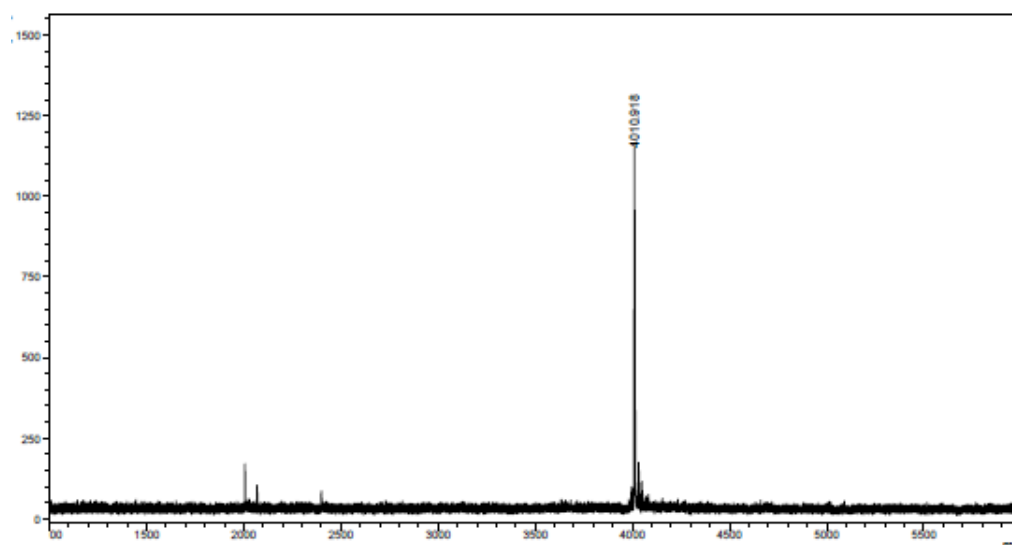
Figure A40. MALDI-TOF mass spectrum of AcLys-TT(Dns)TTTTT(Nr)TT-LysNH$_2$ [**T9(Dns/Nr)**] (calcd for [M+H]$^+$: m/z=4010.91)
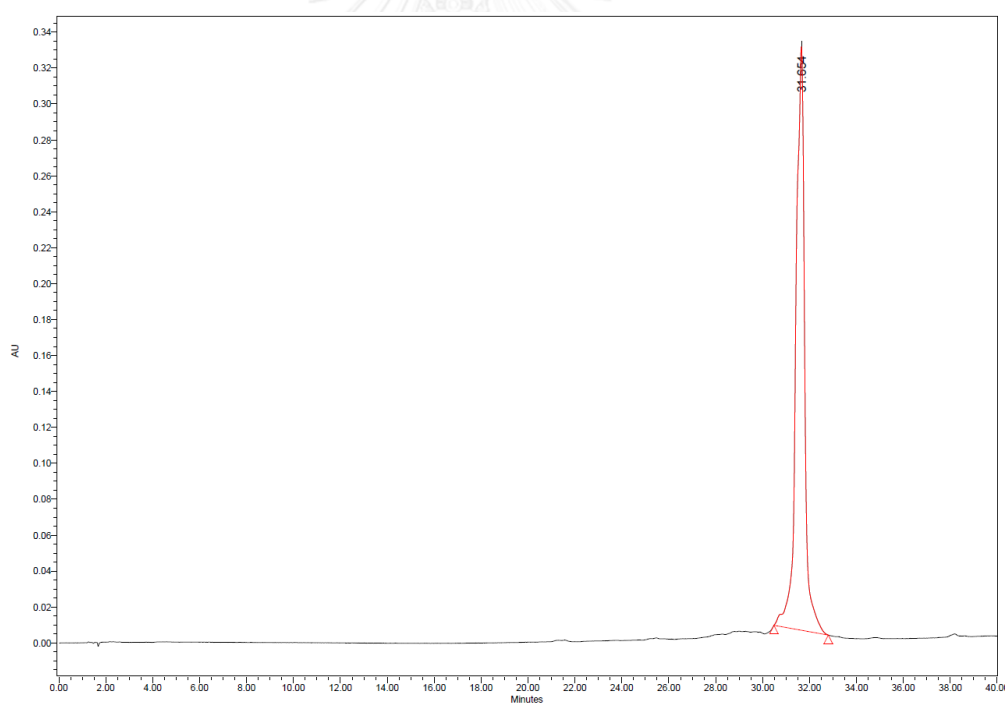
Figure A41. HPLC chromatogram of AcLys-TT(Dns)TTTTT(Nr)TT-LysNH$_2$ [**T9(Dns/Nr)**]
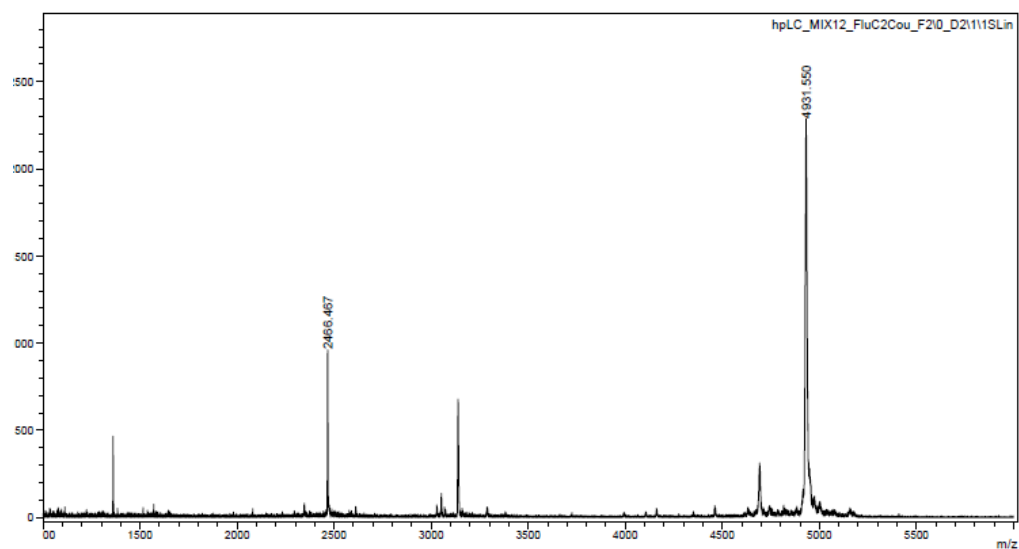
Figure A42. MALDI-TOF mass spectrum of AcLys--AGTT(C2Cou)ATGGG(Flu)TGC-LysNH$_2$ [**M12(C2Cou2/Flu)**] (calcd for [M+H]$^+$: m/z=4931.55)
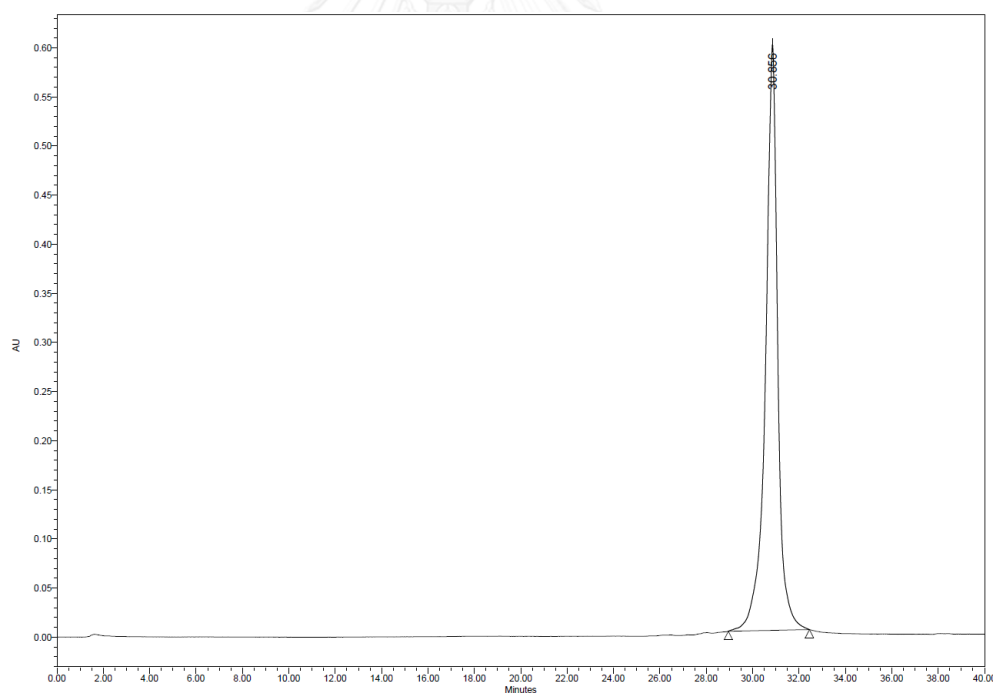
Figure A43. HPLC chromatogram of AcLys-AGTT(C2Cou)ATGGG(Flu)TGC-LysNH$_2$ [**M12(C2Cou/Flu)**]
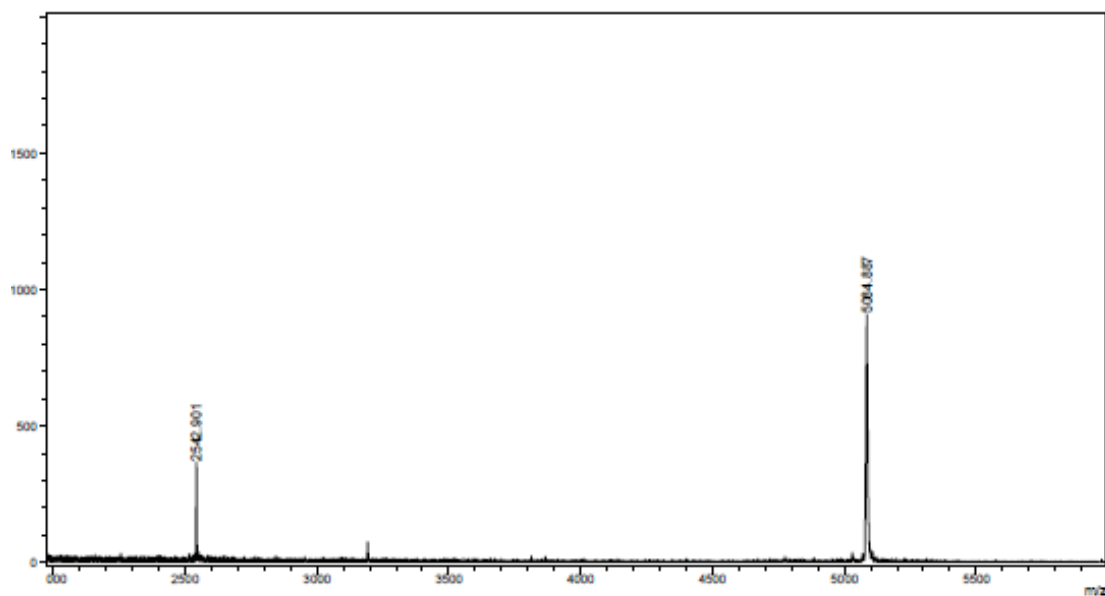
Figure A44. MALDI-TOF mass spectrum of AcLys-AGTT(Flu)ATGGG(TMR)TGC-LysNH$_2$
[**M12(Flu/TMR)**] (calcd for [M+H]$^+$: m/z=5064.85)
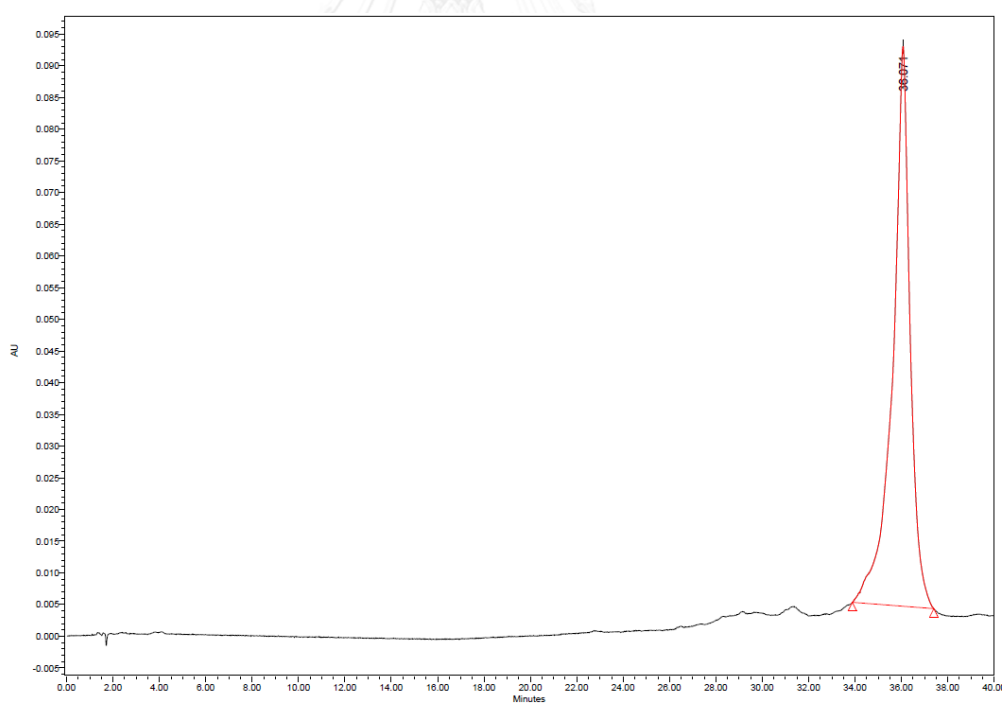
Figure A45. HPLC chromatogram of AcLys-AGTT(Flu)ATGGG(TMR)TGC-LysNH$_2$
[**M12(Flu/TMR)**]
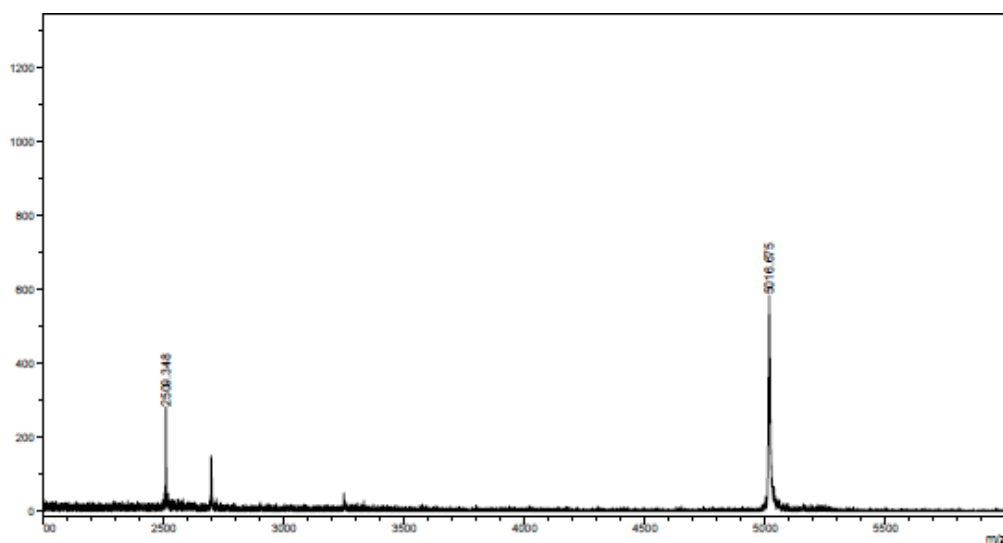
Figure A46. MALDI-TOF mass spectrum of AcLys-AGTT(Dns)ATGGG(Nr)TGC-LysNH$_2$ [**M12(Dns/Nr)**] (calcd for [M+H]$^+$: m/z=5016.67)
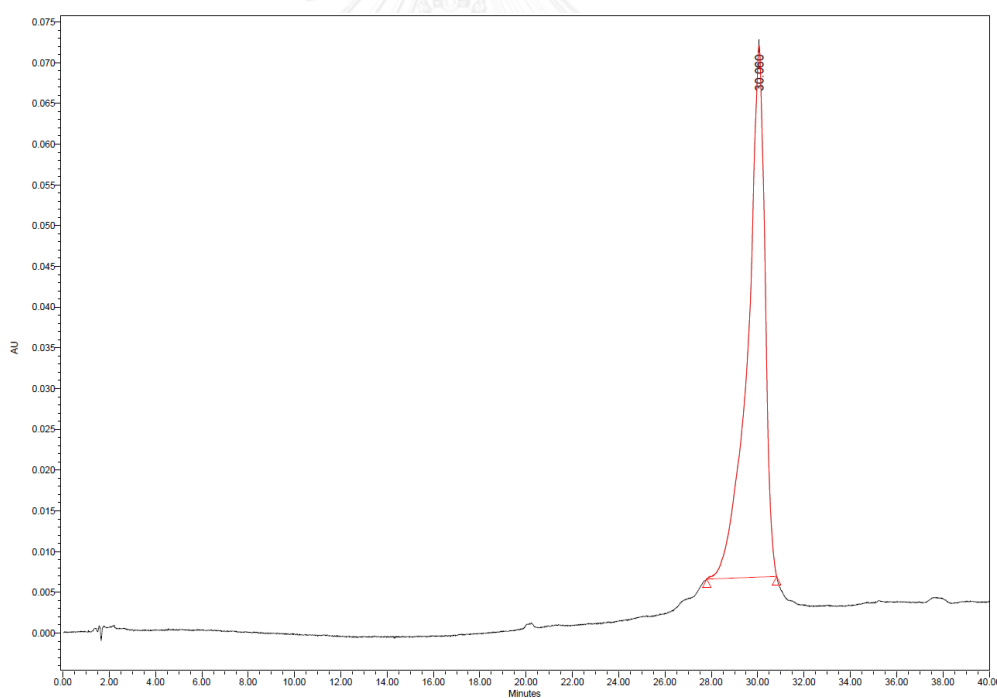
Figure A47. HPLC chromatogram of AcLys-AGTT(Dns)ATGGG(Nr)TGC-LysNH$_2$ [**M12(Dns/Nr)**]
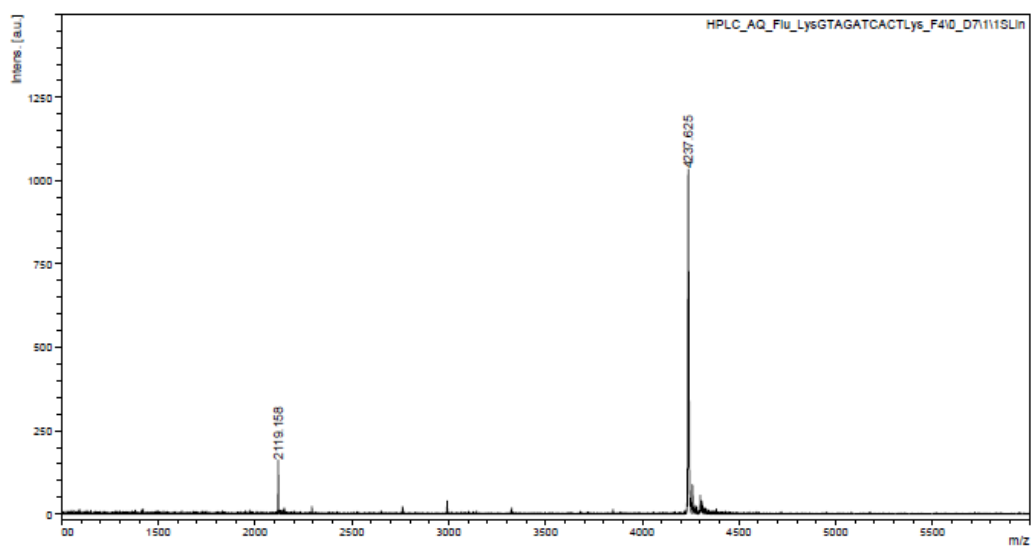
Figure A48. MALDI-TOF mass spectrum of AQFluLys-GTAGATCACT-LysNH$_2$

[**(AQ/Flu)LysM10G**] (calcd for [M+H]$^+$: m/z=4237.62)
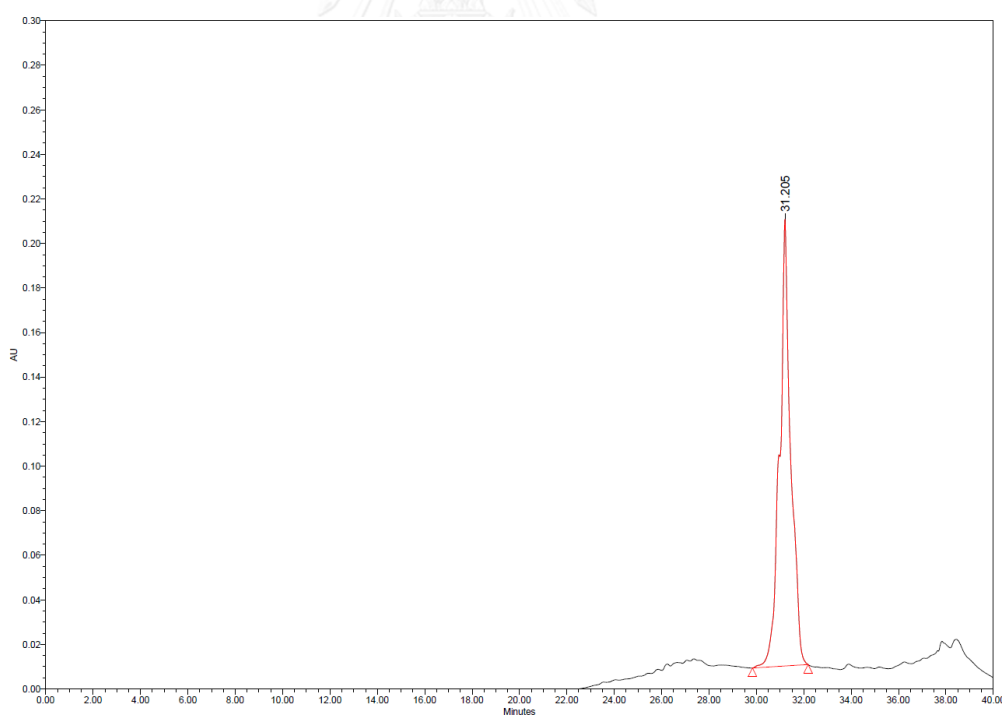
Figure A49. HPLC chromatogram of AQFluLysGTAGATCACT-LysNH$_2$
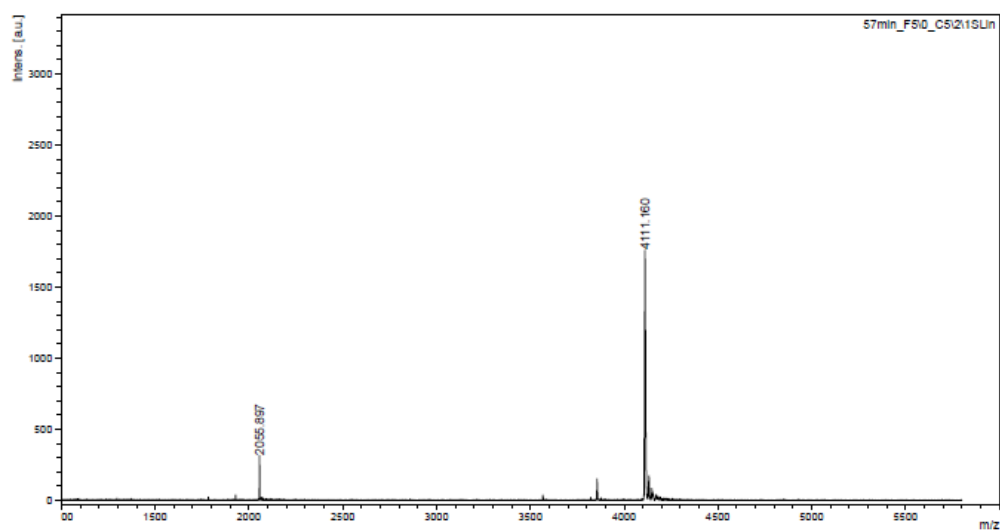
[**(AQ/Flu)LysM10G**]

Figure A50. MALDI-TOF mass spectrum of AQFlu(apc)-GTAGATCACT-LysNH$_2$

[**(AQ/Flu)apcM10G**] (calcd for [*M*+H]$^+$: m/z=4111.16)
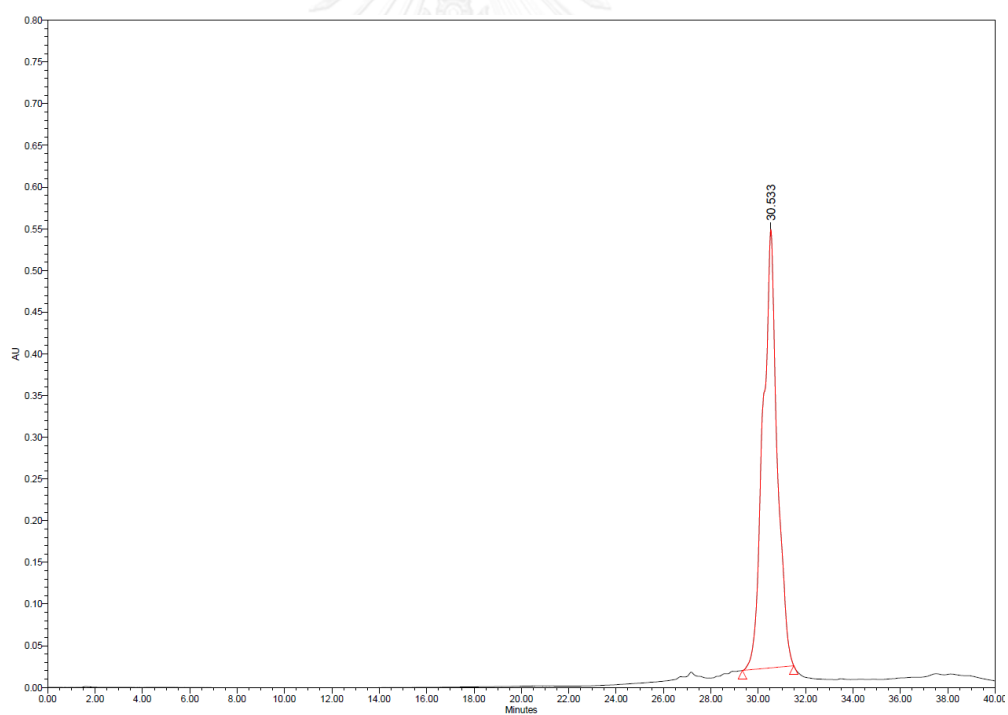
Figure A51. HPLC chromatogram of AQFluapcGTAGATCACT-LysNH$_2$
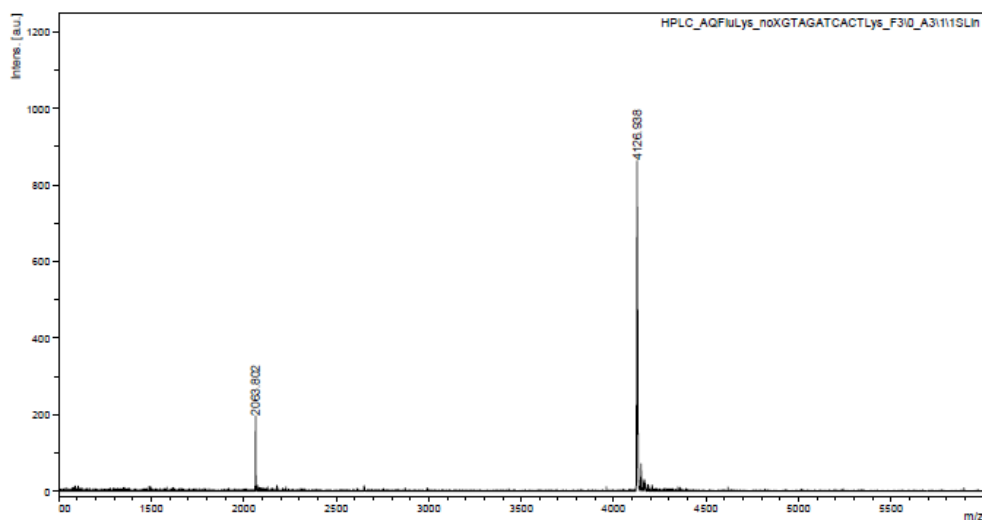
[**(AQ/Flu)apcM10G**]

Figure A52. MALDI-TOF mass spectrum of AQFluLys(-acpc)GTAGATCACT-LysNH$_2$
[**(AQ/Flu)Lys(-acpc)M10G**] (calcd for [M+H]$^+$: m/z=4126.93)
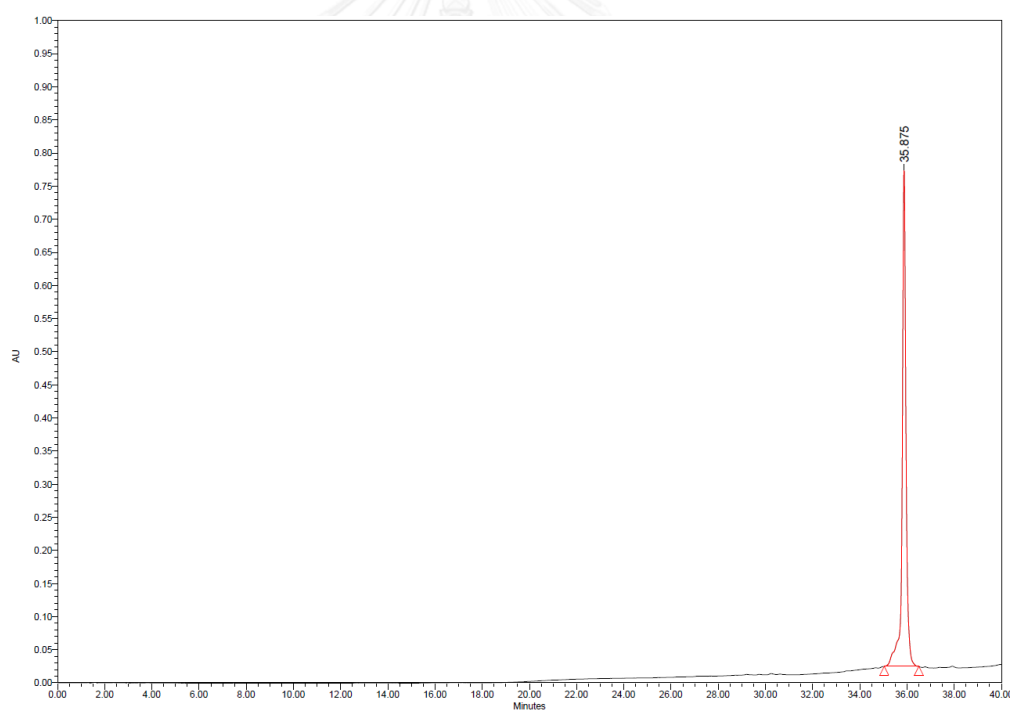
Figure A53. HPLC chromatogram of AQFluLys(-acpc)GTAGATCACT-LysNH$_2$
[**(AQ/Flu)Lys(-acpc)M10G**]
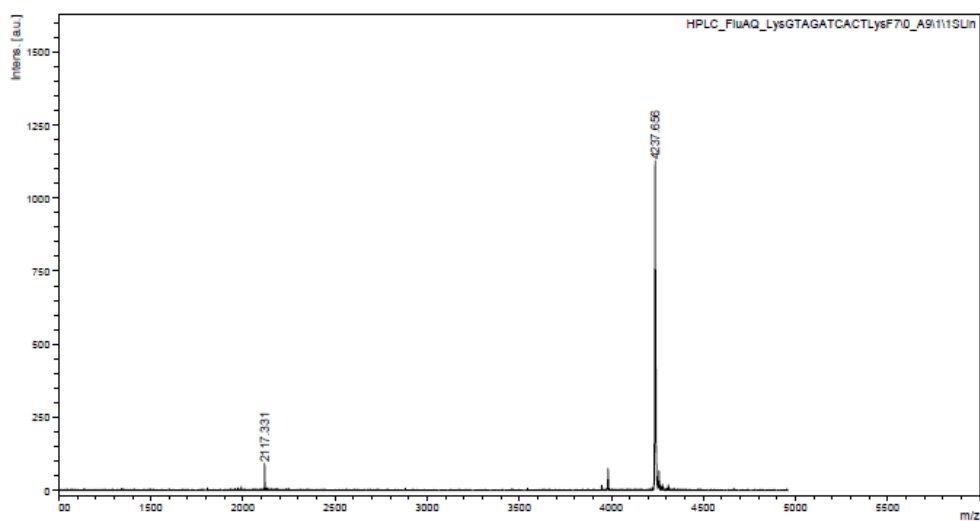
Figure A54. MALDI-TOF mass spectrum of FluAQLys-GTAGATCACT-LysNH$_2$

[**(Flu/AQ)LysM10G**] (calcd for [M+H]$^+$: m/z=4237.65)
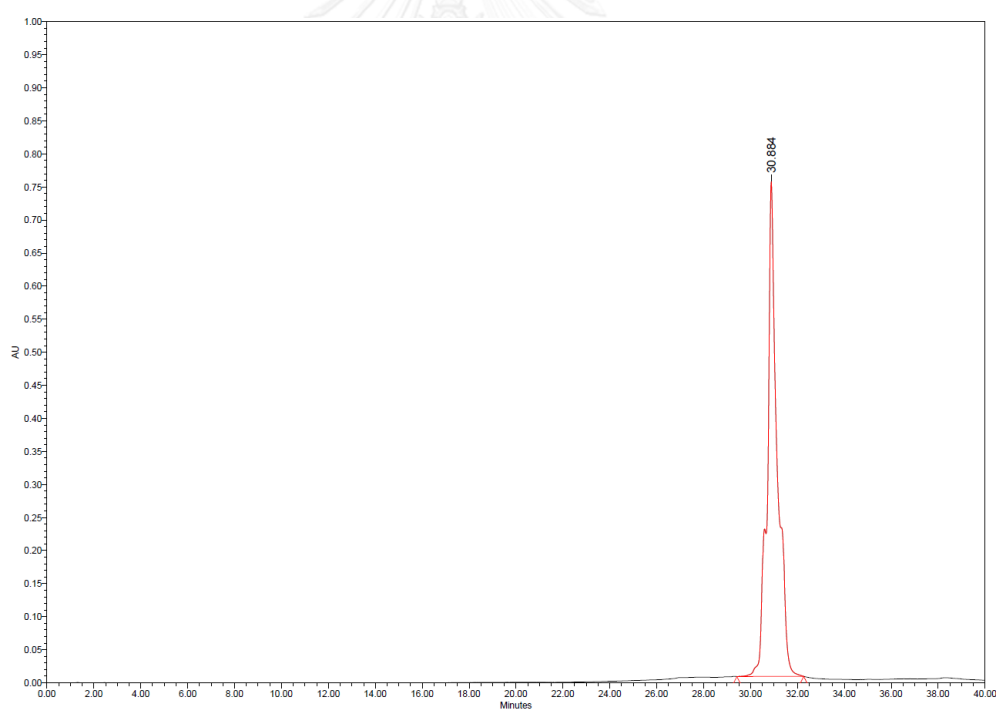
Figure A55. HPLC chromatogram of FluAQLys-GTAGATCACT-LysNH$_2$

[**(Flu/AQ)LysM10G**]
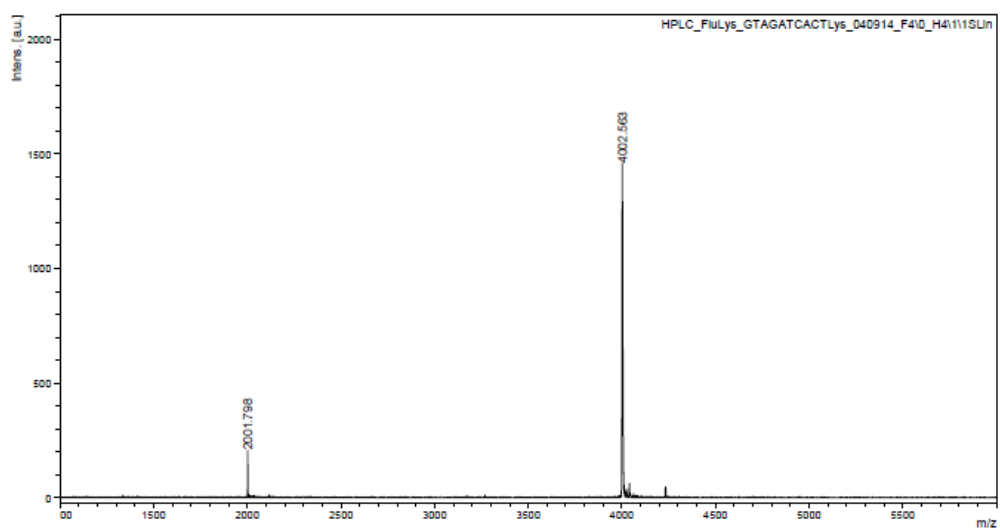
Figure A56. MALDI-TOF mass spectrum of FluLys-GTAGATCACT-LysNH$_2$ [**(Flu)LysM10G**] (calcd for [M+H]$^+$: m/z=4002.56)
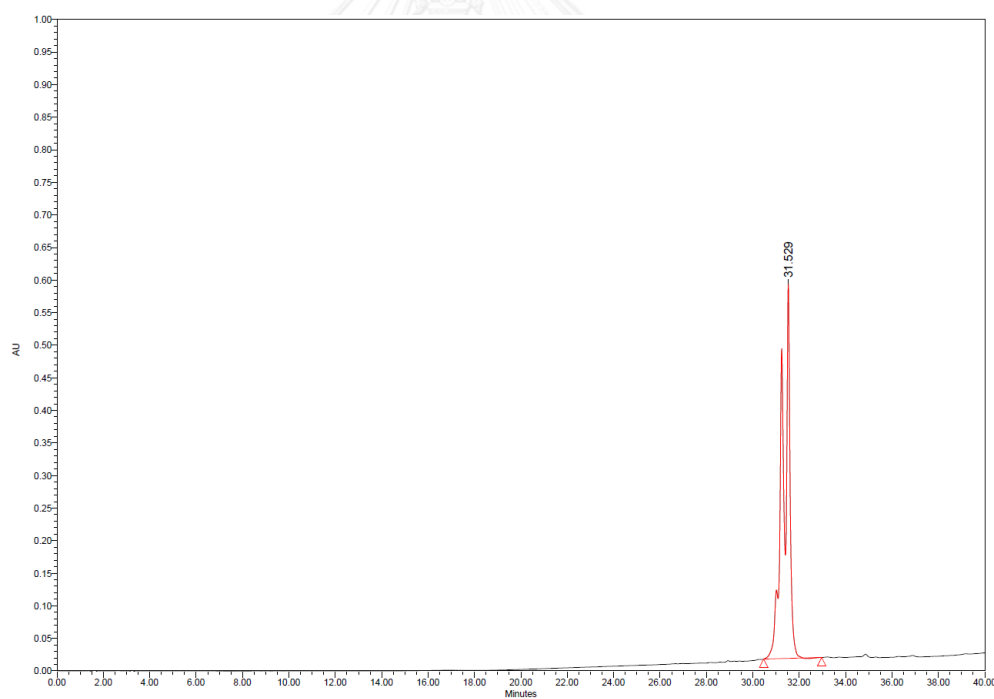
Figure A57. HPLC chromatogram of FluLys-GTAGATCACT-LysNH$_2$ [**(Flu)LysM10G**]
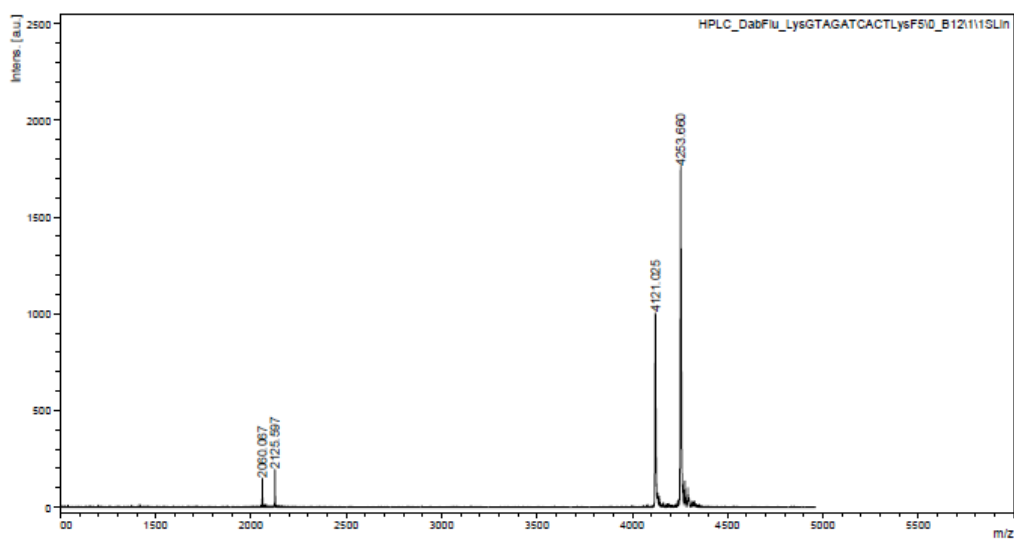
Figure A58. MALDI-TOF mass spectrum of DabFluLysGTAGATCACT-LysNH$_2$
[**(Dab/Flu)LysM10G**] (calcd for [M+H]$^+$: m/z=4253.68)
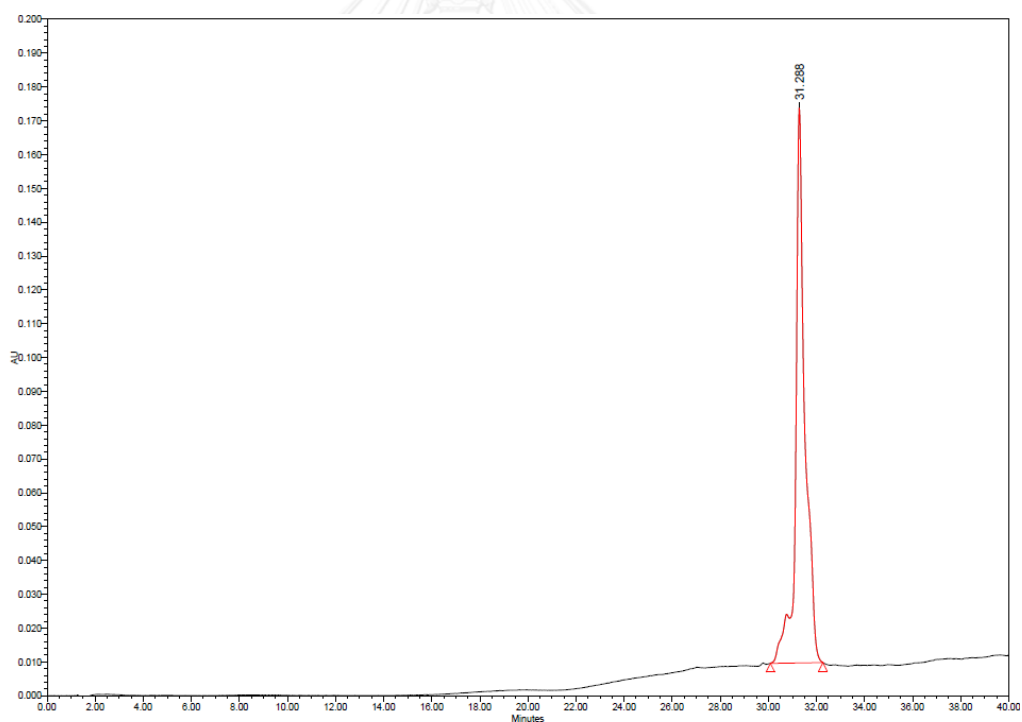
Figure A59. HPLC chromatogram of DabFluLysGTAGATCACT-LysNH$_2$
[**(Dab/Flu)LysM10G**]
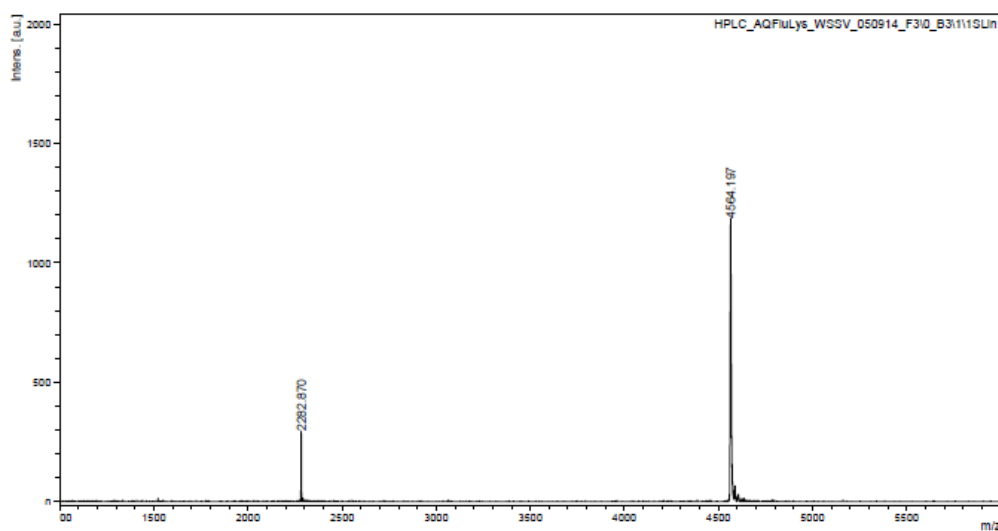
Figure A60. MALDI-TOF mass spectrum of AQFluLys-CTAAATTCAGA-LysNH$_2$

[**(AQ/Flu)LysM11C**] (calcd for [M+H]$^+$: m/z=4564.19)
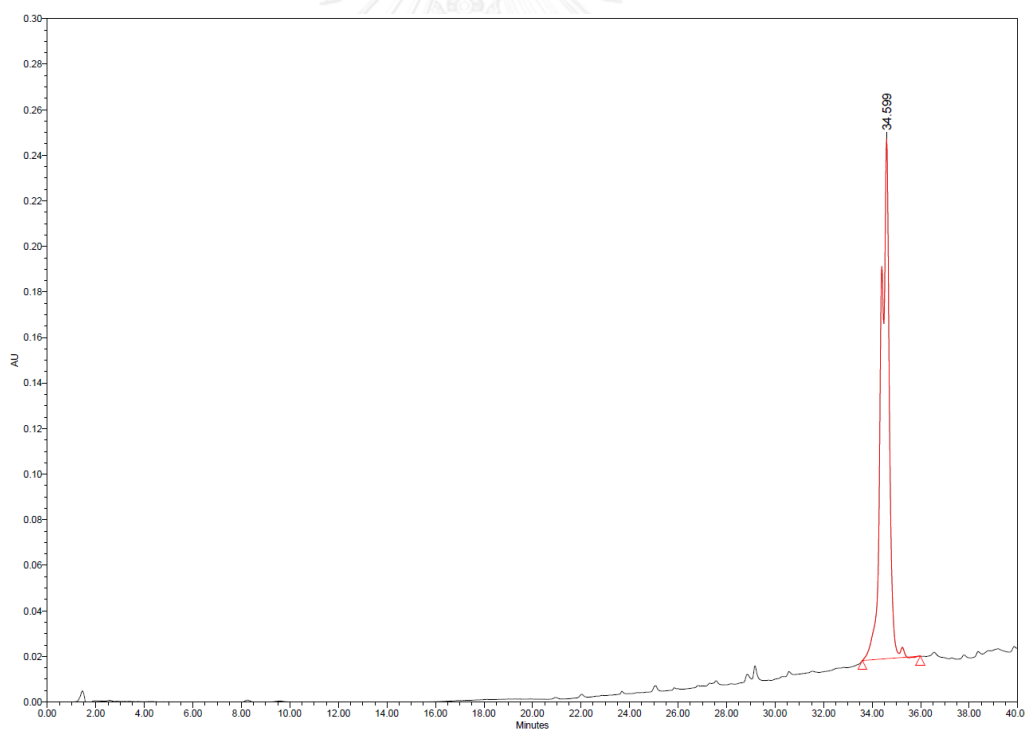
Figure A61. HPLC chromatogram of AQFluLys-CTAAATTCAGA-LysNH$_2$
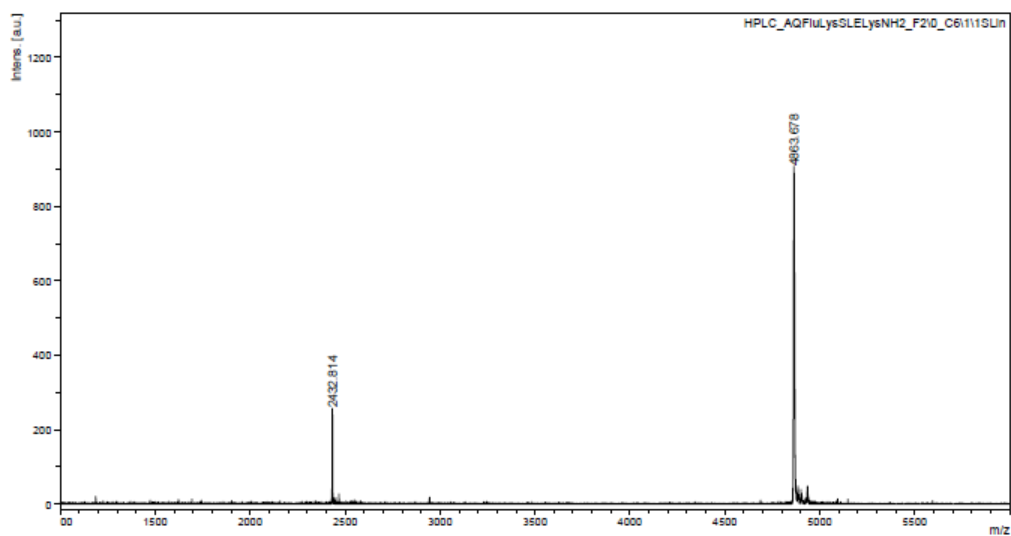
[**(AQ/Flu)LysM11C**]

Figure A62. MALDI-TOF mass spectrum of AcLys-TT(Cou2)TTTTT(Flu)TT-LysNH$_2$ [(AQ/Flu)LysM12A] (calcd for [M+H]$^+$: m/z=4863.67)
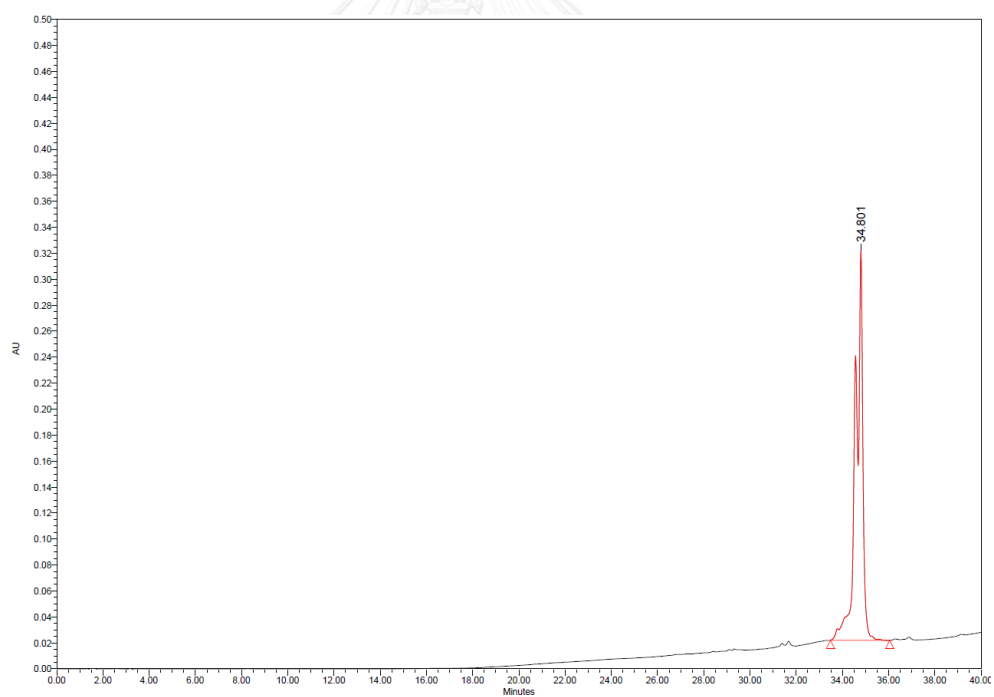
Figure A63 HPLC chromatogram of AQFluLys-AGTTATCCCTGC-LysNH$_2$ [(AQ/Flu)LysM12A]
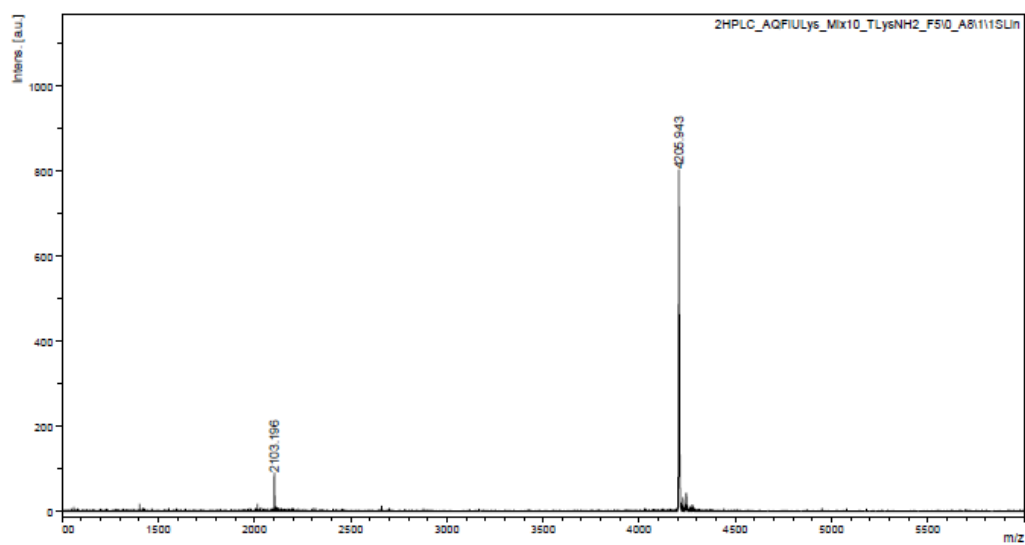
Figure A64 MALDI-TOF mass spectrum of AQFluLys-TACAGACATC-LysNH$_2$

[**(AQ/Flu)LysM10T**] (calcd for $[M+H]^+$: m/z=4205.94)
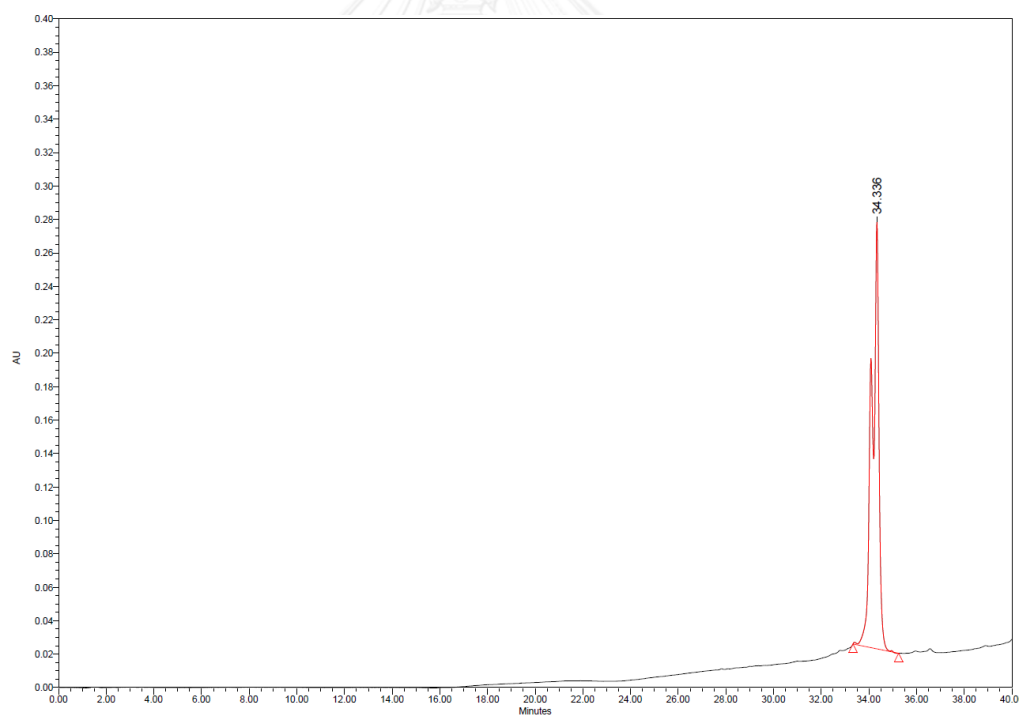
Figure A65 HPLC chromatogram of AQFluLys-TACAGACATC-LysNH$_2$

[**(AQ/Flu)LysM10T**]
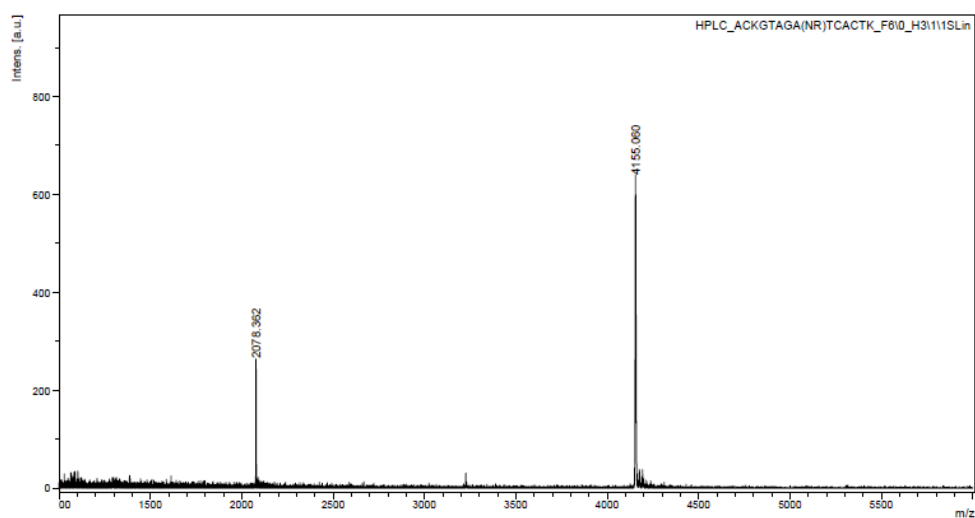
Figure A66. MALDI-TOF mass spectrum of AcLys--GTAGA(Nr)TCACT-LysNH$_2$ [**M10(Nr)**] (calcd for [M+H]$^+$ = 4155.06)
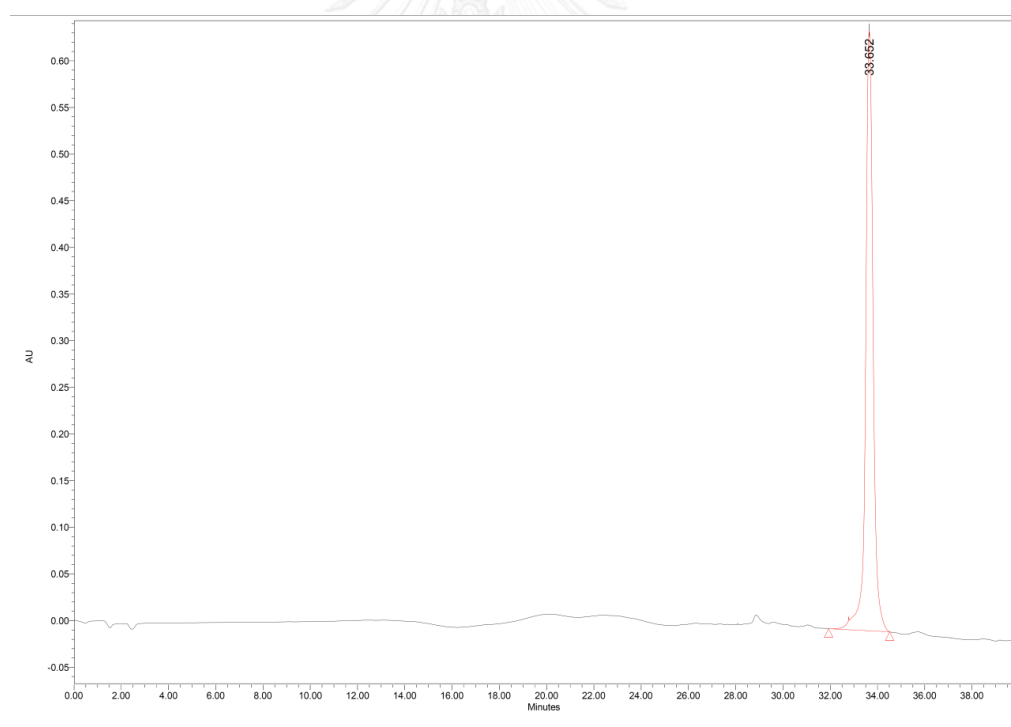
Figure A67. HPLC chromatogram of AcLys--GTAGA(Nr)TCACT-LysNH$_2$ [**M10(Nr)**]
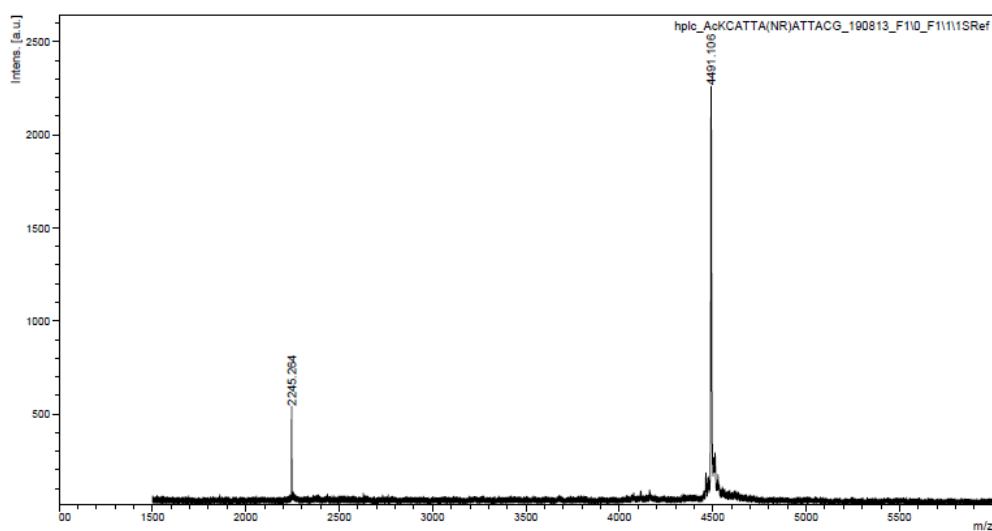
Figure A68. MALDI-TOF mass spectrum of AcLys--CATTA(Nr)ATTACG-LysNH$_2$ [**M11AA(Nr)**] (calcd for [M+H]$^+$ = 4491.10)
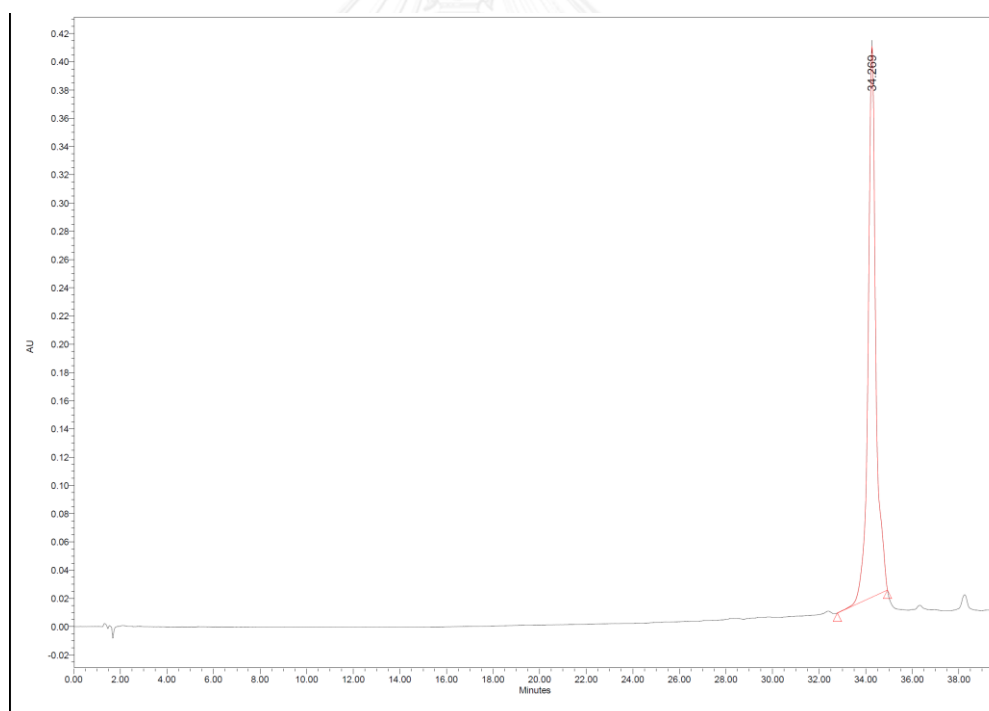
Figure A69. HPLC chromatogram of AcLys--CATTA(Nr)ATTACG-LysNH$_2$ [**M11AA(Nr)**]
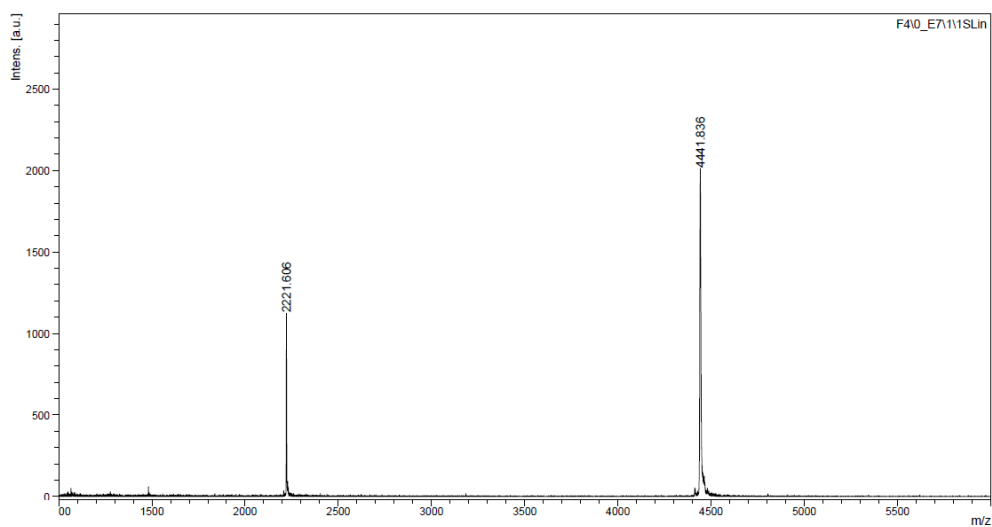
Figure A70. MALDI-TOF mass spectrum of AcLys--CATTC(Nr)CTTACG-LysNH$_2$ [**M11CC(Nr)**] (calcd for [M+H]$^+$ = 4441.83)
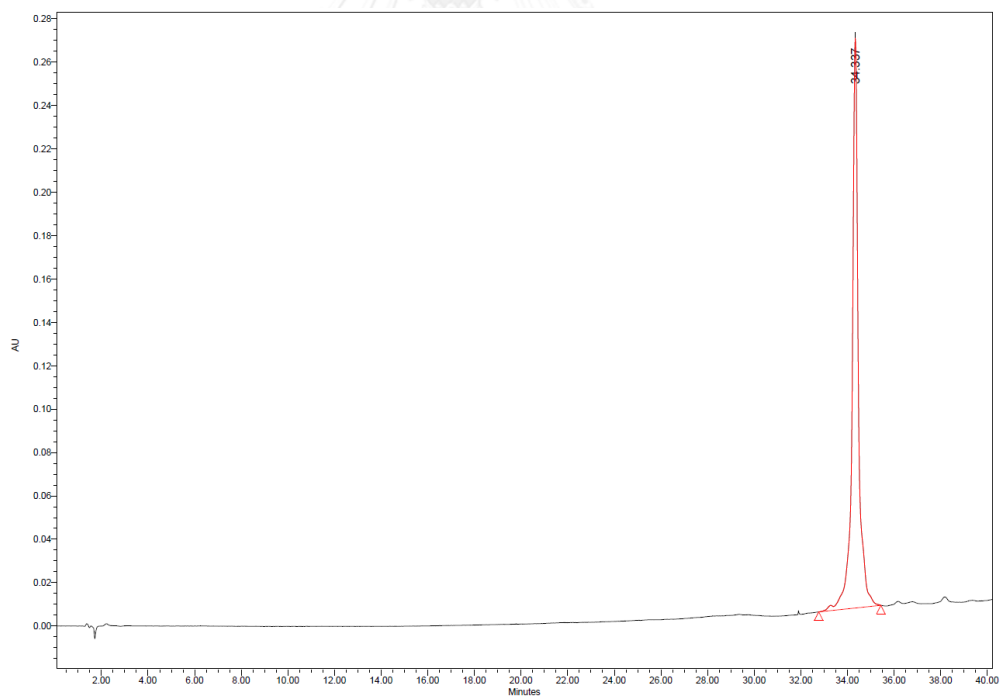
Figure A71. HPLC chromatogram of AcLys--CATTC(Nr)CTTACG-LysNH$_2$ [**M11CC(Nr)**]
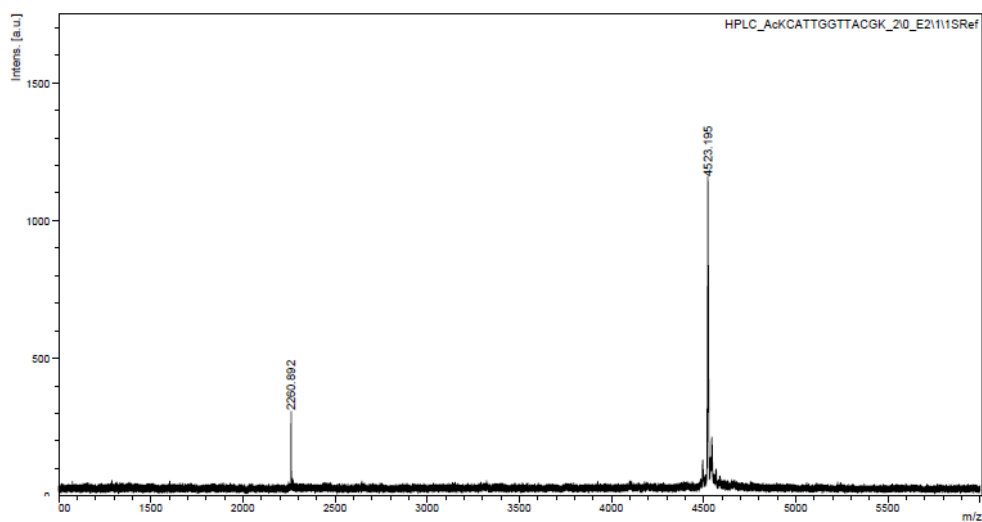
Figure A72. MALDI-TOF mass spectrum of AcLys--CATTG(Nr)GTTACG-LysNH$_2$ [**M11GG(Nr)**] (calcd for [M+H]$^+$ = 4523.19)
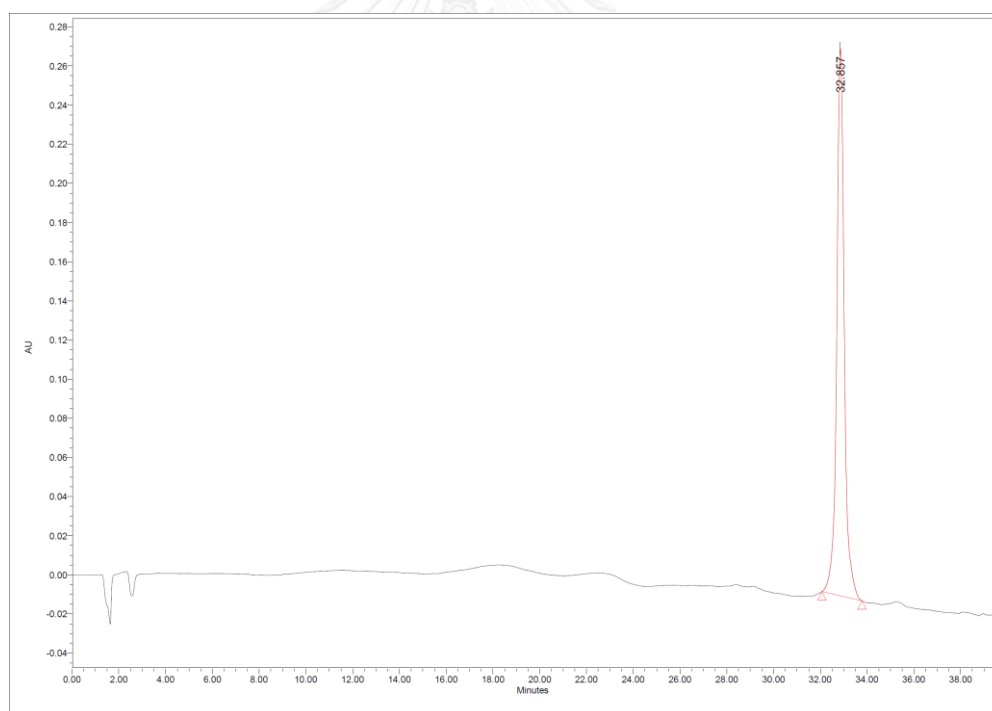
Figure A73. HPLC chromatogram of AcLys--CATTG(Nr)GTTACG-LysNH$_2$ [**M11GG(Nr)**]
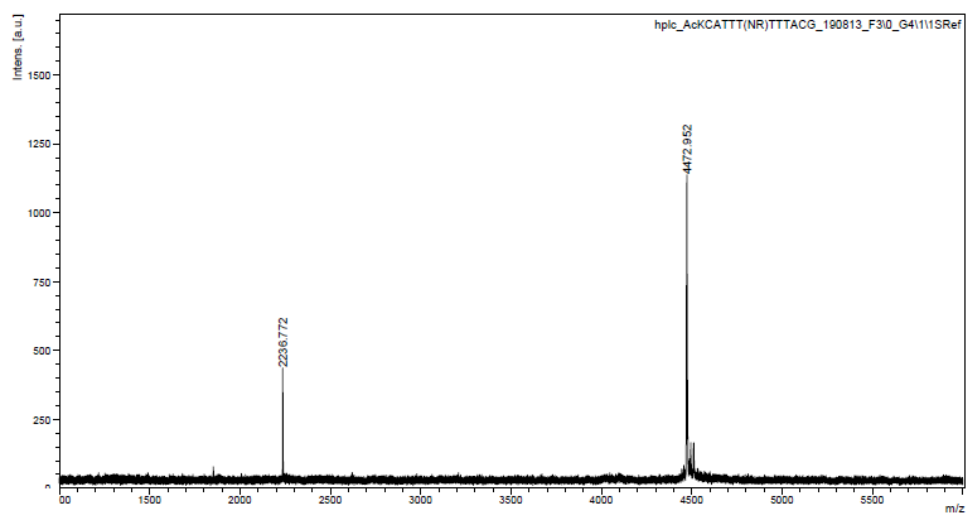
Figure A74. MALDI-TOF mass spectrum of AcLys--CATTT(Nr)TTTACG-LysNH$_2$ [**M11TT(Nr)**] (calcd for $[M+H]^+$ = 4472.95)
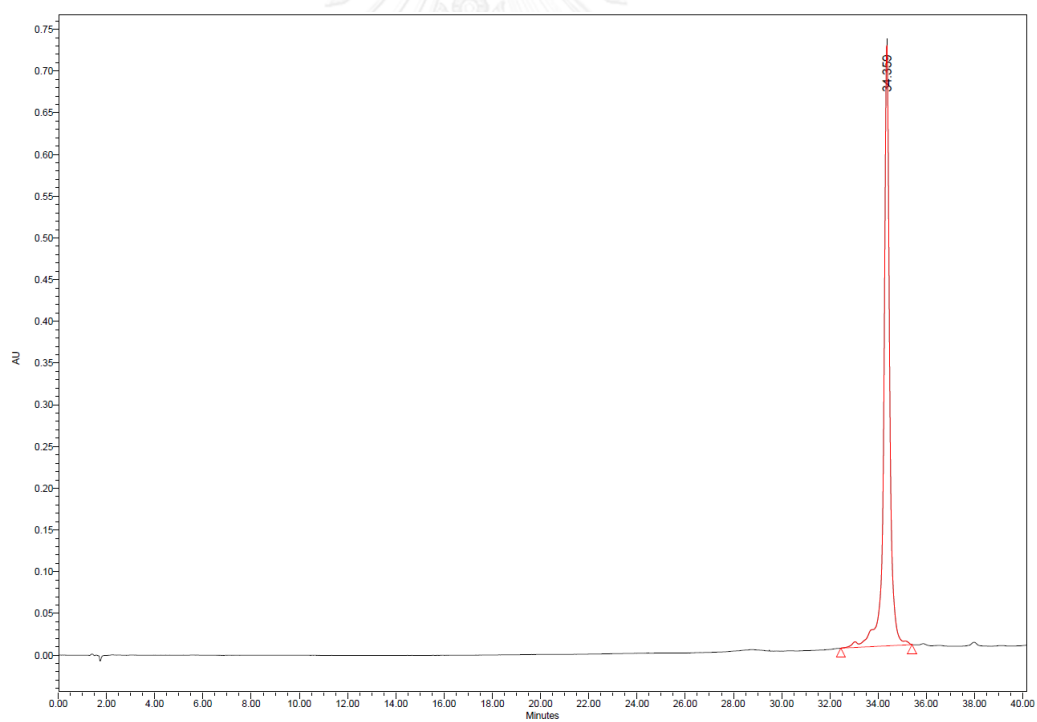
Figure A75. HPLC chromatogram AcLys--CATTT(Nr)TTTACG-LysNH$_2$ [**M11TT(Nr)**] (calcd for $[M+H]^+$ = 4472.95)
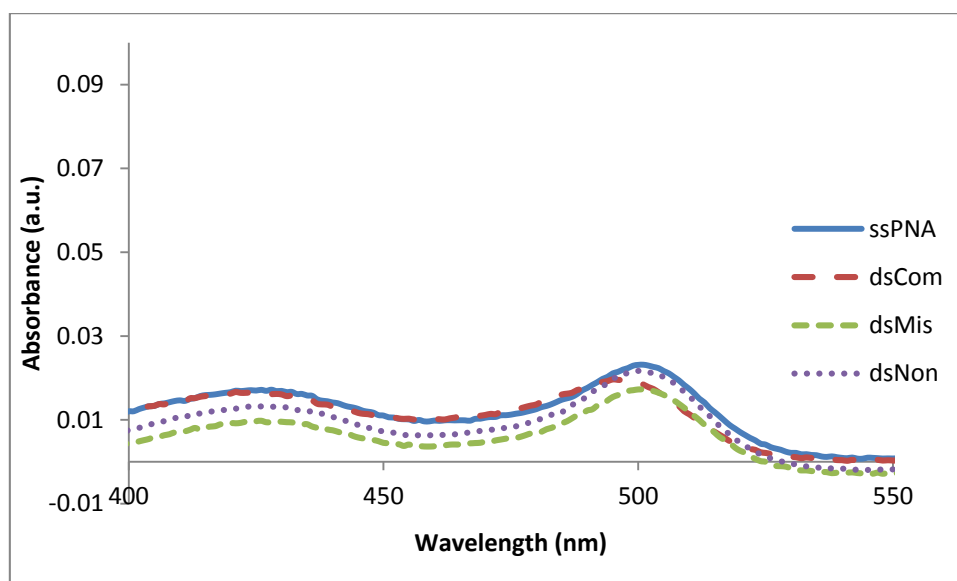
Figure A76. UV-Vis spectra of **T9(Cou1/Flu)** in the absence and presence of DNA target in 10 mM phosphate buffer pH 7.0, [PNA] = 1.0 μM and [DNA] = 1.2 μM.
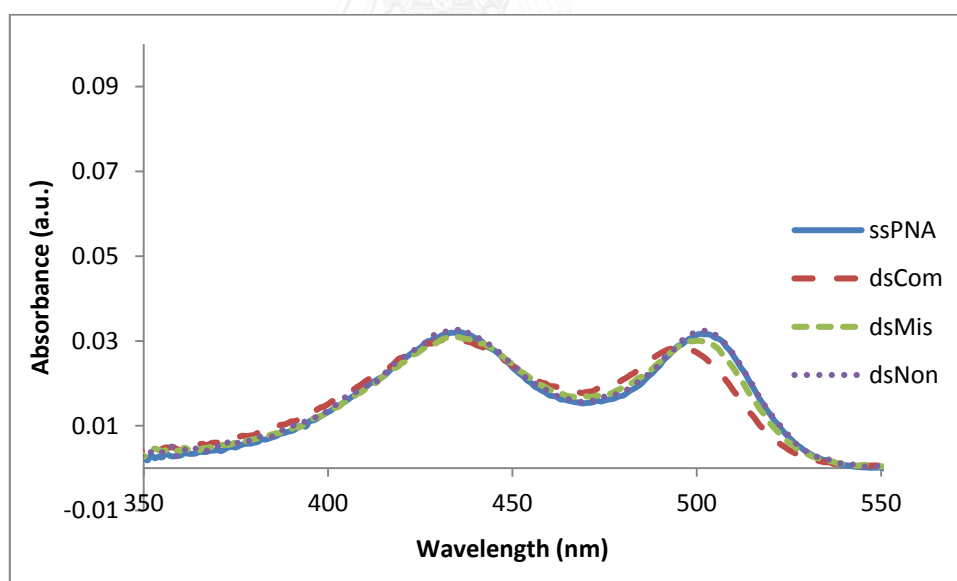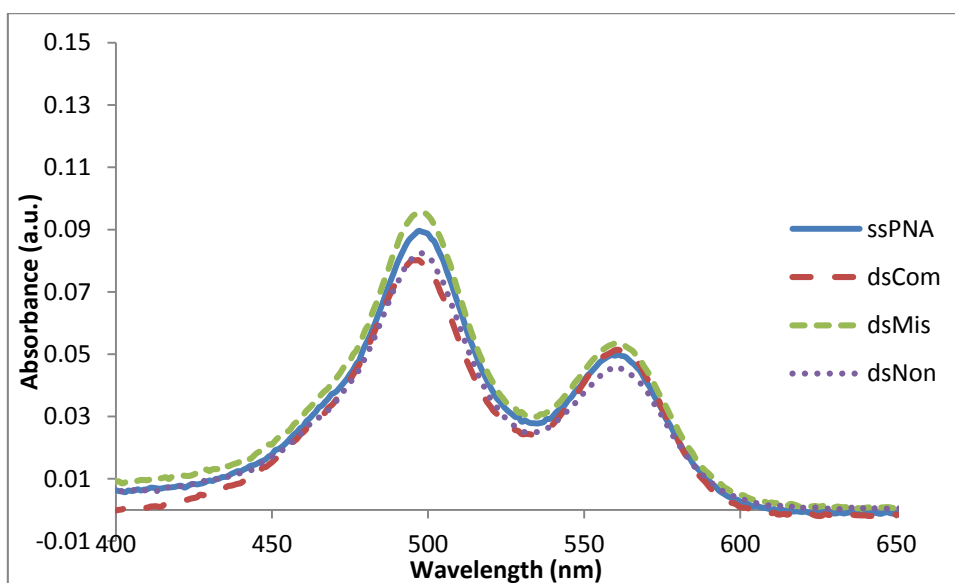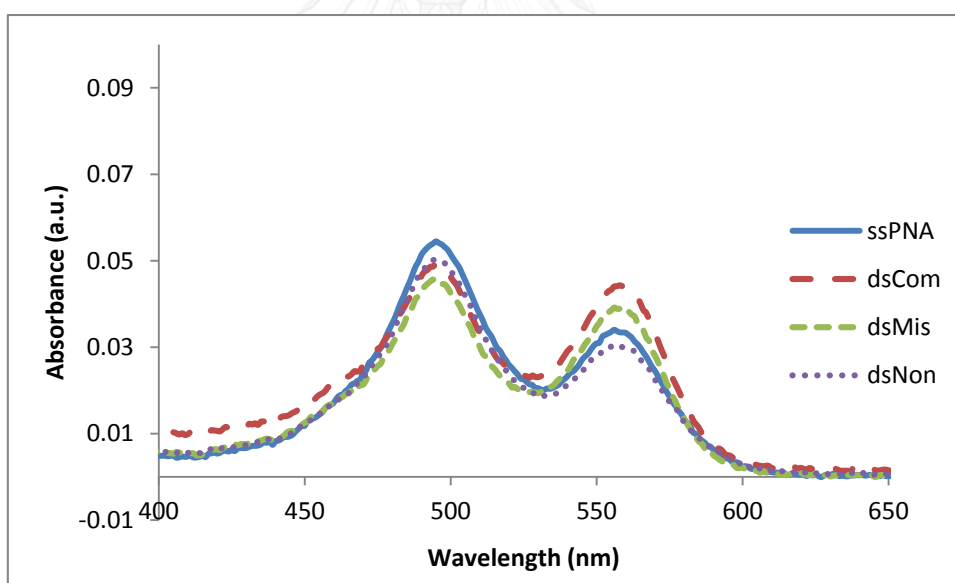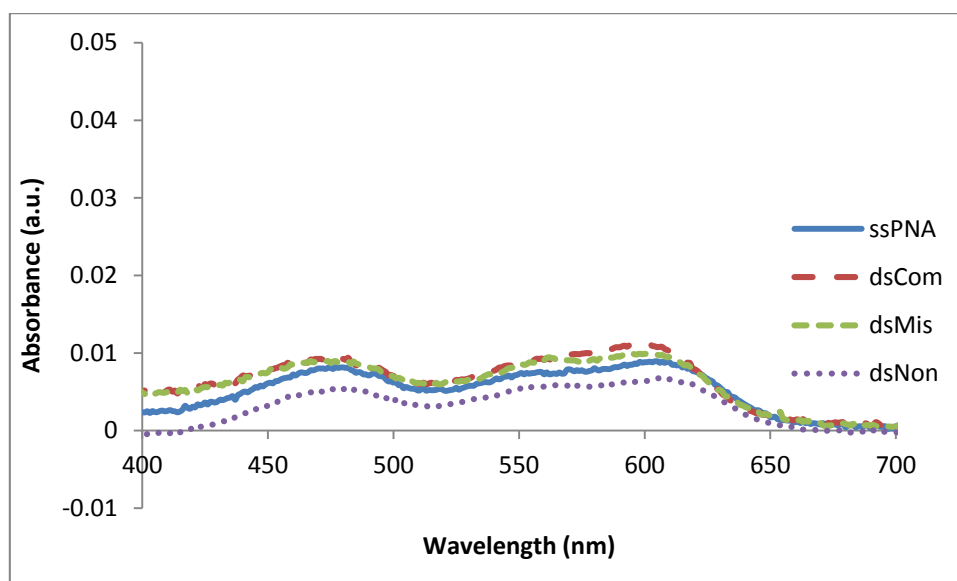

Figure A77. UV-Vis spectra of **T9(C2Cou1/C2Flu)** in the absence and presence of DNA target in 10 mM phosphate buffer pH 7.0, [PNA] = 1.0 μM and [DNA] = 1.2 μM.
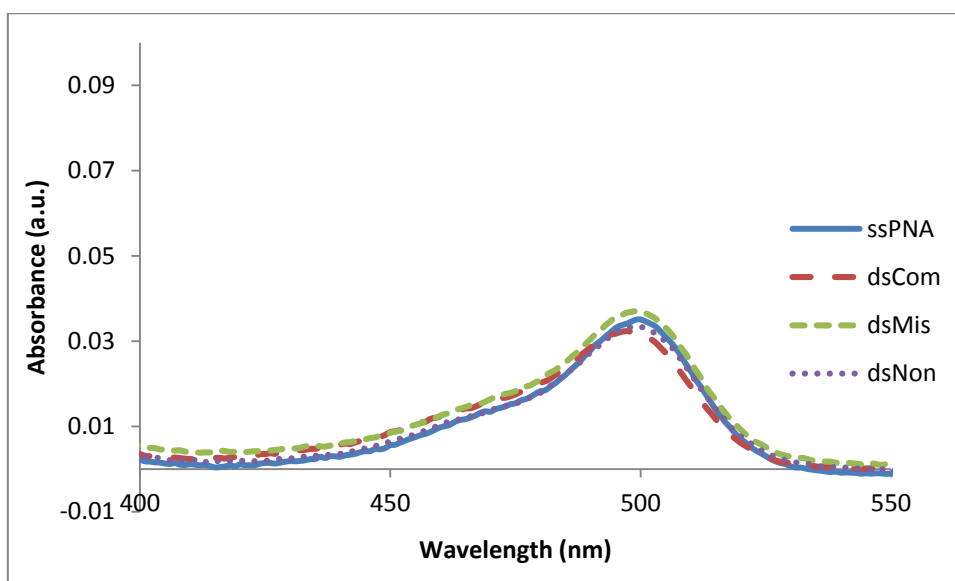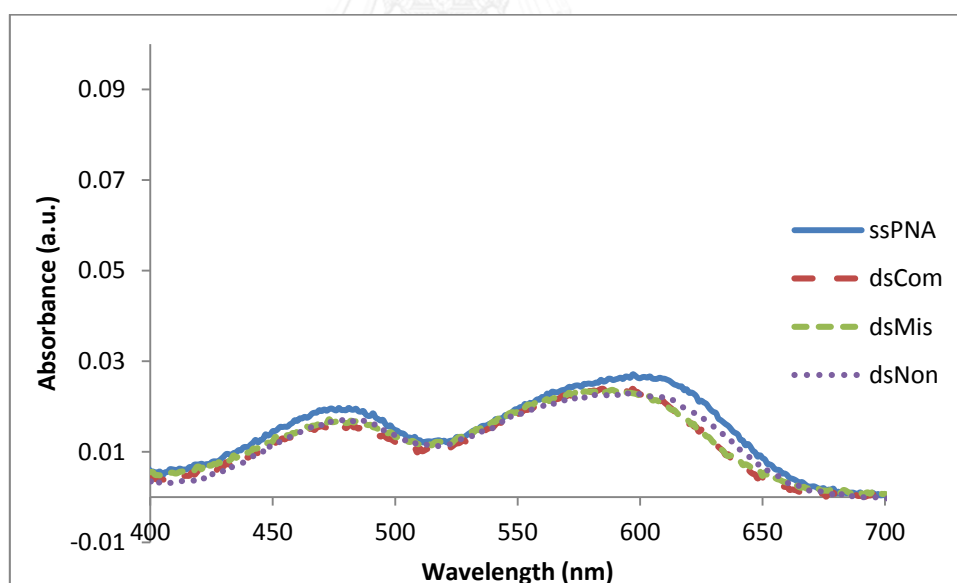
Figure A78. UV-Vis spectra of **T9(Cou2/Flu)** in the absence and presence of DNA target in 10 mM phosphate buffer pH 7.0, [PNA] = 1.0 µM and [DNA] = 1.2 µM.
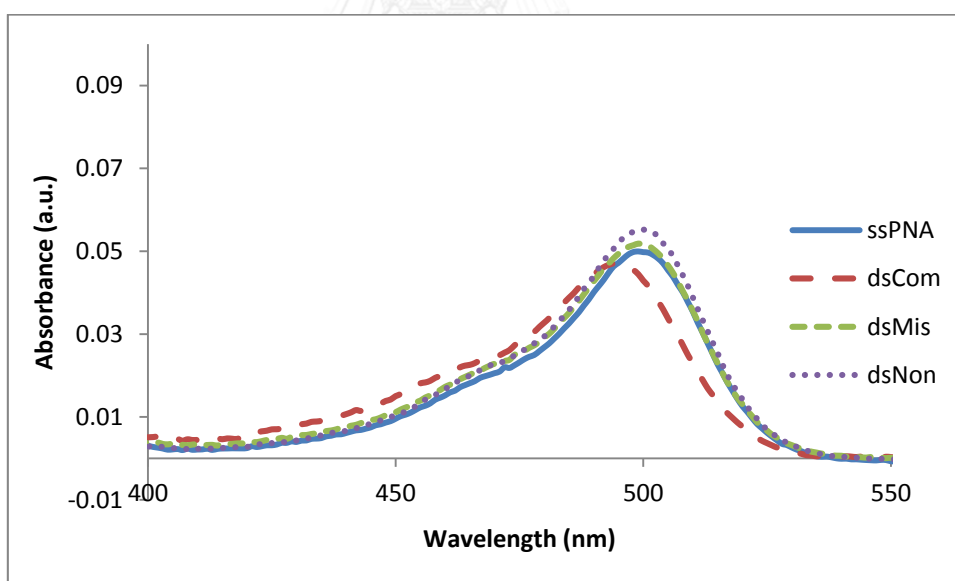
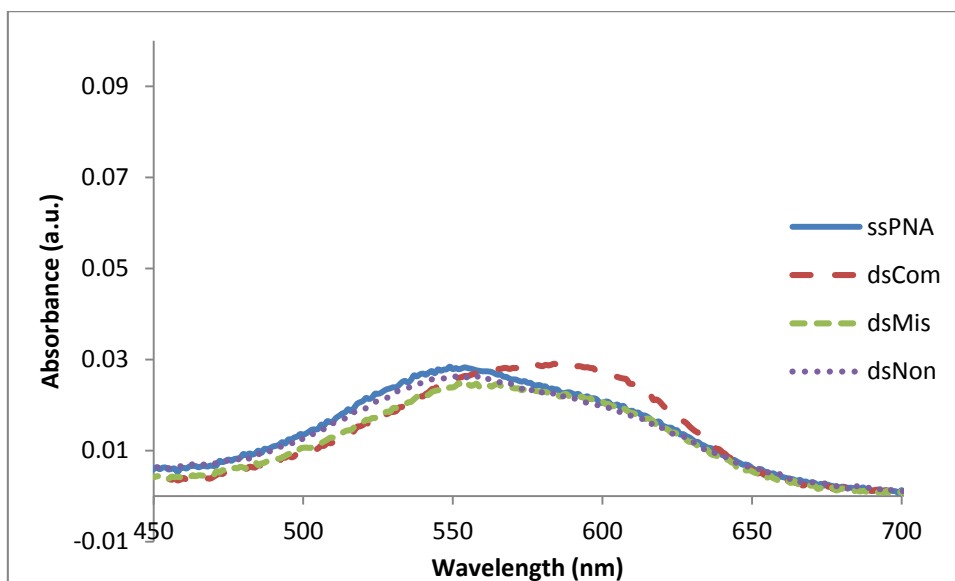**Figure A79.** UV-Vis spectra of **T9(Cou2/C2Flu)** in the absence and presence of DNA target in 10 mM phosphate buffer pH 7.0, [PNA] = 1.0 µM and [DNA] = 1.2 µM.
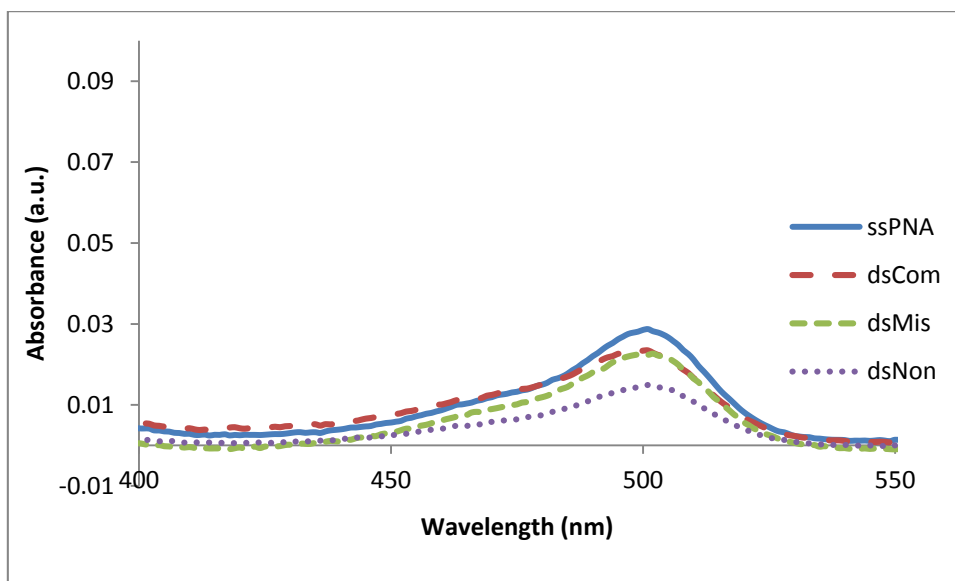
Figure A80. UV-Vis spectra of **T9(C2Cou2/C2Flu)** in the absence and presence of DNA target in 10 mM phosphate buffer pH 7.0, [PNA] = 1.0 µM and [DNA] = 1.2 µM
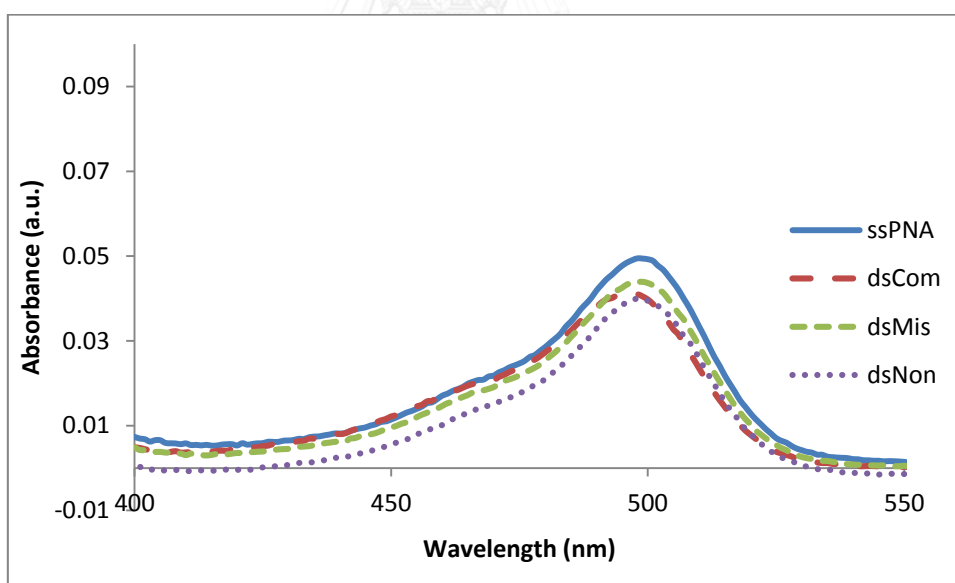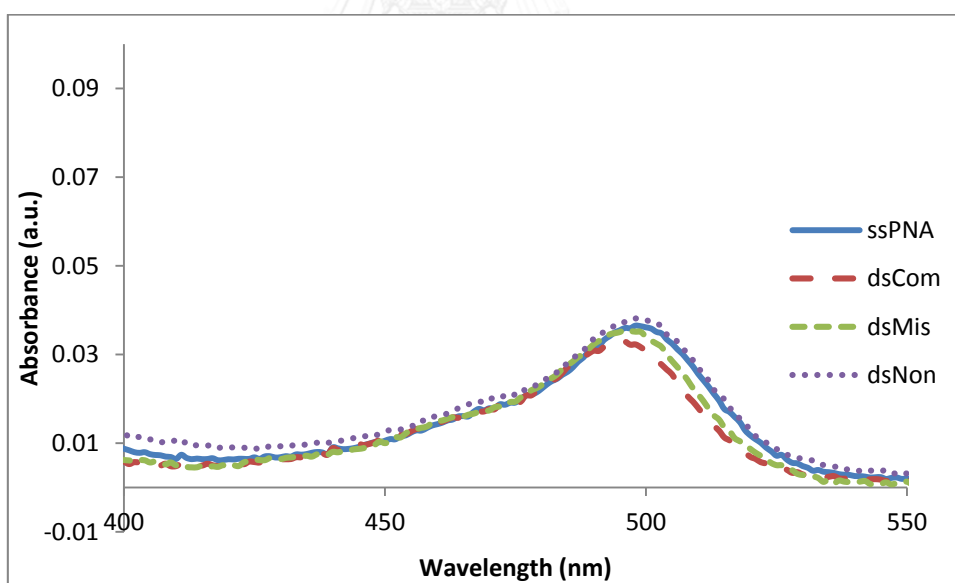

Figure A81. UV-Vis spectra of **T9(C2Cou2/Flu)** in the absence and presence of DNA target in 10 mM phosphate buffer pH 7.0, [PNA] = 1.0 µM and [DNA] = 1.2µM
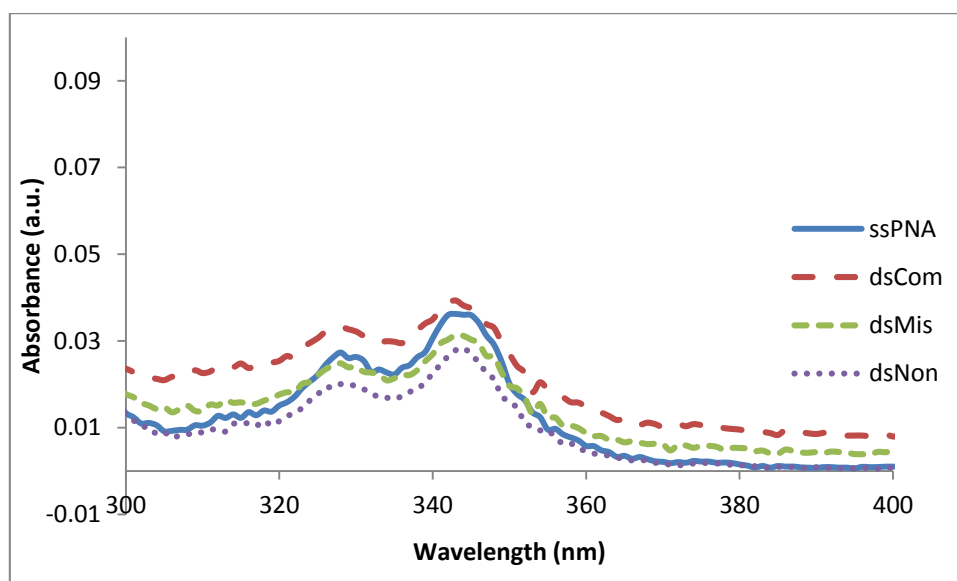
Figure A82. UV-Vis spectra of **T9(DNB/Pyr)** in the absence and presence of DNA target in 10 mM phosphate buffer pH 7.0, [PNA] = 1.0 µM and [DNA] = 1.2µM
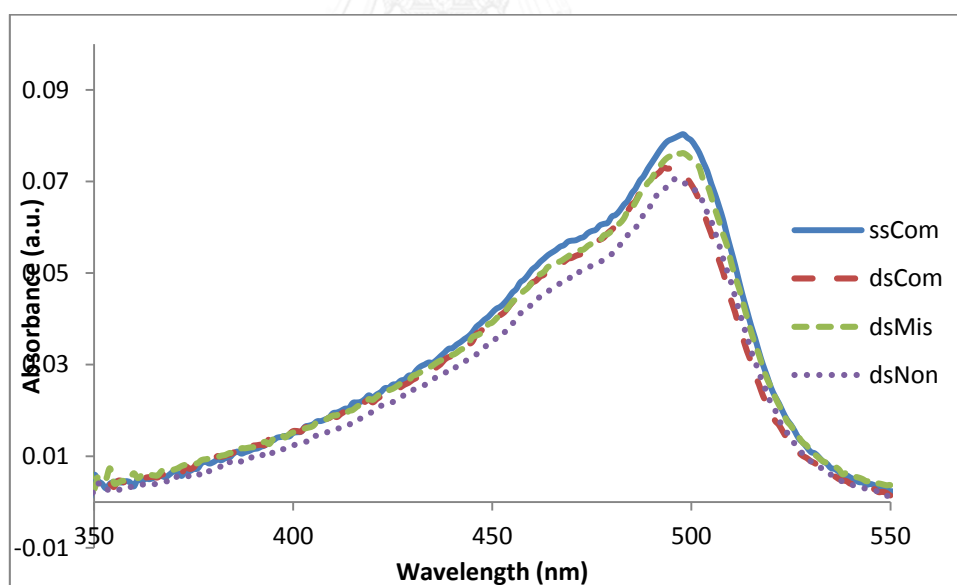
Figure A83. UV-Vis spectra of **T9(Flu/Dab)** in the absence and presence of DNA target in 10 mM phosphate buffer pH 7.0, [PNA] = 1.0 µM and [DNA] = 1.2µM
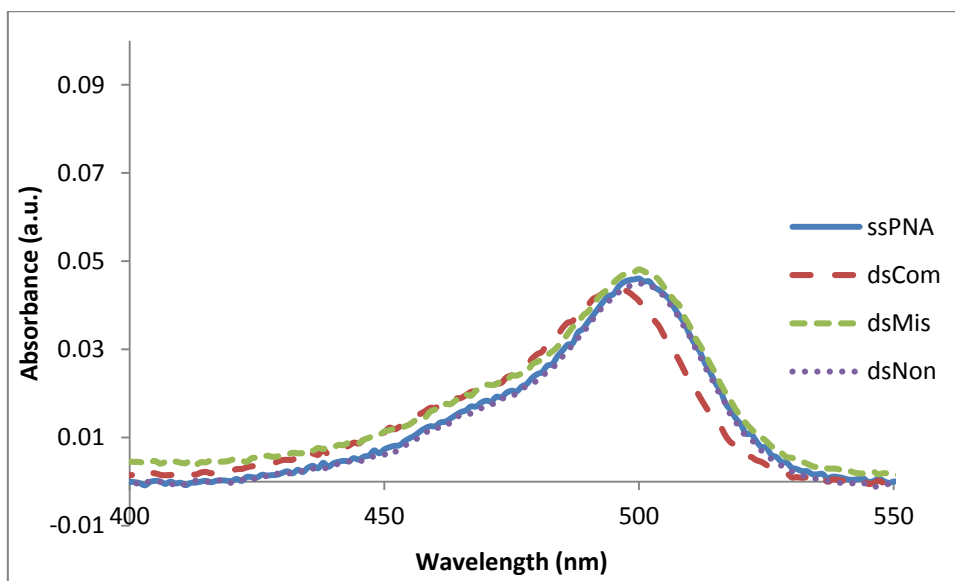
Figure A84. UV-Vis spectra of **T9(Flu/AQ)** in the absence and presence of DNA target in 10 mM phosphate buffer pH 7.0, [PNA] = 1.0 µM and [DNA] = 1.2µM
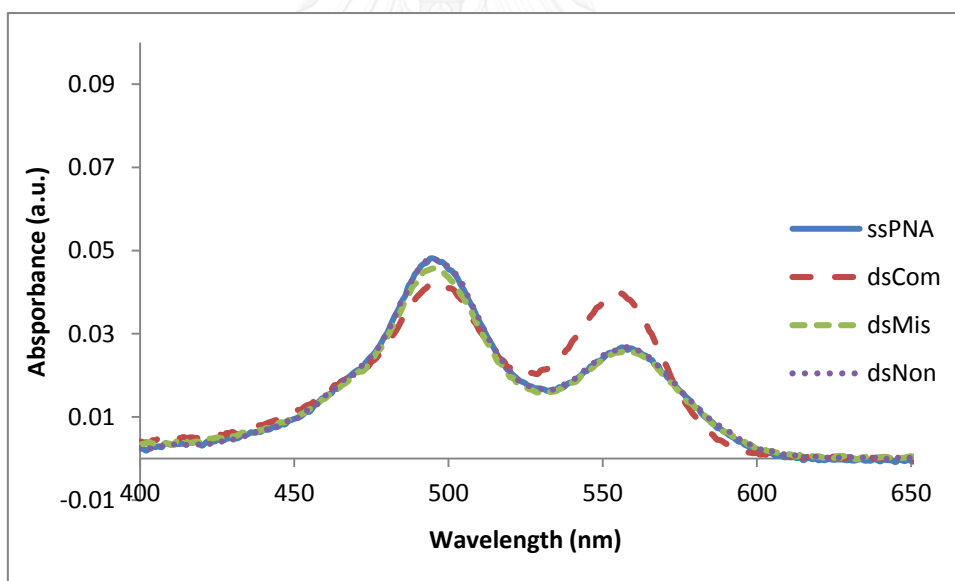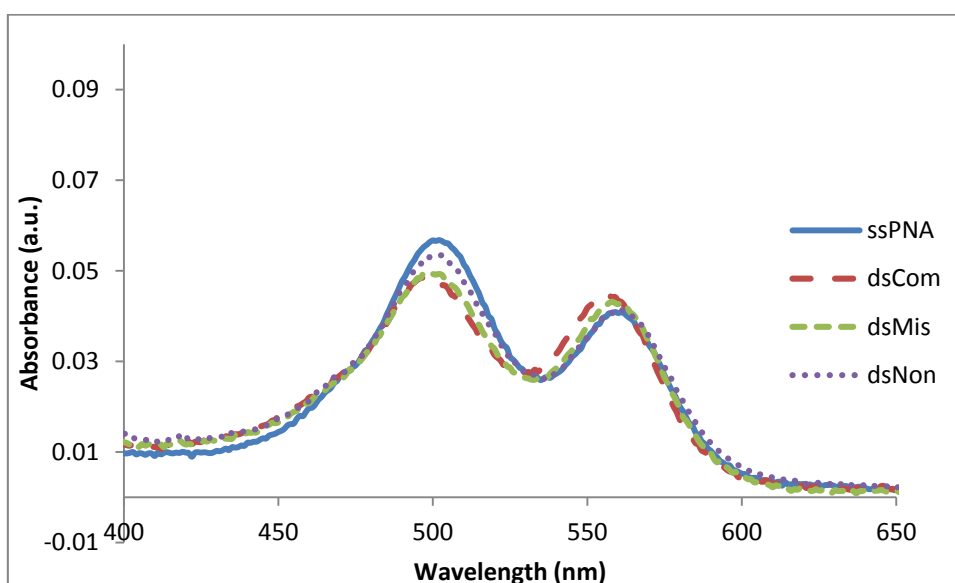

Figure A85. UV-Vis spectra of **T9(Flu/TMR)1** in the absence and presence of DNA target in 10 mM phosphate buffer pH 7.0, [PNA] = 1.0 µM and [DNA] = 1.2µM
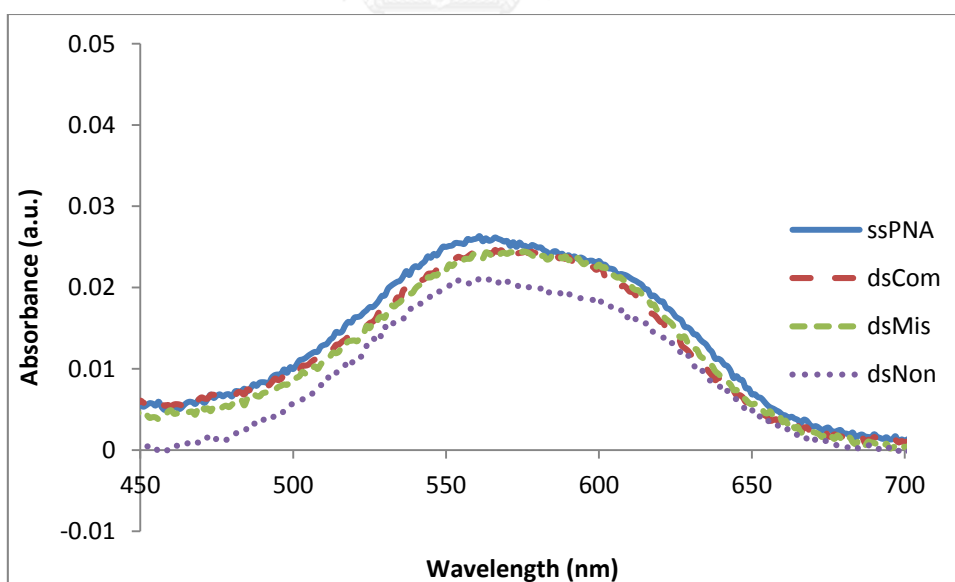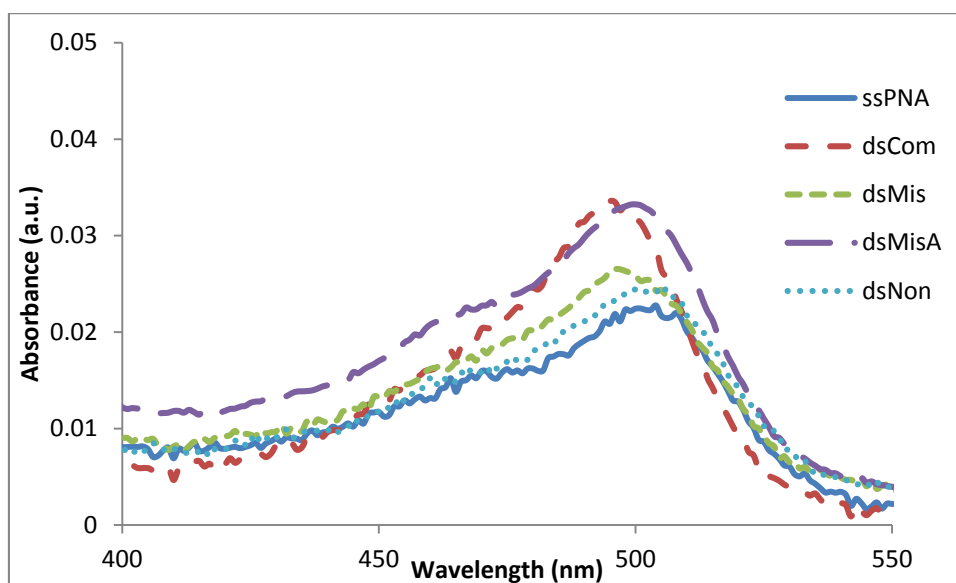
Figure A86. UV-Vis spectra of **T9(Flu/TMR)2** in the absence and presence of DNA target in 10 mM phosphate buffer pH 7.0, [PNA] = 1.0 µM and [DNA] = 1.2µM
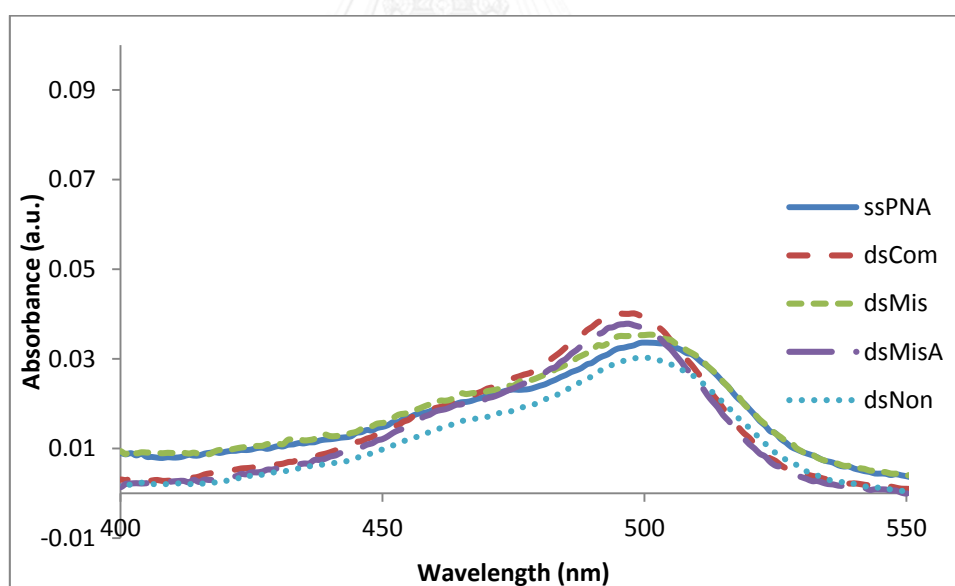

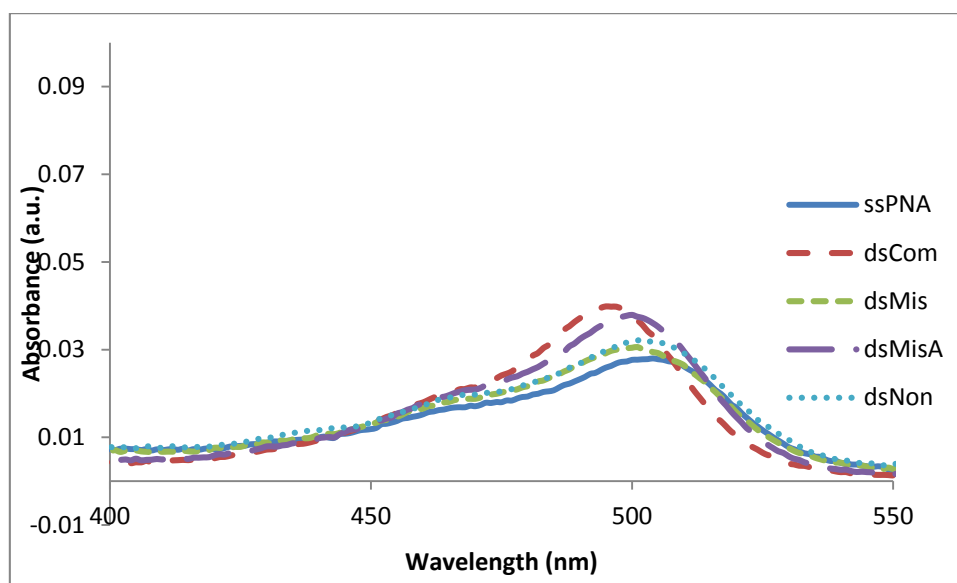**Figure A87.** UV-Vis spectra of **T9(Flu/TMR)3** in the absence and presence of DNA target in 10 mM phosphate buffer pH 7.0, [PNA] = 1.0 µM and [DNA] = 1.2µM

Figure A88. UV-Vis spectra of **T9(NBD/PheR)** in the absence and presence of DNA target in 10 mM phosphate buffer pH 7.0, [PNA] = 1.0 µM and [DNA] = 1.2µM

Figure A89. UV-Vis spectra of **T9(NBD/Nr)** in the absence and presence of DNA target in 10 mM phosphate buffer pH 7.0, [PNA] = 1.0 µM and [DNA] = 1.2µM
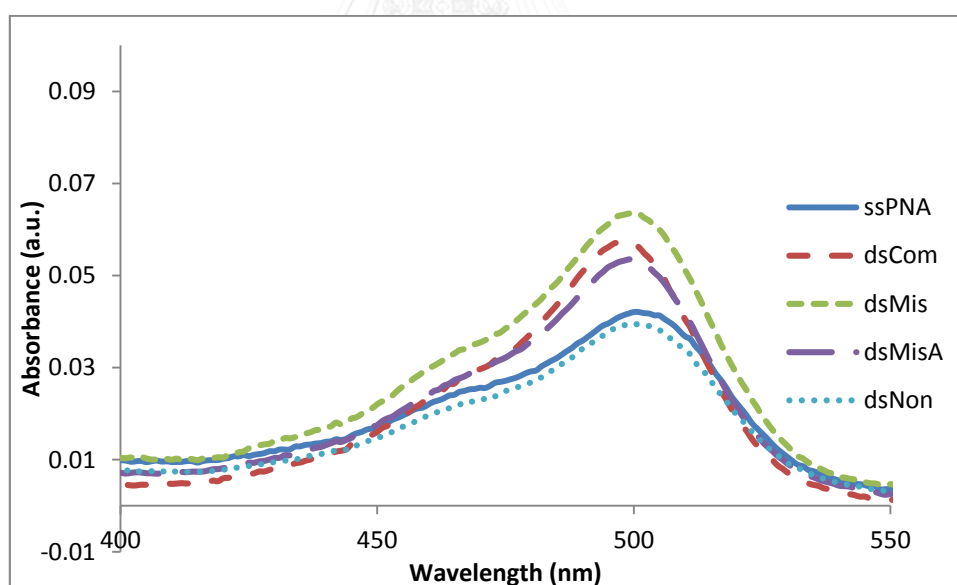
Figure A90. UV-Vis spectra of **T9(Dns/Nr)** in the absence and presence of DNA target in 10 mM phosphate buffer pH 7.0, [PNA] = 1.0 μM and [DNA] = 1.2μM

Figure A91. UV-Vis spectra of **M12(C2Cou2/Flu)** in the absence and presence of DNA target in 10 mM phosphate buffer pH 7.0, [PNA] = 1.0 μM and [DNA] = 1.2μM

Figure A92. UV-Vis spectra of **M12(Flu/TMR)1** in the absence and presence of DNA target in 10 mM phosphate buffer pH 7.0, [PNA] = 1.0 µM and [DNA] = 1.2µM
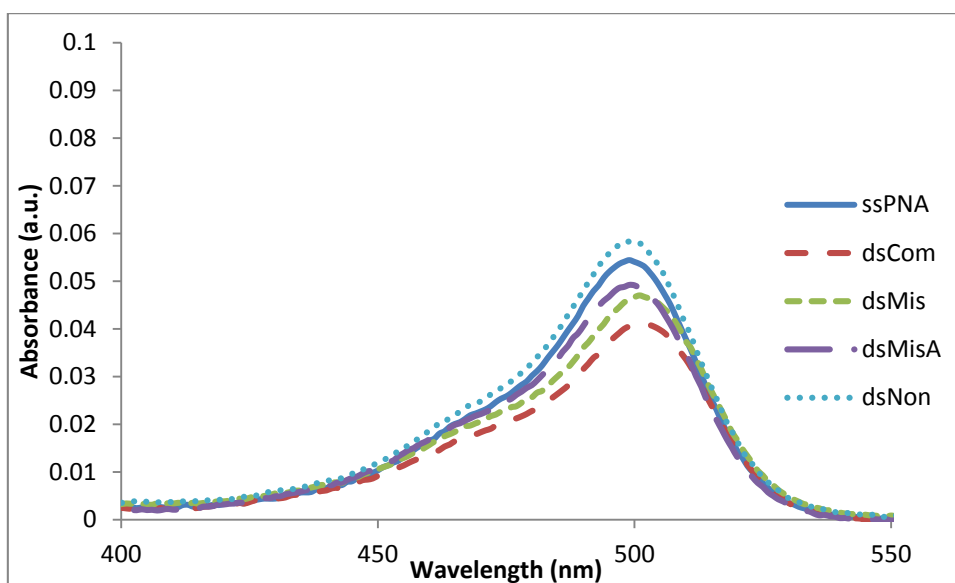

Figure A93. UV-Vis spectra of **M12(Dns/Nr)** in the absence and presence of DNA target in 10 mM phosphate buffer pH 7.0, [PNA] = 1.0 µM and [DNA] = 1.2µM
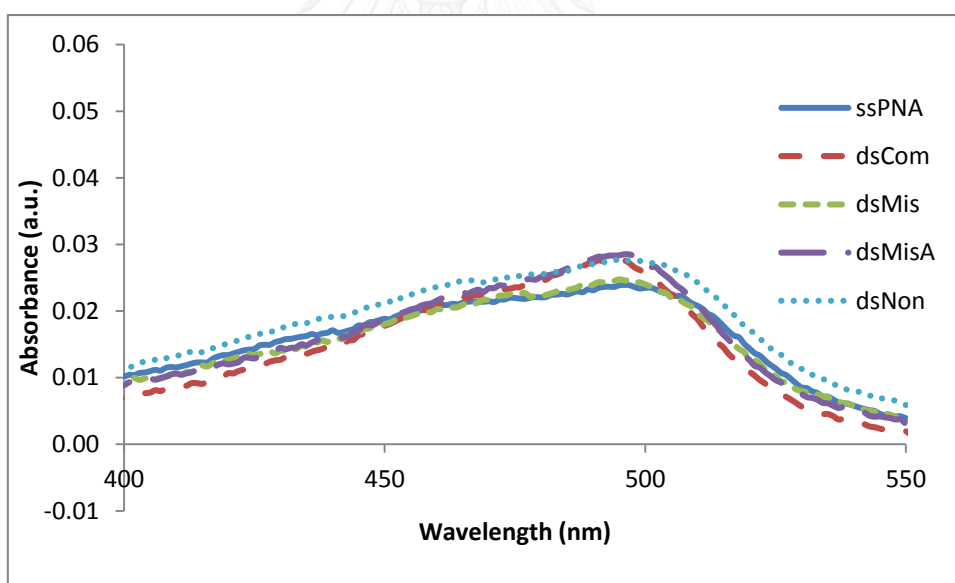
Figure A94. UV-Vis spectra of **(AQ/Flu)LysM10G** in the absence and presence of DNA target in 10 mM phosphate buffer pH 7.0, [PNA] = 1.0 µM and [DNA] = 1.2µM

Figure A95. UV-Vis spectra of **(AQ/Flu)apcM10G** in the absence and presence of DNA target in 10 mM phosphate buffer pH 7.0, [PNA] = 1.0 µM and [DNA] = 1.2µM
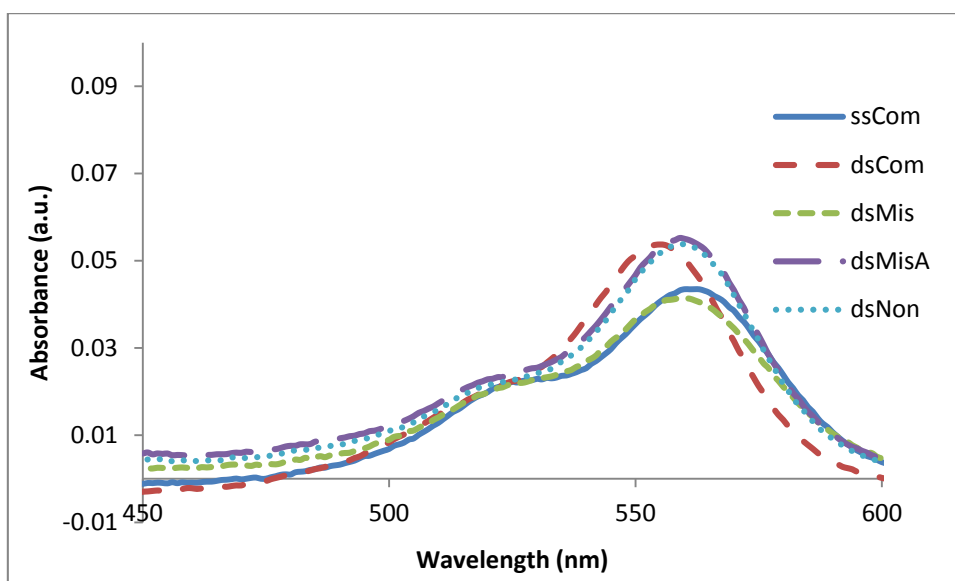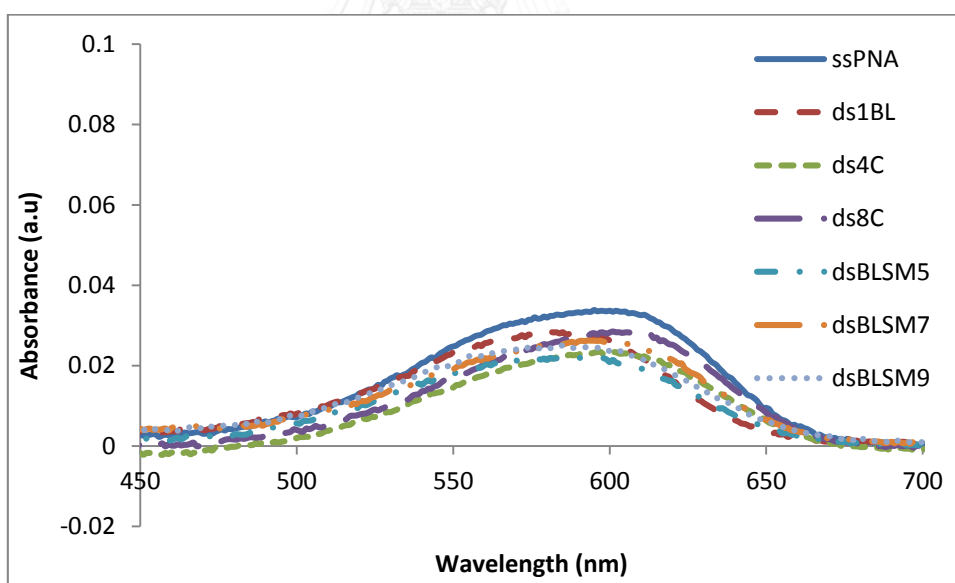
Figure A96. UV-Vis spectra of **(AQ/Flu)Lys(-ACPC)M10G** in the absence and presence of DNA target in 10 mM phosphate buffer pH 7.0, [PNA] = 1.0 µM and [DNA] = 1.2µM

Figure A97. UV-Vis spectra of **(Flu/AQ)LysM10G** in the absence and presence of DNA target in 10 mM phosphate buffer pH 7.0, [PNA] = 1.0 µM and [DNA] = 1.2µM

Figure A98. UV-Vis spectra of **(Flu)LysM10G** in the absence and presence of DNA target in 10 mM phosphate buffer pH 7.0, [PNA] = 1.0 µM and [DNA] = 1.2µM


Figure A99. UV-Vis spectra of **(Dab/Flu)LysM10G** in the absence and presence of DNA target in 10 mM phosphate buffer pH 7.0, [PNA] = 1.0 µM and [DNA] = 1.2µM

Figure A100. UV-Vis spectra of **(AQ/TMR)LysM10G** in the absence and presence of DNA target in 10 mM phosphate buffer pH 7.0, [PNA] = 1.0 µM and [DNA] = 1.2µM

Figure A101. UV-Vis spectra of **M10(Nr)** in the absence and presence of DNA target in 10 mM phosphate buffer pH 7.0, [PNA] = 1.0 µM and [DNA] = 1.2µM
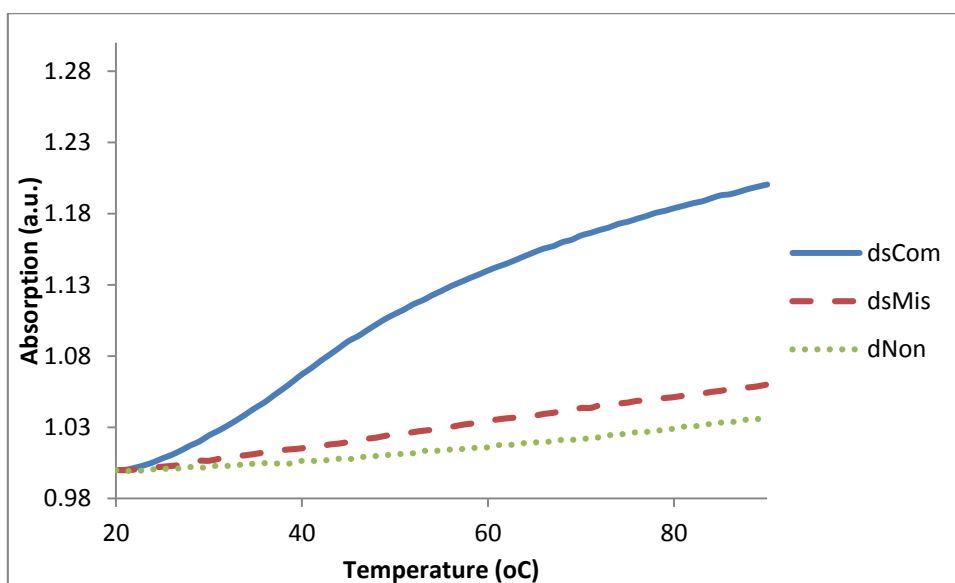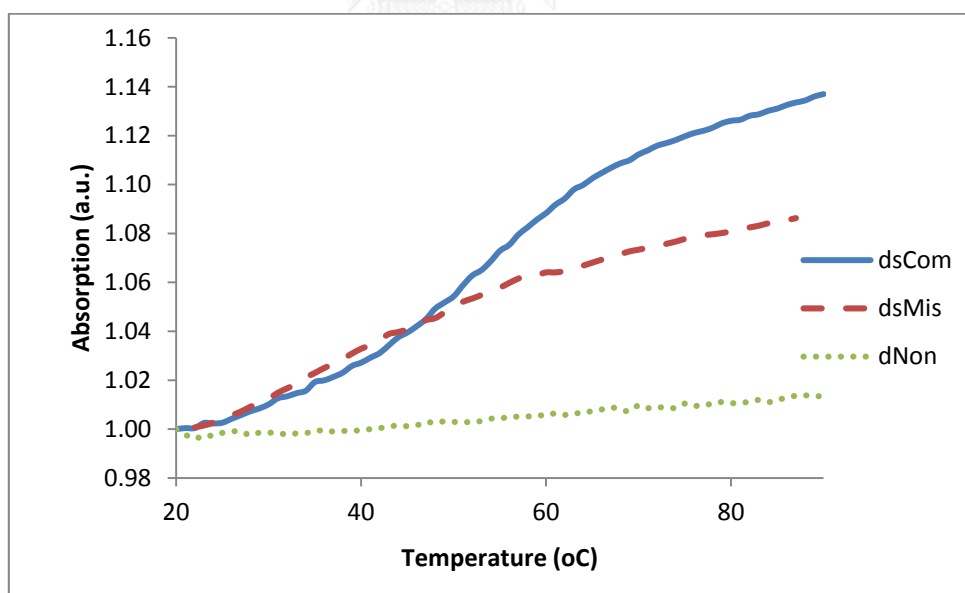
Figure A102. UV- T_m curves with complementary (dsCom), internal mismatch (dsMis), mismatched (dsMisA) and non-complementary (dsNon) DNA of **T9(Cou1/Flu)**
Conditions: 10 mM sodium phosphate buffer pH 7.0, [PNA] = 1.0 µM and [DNA] = 12 µM

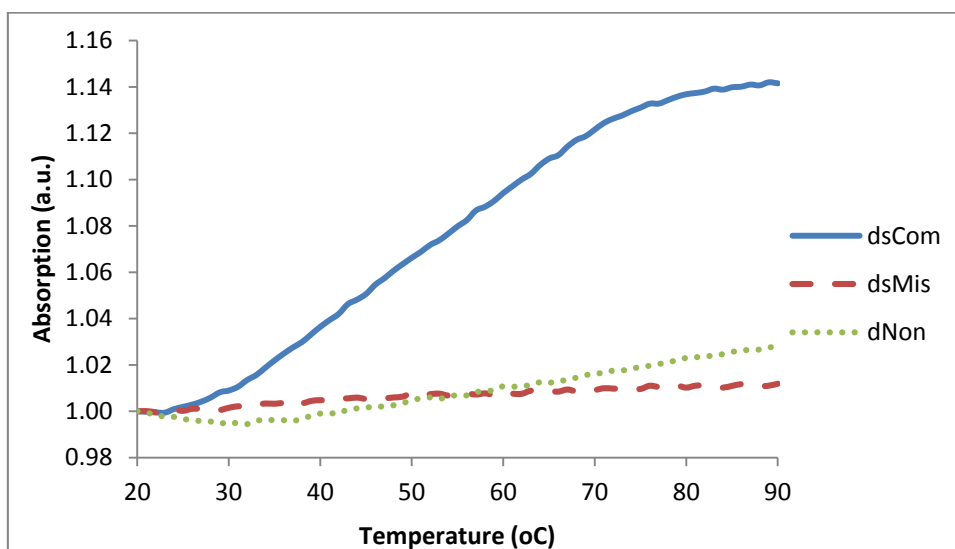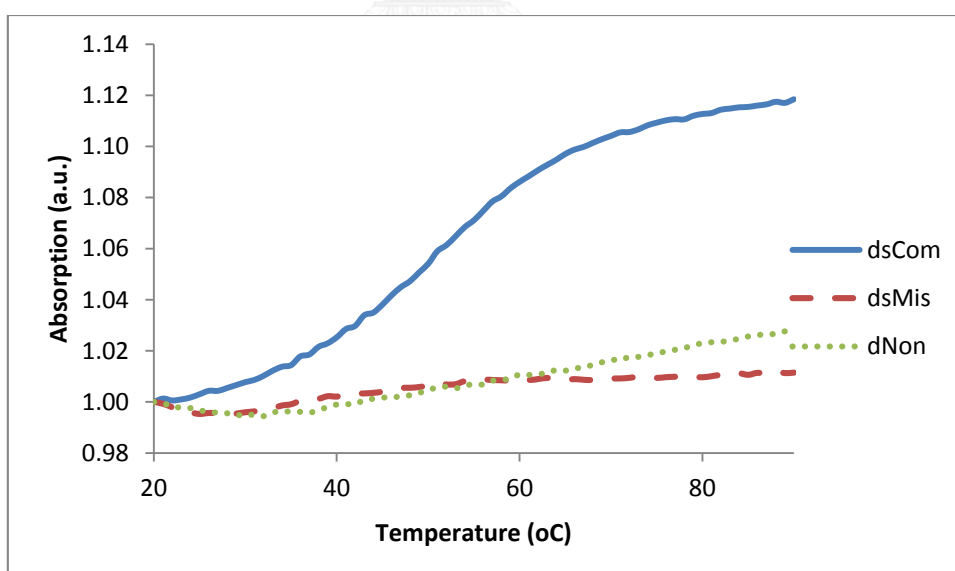**Figure A103** UV- T_m curves with complementary (dsCom), internal mismatch (dsMis), mismatched (dsMisA) and non-complementary (dsNon) DNA of **T9(C2Cou1/C2Flu)**
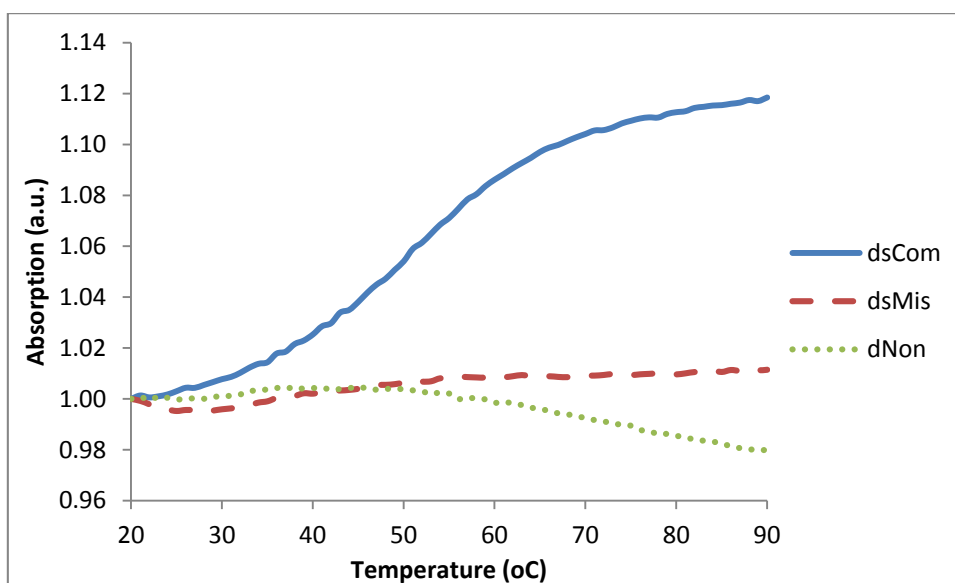Conditions: 10 mM sodium phosphate buffer pH 7.0, [PNA] = 1.0 µM and [DNA] = 1.2 µM

Figure A104. UV- T_m curves with complementary (dsCom), internal mismatch (dsMis), mismatched (dsMisA) and non-complementary (dsNon) DNA of **T9(Cou2/Flu)** Conditions: 10 mM sodium phosphate buffer pH 7.0, [PNA] = 1.0 µM and [DNA] = 1.2 µM

Figure A105. UV- T_m curves with complementary (dsCom), internal mismatch (dsMis), mismatched (dsMisA) and non-complementary (dsNon) DNA of **T9(Cou2/C2Flu)** Conditions: 10 mM sodium phosphate buffer pH 7.0, [PNA] = 1.0 µM and [DNA] = 1.2 µM
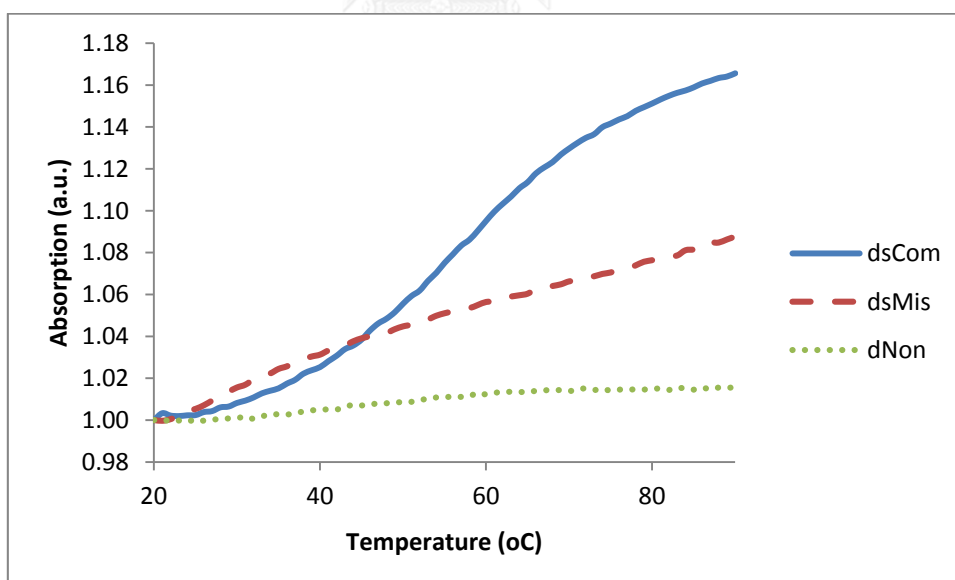
Figure A106. UV- T_m curves with complementary (dsCom), internal mismatch (dsMis), mismatched (dsMisA) and non-complementary (dsNon) DNA of **T9(C2Cou2/C2Flu)** Conditions: 10 mM sodium phosphate buffer pH 7.0, [PNA] = 1.0 μM and [DNA] = 1.2 μM
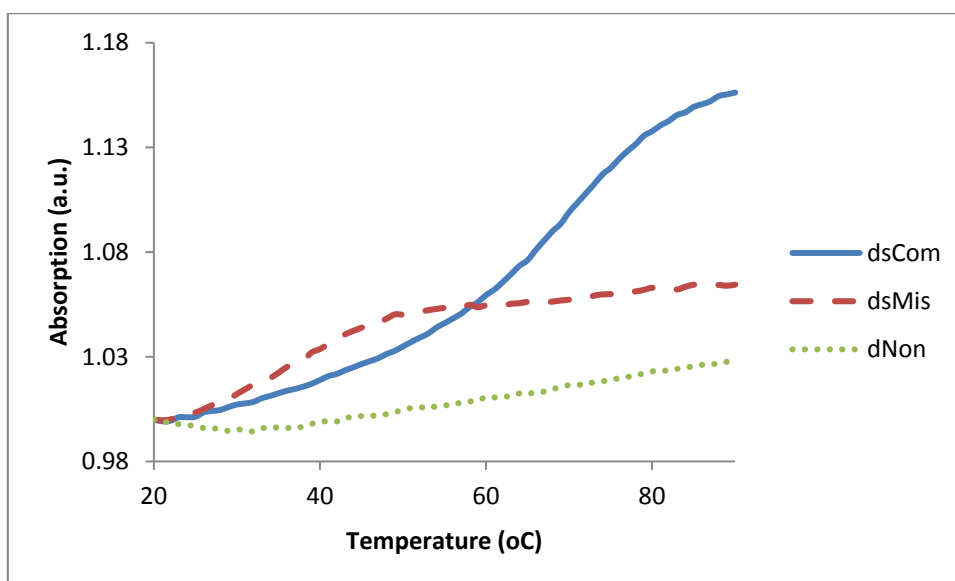

Figure A107. UV- T_m curves with complementary (dsCom), internal mismatch (dsMis), mismatched (dsMisA) and non-complementary (dsNon) DNA of **T9(C2Cou2/Flu)** Conditions: 10 mM sodium phosphate buffer pH 7.0, [PNA] = 1.0 μM and [DNA] = 1.2 μM

Figure A108 UV- T_m curves with complementary (dsCom), internal mismatch (dsMis), mismatched (dsMisA) and non-complementary (dsNon) DNA of **T9(NBD/PheR)** Conditions: 10 mM sodium phosphate buffer pH 7.0, [PNA] = 1.0 μM and [DNA] = 1.2 μM
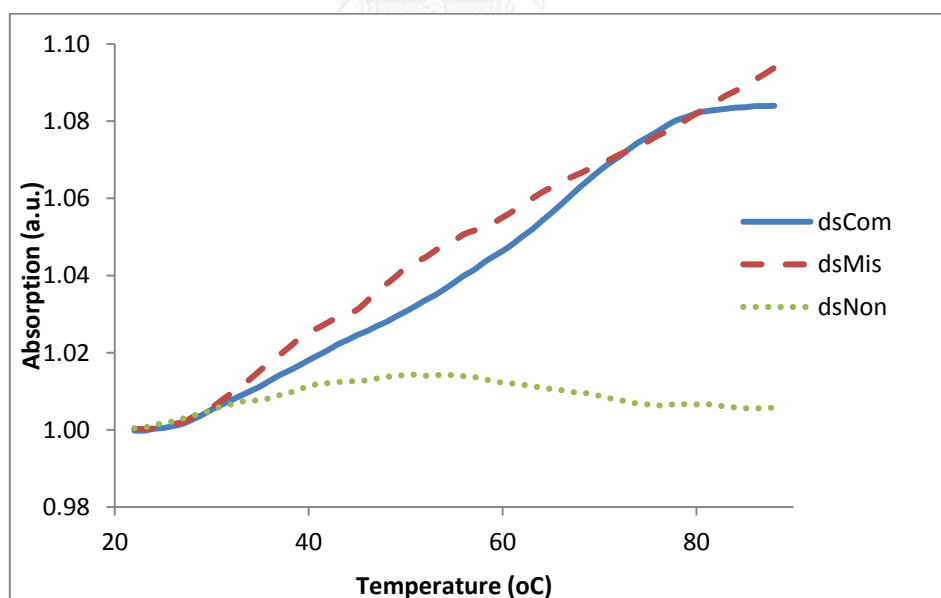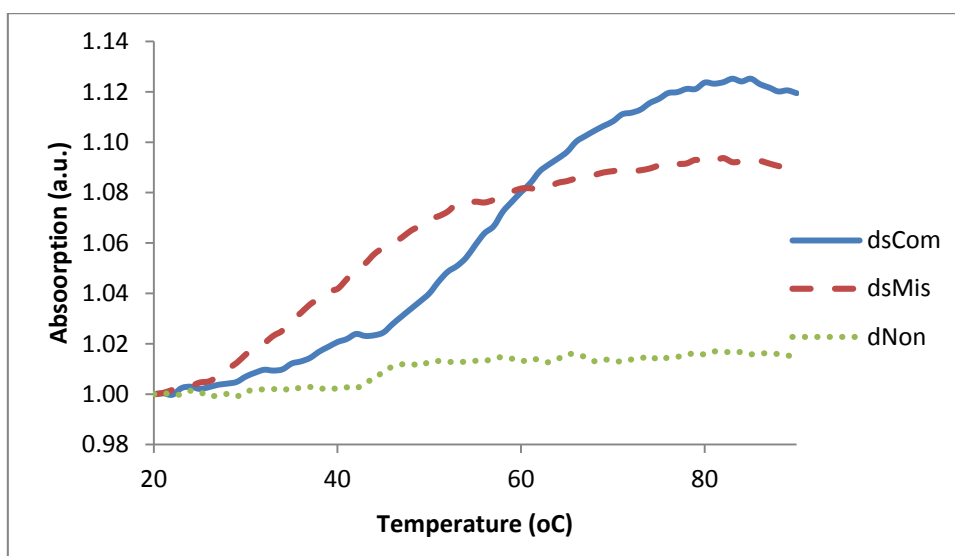

Figure A109. UV- T_m curves with complementary (dsCom), internal mismatch (dsMis), mismatched (dsMisA) and non-complementary (dsNon) DNA of **T9(NBD/Nr)** Conditions: 10 mM sodium phosphate buffer pH 7.0, [PNA] = 1.0 μM and [DNA] = 1.2 μM

Figure A110. UV- T_m curves with complementary (dsCom), internal mismatch (dsMis), mismatched (dsMisA) and non-complementary (dsNon) DNA of **T9(Dns/Nr)**

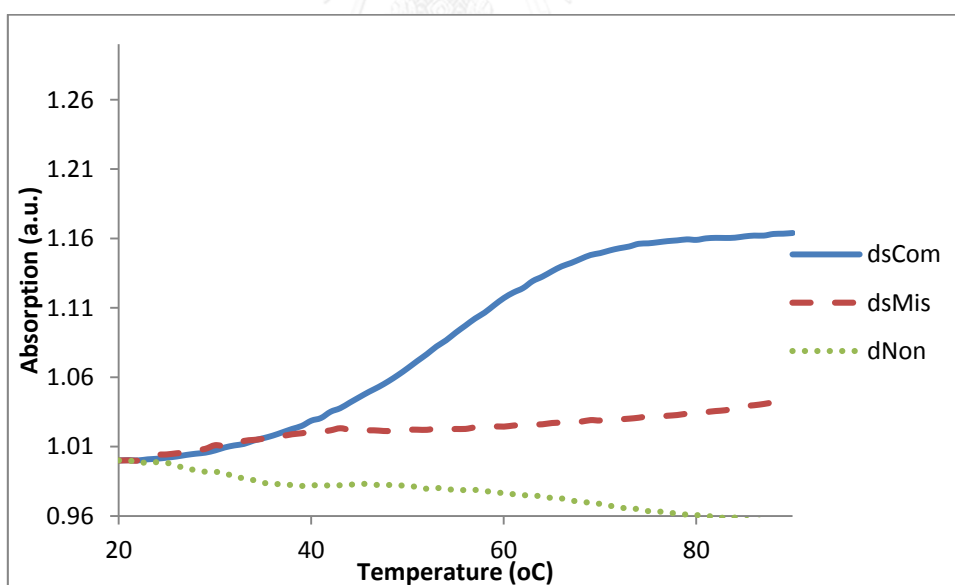Conditions: 10 mM sodium phosphate buffer pH 7.0, [PNA] = 1.0 μM and [DNA] = 1.2 μM

Figure A111. UV- T_m curves with complementary (dsCom), internal mismatch (dsMis), mismatched (dsMisA) and non-complementary (dsNon) DNA of **T9(DNB/Pyr)**

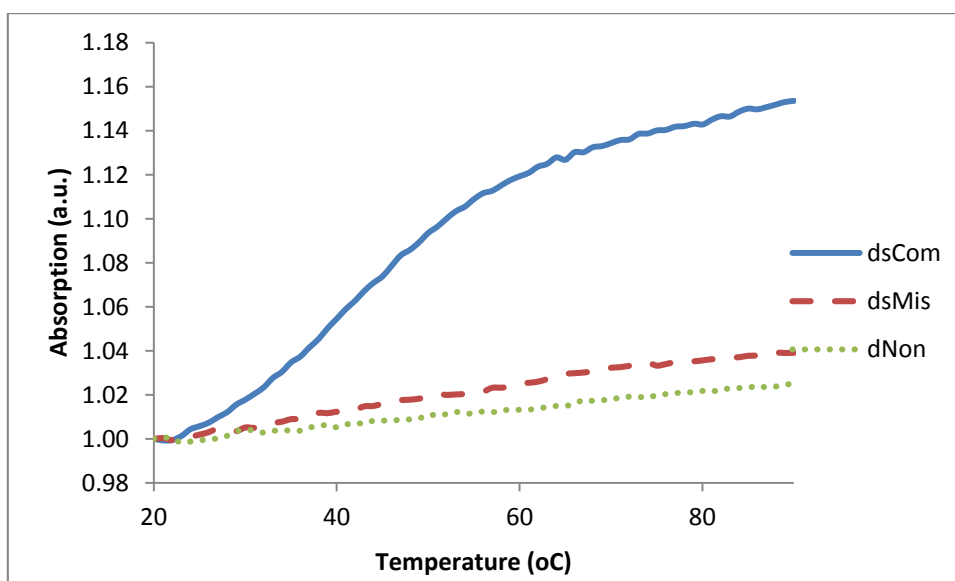Conditions: 10 mM sodium phosphate buffer pH 7.0, [PNA] = 1.0 μM and [DNA] = 1.2 μM

Figure A112. UV- T_m curves with complementary (dsCom), internal mismatch (dsMis), mismatched (dsMisA) and non-complementary (dsNon) DNA of **T9(Flu/Dab)**

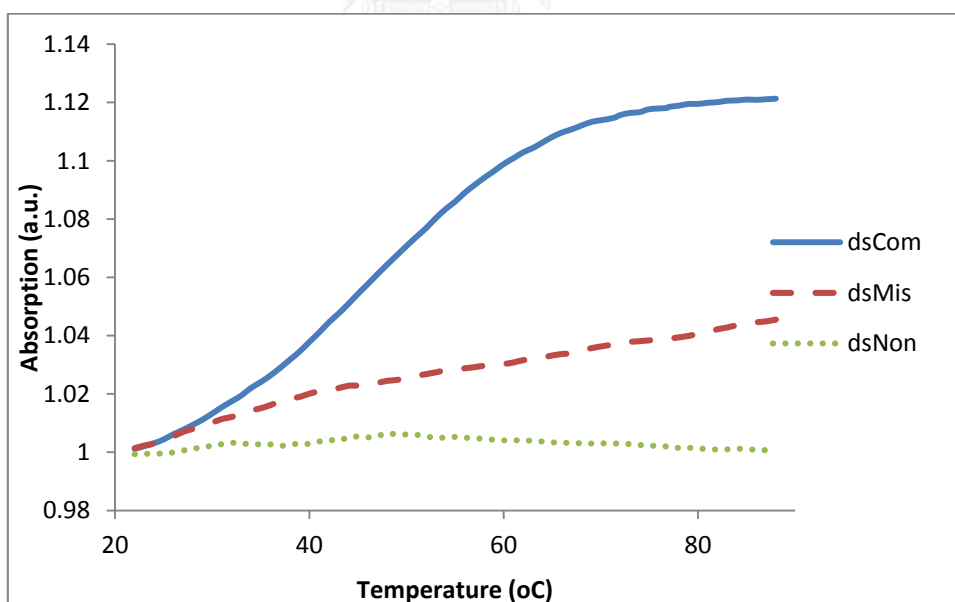Conditions: 10 mM sodium phosphate buffer pH 7.0, [PNA] = 1.0 µM and [DNA] = 1.2 µM

Figure A113. UV- T_m curves with complementary (dsCom), internal mismatch (dsMis), mismatched (dsMisA) and non-complementary (dsNon) DNA of **T9(Flu/AQ)**

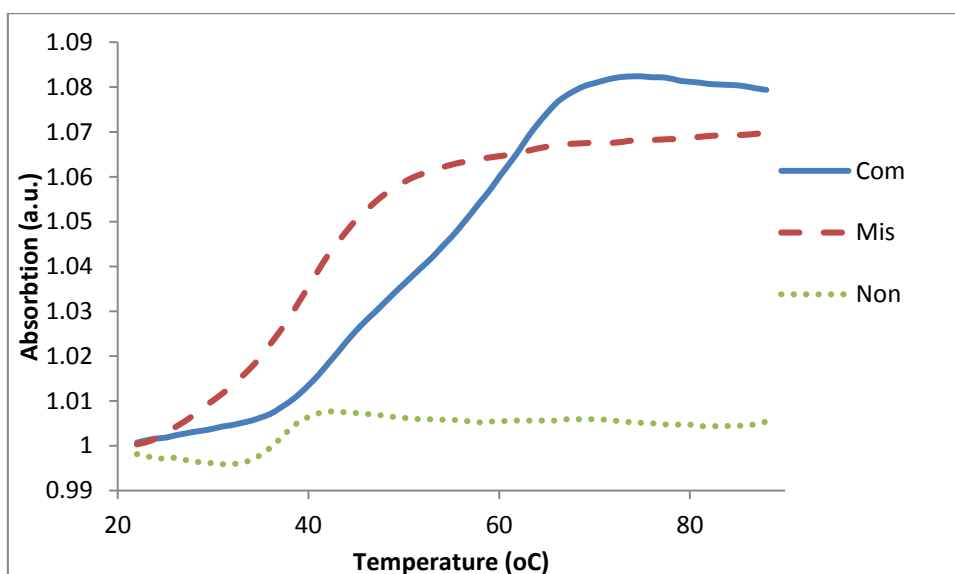Conditions: 10 mM sodium phosphate buffer pH 7.0, [PNA] = 1.0 µM and [DNA] = 1.2 µM

Figure A114. UV- T_m curves with complementary (dsCom), internal mismatch (dsMis), mismatched (dsMisA) and non-complementary (dsNon) DNA **of M12(C2Cou/Flu)**

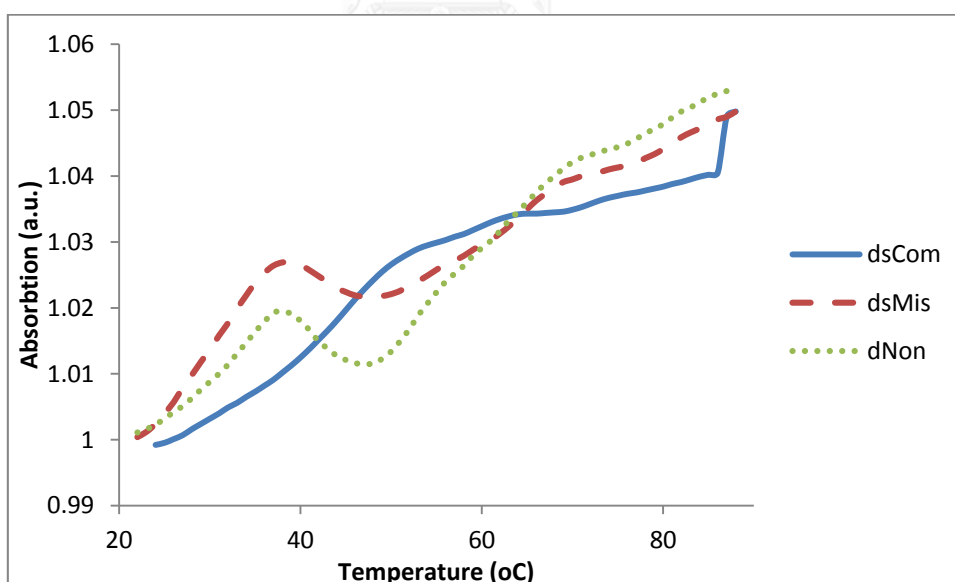Conditions: 10 mM sodium phosphate buffer pH 7.0, [PNA] = 1.0 µM and [DNA] = 1.2 µM

Figure A115. UV- T_m curves with complementary (dsCom), internal mismatch (dsMis), mismatched (dsMisA) and non-complementary (dsNon) DNA of **M12(Flu/TMR)**

Conditions: 10 mM sodium phosphate buffer pH 7.0, [PNA] = 1.0 µM and [DNA] = 1.2 µM
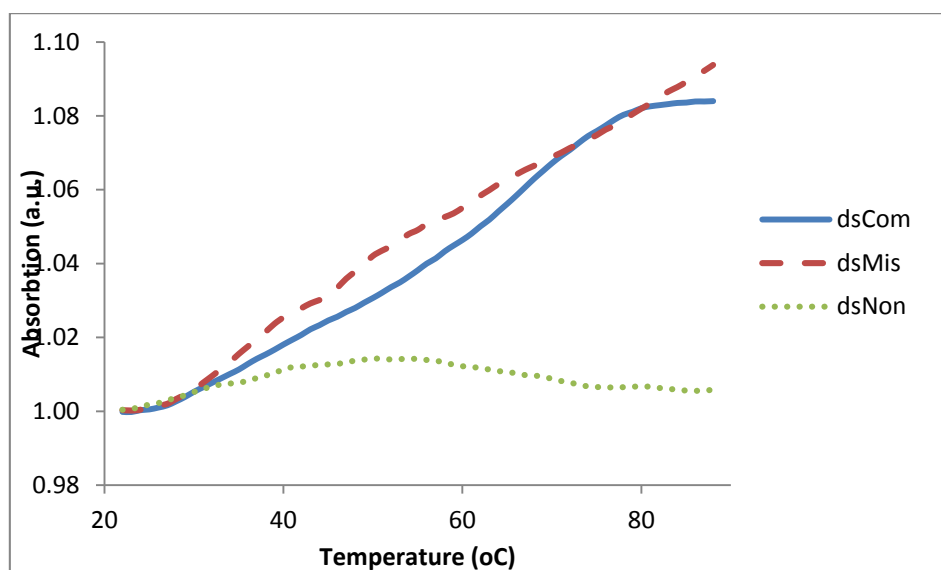
Figure A116. UV- T_m curves with complementary (dsCom), internal mismatch (dsMis), mismatched (dsMisA) and non-complementary (dsNon) DNA of **M12(Dns/Nr)** Conditions: 10 mM sodium phosphate buffer pH 7.0, [PNA] = 1.0 µM and [DNA] = 1.2 µM
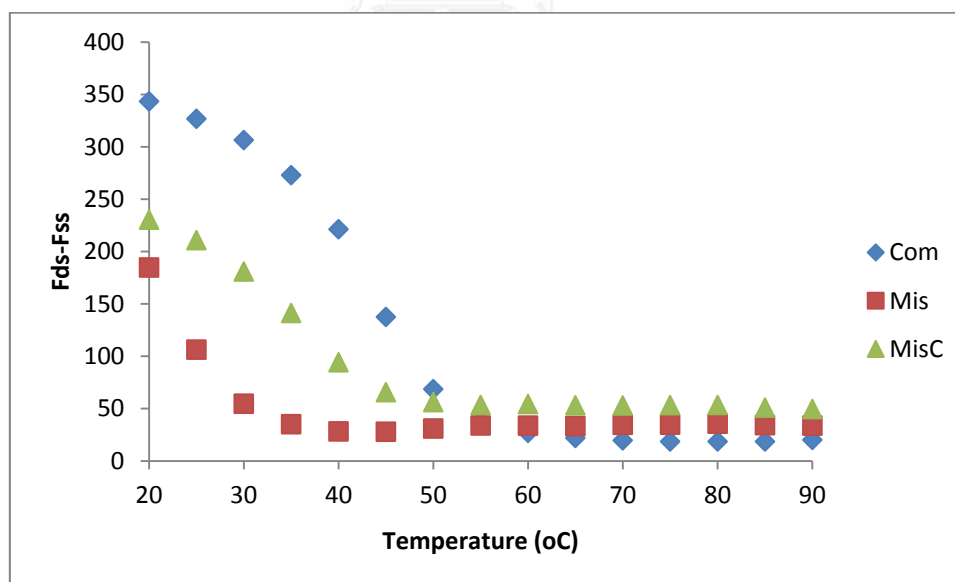

Figure A117. Fluorescence-T_m-curve of **(AQ/Flu)LysM10T** with complementary (dsCom), internal mismatch (dsMis), mismatched (dsMisA) and non-complementary (dsNon). Fluorescence-T_m were measured in 10 mM sodium phosphate buffer pH 7.0, [PNA] = 0.1 µM and [DNA] = 0.12 µM, excitation wavelength was 490 nm, PMT voltage = high

Figure A118. Fluorescence-Tm-curve of **(AQ/Flu)LysM12A** with complementary (dsCom), internal mismatch (dsMis), mismatched (dsMisA) and non-complementary (dsNon). Fluorescence-Tm were measured in 10 mM sodium phosphate buffer pH 7.0, [PNA] = 0.1 μM and [DNA] = 0.12 μM, excitation wavelength was 490 nm, PMT voltage = high.
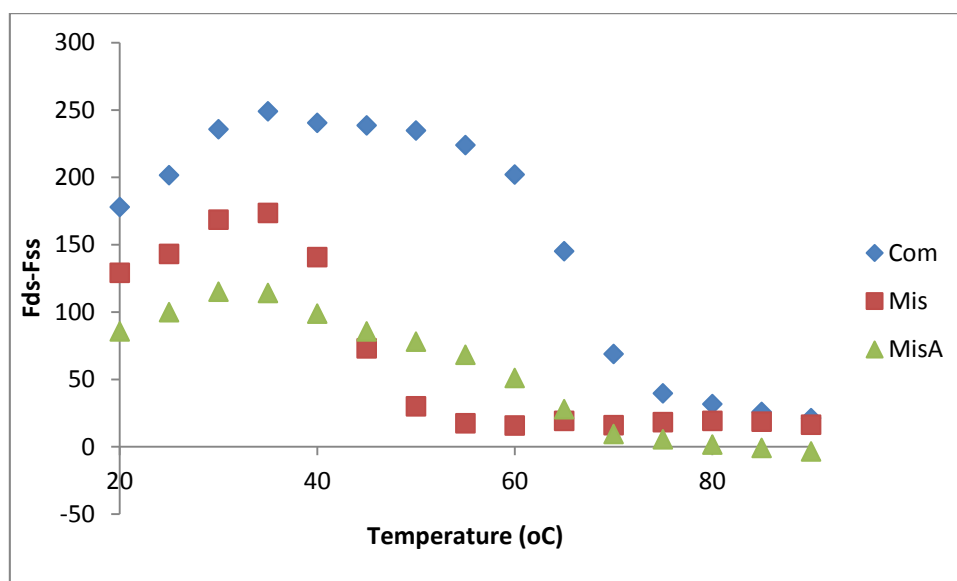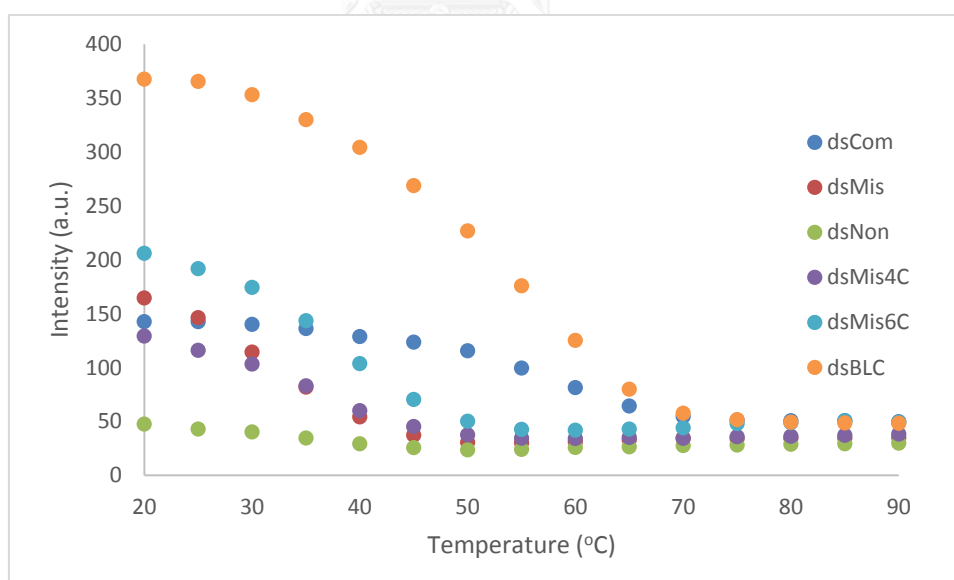

Figure A119. Fluorescence-T_m-curve of **M10(Nr)** with complementary (dsCom), mismatched (dsMis), mismatched (dsMis4C and dsMis6C), non-complementary (dsNon) and inserted base (dsBLC). Fluorescence-T_m were measured in 10 mM sodium phosphate buffer pH 7.0, [PNA] = 1.0 μM and [DNA] = 1.2 μM, excitation wavelength was 580 nm, PMT voltage = 700 PMT.

Figure A120. Fluorescence-T_m-curve of **M11AA(Nr)** with complementary (dsCom), and inserted base (dsBL). Fluorescence-T_m were measured in 10 mM sodium phosphate buffer pH 7.0, [PNA] = 1.0 µM and [DNA] = 1.2 µM, excitation wavelength was 580 nm, PMT voltage = 700 PMT.
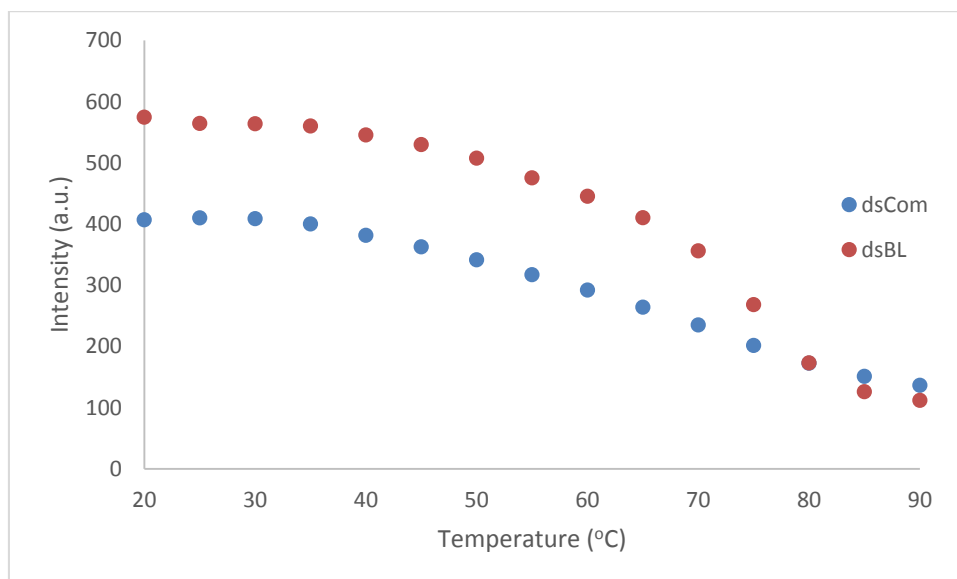

Figure A121. Fluorescence-T_m-curve of **M11TT(Nr)** with complementary (dsCom), and inserted base (dsBL). Fluorescence-T_m were measured in 10 mM sodium phosphate buffer pH 7.0, [PNA] = 1.0 µM and [DNA] = 1.2 µM, excitation wavelength was 580 nm, PMT voltage = 700 PMT.
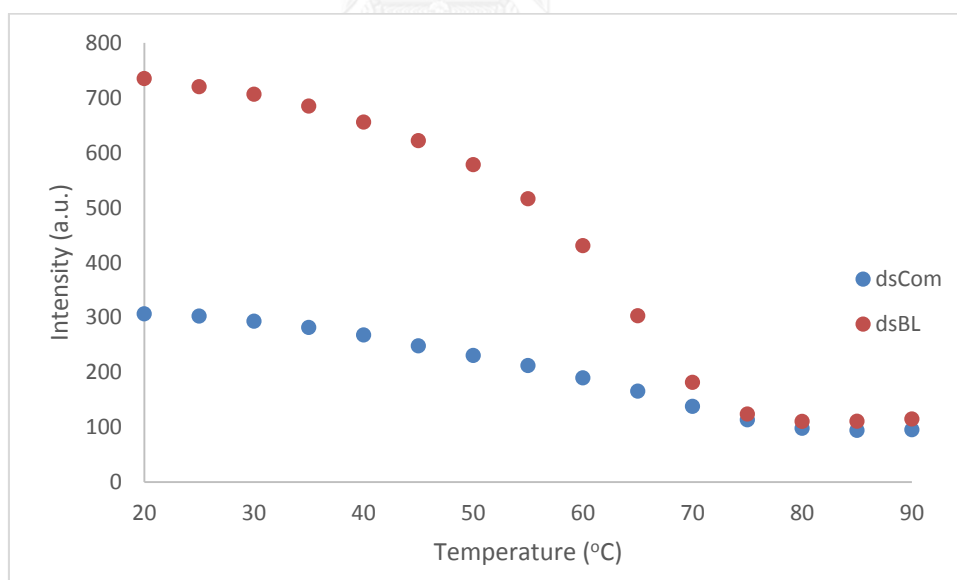
Figure A122. Fluorescence-T_{m}-curve of **M11CC(Nr)** with complementary (dsCom), and inserted base (dsBL). Fluorescence-T_{m} were measured in 10 mM sodium phosphate buffer pH 7.0, [PNA] = 1.0 µM and [DNA] = 1.2 µM, excitation wavelength was 580 nm, PMT voltage = 700 PMT.
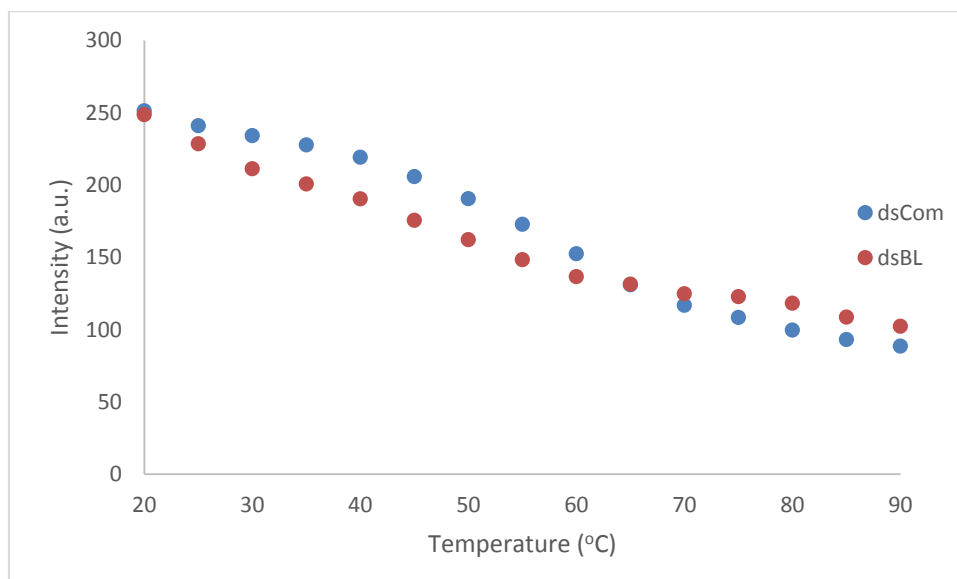

Figure A123. Fluorescence-T_{m}-curve of **M11GG(Nr)** with complementary (dsCom), and inserted base (dsBL). Fluorescence-T_{m} were measured in 10 mM sodium phosphate buffer pH 7.0, [PNA] = 1.0 µM and [DNA] = 1.2 µM, excitation wavelength was 580 nm, PMT voltage = 700 PMT.
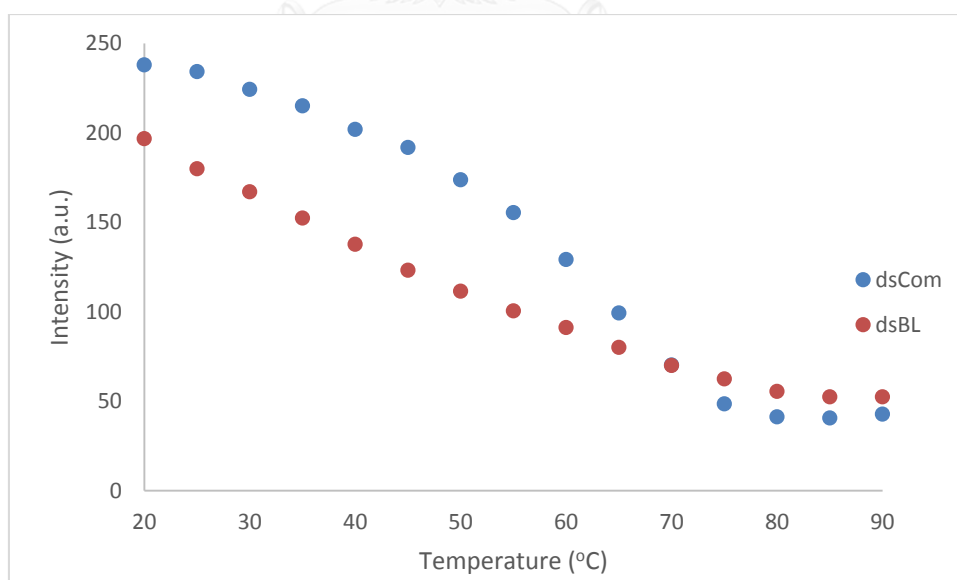
VITA

Mr.Nattawut Yotapan was born on August 10th, 1981 in Lopburi province, Thailand. He received the Bachelor Degree of Science, majoring in Chemistry from Mahidol University in 2002 and graduated with the Master Degree of Organic Chemistry from Faculty of Science, Mahidol University in 2006. He began Ph.D. studying in Program in Chemistry, Faculty of Science, Chulalongkorn University in the academic year of 2008 and graduated in the academic year of 2014.

Publications

Yotapan, N., Charoenpakdee, C., Wathanathavorn, P, Ditmangklo, B, Wagenknecht, H-A., Vilaivan, T. Synthesis and optical properties of pyrrolidinyl peptide nucleic acid carrying a clicked nile red label. Beilstein. J. Org. Chem. 2014, 10, 2166-2174.

Yotapan, N., Paptchikhine, A., Bera, M., Avula, S. K., Vilaivan, T., Andersson P. G. Simple proline derived phosphine-thiazole iridium complexes for asymmetric hydrogenation of trisubstitiuted olefins. Asian. J. Org. Chem. 2013, 2, 674-680.